Carbonate facies on a Lower Carboniferous storm influenced ramp in SW Britain

Thomas Joseph Faulkner B.A.

A thesis submitted to the University of Bristol in accordance with the requirements for the degree of Doctor of Philosophy (Ph.D.) in the Faculty of Science (Geology). May 1989.

Abstract

The Lower Carboniferous ('mid'-Courceyan to early Chadian) Black Rock Limestone ramp succession of SW Britain, accumulated along the southern margin of the Welsh-Brabant Massif during the early stage of development of the SW European foreland basin. Two depositional cycles are recognized which culminate in the subaerial exposure of those sequences in a more landward setting.

The lower depositional cycle includes the Barry Harbour Limestone Formation, which contains a variety of storm-related sedimentary structures including hummocky cross-stratification. This is conformably overlain by the tidally influenced, cross-stratified Brofiscin Oolite Formation which locally displays evidence of subaerial exposure. Seven sedimentary lithofacies are identified in these two formations, which record a distal to proximal, shallowing-upward trend that passes from beneath mean wave-base to above fairweather wave-base.

The upper depositional cycle of the Friars Point Limestone Formation includes the volcanics at Middle Hope, the Waulsortian facies at Castlemartin and Cannington Park, and is capped by the (herein named) Portishead Paleosol Beds (near Bristol). Above the basal transgressive sequence, the Friars Point Limestone consists of two distinct offshore ramp facies belts. The more proximal inner ramp facies belt was more strongly influenced by storm-related currents and exhibits tubular tempestites (storm sediment-filled burrows). The finer-grained, outer ramp facies belt is extensively bioturbated and preserves few features indicative of deposition from storm-related currents. The effects and relative timing of differential subsidence was elucidated by using the well documented biostratigraphy to separate the succession into isochronous units. The onset of pronounced differential subsidence was signified by volcanic activity at Middle Hope (Weston-super-Mare). The volcanic tuffs form a coarsening- and shallowing-upward sequence which records the development of a localised, probably non-emergent, offshore-volcanic high. Recognition of a major eustatic sea level fall at the end of the Courceyan and during the early part of the Chadian, is revealed by studying the decline of the Waulsortian reefs in an offshore ramp setting and evaluating the regional significance of the Portishead Paleosol Beds.

Overall, the development of the Black Rock Limestone ramp was the result of the interplay between eustacy and tectonism.

A full petrographic and geochemical analysis of the Waulsortian dolomites at Castlemartin, including the use of stable isotopes revealed that dolomitization occurred during burial, most probably as a result of basin dewatering.

Acknowledgements

Firstly, I am extremely grateful to Dr V.P. Wright & D. Tucker (ARC), for continual support and expert advice throughout my period of research.

Secondly, I am indebted to Susan Forson for encouragement, and assistance with field logging and editing the text.

Thirdly, I wish to thank the following for help and advice: John Miller, Dick Waters, Jerry Davies, Neil Pickard, Peter Hardy, Trevor Burchette, Alan Lees, Peter Gutteridge, Nigel Hughes, and Shoa Sun.

Fourthly, I thank the technical staff at Bristol, in particular Tony Kemp (geochemistry), Simon Powell (photography) and Gary Webber (preparation of thin-sections).

Lastly, I am grateful for the receipt of a N.E.R.C grant and an Amey Roadstone Case award.

Declaration

I declare that the work contained in this thesis was my own work except where otherwise stated.

Signed 

T.J. Faulkner

May 19th, 1989.

CONTENTS

LIST OF FIGURES & TABLES

Chapter 1 - Introduction

1.1 Introduction

1.2 Geological setting

1.3 Area of study

1.4 Paleogeographic setting

1.5 Previous work

1.1 Introduction

In carbonate sedimentology, the term shelf has become synonymous with the very shallow (less than 10m) flat-topped, and rimmed shelves such as that of southern Florida. Carbonate settings which show a progressive deepening seaward to well below wave-base are referred to as ramps (Ahr 1973) or open shelves (Ginsburg & James 1974). Typically, they exhibit a shallow-water, nearshore sand belt and an offshore, deeper-water region of finer grained sediments. Since there is a general lack of well documented modern analogues (e.g. Persian Gulf, Wilson & Jordan 1983) refinement of the model is dependent upon studies of well exposed ancient successions. Overall, there have been few comprehensive studies of carbonate ramps. Notable exceptions include the work on the Muschelkalk by Aigner (1984 & 1985), Calvet & Tucker (1988), and studies of Palaeozoic ramps by Brett (1983), Markello & Read (1981), Handford (1986), Wright (1986) and Chatellier (1988). In particular, there have been few detailed descriptions of offshore ramp facies types (e.g Calvet & Tucker 1988).

The Lower Carboniferous Black Rock Limestone Group of SW Britain has traditionally been regarded as a monotonous sequence of muddy bioclastic limestones which provide little information on palaeogeography or sea level changes. The main aim of this thesis is to detail the different ramp facies types occurring within the Black Rock Limestone Group and evaluate the evolution of the carbonate province of SW Britain during the mid-Courceyan to early Chadian period. This mainly involves detailed facies analyses of the Black Rock Limestone Group including the Middle Hope volcanics (Weston-super-Mare). In addition, this thesis includes a microfacies and diagenetic study of the Waulsortian mudmounds at Castlemartin and an assessment of the significance of two subaerial exposure units, containing columnar

calcites, immediately above the Black Rock Limestone Group at Portishead (Bristol district).

1.2 Geological setting

In SW Britain, the Lower Carboniferous succession forms a 100Km wide sedimentary wedge (ca. 1500m thick in the south and west) tapering (to 150m) towards the north onto the ancient landmass, the Welsh-Brabant Massif (St George's Land) (Figures 1.1, 1.2 & 1.3). As a result of an early Carboniferous eustatic sea level rise (Johnson 1982) the (Devonian) Old Red Sandstone alluvial plains of southern Britain were drowned to form a southward deepening ramp. The siliciclastic-dominated Lower Limestone Shale Group (Courceyan) records the transgression, at the peak of which it passes transitionally upward into the overlying, mid-Courceyan to early Chadian, Black Rock Limestone Group (Ramsbottom 1984). The latter records the first major phase of carbonate production and establishment of a carbonate ramp (Wright 1986).

As well as sea level changes, differential subsidence played an important role in the development of the pre-Holkerian ramp succession (Wright 1986; Wilson *et al.* 1988). This is reflected in the distribution of the three depth-related ramp facies identifed by Wright (1986) which broadly conform to three distinct tectonic zones (Figure 1.3).

The inner ramp facies, laid-down above fairweather wave-base, include oolitic and peritidal limestones representing shoal and back-shoal environments. Such facies tend to concentrate in the northern zone, that underwent little or no subsidence and contain an attenuated succession with numerous subaerial breaks (Figure 1.3)

Figure 1.1. Schematic diagram of the palaeogeography of Britain and western Europe during the Lower Carboniferous (modified after Varker & Sevastopulo 1985). Insets of the Lower Carboniferous outcrops in southwest Britain, Belgium and southern Germany.

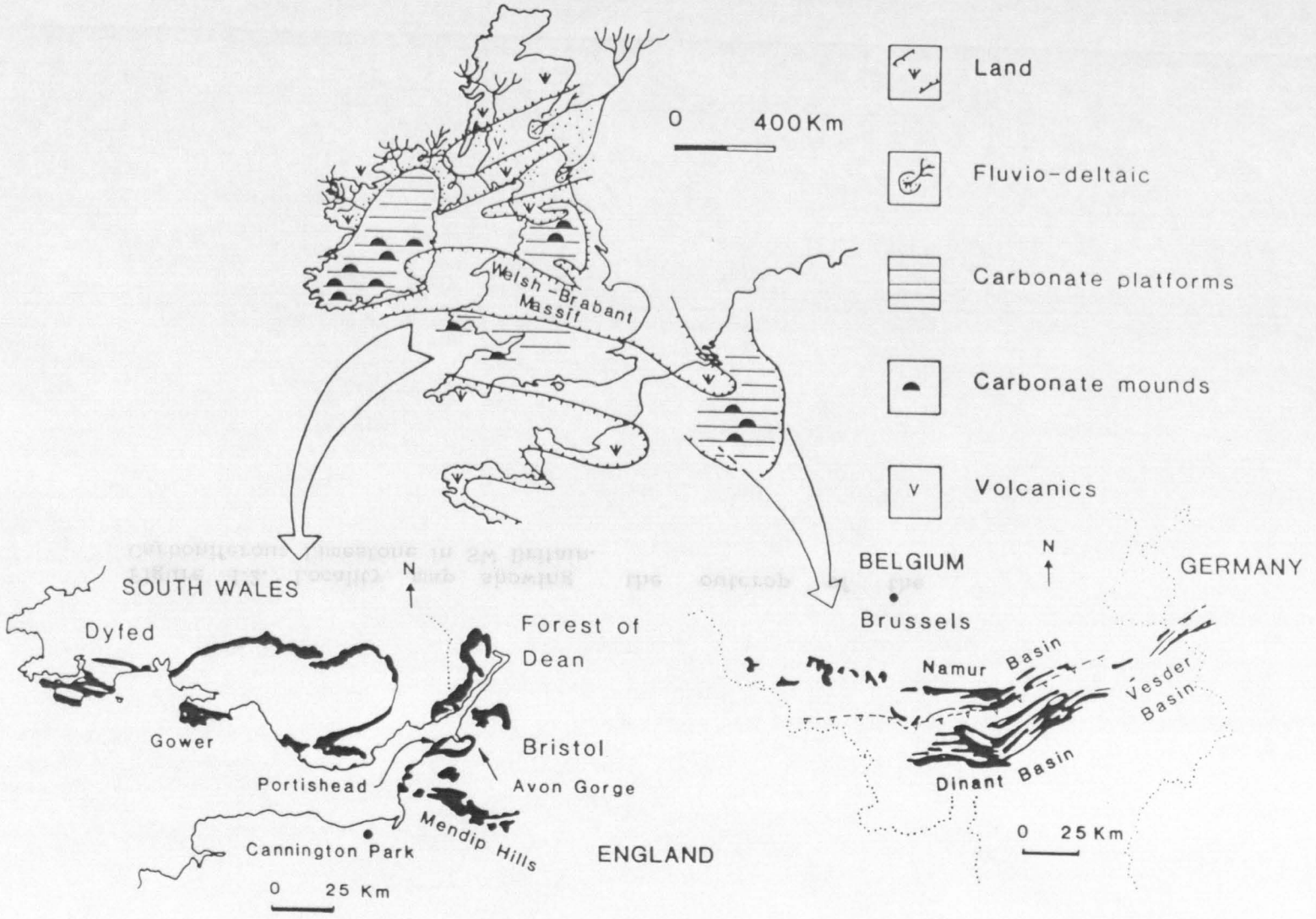
Land
Fluvio-deltaic
Carbonate platforms
Carbonate mounds
Volcanics
0 400Km
Welsh - Brabant Massif
SOUTH WALES
N
Dyfed
Forest of Dean
Gower
Bristol
Portishead
Avon Gorge
Mendip Hills
Cannington Park
ENGLAND
0 25 Km
BELGIUM
Brussels
GERMANY
Namur Basin
Vesder Basin
Dinant Basin
0 25 Km

Figure 1.2. Locality map showing the outcrop of the Carboniferous Limestone in SW Britain.

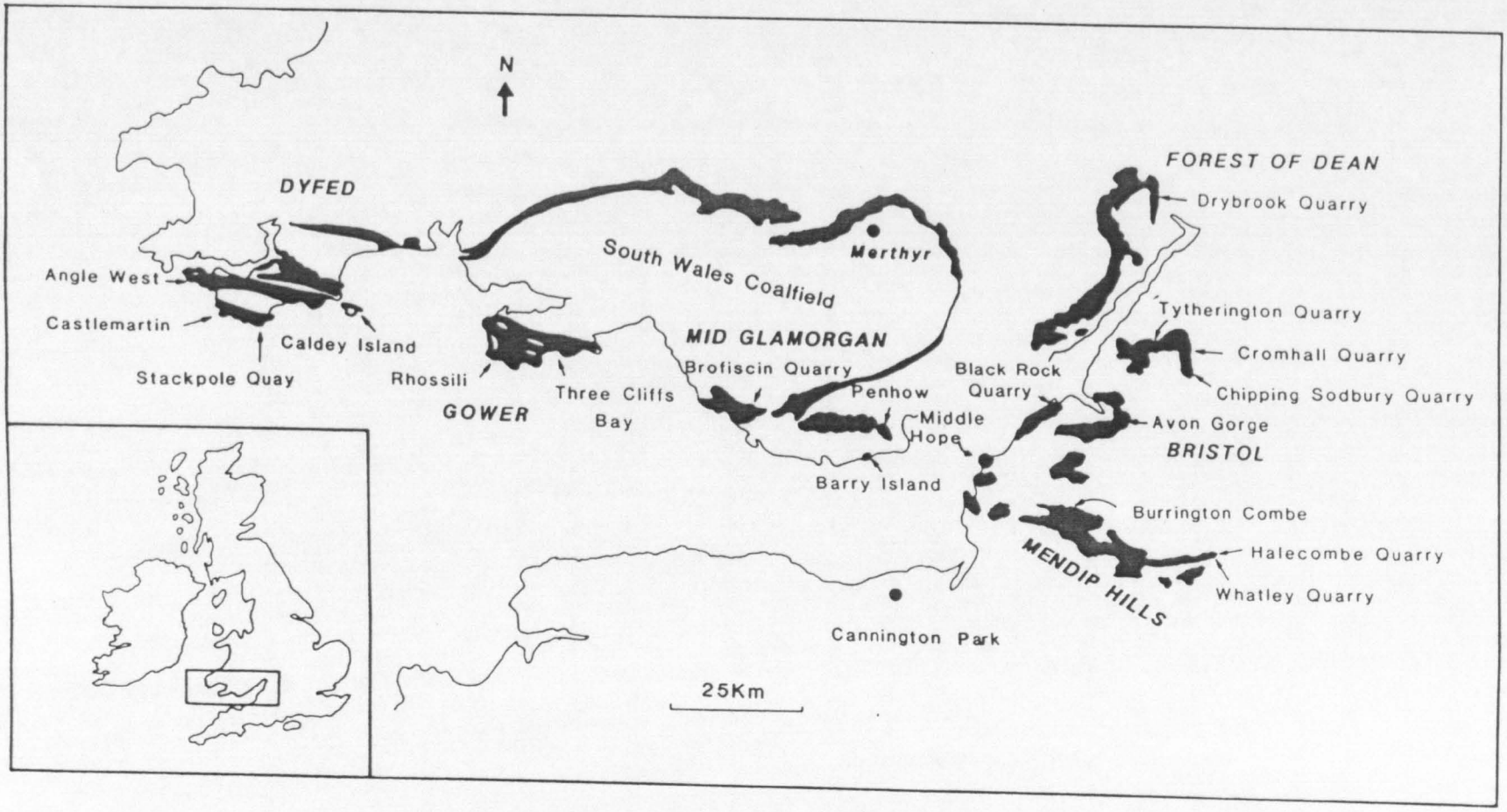
N
DYFED
Angle West
Castlemartin
Caldey Island
Stackpole Quay
Rhossili
GOWER
Three Cliffs Bay
South Wales Coalfield
Merthyr
MID GLAMORGAN
Brofiscin Quarry
Penhow
Middle Hope
Barry Island
Black Rock Quarry
FOREST OF DEAN
Drybrook Quarry
Tytherington Quarry
Cromhall Quarry
Chipping Sodbury Quarry
Avon Gorge
BRISTOL
Burrington Combe
Halecombe Quarry
Whatley Quarry
MENDIP HILLS
Cannington Park
25Km

The mid-ramp facies, laid-down between fairweather and storm wave-base, are represented by a variety of event-beds including hummocky cross-stratification (Wu 1982; Junghanss *et al.* 1984; Wright 1986; Waters & Lawrence 1987; Faulkner 1988). Such facies are prominent in the central zone (Bristol, Gower, Caldey Island and Angle West) which underwent a moderate degree of subsidence (Figures 1.2 & 1.3). Here, the succession mainly consists of bioclastic and oolitic limestones representing a shallow-marine setting predominantly beneath fairweather wave-base, but occasionally influenced by oolite shoal progradation and apparent sea-level falls (Wright 1986; Waters & Lawrence 1987; Faulkner 1988).

The outer ramp facies, deposited beneath storm wave-base include slightly argillaceous, extensively-bioturbated limestones and Waulsortian mounds. Such facies dominate the southern zone of the eastern Mendip Hills, Cannington Park and Castlemartin. These areas underwent a high degree of subsidence and exhibit an expanded succession (Figures 1.2 & 1.3).

The burial history of the Dinantian succession of Gower has been documented by Dickson (1985). The limestones and dolomites were buried to considerable depths (at least 7Kms) by the end of the Carboniferous and were subsequently uplifted and eroded during the Triassic. Subsequent shallow burial (possibly about 2Km) occurred during the Mesozoic and Tertiary. The Dinantian succession has been considerably affected by the Hercynian Orogeny (Donato 1988; Dunne 1983; Hancock *et al.* 1981; Williams & Chapman 1986; Wilson *et al.* 1988) and to a lesser extent by the Alpine Orogeny.

Figure 1.3. Stratigraphic cross-section across South Wales and SW England. For localities see Figure 1.2.

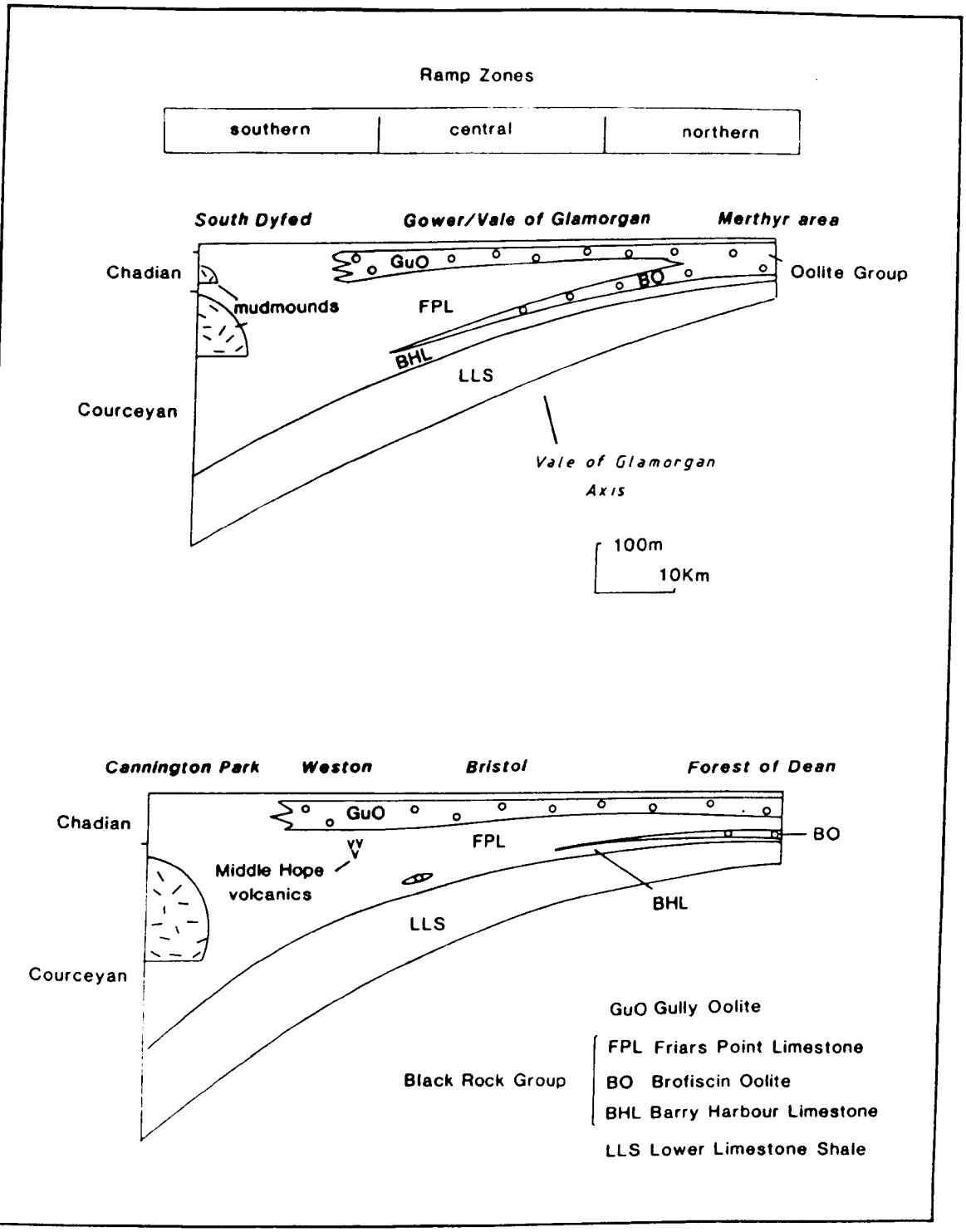
Ramp Zones
southern
central
northern
South Dyfed
Gower/Vale of Glamorgan
Merthyr area
Chadian
GuO
BO
Oolite Group
mudmounds
FPL
BHL
LLS
Courceyan
Vale of Glamorgan
Axis
100m
10Km
Cannington Park
Weston
Bristol
Forest of Dean
Chadian
GuO
FPL
BO
Middle Hope
volcanics
BHL
LLS
Courceyan
GuO Gully Oolite
Black Rock Group
FPL Friars Point Limestone
BO Brofiscin Oolite
BHL Barry Harbour Limestone
LLS Lower Limestone Shale

1.3 Area of study

Outcrop of the Black Rock Limestone Group in the South Wales Coalfield is confined to the South Crop of the Carboniferous Limestone (South Dyfed, Gower, and the Cardiff area) (George *et al.* 1976) (Figure 1.2). Developments in SW England occur within the Forest of Dean area, the Bristol district, and in the Mendip Hills. To the south of the Mendip Hills a borehole has been drilled at (Knap Farm) Cannington Park by the British Geological Survey (Whittaker & Green 1983) (Figure 1.2).

Those sections logged in detail (Appendices A-R) include: West Angle Bay, Castlemartin, Stackpole Quay, and Caldey Island (Dyfed); Rhossili, and Three Cliffs Bay (Gower); Barry Island and a borehole drilled by ARC at Penhow (Vale of Glamorgan); Drybrook Quarry (Forest of Dean); Tytherington Quarry, Cromhall Quarry, Chipping Sodbury Quarry, the Avon Gorge section, Black Rock Quarry, and Middle Hope (Bristol district); Burrington Combe, Halecombe Quarry, and Whatley Quarry (Mendip Hills). These provide a good spread of sections arranged both parallel and normal to depositional strike (Figures 1.2 & 1.3). Information from the Knap Farm borehole is taken from the British Geological Survey memoir by Whittaker & Green (1983).

1.4 Palaeogeographic setting

Reconstructions of the early Carboniferous period, depict two major landmasses Gondwanaland and Euramerica (Laurussia) separated by a seaway known as the Mid-European Ocean (Smith *et al.* 1973; Scotese *et al.* 1979; Turner & Tarling 1975; Rowley *et al.* 1985; Raymond *et al.* 1985; Van der Zwan *et al.* 1985; Leeder 1987). Britain was positioned on the southern border of Euramerica and just to the north of the Mid-European Ocean which was an active subduction zone (Figure 1.4A). Recent palaeomagnetic studies suggest the palaeolatitude of Britain was close to the south of the equator

Figure 1.4.

(A) Palaeogeographic base map for the Lower Carboniferous. The inset shows the position of Britain relative to the equator (Duff 1980). Modified after Leeder 1987.

(B) A geological sketch map of the North European Variscides showing the position and displacement of the proposed Bristol Channel-Bray dextral fault zone. Modified after Holder & Leveridge (1987).

(C) A sketch of the lithospheric section (Scotland to southern France) illustrating the major postulated plate boundaries (Modified after Leeder 1987).

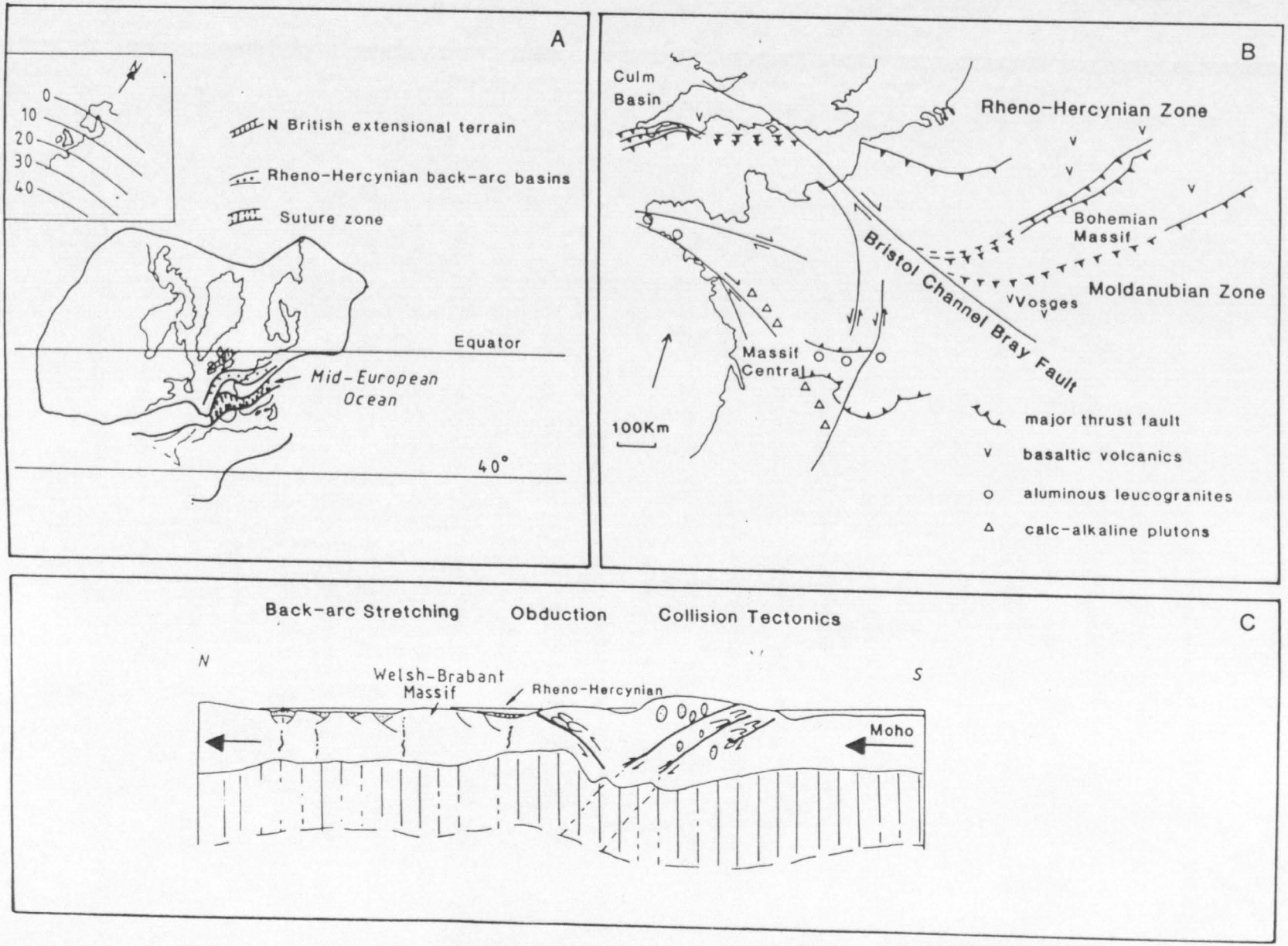
A
0
10
20
30
40
N British extensional terrain
Rheno-Hercynian back-arc basins
Suture zone
Equator
Mid-European Ocean
40°
B
Culm Basin
Rheno-Hercynian Zone
Bohemian Massif
Moldanubian Zone
Vosges
Bristol Channel Bray Fault
Massif Central
100Km
major thrust fault
basaltic volcanics
aluminous leucogranites
calc-alkaline plutons
C
Back-arc Stretching
Obduction
Collision Tectonics
N
S
Welsh-Brabant Massif
Rheno-Hercynian
Moho

(Figure 1.4A) and Britain moved progressively northward, between 15-20°, during the late Devonian to mid-Carboniferous period (Duff 1980; Smith 1981; Van der Zwan *et al.* 1985).

Throughout the Lower Carboniferous northern Britain was subdivided into a series of basins and tectonic highs (platforms) (Leeder 1976; Leeder 1982; Leeder 1987; Bott 1987) (Figures 1.1 & 1.4C). The most southerly emergent area is known as the Welsh-Brabant Massif (Kent 1975; otherwise known as St George's Land, George *et al.* 1976; St George's Platform, Leeder 1976) which formed a low relief 'platform' (Figure 1.1).

The relationship between the southern margin of the carbonate province with the SW England Culm Basin (otherwise known as the Cornubian Basin, George *et al.* 1976) is problematic because the transition is not exposed. In addition, major tectonic displacement has been inferred along the Bristol Channel-Bray Fault (Johnson 1984; Higgs 1986; Holder & Leveridge 1986 & 1987) (Figure 1.4B). Holder & Leveridge (1986) proposed that the Rhenohercynian-Variscides of Belgium, Germany and SW Britain were in tectonic continuity prior to the mid- to late Carboniferous offset (up to 400km) along the Bristol Channel-Bray Fault (Figure 1.4B).

Tectonically, Lower Carboniferous Europe was an active area dominated along its southern margin by platelet collision, as a result of subduction which created a compressional regime (Leeder 1987) (Figure 1.4C). In contrast, an extensional ("stretching") regime dominated NW Europe, causing widespread volcanic activity and subsidence (Leeder 1976; Anderton *et al.* 1979; Leeder 1982; Miller & Grayson 1982; Leeder 1987; Bott 1987; Grayson & Oldham 1987; Gutteridge 1987) (Figure 1.4C). A major phase of subsidence occurred during the late Devonian to early Carboniferous period. This subsidence is postulated as being

related to the progressive closure of the Mid-European Ocean (Leeder 1982 & 1987).

Subsidence was a major cause of the establishment of the Lower Carboniferous block and basins of northern England (Leeder 1976; Leeder 1982; Bott 1987), and the development of a back-arc basin (Reading 1973) along the Rheno-Hercynian zone (Leeder 1987) (Figure 1.4A & C). In which the Culm Basin formed a 'bathyal lull' (Goldring 1962) characteristed by slow, continuous, pelagic sedimentation, interrupted by phases of volcanic activity (Anderton *et al.* 1979; Floyd 1982; Leeder 1982).

Closure of the back-arc sea and platelet collision, occurring during the late Lower Carboniferous period, resulted in the uplift of the northern and southern parts of Europe. This was to set the scene for the subsequent development of the extensive Upper Carboniferous delta plains across central Europe (Leeder 1987). During this period the Culm basin received an input of clastic material, prior to being overridden by the northward migrating Variscan mountain front (Selwood & Thomas 1987). To the north of the mountain front lay the foreland basin of SW Britain (Gayer 1988; Kelling 1988). The onset of Variscan deformation is recorded in South Wales by syn-sedimentary movements on sub-basin structures, influencing subsidence and causing coal seam splits (Gayer 1988). Subsequent thrusting and folding in South Wales and the Bristol-Mendip area, records the progressive northward migration of the Variscan front, telescoping the Palaeozoic sedimentary successions (Dunne 1983; Hancock *et al.* 1981; Williams & Chapman 1986).

1.5 Previous work

The foundations for modern research into the Dinantian succession of SW Britain were laid down at the beginning of this century. Pioneering

palaeontological work by Vaughan (1903 & 1905) established a coral and brachiopod zonal scheme that was shown to be more than of local significance in SW Britain. Correlation of the *Zaphrentis* (Z) and lower part of the *Caninia* (C1) Zone permitted regional sedimentological studies of what is now known as the Black Rock Limestone Group. Notable contributions were from Sullivan (1960 & 1965) and George (1972) who showed that the Z-C1 Zones formed a southerly deepening carbonate 'shelf'. Shallow water, oolite shoal and back-barrier facies dominate the northern attenuated succession e.g. Oolite Group (Figure 1.3). To the south, occur the mainly subtidal facies of bioclastic limestones and the Waulsortian reef mounds at Castlemartin (Dixon 1921) and Cannington Park (Whittaker & Green 1983). Controls upon the southward migration of the nearshore facies belts (e.g. the tongues of southward wedging oolitic limestone) were considered to be strongly influenced by pulses of tectonic subsidence affecting the area to the south of St George's Land (Welsh-Brabant Massif) (George 1972 & 1974).

In contrast, Ramsbottom (1973) proposed that eustatic sea level changes were the major control upon the distribution of the facies in the Dinantian succession. Transgressive phases were represented by the subtidal bioclastic limestones; the regressive phases by oolitic limestones and non-sequences in the more marginal (landward) areas. The first Major Cycle (transgression-regression) in SW Britain includes the Lower Limestone Shale Group and the Black Rock Limestone (Ramsbottom 1973). The regression is represented by a non-sequence (faunal break) at the top of the Black Rock Limestone Group in the Avon Gorge (Mitchell 1971 & 1972; Rhodes *et al.* 1969). Ramsbottom (1984) and Wright (1986), were later to show that sedimentation was not only controlled by eustatic sea level changes but also by differential subsidence across SW Britain (see Geological Setting 1.2). A tectonic "hinge", the Vale of Glamorgan

axis, perhaps a major fault at depth, is known to have centred about the Vale of Glamorgan and eastern Gower (Wright 1984a; Waters 1984; Wright 1986; Waters & Lawrence 1987; Wilson *et al.* 1988) (Figure 1.3). To the south of the axis the Black Rock Limestone and Gully Oolite show a pronounced increase in thickness. Other evidence for tectonic activity is recorded by the Middle Hope volcanics (Weston-super-Mare) (Speedyman 1977; Jeffreys 1979; Jeffreys & Aigner 1982; Whittaker & Green 1983; Faulkner 1989).

Until this study, the only detailed facies studies of the Black Rock Limestone Group have been undertaken upon the superb sections of Gower (Wu 1982; Junghanss *et al.* 1984; Wright 1986; Ramsay 1987), the Cardiff district (Waters & Lawrence 1987) and the borehole drilled at Knap Farm, Cannington Park (Whittaker & Scrivener 1982; Lees & Hennebert 1982). Overall, the outcrop studies have emphasised the storm-generated sedimentary features in the lower part of the Black Rock Limestone (Wu 1982; Junghanss *et al.* 1984; Ramsay 1987). Only a limited amount of work has been undertaken on the upper part of the Black Rock Limestone which consists of a monotonous succession of thickly-bedded, slightly argillaceous, bioclastic limestones recording sedimentation in a below storm wave-base environment (Wright 1986; Ramsay 1987; Waters & Lawrence 1987). This interpretation confirms a detailed microfacies analysis of the borehole at Cannington by Lees & Hennebert (1982). The latter authors showed the mudmound complex cored at Knap Farm to be comparable to the classic Waulsortian mounds of Belgium, indicative of a deepwater, below storm wave-base environment.

Two main types of dolomite have been identified in the Black Rock Limestone Group. Volumetrically the reddish-brown, pervasive stratal dolomites are the most significant. They form the regionally extensive

Black Rock Dolomite which immediately underlies the Gully Oolite (Whittaker & Green 1983; Wright 1986; Waters & Lawrence 1987; Hird *et al.* 1987). In contrast, pale white Waulsortian reef dolomites (Dixon 1921; Lees & Hennebert 1982) have a more limited distribution since they are restricted to the southern ramp zone (Figure 1.3).

The variability of the trace element chemistry of the Black Rock Dolomite was demonstrated by Bhatt (1973 & 1976). A subsequent, more comprehensive, geochemical study using stable isotopes by Hird *et al.* (1987) concluded dolomitization proceeded in a shallow-burial mixing zone environment. Only a limited amount of petrographic work has been undertaken upon the Waulsortian reef dolomites (Dixon 1921; Lees & Hennebert 1982).

Chapter 2 - Stratigraphy

2.1 Dinantian stratigraphy

2.2 Lithostratigraphy

2.3 Biostratigraphy

2.3.1 Macrofauna

2.3.2 Microfauna

2.1 Dinantian stratigraphy

Dinantian stratigraphy of the British Isles is based upon the six regional stages (chronostratigraphic divisions) of George *et al.* (1976) (Figures 2.1 & 2.2). It is still necessary, however, to identify the Tournaisain - Viséan subsystems which are still widely used abroad and represent the only international standard of subdividing the Dinantian (Varker & Sevastopulo 1985). Approximately, but not exactly, the Courceyan (the lowest stage of George *et al.* 1976) is equivalent to the Tournaisian (Mitchell *et al.* 1982; Mitchell *et al.* 1986; Waters & Lawrence 1987) (Figure 2.3). The Black Rock Group is mid-Courceyan (mid-Tournaisian) to early Chadian (Viséan) in age (Figure 2.3) and includes: the Black Rock Limestone, the Blucks Pool Limestone, the Waulsortian mounds at Castlemartin and Cannington Park as well as the overlying Linney Head Beds and lower part of the Cynwir Cherty Limestone (Figure 2.4).

The approach by George *et al.* (1976) is based on precisely defined stratotype stages, each delineated at their base by the incoming of a diagnostic fauna (George *et al.* 1976). The stratotype stages replaced both the faunal zones of Vaughan (1905) and the sedimentary cycles of Ramsbottom (1973 & 1979). Vaughan's coral and brachiopod zones were finally abandoned after numerous stages of emendation and a plethora of inconsistencies had arisen from their use (for a summary see George *et al.* 1976, Table I).

Ramsbottom (1973) interpreted the Dinantian succession of Britain as comprising of six major transgressive-regressive cycles, each correlatable within a given area using his idealised facies model (Figures 2.5 & 2.6). Correlations between regions were based on the incoming of distinctive faunas, at the base of each Major Cycle, which were thought to have been synchronous and in response to eustatic rises in sea level. This approach was extensively critised, in particular by

Figure 2.1. The Dinantian stratigraphy of Bristol and the Mendips. (George *et al.* 1976).

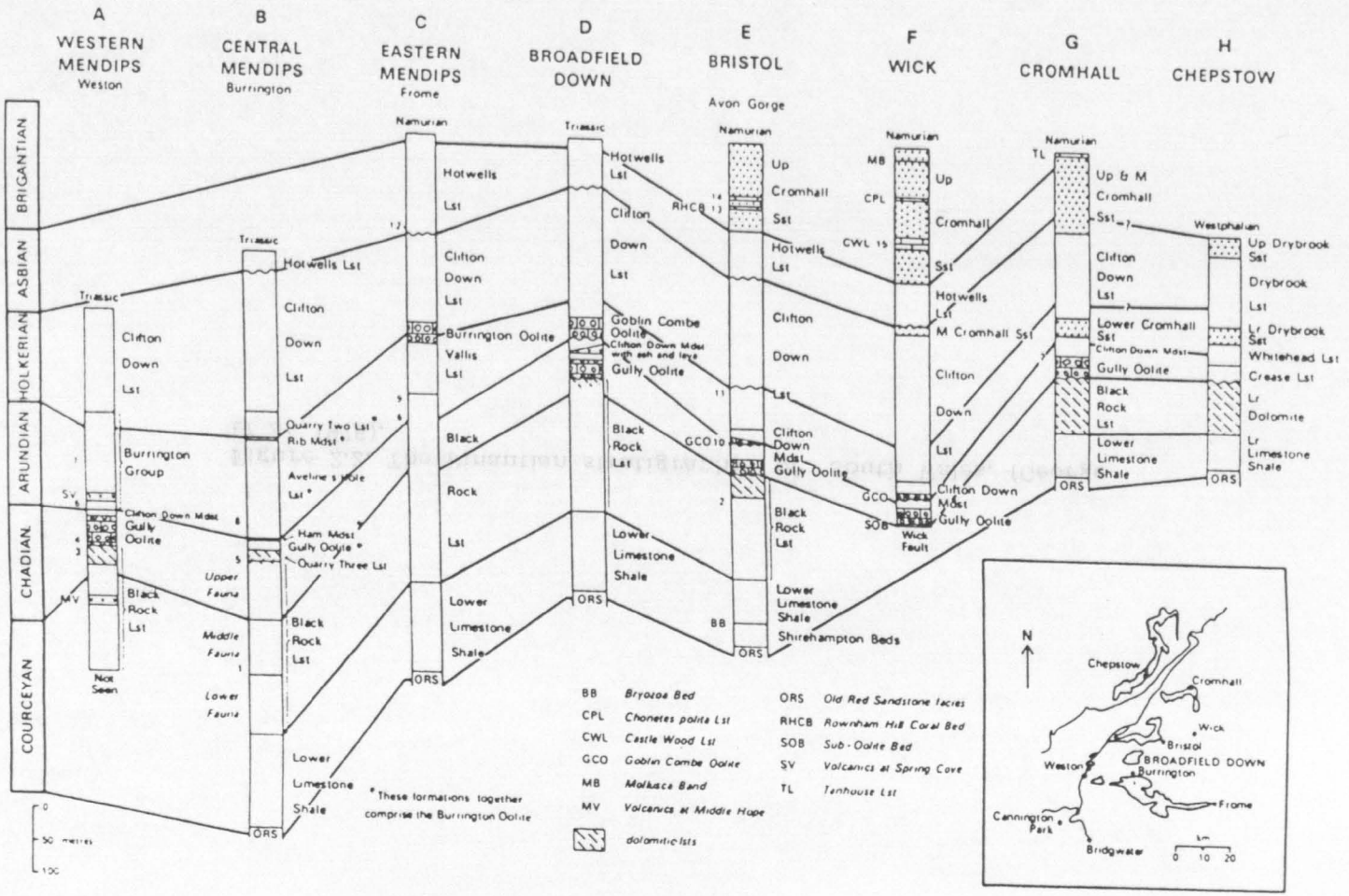
A
WESTERN MENDIPS
Weston
B
CENTRAL MENDIPS
Burrington
C
EASTERN MENDIPS
Frome
D
BROADFIELD DOWN
E
BRISTOL
Avon Gorge
F
WICK
G
CROMHALL
H
CHEPSTOW
BRIGANTIAN
ASBIAN
HOLKERIAN
ARUNDIAN
CHADIAN
COURCEYAN
Namurian
Triassic
Westphalian
Hotwells Lst
Clifton Down Lst
Burrington Group
Clifton Down Mdst
Gully Oolite
Black Rock Lst
Not Seen
Quarry Two Lst *
Rib Mdst *
Avelines Hole Lst *
Ham Mdst
Gully Oolite *
Quarry Three Lst
Upper Fauna
Middle Fauna
Lower Fauna
Lower Limestone Shale
ORS
Burrington Oolite
Vallis Lst
Black Rock Lst
Rock Lst
Lower Limestone Shale
Goblin Combe Oolite
Clifton Down Mdst with ash and lava
Gully Oolite
Lower Limestone Shale
Up Cromhall Sst
Clifton Down Lst
Black Rock Lst
Clifton Down Mdst
Gully Oolite
Lower Limestone Shale
Shirehampton Beds
BB
RHCB
GCO
MB
CPL
CWL
SOB
Wick Fault
M Cromhall Sst
Clifton Down Mdst & Gully Oolite
TL
Up & M Cromhall Sst
Lower Cromhall Sst
Gully Oolite
Black Rock Lst
Lower Limestone Shale
Up Drybrook Sst
Drybrook Lst
Lr Drybrook Sst
Whitehead Lst
Crease Lst
Lr Dolomite
Lr Limestone Shale
SV
MV
* These formations together comprise the Burrington Oolite
BB Bryozoa Bed
CPL Chonetes polita Lst
CWL Castle Wood Lst
GCO Goblin Combe Oolite
MB Malluscs Band
MV Volcanics at Middle Hope
dolomitic lsts
ORS Old Red Sandstone facies
RHCB Rownham Hill Coral Bed
SOB Sub-Oolite Bed
SV Volcanics at Spring Cove
TL Tanhouse Lst
0
50 metres
100
N
Chepstow
Cromhall
Wick
Bristol
Weston
BROADFIELD DOWN
Burrington
Frome
Cannington Park
Bridgwater
km
0 10 20

Figure 2.2. The Dinantian stratigraphy of South Wales. (George *et al.* 1976).

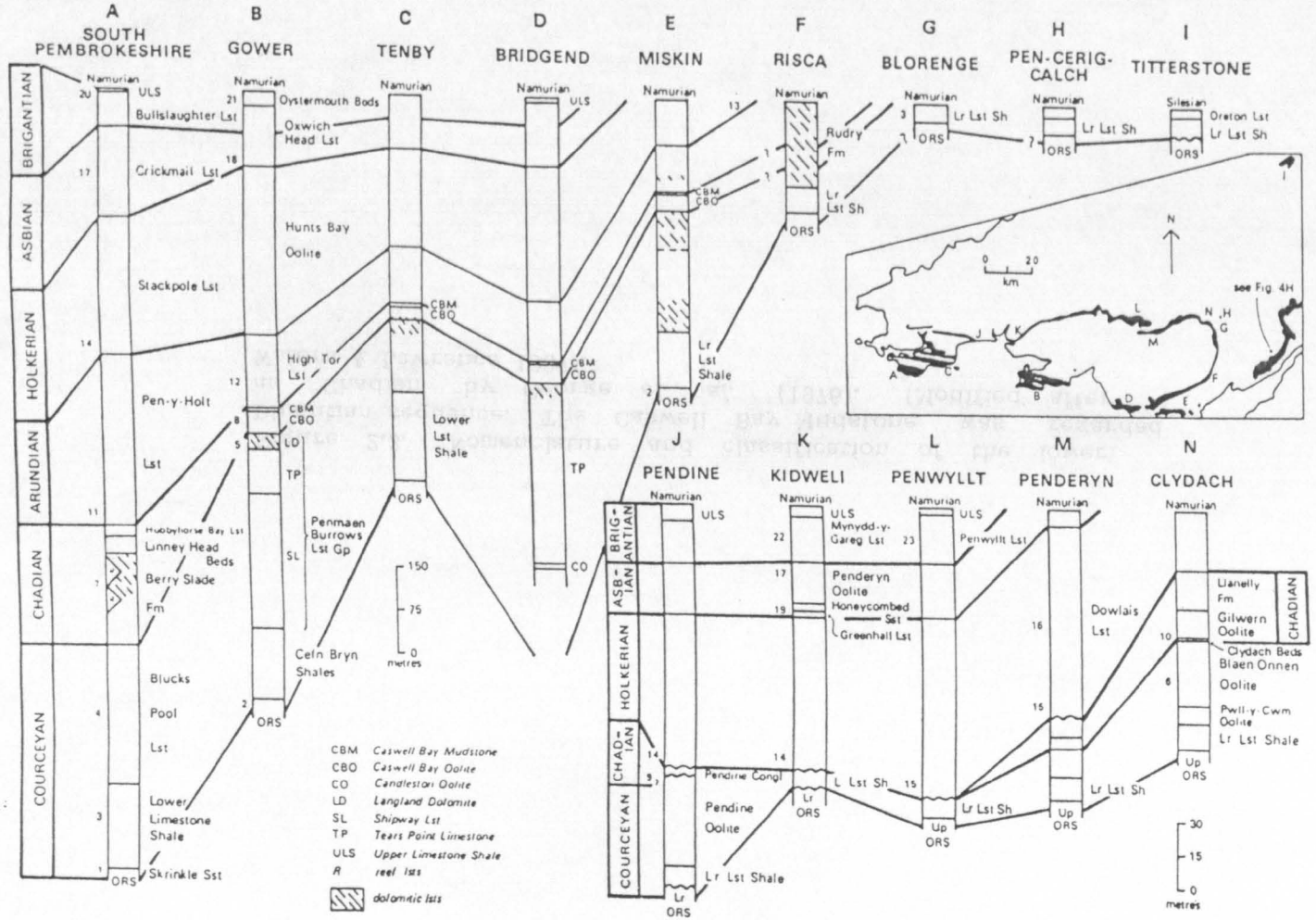
A
SOUTH PEMBROKESHIRE
B
GOWER
C
TENBY
D
BRIDGEND
E
MISKIN
F
RISCA
G
BLORENGE
H
PEN-CERIG-CALCH
I
TITTERSTONE
BRIGANTIAN
ASBIAN
HOLKERIAN
ARUNDIAN
CHADIAN
COURCEYAN
Namurian
Silesian
ULS
Bullslaughter Lst
Crickmail Lst
Stackpole Lst
Pen-y-Holt Lst
Hubbyhorse Bay Lst
Linney Head Beds
Berry Slade Fm
Blucks Pool Lst
Lower Limestone Shale
Skrinkle Sst
ORS
Oystermouth Beds
Oxwich Head Lst
Hunts Bay Oolite
High Tor Lst
CBM
CBO
LD
TP
SL
Penmaen Burrows Lst Gp
Ceiln Bryn Shales
Lower Lst Shale
CO
Rudry Fm
Lr Lst Sh
Lr Lst Shale
Lr Lst Sh
Oreton Lst
Lr Lst Sh
see Fig. 4H
0 20
km
N
J
K
L
M
N
PENDINE
KIDWELI
PENWYLLT
PENDERYN
CLYDACH
ULS Mynydd-y-Gareg Lst
Penderyn Oolite
Honeycombed Sst
Greenhall Lst
Penwylit Lst
Dowlais Lst
Llanelly Fm
Gilwern Oolite
Clydach Beds
Blaen Onnen Oolite
Pwll-y-Cwm Oolite
Lr Lst Shale
Pendine Congl
Pendine Oolite
L Lst Sh
Lr Lst Sh
Up ORS
Lr ORS
150
75
0
metres
30
15
0
CBM Caswell Bay Mudstone
CBO Caswell Bay Oolite
CO Candleston Oolite
LD Langland Dolomite
SL Shipway Lst
TP Tears Point Limestone
ULS Upper Limestone Shale
R reef lsts
dolomitic lsts

Figure 2.3. Nomenclature and classification of the lower Dinantian sequence. The Caswell Bay Mudstone was regarded as Chadian by George *et al.* (1976). (Modified after Waters & Lawrence 1987).

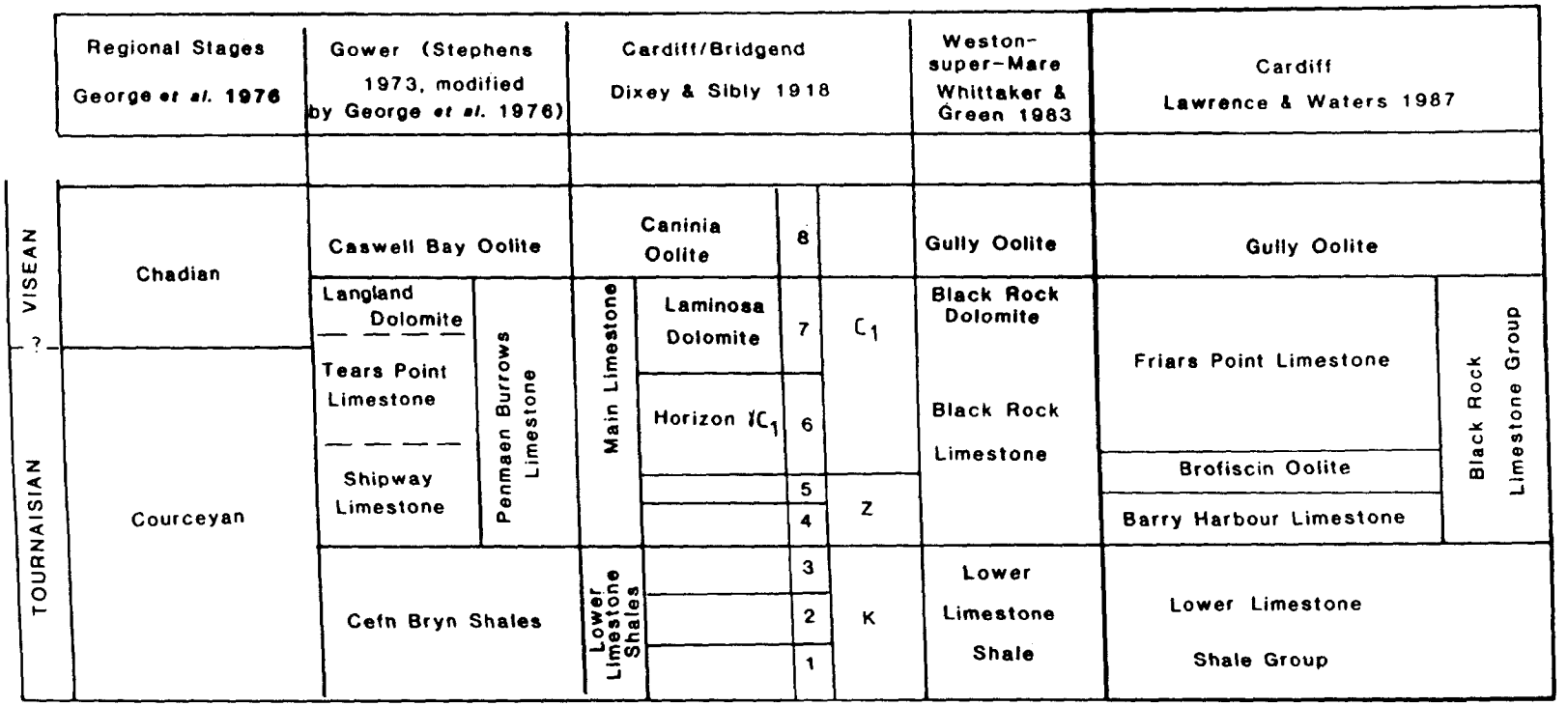
Regional Stages
George et al. 1976
Gower (Stephens 1973, modified by George et al. 1976)
Cardiff/Bridgend
Dixey & Sibly 1918
Weston-super-Mare
Whittaker & Green 1983
Cardiff
Lawrence & Waters 1987
VISEAN
?
TOURNAISIAN
Chadian
Courceyan
Caswell Bay Oolite
Caninia Oolite
8
Gully Oolite
Gully Oolite
Langland Dolomite
Tears Point Limestone
Shipway Limestone
Penmaen Burrows Limestone
Main Limestone
Laminosa Dolomite
7
Horizon IC1
6
5
4
C1
Z
Black Rock Dolomite
Black Rock Limestone
Friars Point Limestone
Brofiscin Oolite
Barry Harbour Limestone
Black Rock Limestone Group
Cefn Bryn Shales
Lower Limestone Shales
3
2
1
K
Lower Limestone Shale
Lower Limestone Shale Group

Figure 2.4. Correlation of some pre-Holkerian sections across SW Britain. (Mitchell *et al.* 1982).

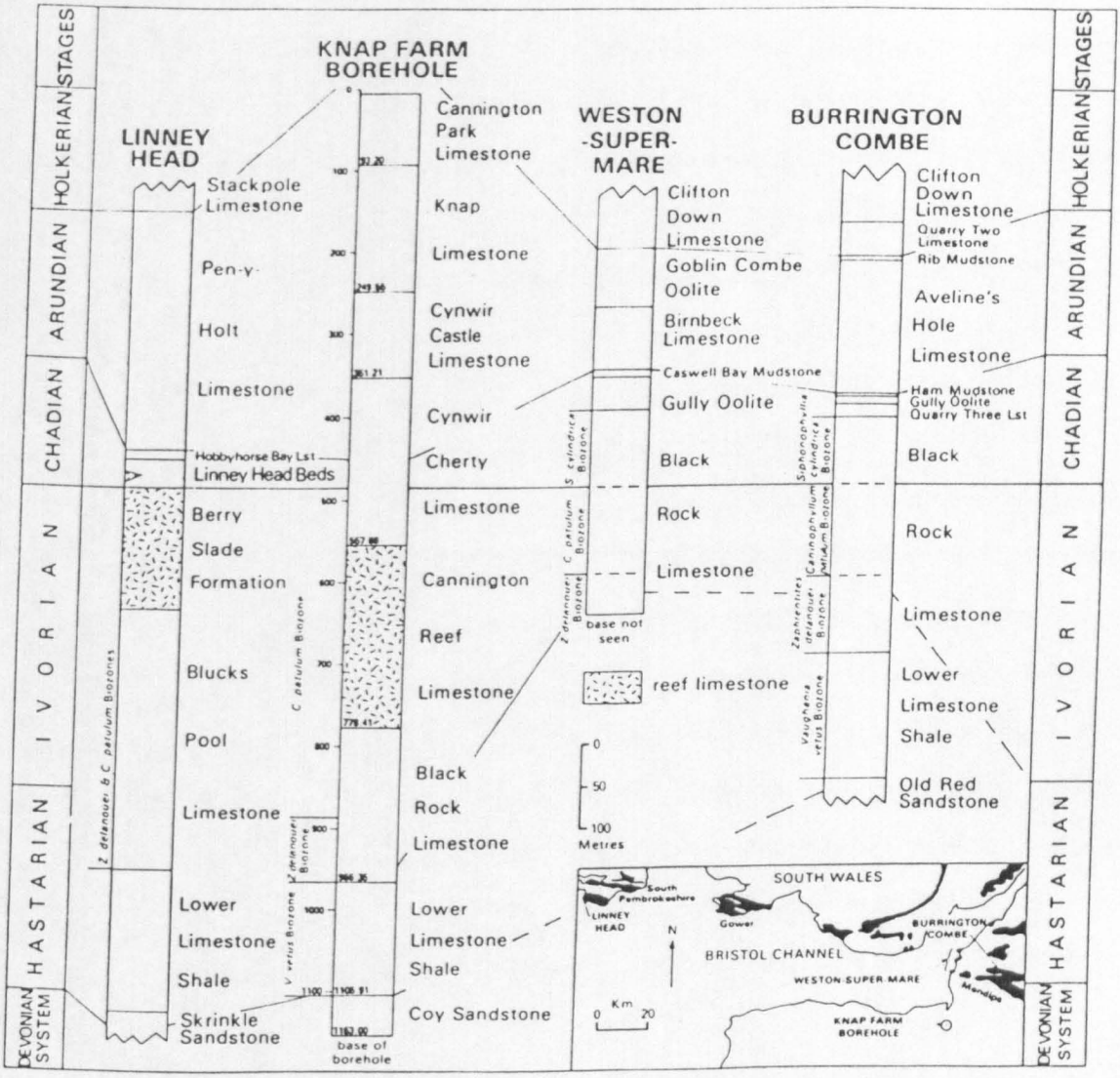
KNAP FARM BOREHOLE
LINNEY HEAD
WESTON -SUPER- MARE
BURRINGTON COMBE
DEVONIAN SYSTEM
HASTARIAN
IVORIAN
CHADIAN
ARUNDIAN
HOLKERIAN STAGES
Stackpole Limestone
Pen-y-
Holt
Limestone
Hobbyhorse Bay Lst
Linney Head Beds
Berry
Slade
Formation
Blucks
Pool
Limestone
Lower
Limestone
Shale
Skrinkle Sandstone
Cannington Park Limestone
Knap
Limestone
Cynwir
Castle
Limestone
Cynwir
Cherty
Limestone
Cannington
Reef
Limestone
Black
Rock
Limestone
Lower
Limestone
Shale
Coy Sandstone
base of borehole
Clifton Down Limestone
Goblin Combe Oolite
Birnbeck Limestone
Caswell Bay Mudstone
Gully Oolite
Black
Rock
Limestone
base not seen
reef limestone
Clifton Down Limestone
Quarry Two Limestone
Rib Mudstone
Aveline's Hole Limestone
Ham Mudstone
Gully Oolite
Quarry Three Lst
Black
Rock
Limestone
Lower Limestone Shale
Old Red Sandstone
Metres
SOUTH WALES
South Pembrokeshire
LINNEY HEAD
Gower
BURRINGTON COMBE
BRISTOL CHANNEL
WESTON-SUPER-MARE
Mendips
KNAP FARM BOREHOLE
Km

George (1978) who noted a number of major defects. It neglected the possibility that the facies may be strongly influenced by tectonic controls as well as eustacy.

2.2 Lithostratigraphy

The base of the Black Rock Limestone Group is transitional with the underlying Lower Limestone Shale Group. The boundary is taken at that horizon where the carbonate content becomes prevalent which is usually quite distinct. Over the northern and central part of the study area the Black Rock Limestone is immediately overlain by the Gully Oolite (Figure 2.1 & 2.2). In the eastern Mendip Hills, at Cannington Park and Castlemartin, the Black Rock Limestone passes upward into the overlying succession of crinoidal limestones (Figures 2.1 & 2.4).

A summary of major developments in the lower Dinantian stratigraphy of SW Britain since Dixey & Sibly (1918) is shown in Figure 2.3. The most recent scheme for subdividing the Black Rock Group has been proposed by Waters & Lawrence (1987) who recognized three lithostratigraphic formations in the Cardiff district: the Barry Harbour Limestone, the Brofiscin Oolite and the Friars Point Limestone which are readily identifiable within the study area and form mappable units. They replace the faunal assemblage zones of the Shipway Limestone Formation and Tears Point Limestone Formation defined on Gower by Dixon & Vaughan 1911 (Figure 2.3)

The Barry Harbour Limestone forms the lower part of the Black Rock Limestone and reaches a maximum thickness of ca. 120m at Castlemartin. It is bounded by the overlying Brofiscin Oolite (up to 20m thick) which outcrops in the northern and central zones (Figure 1.3). The Friars Point Limestone Formation forms the upper part of the Black Rock Limestone and includes the Waulsortian mounds at Castlemartin and Cannington Park.

Figure 2.5. Depth-related Dinantian facies sequence recognized by Ramsbottom (1973).

Figure 2.6. Correlation of Ramsbottom's cycles with Vaughan's Zones. (After Ramsbottom 1973 & 1979).

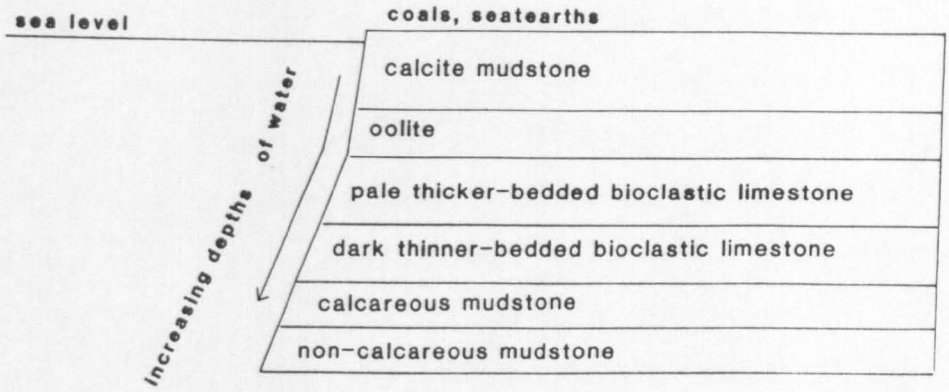

Stages George *et al.* 1976	Succession (Bristol)	Zones Dixon & Vaughan 1912	Major cycle Ramsbottom 1973	Mesothemic cycles Ramsbottom 1979
Chadian	Gully Oolite Sub-oolite Bed	C	2	D2b D2a
Courceyan	Black Rock Group Lower Limestone Shale Group	horizon γ Z K	1	D1c D1b D1a

It also contains the Black Rock Dolomite (otherwise known as the Langland Dolomite or *Laminosa Dolomite*) which occurs immediately beneath the Gully Oolite (Figure 2.3).

The advantage of the lithostratigraphic formations of Waters & Lawrence (1987) is that they are readily identifiable even within the dolomitized sucessions that outcrop in the northern part of the study area e.g Drybrook Quarry (Appendix I). Difficulties arise, however, in distinguishing the boundary between the Barry Harbour Limestone and Friars Point Limestone in those sections where the Brofiscin Oolite is absent. This problem is resolved at Barry Island by the use of a cross-bedded bioclastic unit (Yorke Rock Bed), that occurs at a similar stratigraphic level to the Brofiscin Oolite (Waters & Lawrence 1987). A similar approach has been adopted at Rhossili (Appendix E) on the Gower. In the southern zone and at Chipping Sodbury (Appendix L), the boundary is arbitarily placed in the transition between the thin-bedded bioclastic limestones characteristic of the Barry Harbour Limestone and the more thickly-bedded, bioturbated limestones characteristic of the Friars Point Limestone (e.g. Castlemartin, Appendix B).

2.3 Biostratigraphy

Correlation within the Black Rock Limestone Group is mainly achieved using corals and conodonts (Figure 2.7). The former are particularly important, for inter-regional correlations with the rest of Britain, Belgium and Ireland. Collections of corals and conodonts have mainly been taken from the thickest developments of the Black Rock Limestone Group (Butler 1973; Mitchell *et al.* 1982; Mitchell *et al.* 1986; Waters & Lawrence 1987). Systematic work on the macrofaunas in the thinner successions, towards the north, is extremely difficult owing to the replacement of the corals by dolomite. Unfortunately, there have been

Figure 2.7. The relationship between the conflated conodont zones of Varker & Sevastopulo (1985), the coral assemblage biozones of Ramsbottom & Mitchell (1980) and the Black Rock Formations of Waters & Lawrence (1987). (Modified after Waters & Lawrence 1987).

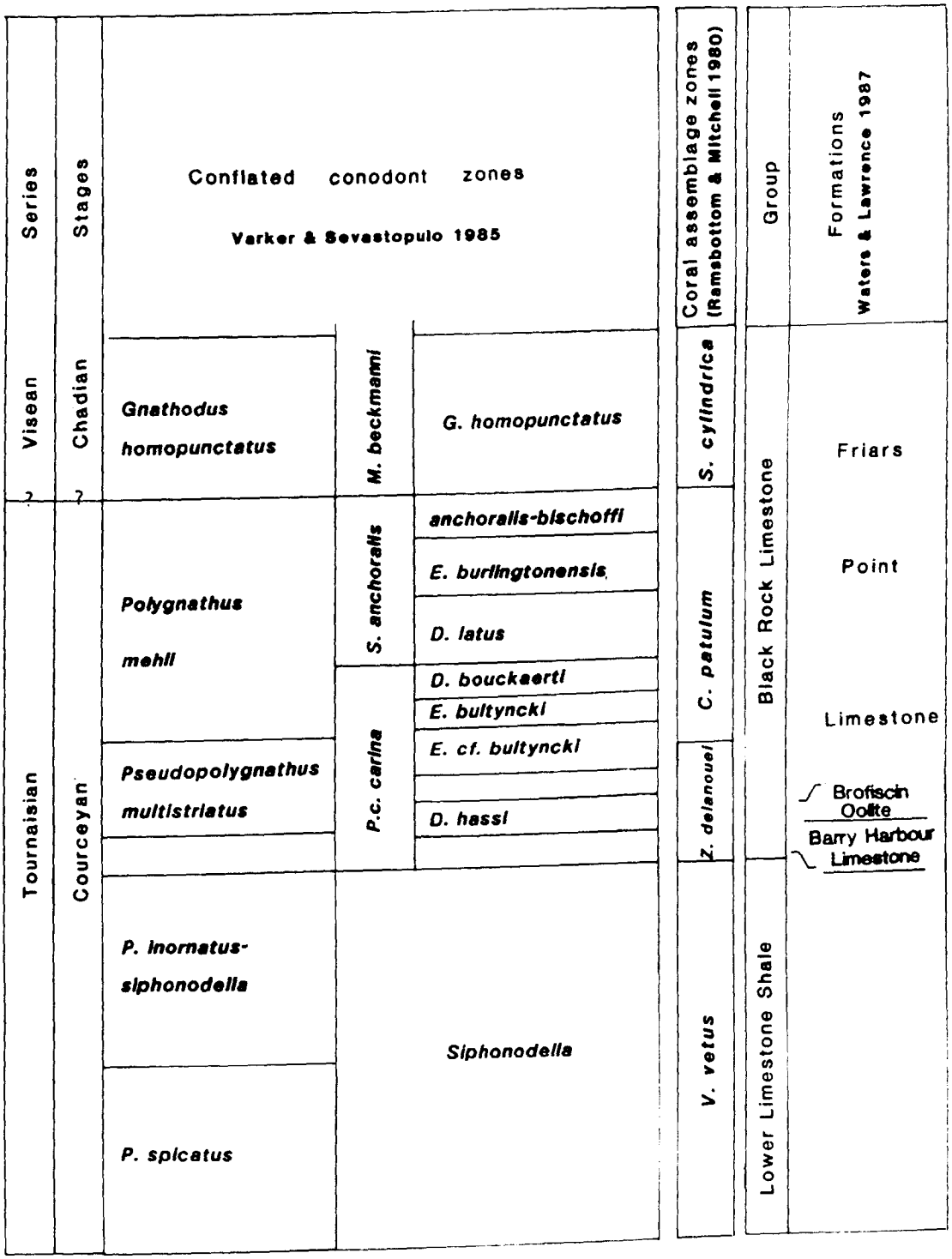
Series
Stages
Conflated conodont zones
Varker & Sevastopulo 1985
Coral assemblage zones (Ramsbottom & Mitchell 1980)
Group
Formations
Waters & Lawrence 1987
Visean
Chadian
Tournaisian
Courceyan
Gnathodus homopunctatus
M. beckmanni
G. homopunctatus
S. cylindrica
Friars
Polygnathus mehli
S. anchoralis
anchoralis-bischoffi
E. burlingtonensis
D. latus
C. patulum
Point
Limestone
Pseudopolygnathus multistriatus
P.c. carina
D. bouckaerti
E. bultyncki
E. cf. bultyncki
Z. delanouei
Brofiscin Oolite
Barry Harbour Limestone
D. hassi
Black Rock Limestone
P. inornatus-siphonodella
Siphonodella
V. vetus
P. spicatus
Lower Limestone Shale

few conodont collections taken from the northern attenuated sequences (e.g. Rhodes *et al.* 1969). Only limited amounts of biostratigraphic work have been undertaken using foraminifera, mainly in connection with the determination of the position of the Tournaisian-Viséan boundary (Austin *et al.* 1973; Mitchell *et al.* 1986).

2.3.1 Macrofauna

Three distinctive coral faunas (Lower, Middle & Upper Fauna) were identified at Burrington Combe by Mitchell & Green (1965). These are now known as the *Zaphrentites delanouei*, *Caninophyllum patulum* and *Siphonophyllia cylindrica* Assemblage Biozones respectively (Mitchell 1980; Ramsbottom & Mitchell 1980). These coral faunas have been used to correlate across the carbonate province of SW Britain (Mitchell 1980; Ramsbottom & Mitchell 1980; Mitchell *et al.* 1982; Mitchell *et al.* 1986) (Figures 2.1 & 2.4). A recent study of the corals, conodonts and foraminifera at the Tears Point section (Rhossili) has shown that the base of the *S. cylindrica* (Upper Fauna) Assemblage Biozone there is approximately coincidental with the Tournaisian-Viséan boundary and in close proximity to the Courceyan-Chadian boundary (Mitchell *et al.* 1986).

The base of the *Z. delanouei* Biozone occurs in close proximity to the contact between the Lower Limestone Shale and the overlying Black Rock Limestone (Mitchell 1980). The *Z. delanouei* Biozone includes the Barry Harbour Limestone, the Brofiscin Oolite and the lower part of the Friars Point Limestone (Figure 2.7). The upper part of the Friars Point Limestone contains the *C. patulum* and the overlying *S. cylindrica* Assemblage Biozones (Figure 2.7).

The *Z. delanouei* Biozone has an almost consistent thickness throughout the region (ca. 100m). While the *C. patulum*

(up to 400m thick) and *S. cylindrica* (up to 50m thick) Biozones show great thickness variations and a pronounced northward attenuation. At Bristol (Avon Gorge & Portway Tunnel) the *S. cylindrica* Biozone is conspicuously absent and the *C. patulum* Biozone is considerably reduced in thickness in comparison to the succession at Burrington Combe (Mitchell 1971, 1972 & 1980).

2.3.2 Microfauna

The conodont biostratigraphical 'framework' used is based on the conflated zonation proposed by Varker & Sevastopulo (1985). This recent synthesis relates the multitude of different zonations which emerged during the late sixties and seventies, to form a zonal scheme of regional significance (Figure 2.7). It includes a synthesis of the 14 conodont zones identified by Rhodes *et al.* (1969) from the Avon Gorge section.

The base of the Black Rock Limestone occurs within the interzone between the *Siphonodella* Zone and the overlying *Pseudopolygnathus multistriatus* Zone. Other zones occurring within the Black Rock Group include the *Polygnathus mehli* Zone and the *Gnathodus homopunctatus* Zone (Figure 2.7). The base of the *Gnathodus homopunctatus* Zone denotes the base of the Viséan and occurs in close proximity to the base of the Chadian Stage (Mitchell *et al.* 1982; Mitchell *et al.* 1986; Waters & Lawrence 1987).

The Barry Harbour Limestone occurs within the *Siphonodella-Ps. multistriatus* interzone (Waters & Lawrence 1987; Mitchell *et al.* 1982) (Figure 2.7). At Brofiscin Quarry, the base of the *Ps. multistriatus* Zone occurs within the Brofiscin Oolite (Waters & Lawrence 1987). While at Barry, it occurs at the base of the Yorke Rock Bed (Waters & Lawrence

1987). The Friars Point Limestone includes the upper part of the *Ps. multistriatus* Zone, *P. mehli* Zone and the *Gnathodus homopunctatus* Zone (Figure 2.7).

Complete faunal successions have been documented in the thicker sequences in the Mendip Hills (Butler 1972 & 1973), at Cannington Park (Mitchell *et al.* 1982), Weston-super-Mare (Whittaker & Green 1983), Tears Point (Mitchell *et al.* 1986), and Barry Island (Waters & Lawrence 1987). Notably absent in the attentuated succession of the Avon Gorge is the conodont *Scaliognathus anchoralis* (Rhodes *et al.* 1969). Rhodes *et al.* (1969) proposed that the absence of *S. anchoralis* could either be due to factors influencing its distribution (e.g. facies control) or as a result of a non-sequence at the top of the Black Rock Group. Subsequently, *S. anchoralis* has been recorded in a laterally equivalent section at Llanstrisant (Wales) by Waters & Lawrence (1987).

Chapter 3 - Storm sedimentation on an early Carboniferous ramp: the Barry Harbour Limestone & the Brofiscin Oolite

3.1 Introduction

The carbonate ramp model is increasingly being applied to ancient carbonate sequences. A typical regressive sequence consists of thickening- and coarsening-upward storm layers, overlain by a sandy unit representative of deposition in a nearshore, shallow water environment (Ahr 1973; Brett 1983; Aigner 1984 & 1985; Markello & Read 1981; Wu 1982; Read 1985; Handford 1986; Wright 1986; and Chatellier 1988). There have, however, been few regional (basin) studies of the nature of regressive carbonate ramp sequences. Notable exceptions include the work on the Muschelkalk of Germany by Aigner (1984 & 1985), the Lower Carboniferous, Banff Formation of Canada by Chatellier (1988) and the Upper Cambrian of Southwest Virginia by Markello & Read (1981).

The aim of this chapter is to describe and interpret the carbonate facies of the lower part of the Black Rock Limestone Group (the Barry Harbour Limestone Formation and the Brofiscin Oolite Formation) of SW Britain. This regional study includes the detailed facies analysis undertaken at Three Cliffs Bay (Gower) by Faulkner (1988). Here, the Barry Harbour Limestone forms a shallow marine, predominantly subtidal, shallowing-upward sequence which is capped by the subaerially exposed Brofiscin Oolite (Hird 1986). Subsequent to an assessment of the spatial and temporal distribution of the lithofacies, a general model is offered for the environment of deposition.

3.2 Sedimentary facies

Six lithofacies have been identified in the Barry Harbour Limestone, the Brofiscin Oolite and its probable cross-bedded bioclastic limestone equivalents e.g. Yorke Rock Bed (Waters & Lawrence 1987). These are similar to the lithofacies described by Faulkner (1988) from Three Cliffs Bay. An additional, minor lithofacies (7) has been recognized immediately

beneath the Friars Point Limestone at Drybrook Quarry (Appendix I). The lithofacies are characterised using the following sedimentary features: grain-size variation, sedimentary structures, trace fossil assemblages and bedding thickness.

3.2.1 *Lithofacies 1:* Planar laminated facies containing minor scours filled with shelly lags

Lithofacies 1 is dominated by planar laminated packstones (Figures 3.1A & 3.2A) which are commonly moderately to extensively dolomitized. Locally, the planar laminae are cut by minor scours (10-15cm wide and 1-2cm deep) filled with a basal lag of disarticulated brachiopod valves and coarse crinoidal debris (2-5mm in diameter) (Figure 3.2A). Separating the metre thick accumulations of planar lamination are extensively bioturbated horizons (<5cm thick), and rare rippled horizons (usually 1-6cm thick). Internally the ripples are similar to the bi-directional bundled cross-lamination described from the Lower Carboniferous of Ireland by de Raaf *et al.* (1977). Immediately overlying the rippled horizons there are bioturbated structureless micrite layers (<1cm thick).

The planar laminae are 1-3mm thick and show no obvious sign of bioturbation or grading. Crinoid fragments (0.2 to 2mm in diameter) and convex-upward orientated brachiopod valves make up the bulk of the rock, and in thin section silt sized quartz grains and crystals of framboidal pyrite (50 microns in diameter) occur ubiquitously. The interstices are filled with clay minerals and a microsparite cement.

Those brachiopods which are particularly common in Lithofacies 1 include *Spirifer cf. tornacensis* and *Chonetes cf. hardrensis*. The latter dominates the section on Caldey Island. Complete crinoid calyxes are rare. Orientation of crinoid calyxes from a bedding plane surface at Castlemartin reveal a poorly defined orientation towards the NE and the W

Figure 3.1. Schematic summary diagrams showing the interpretation of the sedimentary features, the trace fossil assemblages and the body fossil contents found within Lithofacies 1,2 & 3; A, B, and C, respectively.

A Planar laminated facies containing minor scours filled with shelly lags (Lithofacies 1)

Sedimentary Structures	Lithology	Trace Fossils	Body Fossils	Interpretation
Planar lamination minor scours	Packstone	Rare horizontal burrows	Crinoids & convex- upward brachiopod valves	Low energy suspension deposition from period currents

B Ungraded thin sedimentary couplets (Lithofacies 2)

Sedimentary Structures	Lithology	Trace Fossils	Body Fossils	Interpretation
Rare horizontal planar lamination	Wackestone	Zoophycos Planolites & horizontal burrows	Orthids spirifers & strophomenids	Waning current flow & suspension deposition
Sharp base	Packstone	Rare	Parautochthonous convex-upward brachiopod valves	Suspension deposition from periodic low energy currents

C Graded beds containing planar stratification &/or HCS (Lithofacies 3)

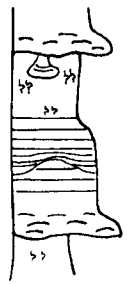

Sedimentary Structures	Lithology	Trace Fossils	Body Fossils	Interpretation
	Micritic lst	Zoophycos Chondrites & Planolites		Waning current flow & suspension deposit
HCS &/or planar lamination	Packstone	Vertical burrows & rare Rhizocorallium	Fragmented bioclasts	Storm generated deposit
Erosive base	Packstone		Shell lag	

Figure 3.2

(A) Lithofacies 1: planar stratified packstone, exhibiting minor scour (S), and chert nodules. (Caldey Island).

(B) Lithofacies 2: stacked ungraded sedimentary couplets. Sharp based bioclastic packstone layer (P) is overlain by wackestone layer (W). (Three Cliffs Bay).

(C) Arcuate trace fossil, *Zoophycos* (Z), extensively identifed in a wackestone layer which forms the upper part of an ungraded sedimentary couplet (Lithofacies 2) (see Figure 3.2B). (Three Cliffs Bay).

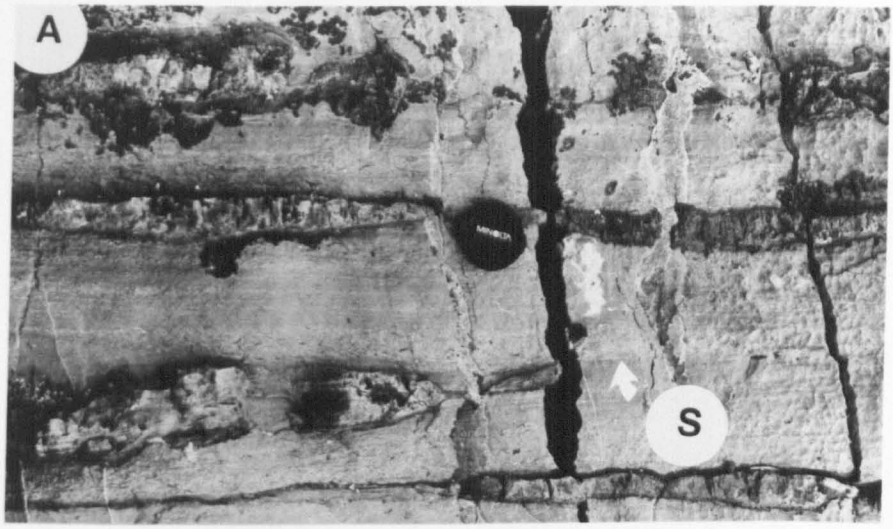
A
S

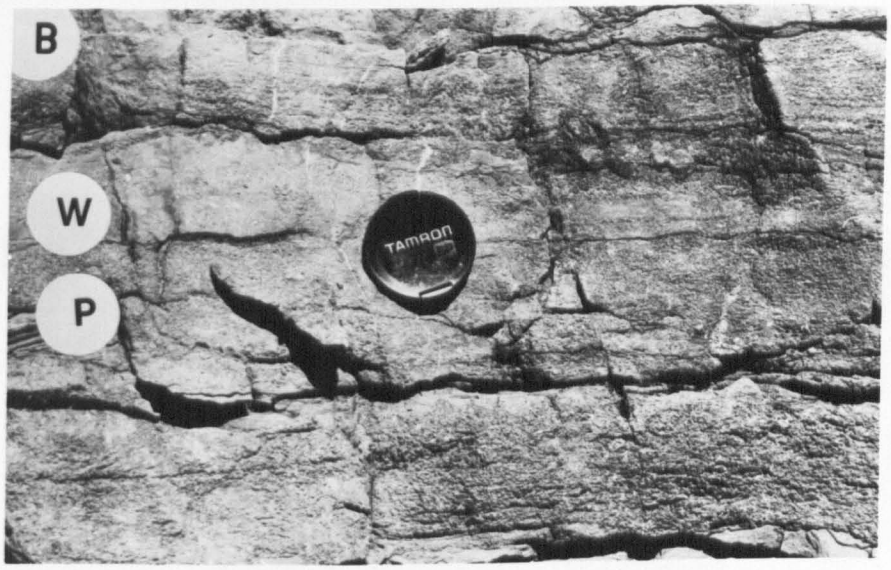
B
W
P
TAMRON

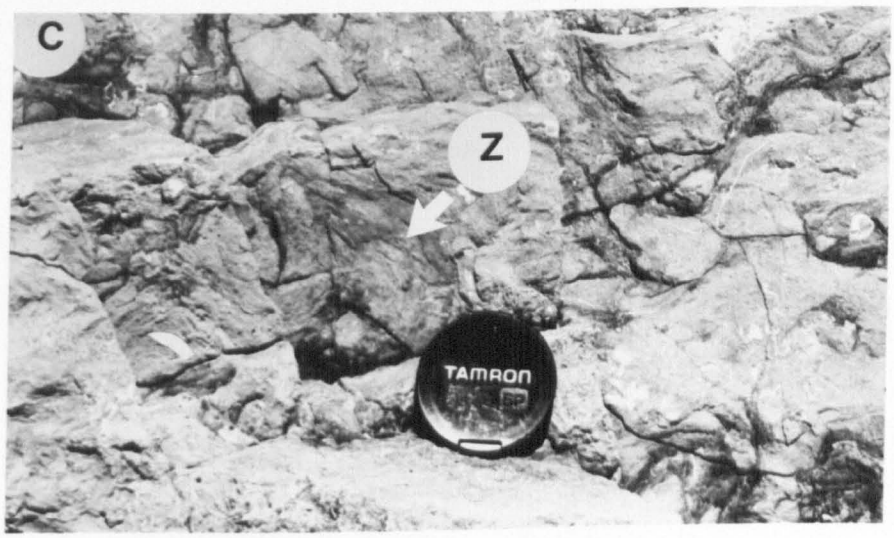
C
Z
TAMRON

(Figure 3.3, denoted by I).

Interpretation: The fragmented brachiopod and crinoid allochems were probably transported and disarticulated by marine currents which at times were of sufficient energy to cause localised scouring prior to deposition. The absence of primary current lineation and poor sorting in the laminites suggests deposition from suspension and not from upper flow regime conditions. The internal structure of the wave ripples is similar to the wave generated structures described by de Raaf *et al.* (1977). However, their minor occurrence in Lithofacies 1 suggests that they represent rare sedimentary events. The distinct contact between the ripples and the overlying micrite layer indicates a change in the hydrological regime from the higher energy oscillatory currents to low energy suspension deposition. The formation of the wave ripples is most likely to be due to rare (storm?) events, allowing oscillatory currents to interact with the sea floor sediment at a greater depth than the mean level of wave-base. Such an occurrence is not unusual, as wave-ripples have been documented developing beneath mean wave-base (in water depths exceeding 100m) during major storms, by Komar *et al.* (1972) and Channon & Hamilton (1976).

Below wave-base, planar laminated turbidite-like (tempestite) storm sandstones have been described from both the recent (Reineck & Singh 1972; Nelson 1982; Aigner & Reineck 1982) and the ancient (Handford 1986; Hamblin & Walker 1979; Soegaard & Eriksson 1985; Brenchley *et al.* 1979). Observations from the North Sea, led Aigner & Reineck (1982) to interpret the thin bedded, planar laminated sands as having been deposited from low energy storm flows (distal tempestites). These low energy deposits are lateral (down depositional dip) equivalents of the thicker bedded higher energy tempestite flow deposits found accumulating nearer to shore at shallower depths. There is some similarity between the laminates described

Figure 3.3. Graphic sedimentary logs of the Barry Harbour Limestone and Brofiscin Oolite in South Wales; including rose diagram plots of cross-bed sets and the orientation of crinoid stems (denoted by I) and brachiopod valve umbones (denoted by II & III).

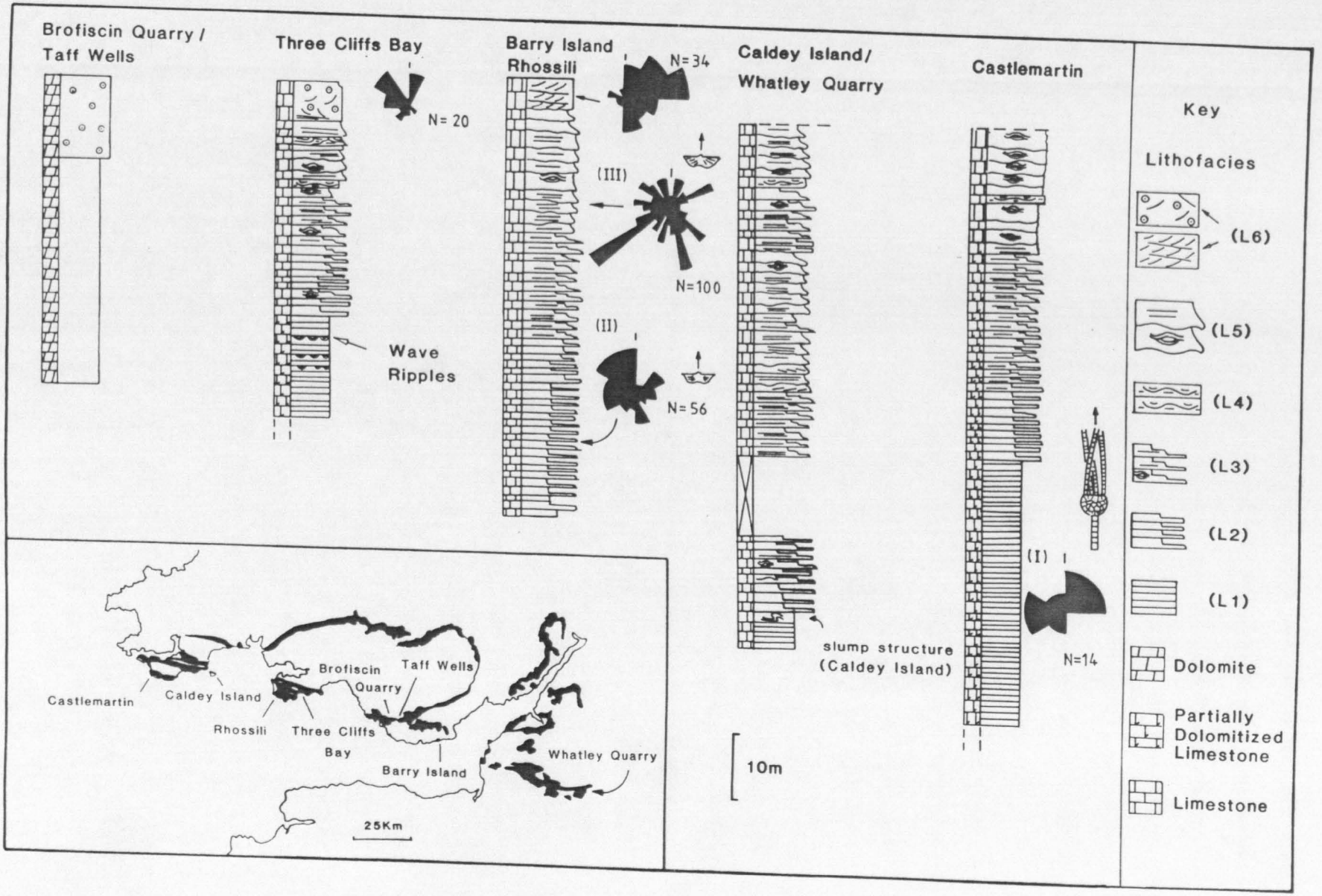
Brofiscin Quarry /
Taff Wells
Three Cliffs Bay
N= 20
Wave
Ripples
Barry Island
Rhossili
N=34
(III)
N=100
(II)
N=56
Caldey Island/
Whatley Quarry
slump structure
(Caldey Island)
Castlemartin
(I)
N=14
10m
Key
Lithofacies
(L6)
(L5)
(L4)
(L3)
(L2)
(L1)
Dolomite
Partially
Dolomitized
Limestone
Limestone
Castlemartin
Caldey Island
Rhossili
Brofiscin
Quarry
Taff Wells
Three Cliffs
Bay
Barry Island
Whatley Quarry
25Km

by Aigner & Reineck (1982) and Lithofacies 1. Both are dominated by planar lamination and there is a conspicuous lack of cross-lamination. However the two differ because in Lithofacies 1 there is a paucity of bioturbated, finer grained layers separating the storm-related deposits. These finer grained layers are representative of fairweather, low energy, suspension deposition between storm events. The absence of mud-rich layers could be due to crinoidal material diluting the fine grained suspension input.

In conclusion it seems likely that the planar laminated Lithofacies 1 was deposited from low energy storm currents beneath the mean level of wave-base. The absence of bioturbation, which is common in the other overlying lithofacies is problematical. There are three important factors that can affect bioturbation: these include the nature of the substrate, the rate of sedimentation and the supply of oxygen. The episodic nature of sedimentation as envisaged here would have been unlikely to inhibit bioturbation altogether and more likely to concentrate it within layers. Extensively bioturbated horizons are found in Lithofacies 1 but there is a paucity of bioturbation in the metre thick accumulations of planar lamination. There is no evidence to suggest that the nature of the substrate was unsuitable for bioturbation, therefore anaerobic conditions are the most likely cause for the preservation of the planar-lamination. Framboidal pyrite is generally accepted as an early diagenetic product of reducing conditions (Berner 1971; Hudson 1982). However, the sparse, evenly disseminated pyrite within these rocks need not necessarily imply totally anaerobic conditions. Overall, the combined sedimentary and diagenetic evidence favours oxygen depleted sea floor sediments.

3.2.2 *Lithofacies 2:* Ungraded thin sedimentary couplets.

Lithofacies 2 consists of thinly bedded (5-10cm thick) sedimentary couplets, of structureless or planar laminated bioclastic packstones,

overlain by bioturbated wackestones (Figures 3.1B & 3.2B). The bases of the couplets are usually sharp, although locally there are indications of shallow scouring (invariably less 1cm deep). The fauna of the beds include thin-shelled valves of orthids, strophomenids, spiriferoids, and crinoid fragments which are 1-5mm in diameter. The majority of the allochems are disarticulated and when inequidimensional the long axes are generally concordant to bedding.

The junction between each packstone coquina layer and the overlying wackestone is gradational and distinct. The wackestone layer is predominantly extensively bioturbated, although occasional relict horizontal lamination may be found. The diverse assemblage of biogenic structures includes *Zoophycos* (Figure 3.2C), simple horizontal burrows and shallow vertical burrows.

The orientations of spiriferoids have been recorded on bedding plane surfaces at Barry. Results from two surfaces considered to be representative of the sedimentary couplet, reveal a strong alignment of the hinge-lines in the packstone layer towards the ENE and WSW (Figure 3.4B). In the wackestone layer, the brachiopod hinge-lines show a more poorly defined trend towards the NW-SE (Figure 3.4A). However, the sample sizes were very small. The collation of composite results, taken from numerous packstone bedding plane surfaces, confirms a preferred orientation of the hinge-lines towards the ENE-WSW (Figure 3.3, denoted by II).

Interpretation: The alternation of packstone layers and extensively bioturbated wackestone layers is indicative of two contrasting energy regimes. Episodic flows probably disarticulated and fragmented the faunal constituents into packstone layers. This is reflected in the prefered orientation of the brachiopods in the lags.

Wackestone layers accumulated from low energy suspension

Figure 3.4. Rose diagram plots of the orientation of spiriferoid valve umbones. The measurements were taken from two bedding plane surfaces, representative of the wackestone and packstone lithologies which comprise the ungraded sedimentary couplets (Lithofacies 2); A and B respectively.

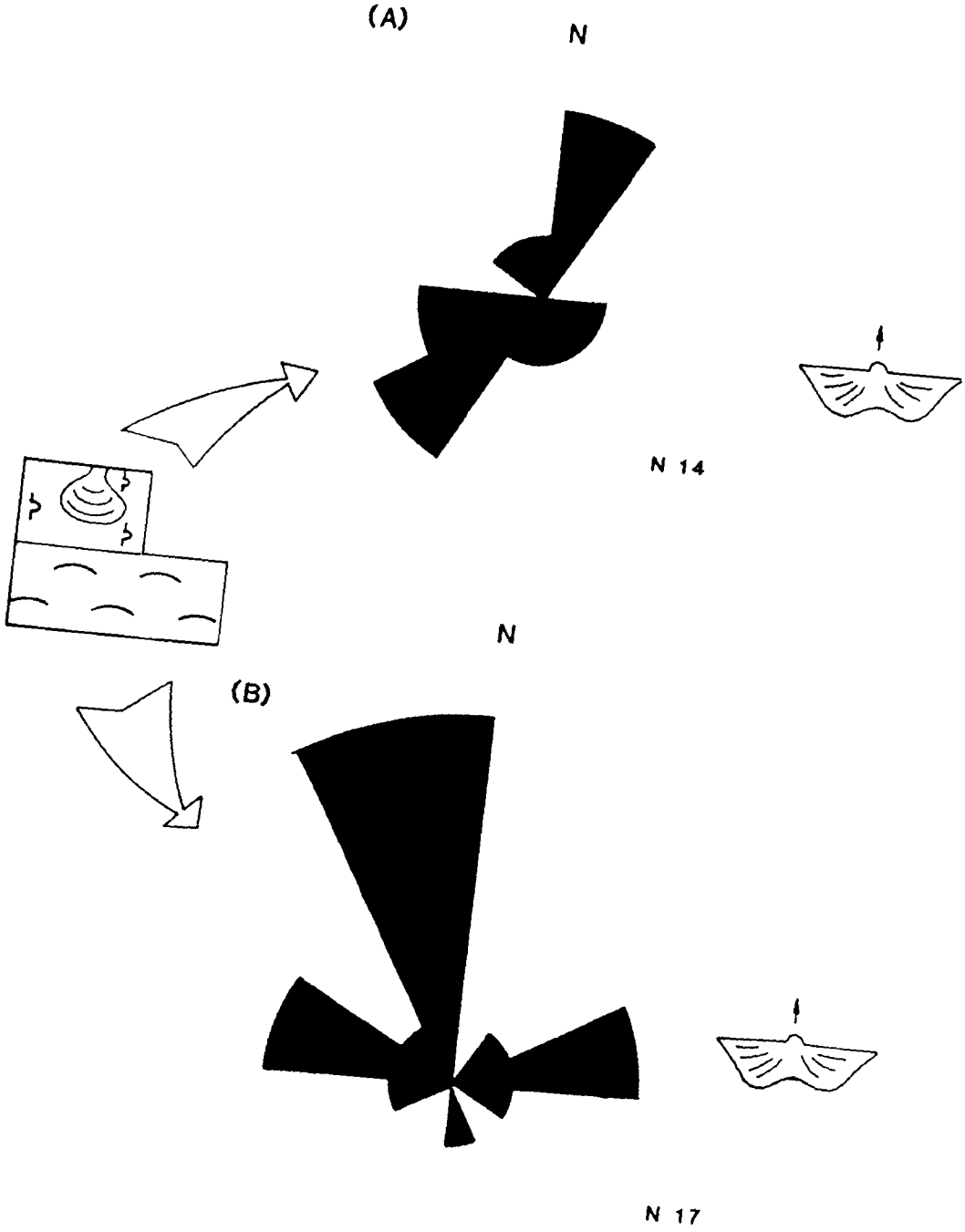
(A)
N
N 14
N
(B)
N 17

deposition. Since there is a similarity between the brachiopod content in the packstone and the overlying wackestone layers, the faunal assemblage was most likely locally derived and reworked into (parautochthonous) packstone layers. The episodic nature of sedimentation was most likely due to low energy storm flows operating beneath mean wave-base.

3.2.3 *Lithofacies 3:* Graded beds containing planar stratification and/or HCS.

Lithofacies 3 is equivalent to type B bedding described and figured by Wu (1982, page 194) from Three Cliffs Bay. This lithofacies is bedded on a 10-20cm scale and charcterized by its tripartite grain-size variation and sedimentary structures (Figure 3.1C). The basal contact is sharp and planar, but locally there are shallow scours (first order boundary surfaces). The basal skeletal lag (2-3cm thick) is a coarse continuous bioclastic pack/grainstone that increases in thickness into the scours. The second layer is finely laminated (on a 2-5mm scale), and contains isolated, coarser bioclastic lenses (1-2cm thick and 10-15cm wide). Vertically, over a 5-10cm scale, the lamination diminishes in thickness. Within the second layer, there are two distinct sedimentary structures: horizontal planar lamination and, more rarely, hummocky cross-stratification (HCS) (Figure 3.5A & B). The HCS consists of lamination draping over a scoured topography (second order surfaces) of convex-upward surfaces (hummocks), and convex downward surfaces (swales) (Figure 3.5B). Laterally, the laminae expand noticeably in thickness from the crest of the hummocks into the swales. The wavelength of the hummocks is between 0.3 and 2m. A maximum vertical relief of 10cm was recorded for the hummocks which invariably pass upward into planar horizontal lamination although rarely wave ripples may be found. In the HCS in the Barry Harbour Limestone there is commonly only one second order scour

Figure 3.5

(A) Hummocky cross-stratification. (Three Cliffs Bay).

(B) Hummocky cross-stratification. Note the undulatory, scour, first order boundary surface (F), and the second order scour surface (S). (Caldey Island).

(C) Lithofacies 4: planar stratified grainstone exhibiting escape burrows (E). (Three Cliffs Bay).

(D) Lithofacies 5: amalgamated planar-stratified graded bioclastic packstones; exhibiting a sharp based skeletal lag (L), planar stratification (P), and chert nodules. (Barry Island).

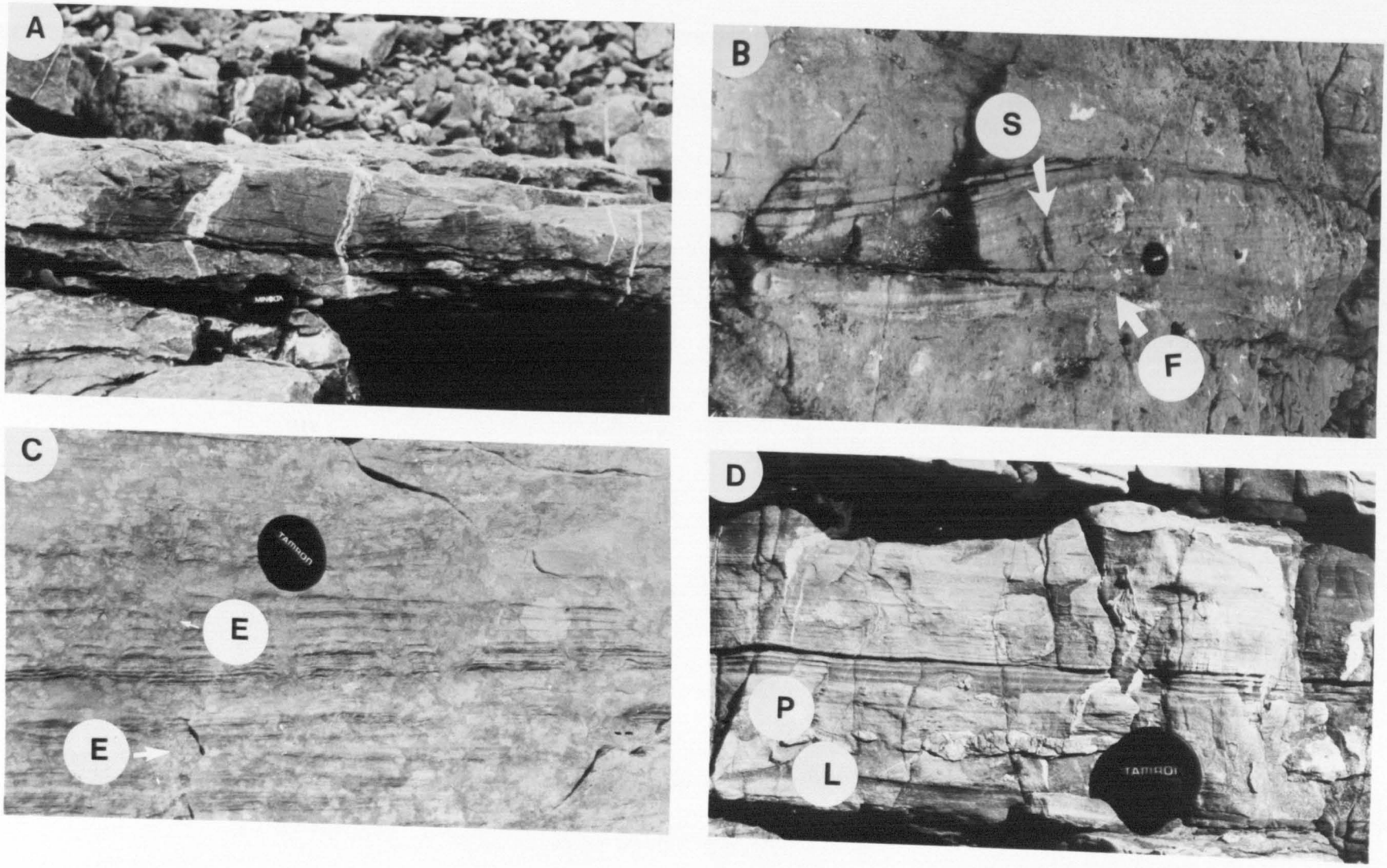
A
B
S
F
C
E
E
D
P
L

surface (Figure 3.5B), although rarely two or more surfaces are found to have scoured into each other.

The top layer consists of either a black micritic limestone or, more rarely an argillaceous micrite. Both are commonly extensively bioturbated, although scarce relict horizontal lamination may be found. Generally, there is an upward increase in the intensity of bioturbation from the base (Figure 3.1C). The base is usually poorly bioturbated, but escape burrows can be found. The middle layer is usually poorly to moderately bioturbated, but shows a high diversity of biogenic structures. These include simple vertical burrows, *Zoophycos*, *Arenicolites*, *Diplocraterion*, rare *Rhizocorallium* (Wu 1982) and *Planolites*. The top layer is normally rich in the biogenic structures mentioned above with the most obvious burrow system being *Planolites*.

Interpretation: High energy currents would be required to produce the first order boundary surface and fragment and transport the allochems. Overall, the upward decrease in grain size and the contrasting upward increase in bioturbation, is indicative of a reduction in depositional rate, a waning of current energy and recolonization of the upper sediment surface.

Although there is great debate at the moment concerning the origin of HCS, there is agreement that oscillatory currents, due to storm surface gravity waves, play a part in its formation (Allen 1985; Brenchley 1985; Dott & Bourgeois 1982; Harms *et al.* 1975; Duke 1985 & 1987; Greenwood & Sherman 1986; Klein & Marsaglia 1987; Leckie 1988; Nottvedt & Kreisa 1987; Swift *et al.* 1983; Swift & Nummedal 1987; and Walker *et al.* 1983). Unequivocally, HCS has been reported from a number of depositional environments which include lacustrine (Duke 1985) and coastal sediments (Greenwood & Sherman 1986) but it is most commonly reported in deposits in

ancient epicontinental seas (Brenchley 1985, Dott & Bourgeois 1982; Harms *et al.* 1975; Duke 1985 & 1987; Swift & Nummedal 1987 and Wu 1982). The top layer of each Lithofacies 3 bed was not reworked by currents, which would suggest deposition from suspension probably below fairweather wave-base (Figure 3.1C).

3.2.4 *Lithofacies 4:* Dish-like scours overlain by horizontal planar stratified bioclastic grainstones

Lithofacies 4 is a parallel to sub-parallel, stratified, coarse bioclastic grainstone, bedded on a 10–30cm scale (Figures 3.5C & 3.6A). The base of each bed is sharp, and commonly undulatory due to scouring. It is uncommon for the scours to cut-into each other. Generally they are laterally spaced on a metre scale and cut-down (5–8cm) into the underlying beds. Studying the sedimentary structures on perpendicular joint-set faces, reveals a dish-like geometry. Solitary scour margins have also been found which have inclined concave-upward surfaces that pass along their lower margin into subhorizontal parallel stratification. At the base of the dish-like scours there is commonly a shell-lag layer (less than 5cm thick). This lag consists of abundant, broken and disarticulated crinoid ossicles, brachiopod valves, and rare crinoid stems. Into the partially filled scours, a finely laminated, bioclastic grainstone was deposited. The alternately thick and thin layers are parallel to subparallel and at the scour margins dip at less than 15 degress toward the centre of the depression. It is noticeable that the scour depressions were infilled before the deposition of overlying horizontally stratified blanket layers (each layer is 3mm to 2cm thick). Locally there are signs of erosion planing-off the swells between the scours before the deposition of the blanket layers.

Constituents of both the inclined and blanket laminae include

Figure 3.6. Schematic summary diagrams showing the interpretation of the the sedimentary features, the trace fossil assemblages, and the body fossil contents found within Lithofacies 4, 5 & 6; A, B, and C, respectively.

A Dish-like scours overlain by planar stratified bioclastic grainstones (Lithofacies 4)

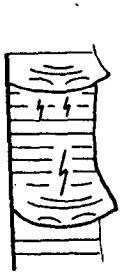

Sedimentary Structures	Lithology	Trace Fossils	Body Fossils	Interpretation
Planar stratified	Grainstone	Short vertical & escape burrows	Fragmented crinoids	Amalgamated high energy storm generated deposit
Dish-like scours			Lag	

B Amalgamated, planar stratified, graded bioclastic packstones (Lithofacies 5)

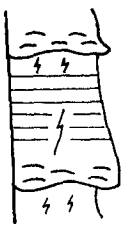

Sedimentary Structures	Lithology	Trace Fossils	Body Fossils	Interpretation
HCS &/or planar lamination	Packstone	Escape & short vertical burrows	Abraded crinoid & brachiopod fragments	Amalgamated storm generated deposit
Planar laminated or structureless	Packstone	Escape burrows	Lag	
Erosive base				

C Cross-bedded oolitic & bioclastic grainstones (Lithofacies 6)

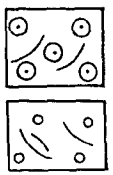

Sedimentary Structures	Lithology	Trace Fossils	Body Fossils	Interpretation
Cross-beds	Grainstone	Rare	Fragmented crinoids & brachiopods	Fairweather currents

broken crinoid and brachiopod fragments, mainly of 0.7mm grade and rarely up to 4mm. Individual laminae may show internal grading. One of the characteristic features of this lithofacies is the lower diversity of biogenic structures, consisting predominantly of escape burrows (up to 17cm long) and shorter vertical burrows (Figure 3.5C).

Interpretation: The combination of sedimentary structures (shallow dish-like scours, overlain by planar laminated, bioclastic grainstones) suggests Lithofacies 4 was deposited in high energy conditions. Accumulation rates must have been very rapid due to the length of the escape burrows (up to 17cm). The absence of fine grained suspension deposits both as micrite drapes and reworked intraclasts suggests that Lithofacies 4 probably represents stacked, high-energy, storm-deposits. The dish-like scours at the base of the facies is likely to be due to storm waves scouring into the sea floor. The infilling of the swales levelled the sea floor before the blanket layers rapidly accreted.

3.2.5 *Lithofacies 5:* Amalgamated graded bioclastic/oolitic packstones

This bedded (20-40cm thick) graded lithofacies consists of two packstone layers above either a planar or a rarely undulatory basal (first order) scour surface (Figures 3.5D & 3.6B). The lower bioclastic layer is commonly structureless, and contains rare wackestone intraclasts (1-3cm in diameter). Measurement of the orientation of the hinge-lines of spiriferoids on bedding plane surfaces at Barry Island shows a preferred orientation of NW to SE (Figure 3.3, denoted by III).

The upper layer shows a variety of sedimentological features. The oolitic packstones tend to be structureless whereas the bioclastic packstones are commonly stratified. Invariably the stratification is horizontal (Figure 3.5D) and/or inclined but occasionally HCS is also

present (Figures 3.7 & 3.8). The inclined layers predominantly accreted vertically and are usually parallel/subparallel to the first order boundary surface. Locally, the inclined layers shows a progressive increase in the forset dip from less than 10° to 15°.

Hummocks can consist of one or more second-order scour surface/s creating a hummocky topography, onto which the overlying laminae have been passively laid-down. Similar to the HCS of Lithofacies 3, the laminae show a progressive increase in thickness from the crest of the hummocks towards the swales (Figure 3.7). Lithofacies 5 beds show many similarities with Lithofacies 3 beds, but the former are amalgamated and so invariably lack a fine grained upper layer due to scouring (compare Figures 3.1C & 3.6B). If a micrite-rich layer is present, it is either very thin, or locally preserved in thin discontinuous 'pockets'. Overall, Lithofacies 5 is thicker, coarser grained, and contains a lower diversity of biogenic structures than Lithofacies 3. Simple vertical burrows are the commonest burrow system and tend to concentrate in the upper packstone layer. Occasionally both layers are seen to be extensively bioturbated.

Interpretation: The sedimentary features strongly suggest that Lithofacies 5 was deposited by episodic, high energy (probably storm-related) events. The presence of HCS is used to infer deposition above storm wave base. The poor development and lack of the upper fine grained layer in Lithofacies 5 is most likely due to erosional removal, prior to the deposition of the overlying storm bed. Similar stacked, amalgamated storm (event) deposits have been described and interpreted by Goldring & Bridges (1973). Subsequently there have been a number of papers that have described a similar lithofacies, but in particular have emphasised the presence and significance of hummocky cross-stratification (e.g Hamblin & Walker 1979; Bourgeois 1980; Dott & Bourgeois 1982; and Walker *et al.* 1983). There is general agreement that the occurrence of

Figure 3.7. Photographic mosaic of the hummocky cross-stratification within Lithofacies 5 beds. The hummocks (H) are separated by the swales (S). (The Pole, Castlemartin).

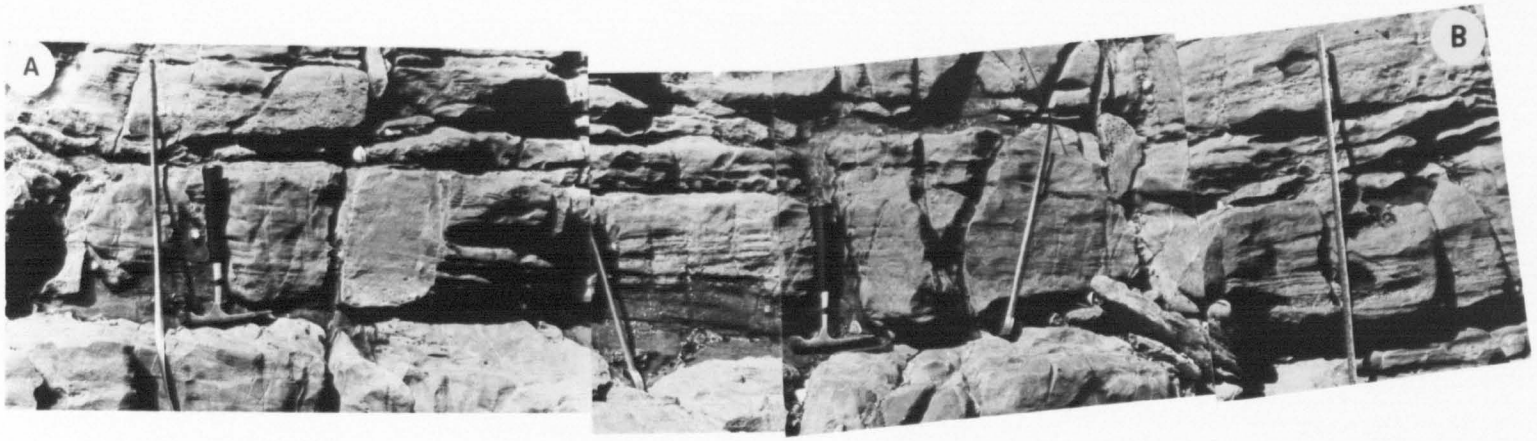
A
B

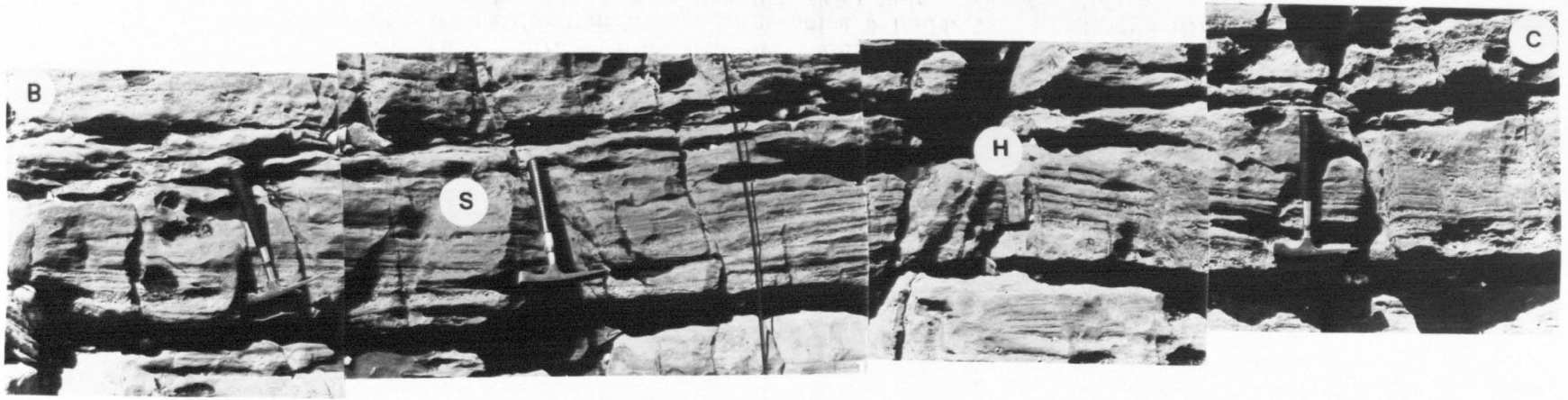
B
S
H
C

amalgamated HCS storm deposits indicate shallow water environments, commonly in close-proximity to fairweather wave-base (Brenchley 1985). Such an interpretation is consistent with Lithofacies 5. This interpretation is supported by the presence of ooids within some of the graded beds, which are likely to have been locally derived from active shoal facies.

Wu (1982) interpreted the low angle inclined stratification, in his proximal to shoreline facies type D, as megaripples. Ramsay (1987) extended this interpretation and proposed that the inclined stratification in the upper part of the Barry Harbour Limestone represents migratory storm megaripples. Many of these layers are inclined because they are parallel/subparallel to the inclined first order boundary scour surface (as shown in Figure 14.3, page 270, Ramsay 1987). It is uncommon for the inclined stratified layers to dip at angles greater than the first order boundary scour surface. Vertical accretion was the dominant mode of sedimentation during storms and a significant component of real lateral accretion was rarely developed. It is important to distinguish between accentuated lateral accretion due to an uneven or low angle inclined sea floor surface and genuine migratory megaripples. There are, however, several beds with a persistent inclination. These show a progressive increase in the foreset dip from less than 10 degrees to 15 degrees; such beds are interpreted as migratory megaripples. There is an absence of reactivation surfaces and so it seems likely that migration only presisted for single storm events.

3.2.6 *Lithofacies 6:* Cross-bedded grainstones

Lithofacies 6 includes cross-bedded, bioclastic (3-4m thick) and oolitic grainstones (3-20m thick) (Figure 3.6C). The medium scale trough and planar cross-beds (5-30cm thick) commonly have a sharp and erosive base

Figure 3.8. Three, vertical and lateral graphic profiles of the HCS ocurring within Lithofacies 5 beds at Castlemartin. Also see Figure 3.7.

Figure 3.9.

(A) Lithofacies 6: scour based, cross-bedded oolitic limestone. (Three Cliffs Bay).

(B) Lithofacies 7: outcropping above the Brofiscin Oolite Formation (BO) and exhibiting low angle lateral accretion surfaces (S) defined by clay seams. (Drybrook Quarry).

(C) Lithofacies 7: fine-grained dolomite, exhibiting diffuse layering. (Drybrook Quarry).

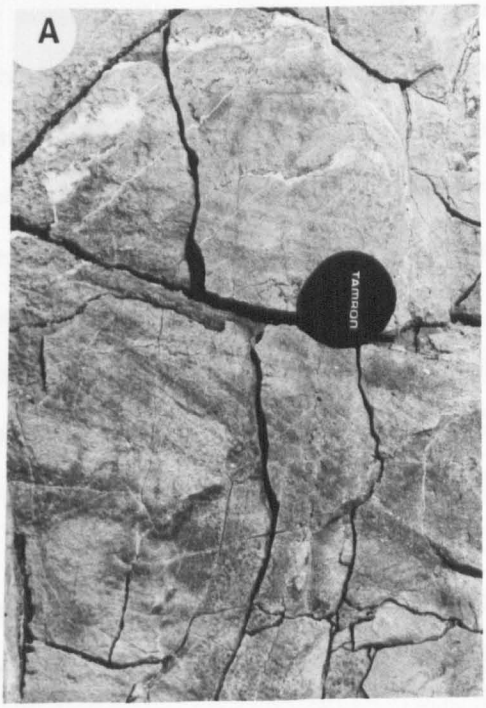
A
TAMRON

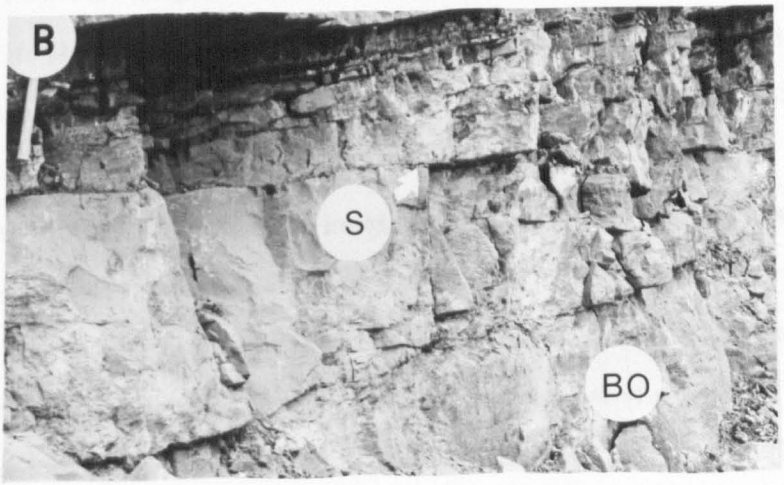
B
S
BO


C
MINOLTA

(Figure 3.9A). They consist of moderate to well sorted allochems which either form graded or ungraded sets (0.5cm to 4cm thick). Generally, the cross-bedded bioclastic limestones tend to be more laterally persistent (up to 10m). In such cases, it is common for the sets to progressively steepen before petering-out into a structurless bioclastic limestone.

Other sedimentary features contained within the cross-bedded limestones include rare biogenic structures, and asymmetrical ripples (Figure 3.10). Separating the oolitic cross-beds at Tytherington Quarry (Appendix J) and Cromhall Quarry (Appendix K) are micritic drapes, up to 5cm thick.

From a palaeocurrent analysis of the oolite at Three Cliffs Bay the dominant current direction is towards the N and NW with minor vector flows to the SW and SE (Figure 3.11). In contrast, the dominant palaeocurrent directions in the cross-bedded bioclastic limestones at Rhossili (Appendix E) and the Yorke Rock Bed (Appendix H) at Barry are towards the W and the NE respectively (Figure 3.11).

Interpretation: The cross-bedded bioclastic and oolitic limestones were deposited in a shallow water environment. The lack of interparticular fines, and the lateral persistence (up to 10m) of some of the cross-beds suggests deposition in a high energy, active shoal environment.

Palaeocurrent readings of the cross-bedded bioclastic limestones reveal a strong longshore component towards the W and the NE (Figure 3.11). While the cross-bedded oolite at Three Cliffs Bay shows both a longshore component towards the NW and shoreline perpendicular vectors towards the N and the SW (Figure 3.11). The dominance of medium scale, bipolar cross-beds indicates tidally influenced deposition (Ramsay 1987). Ramsay (1987) also recorded undulatory erosion surfaces in the oolite at Three Cliffs Bay with dips of 5 to 8°. The presence of these inclined master bedding surfaces led him to propose that the oolite is a migratory

Figure 3.10. Vertical and lateral graphic profile of the cross-bedded Yorke Rock Bed at Barry Island. Palaeocurrent readings and stratigraphic position is shown in Figure 3.3.

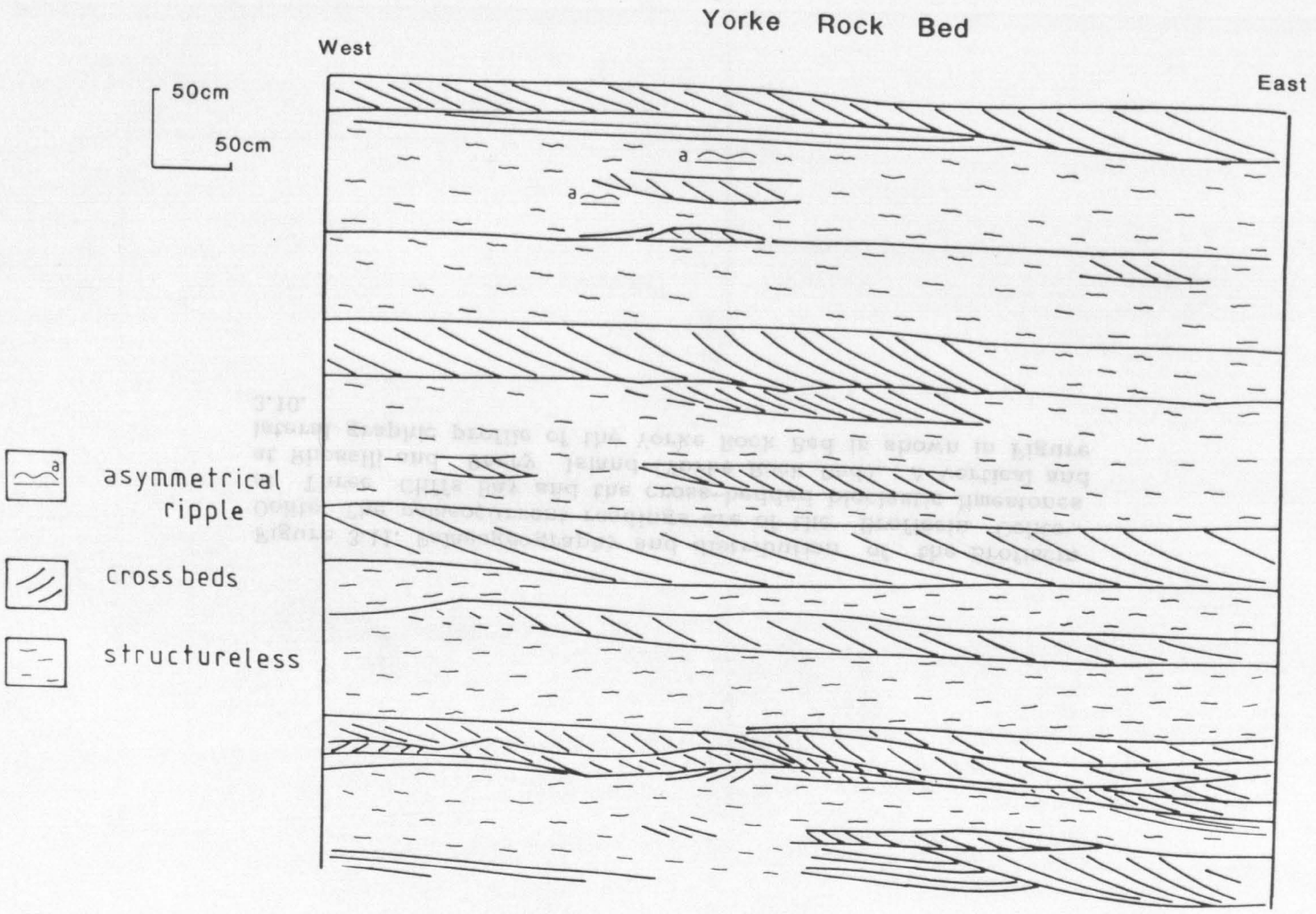
Yorke Rock Bed
West
East
50cm
50cm
a
a
asymmetrical ripple
cross beds
structureless

Figure 3.11. Palaeogeography and distribution of the Brofiscin Oolite. The palaeocurrent readings are of the Brofiscin Oolite at Three Cliffs Bay and the cross-bedded bioclastic limestones at Rhossili and Barry Island (Yorke Rock Bed). A vertical and lateral graphic profile of the Yorke Rock Bed is shown in Figure 3.10.

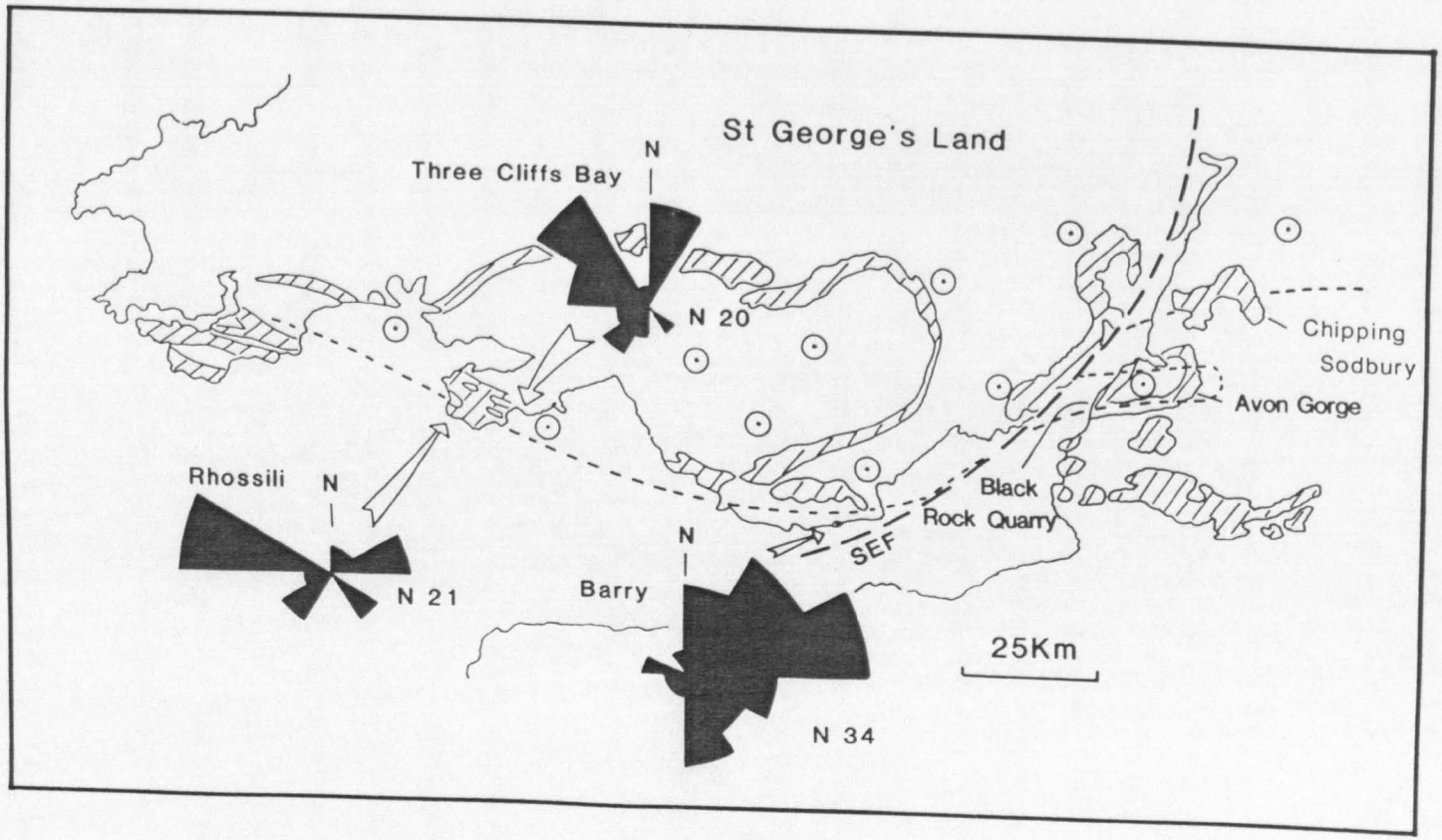
St George's Land
Three Cliffs Bay
N
N 20
Rhossili
N
N 21
Barry
N
N 34
Chipping
Sodbury
Avon Gorge
Black
Rock Quarry
SEF
25Km

sandwave. Unfortunately, minimal sedimentary evidence can be obtained from the more northerly outcrops of the Brofiscin Oolite to support the tidal interpretation because the oolite is dolomitized and it is difficult to see much detail.

Contained within the oolitic limestones of South Wales are vadose cements, indicative of subaerial exposure (Hird 1986). In contrast, there is a conspicuous absence of such features in the cross-bedded oolitic limestones of the Bristol district (e.g. Tytherington, Cromhall, & Chipping Sodbury) and in the cross-bedded bioclastic limestones of South Wales (Rhossili & Barry Island). The latter pass transitionally upward into the overlying Friars Point Limestone and probably occur in a slightly deeper water environment and represent a more marginal, seaward part of the shoal than the cross-bedded oolitic limestones of South Wales (Figure 3.11).

3.2.7 *Lithofacies 7* Structureless fine grained dolomites interbedded with shales

Invariably, immediately overlying the Brofiscin Oolite are the crinoidal packstones of the Friars Point Limestone. Separating these lithologies at Drybrook Quarry (Appendix I) is a non-fossiliferous, diffusely laminated dolomite (ca. 120cm thick) (Figure 3.9B & C). Interbedded with the pale tan dolomites (bedded on a 30-50cm scale) are thinly-bedded, black/bluey-green shale layers (1-2cm thick). The latter define low angle (<10°) lateral accretion surfaces which are convergent towards the west (Figure 3.9B).

Interpretation: The association of interbedded, thin shale layers and non-fossiliferous, fine grained dolomites is indicative of deposition in a low energy, probably restricted (lagoonal?) environment. Similar lithologies have been recorded in the Clifton Down Mudstone

immediately overlying the Gully Oolite, and interpreted as back-barrier deposits by Riding & Wright (1981), Wright (1986), Ramsay (1987) and Weedon (1988). The low angle, lateral accretions surfaces (Figure 3.9B) are thought to represent migratory tidal channel bars. Such surfaces have been recorded within the clastic tidal channel fills of the North Sea by Weimer *et al.* (1982) and in a carbonate setting on Andros by Shinn *et al.* (1969). Recognition of low angle accreting surfaces in back-barrier deposits are considered by Wright (1984b), to be diagnostic of tidal channels in ancient sequences.

3.3 Distribution of the lithofacies

This study concentrates upon the coastal sections in South Wales where the lithofacies are readily identifiable. Recognition of the lithofacies was hampered in the quarry sections due to the lack of detail in the 'fresh' (unweathered) rock faces, particularly in the northern and central parts of the area. Here, the succession has been extensively dolomitized. Fortunately, the oolitic grainstones are readily identifiable mainly because of secondary reddening of the ooliths.

From north to south the Barry Harbour Limestone Formation forms a southerly thickening wedge. The measured thickness increases from ca. 5m at Drybrook Quarry to over 90m at Castlemartin (Figures 3.3 & 3.12). In contrast, the Brofiscin Oolite Formation (up to 16m thick at Brofiscin Quarry) forms a southerly thinning sedimentary wedge which 'feathers-out' in the central ramp zone (Figures 3.3 & 3.12).

A summary of the distribution of the lithofacies is shown in Figure 3.13. The planar laminated facies (Lithofacies 1) forms the lower part of the Barry Harbour Limestone in the central and southern ramp zones. In stratigraphic order it is overlain by the ungraded sedimentary couplets of Lithofacies 2, the graded beds of Lithofacies 3, and the

Figure 3.12. Graphic sedimentary logs of the Barry Harbour Limestone and the Brofiscin Oolite in SW England. The symbols for the lithofacies are the same as that used in Figure 3.3, except for Lithofacies 7 which is only developed at Drybrook Quarry.

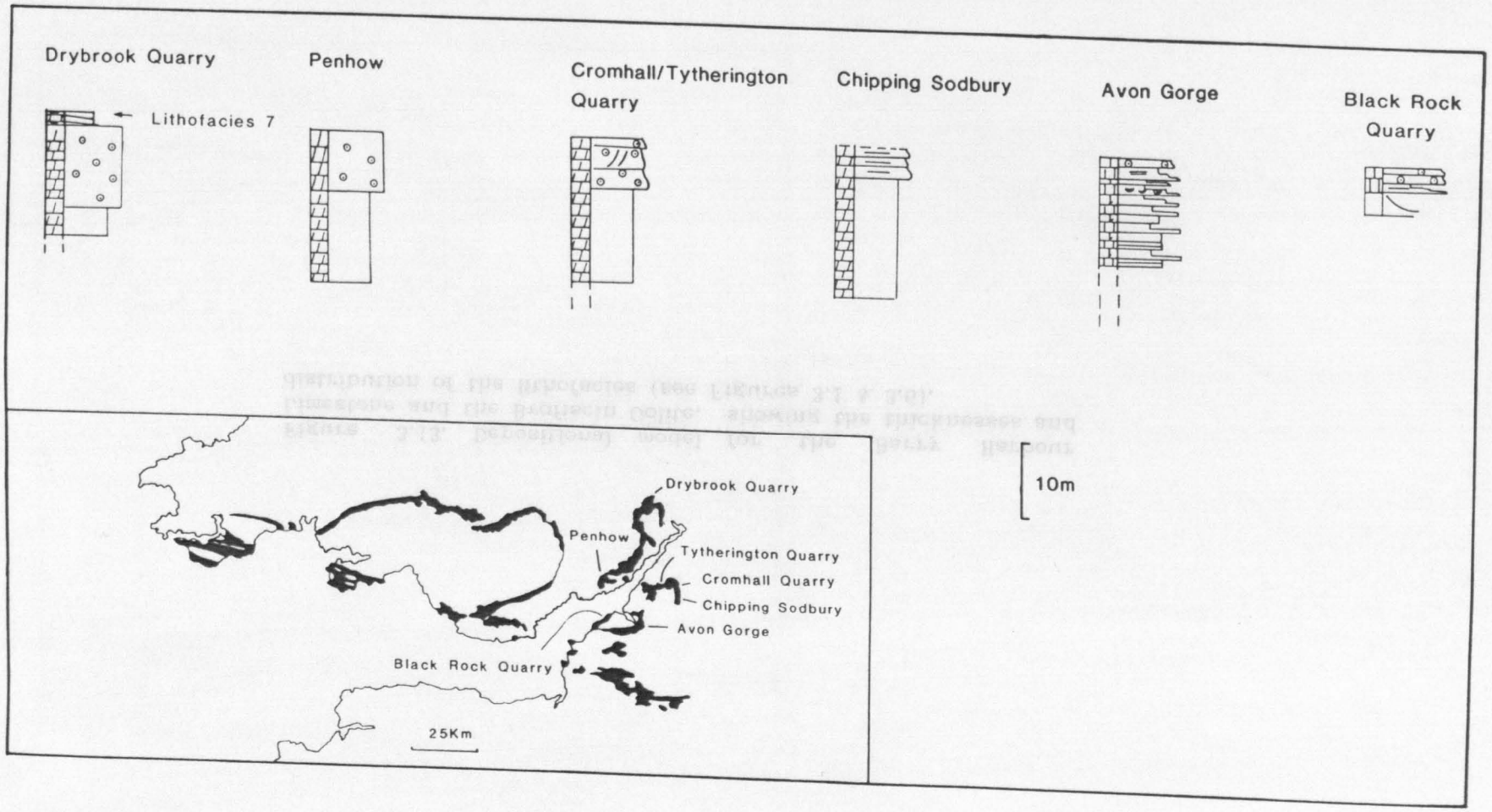
Drybrook Quarry
Lithofacies 7
Penhow
Cromhall/Tytherington Quarry
Chipping Sodbury
Avon Gorge
Black Rock Quarry
10m
Drybrook Quarry
Penhow
Tytherington Quarry
Cromhall Quarry
Chipping Sodbury
Avon Gorge
Black Rock Quarry
25Km

Figure 3.13. Depositional model for the Barry Harbour Limestone and the Brofiscin Oolite, showing the thicknesses and distribution of the lithofacies (see Figures 3.1 & 3.6).

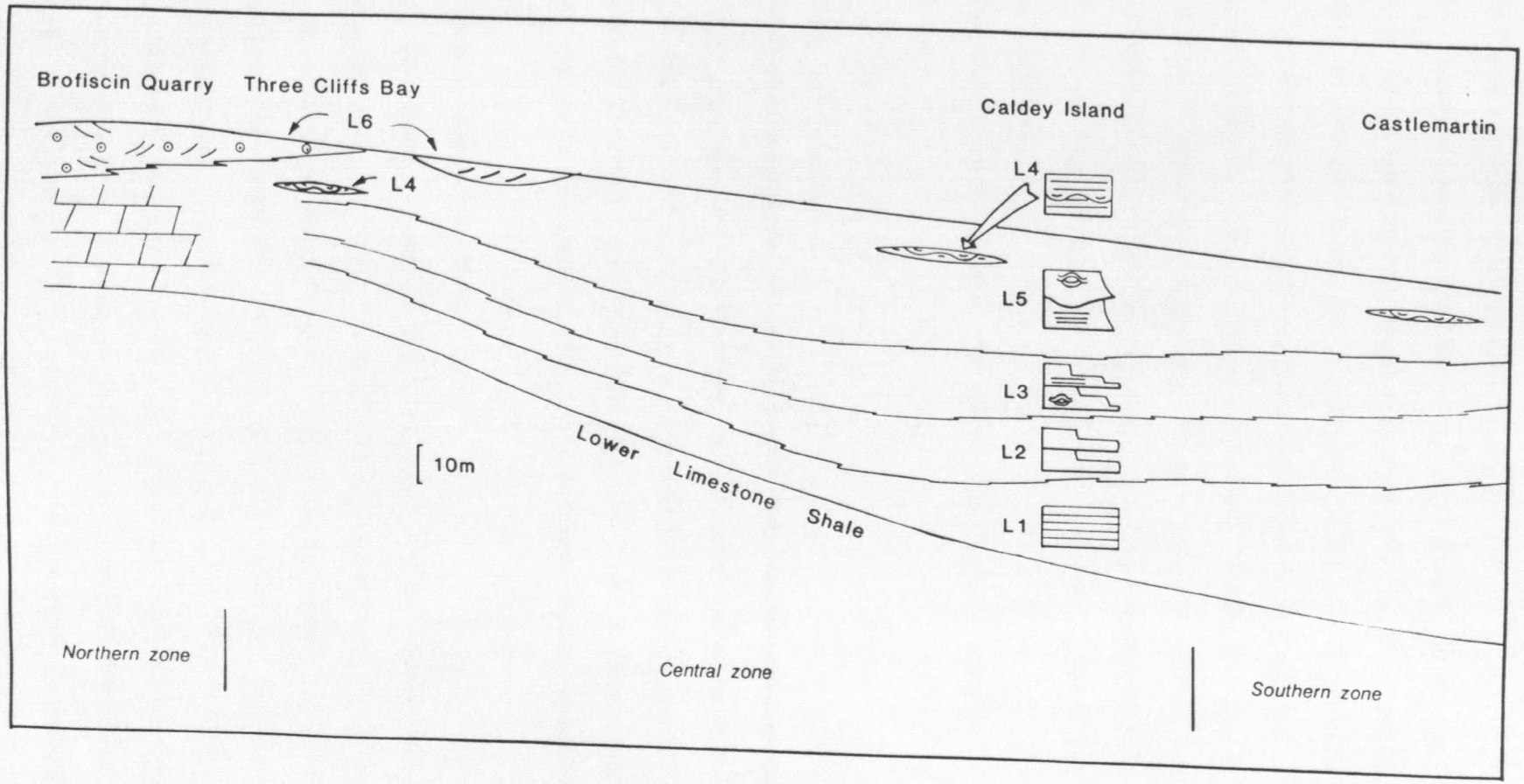
Brofiscin Quarry
Three Cliffs Bay
L6
L4
Caldey Island
Castlemartin
L4
L5
L3
L2
L1
10m
Lower Limestone Shale
Northern zone
Central zone
Southern zone

amalgamated graded beds of Lithofacies 4 and 5.

The northern and central parts of the study area are mainly dominated by the cross-bedded limestones of Lithofacies 6 (Figures 3.3, 3.11 & 3.12). In South Wales the southern fringe of the sandbody is recorded by the cross-bedded bioclastic limestones at Rhossili and Barry Island. In SW England the cross-bedded oolite 'feathers-out' before Chipping Sodbury (Figures 3.11 & 3.12). However, graded oolitic limestone units (Lithofacies 5) are found to the south of Chipping Sodbury: in the Avon Gorge (1m thick unit) and at Black Rock Quarry (2m thick unit) (Figures 3.11 & 3.12).

Lithofacies 7 has only been identified at Drybrook Quarry in the Forest of Dean.

3.4 Discussion

The purpose of this discussion is to evaluate the significance of the lithofacies and discuss the processes operating in the middle and inner ramp environments. In addition, there is a re-evaluation of the idealized shallow marine facies model described by Wu (1982) and an assessment of the nature of the Barry Harbour Limestone and Brofiscin Oolite regression.

3.4.1 Storm versus wave domination

Within the literature there are two alternative sedimentary interpretations offered for the Barry Harbour Limestone on Gower. Junghanss *et al.* (1984) and Wright (1986) agree upon a storm dominated interpretation with HCS, whereas Ramsay (1987) is in favour of it being storm and wave-dominated without HCS. Wave generated structures are present but they have a low abundance in comparison with the storm generated sedimentary structures. The paucity of wave-ripples and the absence of beach facies in the Brofiscin Oolite suggest deposition

under low wave-energy conditions. From the lithofacies descriptions in this study it is apparent that the Barry Harbour Limestone is a storm-dominated sequence with HCS (Figures 3.7 & 3.8).

3.4.2 Nature of the hummocky cross-stratification

Ramsay (1987) reinterpreted the hummocks at Three Cliffs Bay, as symmetrical or possibly three dimensional ripples and uniformly dipping low angle cross-lamination. This reappraisal of the sequence favours the interpretation of Wu (1982) and Wright (1986). The HCS in the Barry Harbour Limestone has been identified by several diagnostic characteristics:- the lower erosional surface gently curves upwards with a maximum slope of 20 degrees (Figures 3.5A & B, 3.7 & 3.8) and clearly truncates the parallel laminae below; the laminae immediately above this surface are subparallel to it; there are some intersections between laminae, but the angles are generally less than 5-10 degrees; the wavelength of the hummocks is between 0.3m and 3m.

The majority of examples of HCS in the Barry Harbour Limestone are simple compared to the classical form of HCS as described by Dott & Bourgeois (1982). The classical form consists of several scour and depositional drape phases (Brenchley 1985) which is in contrast to the single scour and drape phase commonly seen in the HCS of the Barry Harbour Limestone (Figures 3.5B & 3.8A). The formation of HCS is dependent upon the appropriate current type, current strength and suitable grain size. Consequently the absence of HCS in many of the Lithofacies 3 and 5 beds could be due to one or more of the above factors being inappropriate for its formation. It would seem that current intensity and grain size are both related, since without scouring the HCS in the Barry Harbour Limestone will not develop. Dott & Bourgeois (1982) noted that in clastic sequences, HCS preferentially developed in silt to fine sand

grade. This observation has been supported by Leckie (1988), who noted the close association of coarse-grained wave-ripples and finer grained beds exhibiting HCS. Experimental work by Blyth Cain (1968) revealed that crinoid ossicles can be hydrodynamically compared to quartz grains 2-3 phi-sizes smaller due to their relatively low effective density in seawater. Even so, the abundance of coarse bioclastic material (2-5mm in diameter) in the Barry Harbour Limestone may have played an important part in inhibiting the formation of HCS. A similar conclusion was reached by Dodd *et al.* (1987), who documented less well developed forms of HCS, in the Mississippian Ramp Creek and Harrodsburg Limestones, and proposed that this was the result of the insufficient supply of grains of the appropriate size.

There is some evidence that the finer-grained and better sorted tempestite facies exhibit HCS but this is not always the case. The best developed multiple scour and drape form of HCS in the Barry Harbour Limestone occurs at Castlemartin (Appendix B) (Figures 3.7 & 3.8) which contains abundant coarse crinoidal material (also see Dodd *et al.* 1987, page 217 Figure 8). This is not surprising since the intensity and type of storm plays an important part in affecting the hydrographic regime and hence the sedimentary structures produced. Attempts have been made to relate the style of storm-deposited sedimentary associations with latitude in an attempt to recognize hurricane and intense winter storm belts (Duke 1985 & 1987).

The origin of HCS is problematical since the conditions by which it forms have not been successfully reconstructed in a flume tank (Dott & Bourgeois 1982; Brenchley 1985). This is due to its large wavelength, and the problems associated with reconstructing open marine conditions within a confined area. There are three models in the literature which attempt to explain the origin of HCS (Dott & Bourgeois 1982; Harms *et al.* 1975;

Walker *et al.* 1983; Swift *et al.* 1983; Nottvedt & Kreisa 1987). Harms *et al.* (1975) described a scour and drape feature, which is interpreted as being transitional between straight crested symmetrical wave ripples and the upper flat bed of intense oscillatory sheet flow. Each lamina is thought to represent deposition from a single wave or wave train, and the scouring is due to fluctuations in the intensity of the oscillatory current (Dott & Bourgeois 1982).

In their Canadian sections Walker *et al.* (1983) recorded turbiditic type sole structures at the base of many of the HCS beds, and vertical hummock growth without scouring. They argued that the unidirectional turbiditic flow currents waned to allow oscillatory currents to dominate, producing the hummocks by vertical accretion.

The third theory concerning the origin of HCS comes from modern studies of the inner Atlantic shelf of North America, by Swift *et al.* (1983). They found symmetrical hummocky megaripples, and interpreted them as being produced by combined-flow storm currents. These along-coast geostrophic flows are often jetlike, and down-well with high velocities at the coastal margin. Second order scouring into the sea floor formed the incipient megaripples. There followed a period of sea floor aggradation, interrupted by episodic, erosive, fluctuations in turbulence. During the accretion of the megaripples the troughs were kept open by scouring. The basal fill of the troughs are lined with laminae that thicken away from the centre of the troughs, towards the megaripples.

The sedimentary features of the HCS beds in the Barry Harbour Limestone are comparable with the scour and drape model of Dott & Bourgeois (1982) and Harms *et al.* (1975). The laminae overlie second-order, undulatory, scour surfaces and fan in thickness from the hummocks into the swales, and thus differ from the sedimentary features described by Swift *et al.* (1983). The Walker *et al.* (1983) model is

unsuitable because there is a notable absence of turbiditic type sole structures and the hummocks do not develop by vertical growth.

The study of ancient examples has shown that there are two phases to the formation of HCS. The first involves offshore transportation of sediment from the shoreline by unidirectional-dominated currents, and the second is a wave-dominated phase which reworks the sediment. The general consensus is that combined flows with a dominant oscillatory component, may have been responsible for the genesis of HCS (Dott & Bourgeois 1982; Hunter & Clifton 1982; Swift *et al.* 1983; Allen 1985; Nottevedt & Kreisa 1987). It is impossible to resolve the hydrographic processes responsible for the formation of HCS in the Barry Harbour Limestone due to the poor three dimensional exposure. Other studies have been able to place useful contraints upon a probable current-wave regime by using information from the associated rippled horizons. Brenchley (1985) described wave ripples overlying HCS that are polygonal in shape which indicates that wave-formed oscillatory currents can be multidirectional and complex. The close lateral and stratigraphic association of coarse-grained wave-ripples and HCS, led Leckie (1988) to suggest they developed under similar wave-dominant conditions. Rippled horizons are notably lacking in the Barry Harbour Limestone, but when present they are usually locally concentrated. If the hummocks in the Barry Harbour Limestone are due to combined flow currents, then as the currents waned, rippling could have occurred as in storm-dominated clastic sequences. The absence of ripples need not imply a total change in hydrographic regime or a dramatic decrease in current activity. A likely explanation is that the coarse grain size inhibited the formation of ripples.

3.4.3 Depositional environment

The deposits of the Barry Harbour Limestone and the Brofiscin Oolite accreted on a gently, southerly and westwardly, inclined (ramp) sea floor surface. The southerly tapering 'feather' margin of the oolitic sandbody can be correlated down the palaeo-depositional slope and into the below fairweather wave-base facies containing the storm-related sedimentary structure, hummocky cross-stratification (Figure 3.13). Contained within the regressive sequence are a large variety of sedimentary facies, representing deposition from below mean wave-base to above fairweather wave-base. In addition, a minor development of back-barrier facies is found overlying the Brofiscin Oolite at Drybrook Quarry (Appendix I).

The Barry Harbour Limestone

The offshore facies, laid-down below mean wave-base, are represented by the thinly bedded, distal tempestites of planar laminates (Lithofacies 1) and the ungraded sedimentary couplets (Lithofacies 2) (Figure 3.14). The shoreface-offshore transition zone is characterized by an increase in bed thickness, the appearance of HCS, and a low degree of bed amalgamation (Lithofacies 3). In contrast the shoreface deposits (Lithofacies 4 & 5) are characterised by a high degree of bed amalgamation and a notable increase in the average relief of the basal scour (Figure 3.14), yet evidence of major wave action is lacking.

The long length of the escape burrows and better sorting of Lithofacies 4 suggest it was deposited in a higher energy environment than Lithofacies 5. Ramsay (1987) interpreted the massive-bedded units and thinner-bedded units as shoal and intershoal complexes. The minor (thin) developments of Lithofacies 4 within Lithofacies 5 would seem consistent with a shoal and intershoal interpretation (Figure 3.13).

Figure 3.14. Storm beds of the Barry Harbour Limestone at Three Cliffs Bay. The upper part of the diagram shows the depositional setting of a gently inclined ramp surface and the relationship of the lithofacies to storm wave base and fairweather wave base. The lower part of the diagram shows plots of the variation in bed thickness, relief of the basal scour and the relative degree of bed amalgamation down the slope of the ramp.

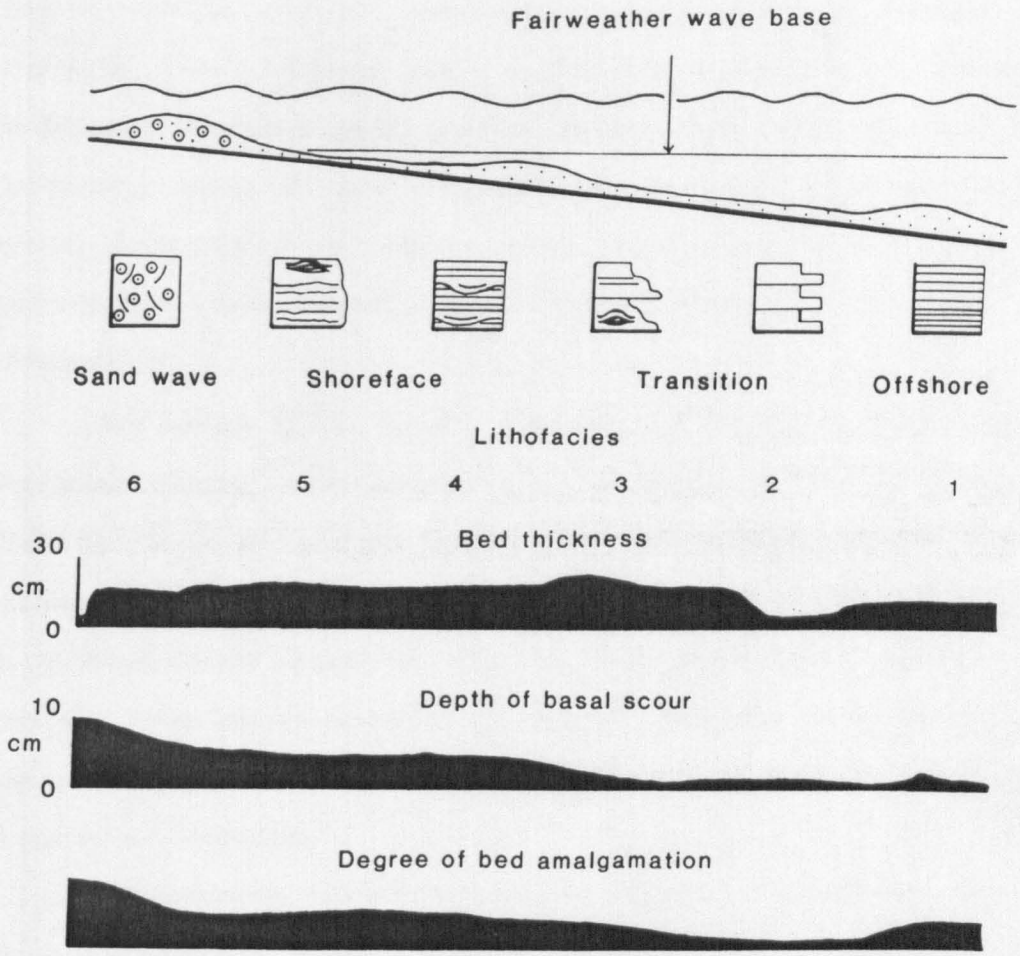
Fairweather wave base
Sand wave
Shoreface
Transition
Offshore
Lithofacies
6
5
4
3
2
1
Bed thickness
30
cm
0
Depth of basal scour
10
cm
0
Degree of bed amalgamation

The Brofiscin Oolite & its lateral cross-bedded equivalents

The cross-bedded Brofiscin Oolite and its lateral bioclastic cross-bedded equivalents record sedimentation in an above fairweather wave-base environment. The palaeocurrent readings show a strong longshore component and a weaker shoreline perpendicular, tidal component (Figure 3.11). Deposition of the Brofiscin Oolite in the Bristol district is interpreted as being in a slightly lower energy regime than that in South Wales. Separating many of the cross-beds at Cromhall Quarry (Appendix K) are micrtic drapes (up to 5cm thick) which contain biogenic structures. Such features are notably absent in the Brofiscin Oolite of Three Cliffs Bay (Appendix F).

The nature of the contact between the Brofiscin Oolite and the overlying Friars Point Limestone is variable. In South Wales the Brofiscin Oolite has a sharp contact with the overlying beds and contains meniscus cements which are indicative of subaerial exposure (Hird 1986). At Cromhall Quarry (Appendix K) and Tytherington Quarry (Appendix J), the Brofiscin Oolite passes transitionally upward into the overlying Friars Point Limestone without any evidence of subaerial exposure or a major break in sedimentation.

Unfortunately, there is insufficient evidence to determine whether the back-barrier tidal deposits (Lithofacies 7) overlying the extensively dolomitized oolite at Drybrook Quarry (Appendix I) were laid-down penecontemporaneously. The alternative is that the back-barrier facies developed landward of a shoreward migrating shoal, during the basal Friars Point Limestone transgression. In such a scenario, the shoal facies would be represented by the sheet deposit of coarse crinoidal material (ca. 10cm) which immediately overlies Lithofacies 7.

In conclusion, at the peak of the regression much of South Wales was subaerially exposed whereas the palaeo-shoreline in SW England was most probably located to the north of the Cromhall Quarry and Tytherington Quarry (Figure 3.11). The Bristol area probably formed a marine embayment, perhaps partially protected by the oolite shoal facies and the emergence surface which developed in South Wales (Figure 3.11).

It is notable that there there is a paucity of re-sedimented ooids in the more proximal tempestite facies. This is significant as it is well established that barometric and wind effects during major hurricanes and mid-latitude storms can cause the build-up of sea water against the shoreline (Morton 1981; Leckie & Walker 1982; Swift et al. 1983; Swift & Nummedal 1987; Swift et al. 1987). The build-up of a significant head of water against the shore is counteracted by gravity which creates downwelling currents that flow offshore. These returning currents are capable of carrying sediment from the nearshore region offshore (Swift et al. 1983). However, it is only the most intense storms which mobilise large volumes of water that cause significant set-up along a coastline (Swift et al. 1983) and are capable of transporting material offshore. The less intense short-lived storms (e.g. Cyclone Winifred) that affect only a relatively small area of coastline do not cause significant set-up against the coastline (<1.6m) and create high-energy downwelling currents (Gagan et al. 1988). These types of storm events merely cause in situ resuspension of shelf sediment, without significant net-transportation offshore (Gagan et al. 1988).

It is significant that the developments of graded oolitic limestone in the Avon Gorge and at Black Rock Quarry are not attached to the main part of the oolite shoal, located to the north of Chipping Sodbury (Figure 3.11). The absence of re-sedimented ooids at Chipping Sodbury (Figure 3.11) militates against the ooid supply being from the north by means of

storm-related relaxation currents.

The well developed ooids are likely to have originated in a nearshore environment and were subsequently transported to below fairweather wave-base. The two-fold westward thickening of the graded oolite units indicates the most likely source of supply. Palaeocurrent readings of the cross-bedded Yorke Rock Bed at Barry show a strong prefered orientation towards the east (Figures 3.10 & 3.11). This would support the proposal that longshore (fairweather) currents were responsible for transporting the ooids offshore into the marine embayment of the Bristol area.

Regardless of the mode of supply of the ooids, sedimentation of the graded oolitic limestones was ultimately from high energy, (storm-related?) currents. The fairweather, offshore transportation of the ooids may have been enhanced by storm processes. Alternatively, the graded oolitic limestone beds may just represent *in situ* resuspension of bioclastic and oolitic material without significant net-transportation offshore (e.g. Gagan *et al.* 1988).

3.4.4 Reanalysis of the facies model of Wu (1982)

This re-analysis of the depositional environments of the Barry Harbour Limestone at Three Cliffs Bay has resulted in a reappraisal of the four distal to proximal, graded facies types described by Wu (1982) (Figure 3.15). His facies model was constructed from his analysis of two lower Dinantian sequences in South Wales. Wu's "below storm wave base facies, type A" is a thickly bedded, bioturbated packstone characterized by reorientated horn corals in the basal lag. This facies is not present in the Barry Harbour Limestone Formation. Types B and C contain HCS, and are interpreted by Wu (1982) as representing deposition between storm and fairweather wave-base (Figure 3.15). The former is analogous to

Figure 3.15. Zonation of depositional types in Ogmore-by-Sea and Three Cliffs Bay. Wu (1982).

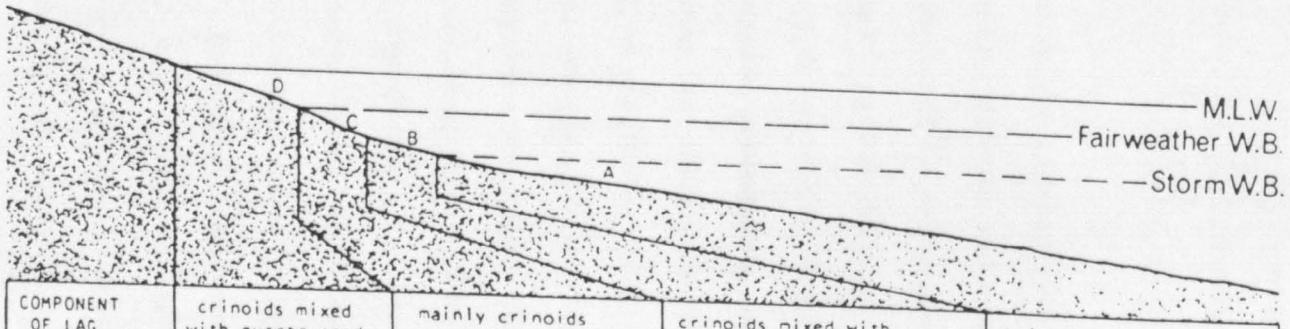

COMPONENT OF LAG	crinoids mixed with quartz sand	mainly crinoids	crinoids mixed with brachiopods & gastropod sheils	whole horn coral, less abraded brachiopods
STRUCTURES	large scale low angle cross-bedding	long wavelength hummocky cross-bedding	short wavelength hummocky cross-bedding	
PATTERN OF LAMINAE	thick laninae	thin laminae alternating with thick laminae	only thin laminae	non-laminated in hand specimen
BIOTURBATION	sporadic to no bioturbation	weakly to sporadic bioturbation	medium to weak bioturbation	strong bioturbation
TRACE FOSSILS	borings	escape burrows	small (arcuate) *Zoophycos*, small *Planolites*-type burrows	large (regular) *Zoophycos*, large *Planolites*-type burrows
TEXTURE	matrix free	→ matrix moderate →		matrix rich

Lithofacies 3. Types C and the megaripple facies Type D are represented by Lithofacies 5 which contains HCS. Important additional sedimentary features found in the Barry Harbour Limestone include the two distal-tempestite Lithofacies 1 and 2, and the subaerially exposed cross-bedded oolite. It is suprising that the latter lithofacies was not included in Wu's facies model because oolitic sandbodies are particularly useful both as palaeobathymetric and environmental indicators (section 3.4.3).

3.4.5 The Barry Harbour Limestone & the Brofiscin Oolite regression

The Barry Harbour Limestone and the Brofiscin Oolite record the establishment of a carbonate ramp and the first major regression in the Dinantian succession of SW Britain. The regression in the central and southern ramp zone is recorded by the sequence of storm-related sedimentary structures in the Barry Harbour Limestone (Lithofacies 1-5) (Figure 3.13).

It is significant that the depth-related facies show a high degree of provinciality (Figure 3.13). The Brofiscin Oolite is thickest in the northern ramp zone (Figure 3.12 & 3.13). In contrast the central ramp zone contains an expanded sequence consisting mainly of the graded beds of Lithofacies 3 and the amalgamated storm beds of Lithofacies 4 and 5. The above facies form an attenuated succession in the southern ramp zone which is dominated by the distal tempestites of Lithofacies 1 and 2. The provinciality of the facies would suggest sediment aggradation was the main process of sediment accumulation. The basinward petering-out of the Brofiscin Oolite in the central ramp zone, represents an unsuccessful, late stage attempt at progradation. For sediment aggradation to have dominated over lateral accretion, and for the expanded sequence in the central ramp zone to have developed,

there must have been a relative rise in sea level.

Eustatic controls upon sedimentation

Ramsbottom (1977 & 1979) and later Ross & Ross (1985 & 1987) suggested that there were three significant depositional (mesothemic) cycles during the Courceyan and two during the Chadian. The three Courceyan mesothems (D1a, D1b & D1c) are part of Ramsbottom's (1973) transgressive-regressive 'First Major Cycle' of which there are six during the Carboniferous.

The first mesothemic cycle, D1a, includes the Lower Limestone Shale Group. The start of the second cycle, D1b, occurs at the base of the Black Rock Limestone. It includes the Barry Harbour Limestone, the Brofiscin Oolite and the lower part of the Friars Point Limestone. The third mesothemic cycle, D1c, comprises the upper part of the Friars Point Limestone and records the major sea level fall at the end of the Courceyan (Ramsbottom 1973; Lees & Hennebert 1982; Ross & Ross 1985 & 1987).

A sea level fall at the base of the Barry Harbour Limestone is difficult to detect, although it may well have prompted carbonate production. According to the sea level curves of Ramsbottom (1977 & 1979) the Barry Harbour Limestone, the Brofiscin Oolite and the lower part of the Friars Point Limestone accumulated during a eustatic rise in sea level. However, the geometry of the Brofiscin Oolite is inconsistent with that of an oolitic sandbody which developed during a eustatic rise in sea level, such as the Castell Coch Limestone (Lower Limestone Shale Group) (Burchette 1987).

Both the Brofiscin Oolite and the Castell Coch Limestone were laid-down in a storm and tide-dominated regime (Burchette *et al. submitted*) and under humid climatic conditions (Hird & Tucker 1988;

Burchette pers. comm.). They both form an oolitic sand belt of tidal shoals which pass seaward into below fairweather wave-base, storm-dominated facies. The palaeocurrent readings show a strong longshore component and a weaker shoreline perpendicular tidal component (Figure 3.11; Burchette 1987, page 250, figure 13.6).

However, the geometries of the Castell Coch Limestone and the Brofiscin Oolite differ. The thickest development of the Castell Coch Limestone occurs basinward along the southern fringe of the oolitic sandbody. A shallow marine embayment/'lagoon' developed landward of the sand belt and prograded basinward during the eustatic rise in sea level (Burchette 1987). The southward thinning of the Brofiscin Oolite and poor development of back-barrier facies (Lithofacies 7), if at all, suggests the Brofiscin Oolite accumulated during a period of relative sea level stasis.

In conclusion the Barry Harbour Limestone and the Brofiscin Oolite depositional cycle is not equivalent to the depositional D1b cycle of Ramsbottom (1977 & 1979). This would suggest the above regressive sequence was a localised phenomenon in SW Britain.

Tectonic controls upon sedimentation

The Barry Harbour Limestone and the Brofiscin Oolite sequence shows over a six fold thickness increase from Drybrook Quarry (Appendix I) to Castlemartin (Appendix B) (Figures 3.3 & 3.12). This would suggest that sedimentation was influenced by differential subsidence. A progressive increase in the rate of subsidence into the basin (flexure) would limit the degree of lateral progradation and maintain the ramp facies belts. A minor drop in sea level exposed the Brofiscin Oolite and caused a seaward shift of the shoal facies belt into the central ramp zone (Figure 3.13).

The only direct evidence of tectonic activity upon sedimentation is

Figure 3.16. Slump structure occurring towards the base of the Barry Harbour Limestone, containing chert nodules. Stratigraphic position is shown in Figure 3.3. (Caldey Island).

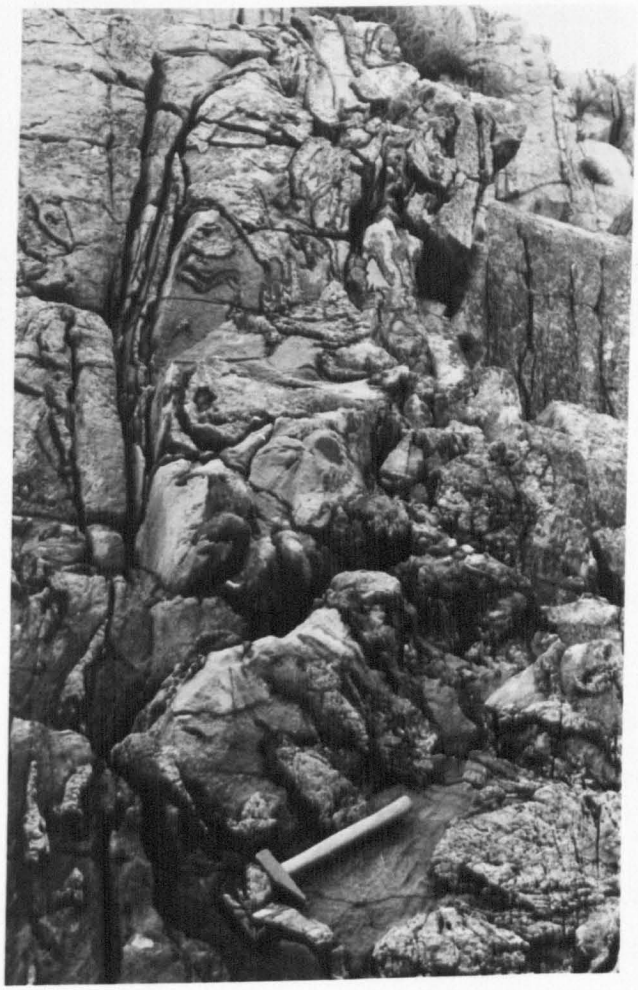

to be found at Caldey Island (Appendix D) where a slump structure occurs in the basal part of the Barry Harbour Limestone (Figures 3.3 & 3.16). Similar slump structures have been documented in the Lower Limestone Shale Group in sections located just to the south of the Ritec Fault (Dyfed). These structures have been recorded at West Angle Bay, Skrinkle Haven, and Caldey Island (Figure 1.2) by Kelling & Williams (1966). The latter authors proposed that seismic activity along the Ritec Fault was the most likely trigger for slumping. Such an origin is consistent with the presence of slumping in the Barry Harbour Limestone at Caldey Island.

In conclusion the nature of the Barry Harbour Limestone and the Brofiscin Oolite regression was as a result of carbonate production 'catching-up' with sea level. The persistence of the depth-related ramp facies belts was probably assisted by differential subsidence as a result of flexure.

3.5 Conclusions

1) The Barry Harbour Limestone and the Brofiscin Oolite form a shallow marine, predominantly subtidal, shallowing-upward sequence which is capped by a subaerially exposed oolite in South Wales.

2) Hummocky cross-stratification was identified within the succession. Many of the HCS beds exhibit only one phase of second-order scour, onto which the overlying laminae drape. The lack of successive scour and drape events as seen as the classical form of HCS is thought to be due to the coarse grain-size of the bioclasts, inhibiting the successive scour events.

3) An assessment of the major controls affecting the sedimentation of the Barry Harbour Limestone favours a storm-dominated interpretation.

4) Wu's (1982) distal to proximal facies trend model is modified to include two additional distal tempestite lithofacies and a proximal oolite

sandbody.

5) The oolitic sandbody is a low wave energy, tidally influenced, sand shoal deposit which prograded across the gently inclined ramp from the north.

6) The area to the north of Bristol formed a marine embayment whose southern limit is a subtidal bar containing re-sedimented ooids derived from the west by longshore currents.

7) The Barry Harbour Limestone and the Brofiscin Oolite record the first major basin-wide, shallowing-upward phase subsequent to the early Carboniferous transgression.

Chapter 4 - Sedimentology and tectonic evolution of an offshore muddy ramp sequence: the Friars Point Limestone Formation

4.1 Introduction

Considerable attention has been devoted to the study of above storm wave-base facies in Carboniferous ramp successions (e.g. Wu 1982; Handford 1986; Wright 1986; Faulkner 1988; Dodd *et al.* 1987), whereas, there have been few detailed accounts of those facies types which form the deeper ramp sequences. Notable exceptions include work on the Arundian of South Wales by Simpson (1987), and studies of the Muschelkalk in Germany and NE Spain by Aigner (1984 & 1985) and Calvet & Tucker (1988), respectively. This disparity of work is more acute in the knowledge that below storm wave-base facies dominate the Lower Carboniferous ramp succession of SW Britain. In particular, these facies form the thick assemblages occurring in the southern ramp zone (Lees *et al.* 1977; Wright 1986; Waters & Lawrence 1987).

The aim of this chapter is to describe and interpret the moderately to extensively bioturbated succession of the Friars Point Limestone Formation (up to 280m thick). Emphasis will be placed upon distribution of the lithofacies and current indicators (e.g. storm-sediment filled burrows). A model is offered for the environment of deposition which consists of two broad depth-related offshore facies belts. The timing of differential subsidence and its effect upon sedimentation is assessed using established conodont biostratigraphy, in order to identify seemingly isochronous sedimentary assemblages.

Also contained within the Friars Point Limestone are the Middle Hope (Weston-super-Mare) volcanics and the Waulsortian buildups of Castlemartin and Cannington Park, these topics are dealt with separately in Chapters 5 and 6 respectively.

4.2 Geological Setting

The Friars Point Limestone Formation (Figure 1.3) overlies the regressive sequence of the Barry Harbour Limestone and Brofiscin Oolite. The peak of the regression culminated in the local emergence of the Brofiscin Oolite, which can be correlated, southward and westward, down the palaeoslope into the subtidal facies of the uppermost Barry Harbour Limestone. The Friars Point Limestone commonly displays a sharp, truncated contact with the immediately underlying Brofiscin Oolite but a gradational contact with the Barry Harbour Limestone, in more distal settings.

4.3 Lithofacies and their interpretation

Three main lithofacies types are recognized (Figure 4.1) and their numbering (Lithofacies 8-10) follows on from those described in Chapter 3. Many of the lithofacies described from the Barry Harbour Limestone are also present in the lower part of the Friars Point Limestone; where necessary the reader is referred to Chapter 3.

Across much of the study area, the Black Rock Dolomite forms the upper part of the Friars Point Limestone Formation (Figures 2.1, 2.2 & 2.3). Unfortunately, the pervasive dolomite almost totally obscures the sedimentary features, except for rare limestone pods in which the precursor limestone may occasionally be identified. Only the latter features are described in detail, since a full petrographic and geochemical study of the Black Rock Dolomite has been documented elsewhere by Hird (1986) and Hird *et al.* (1987).

4.3.1 *Lithofacies 8:* Decimetre-bedded, bioturbated packstone/wackestone beds with shell lags

Lithofacies 8 forms decimetre-thick, bioturbated, pale grey packstone/wackestone beds (Figures 4.1A & 4.2A). The base of each bed is

Figure 4.1. Schematic summary diagrams showing the interpretation of the sedimentary features, trace fossil assemblages, and body fossil contents found within Lithofacies 8, 9 and 10; A, B, and C, respectively.

A

Lithology	Trace Fossils	Body Fossils	Interpretation
Wackestone/ packstone	Zoophycos, Chondrites, Thalassinoides-type?, simple vertical & horizontal burrows.	Diverse assemblage including crinoids, brachiopods, corals & bryozoans	Low energy suspension deposition
Packstone			Deposition from low energy currents

B

Lithology	Trace Fossils	Body Fossils	Interpretation
Marl	Zoophycos, Chondrites, Thalassinoides-type?, simple vertical & horizontal burrows.	Diverse assemblage of crinoids, brachiopods, corals, & bryozoans	Low energy suspension deposition.
Wackestone/ packstone			

C

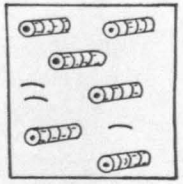

Lithology	Trace Fossils	Body Fossils	Interpretation
Packstone	Simple vertical & horizontal burrows	Mainly crinoid stems calyxes & occasional brachiopod valves	Low energy suspension deposition

Figure 4.2

(A) Lithofacies 8: bioturbated packstone containing discontinuous shelly lags, cross-cut by burrows. (Barry Island).

(B) Parallel orientated crinoid stems occurring within the skeletal lag of a Lithofacies 8 bed (Barry Island). (Rose diagram plot is shown in Figure 4.3 denoted by a).

(C) Storm sediment burrow fill (T), surrounded by a finer grained wackestone (W), and connected to the overlying skeletal lag (L). (Rhossili).


A

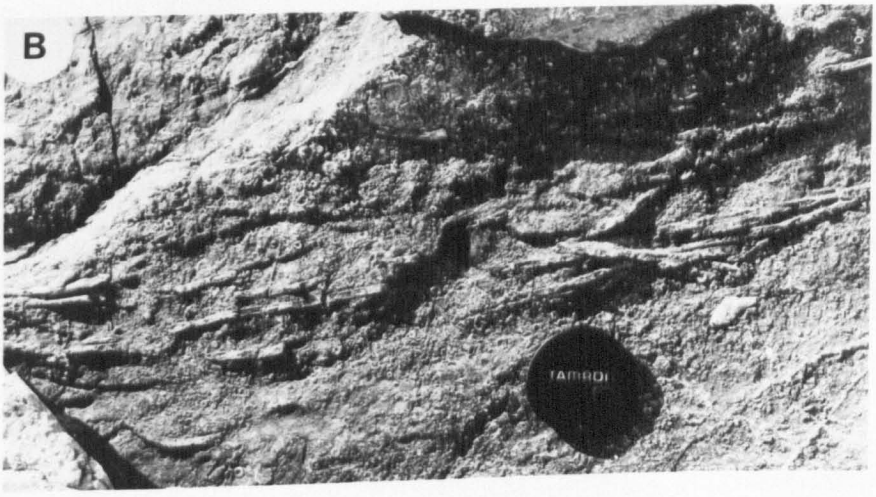
B
TAMRON

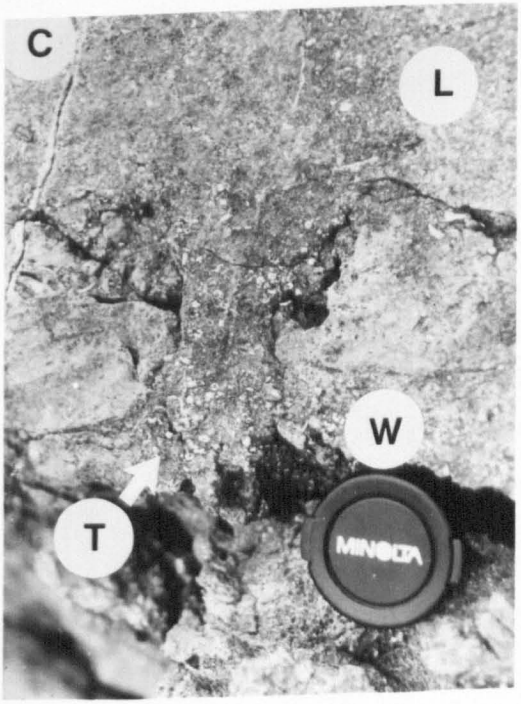
C
L
W
T
MINOLTA

delineated by a laterally-discontinuous skeletal lag (invariably less than 5cm thick) which is traceable up to a maximum distance of 10m. Disrupting the continuity of the lags are cross-cutting burrows (Figure 4.2A). The main constituents of the lags include convex-upward brachiopod valves and crinoid debris including stems. Measurements of the orientation of closely-packed crinoid stems (>>15cm in length) (Figure 4.2B) on a bedding plane surface at Barry, revealed a strong preferred NE-SW orientation (Figure 4.3 denoted by a). Composite results, taken from numerous bedding plane surfaces confirmed the NE-SW trend, although it was less well defined (Figure 4.3 denoted by b).

Lithofacies 8 contains a diverse fauna of crinoids, corals (mainly zaphrentoids), brachiopods and bryozoans. The faunal constituents are commonly disarticulated and apart from the bryozoans there is a minimal amount of fragmentation. The skeletal elements occur within a pale grey micrite which exhibits a diverse assemblage of trace fossils including *Thalassinoides*-type burrows, *Chondrites*, *Zoophycos*, and simple vertical and horizontal burrows. Two types of burrow fill have been recorded: coarse bioclastic packstones, and wackestones. The finer grained burrow fills are prevalent and include those burrows that disrupt the continuity of the skeletal lags (Figure 4.2A). The coarser grained burrow fills only occur immediately beneath the skeletal lags. The coarse skeletal burrow infill is connected to the overlying skeletal lag (Figure 4.2C).

Lithofacies 8 contains abundant dissolution seams, along which black argillaceous material is concentrated. Locally they occur immediately beneath the skeletal lags and exaggerate true bedding. More commonly, however, they are observed occurring within beds, giving the succession a 'pseudo-bedded' appearance (*sensus* Simpson 1985).

Chert nodules are present within Lithofacies 8, although

Figure 4.3. Graphic sedimentary logs of the Friars Point Limestone of South Wales. Including rose diagram plots of orientation of zaphrentoid corals and crinoid stems (denoted by a, b, c, d).

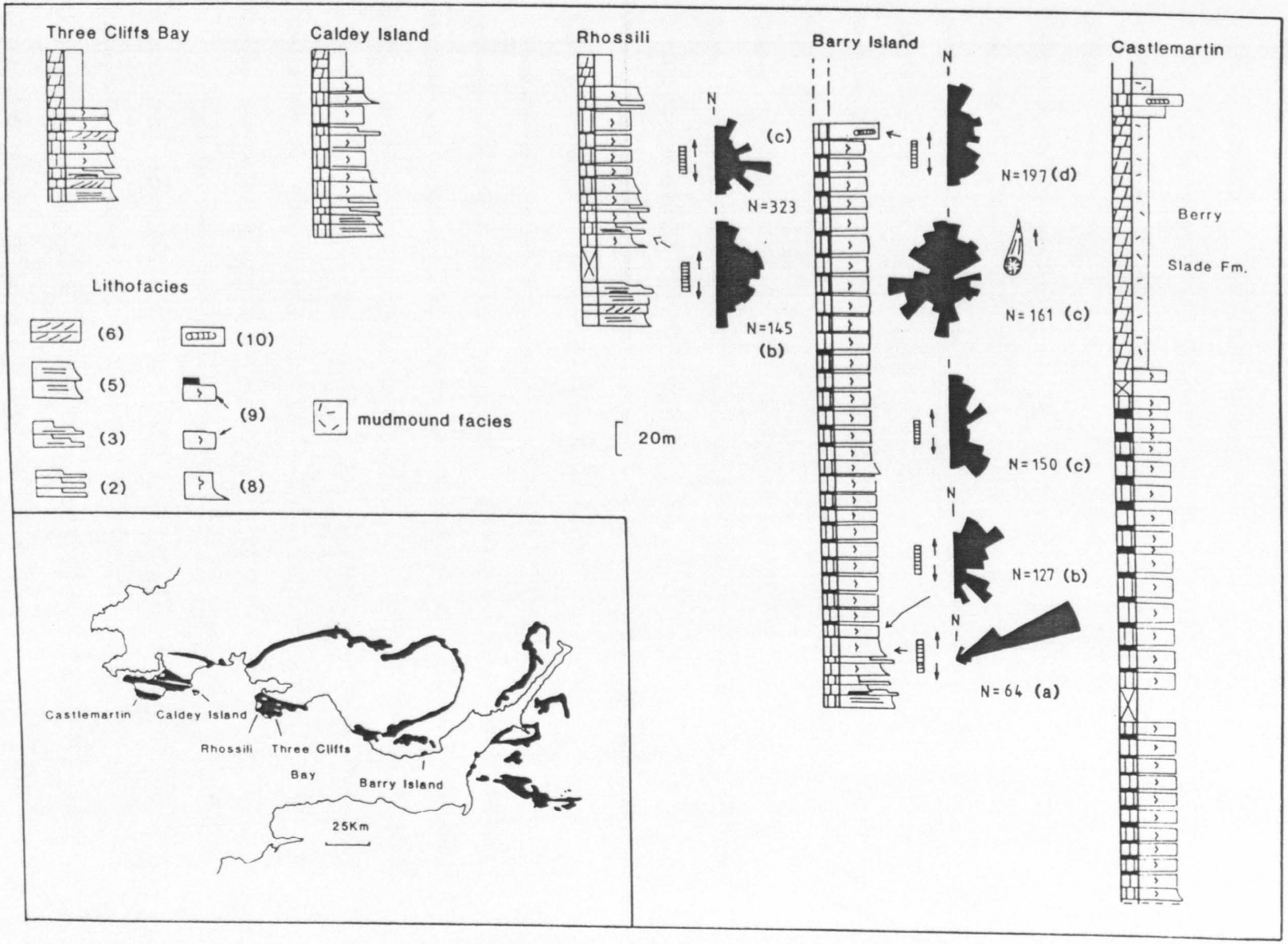
Three Cliffs Bay
Caldey Island
Rhossili
Barry Island
Castlemartin
Lithofacies
(6)
(5)
(3)
(2)
(10)
(9)
(8)
mudmound facies
20m
N
(c)
N=323
N=145
(b)
N=197 (d)
N=161 (c)
N=150 (c)
N=127 (b)
N=64 (a)
Berry
Slade Fm.
Castlemartin
Caldey Island
Rhossili
Three Cliffs
Bay
Barry Island
25Km

they are not particularly abundant. Where developed they tend to be small (<10cm in diameter) and black in colour.

Interpretation: The diverse fauna and array of biogenic structures record deposition in an open marine, low energy environment, below mean wave-base. Sedimentation was, however, influenced by (storm-related?) currents: as testified by the NE-SW alignment of the crinoid stems (Figure 4.3 denoted by a & b); the presence of laterally discontinuous skeletal lags and associated coarse-grained, bioclastic burrow fills (Figure 4.4). The burrow systems are considered to have been infilled penecontemporaneous with deposition of the overlying skeletal lag. Recently, a possible modern analogue has been described from Caicos Platform, British West Indies by Wanless *et al.* (1988). Here, tubular tempestites (storm sediment filled burrows) were deposited during the passage of Hurricane Kate.

4.3.2 *Lithofacies 9:* Thickly-bedded, bioturbated wackestones/packstones separated by shaly horizons

Lithofacies 9 forms decimetre to metre-thick beds of bioturbated, slightly argillaceous wackestones/packstones separated by fissile shaly/marly units (up to 1m thick) (Figures 4.1B, 4.5A). The latter commonly contain a plethora of dissolution seams along which clay material has been concentrated. The transitional contacts between the limestones and the fissile layers are slightly sinuous and laterally extensive.

Both the hard limestones and the fissile units contain a diverse fauna and ichnofauna. The fossil allochems include disarticulated crinoids; productid and chonetid brachiopods; stick and fenestral bryozoans; *Syringopora*, *Michelinia*, zaphrentoid and caninioid corals. The corals usually occur in life position, less commonly they are found on their sides and rarely upside-down (Figure 4.5B). Several of the

Figure 4.4. Proximality trend recognized within the Friars Point Limestone, showing the distribution of lithofacies as well as the occurence of tubular tempestites.

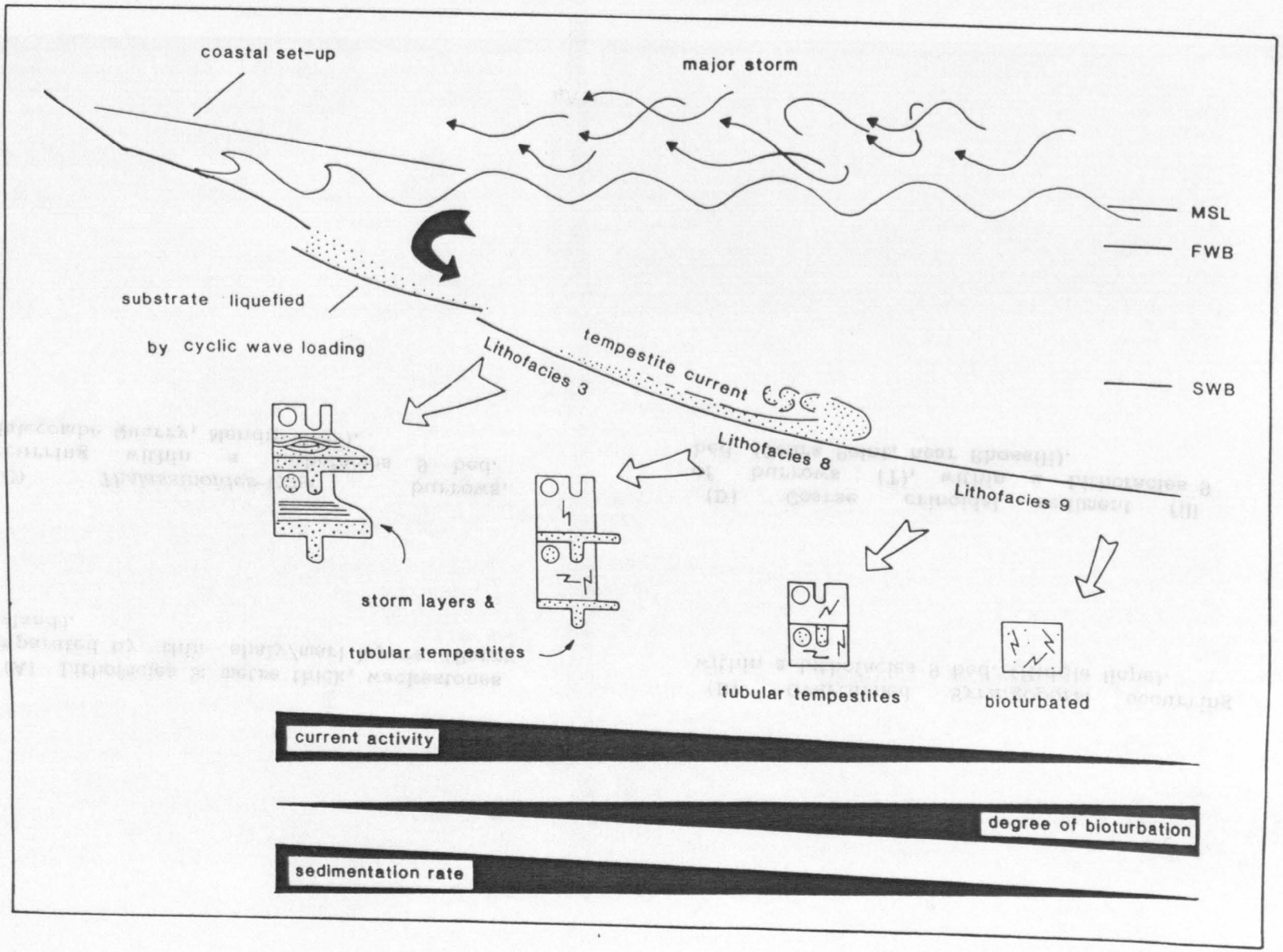
coastal set-up
major storm
MSL
FWB
SWB
substrate liquefied
by cyclic wave loading
tempestite current
Lithofacies 3
Lithofacies 8
Lithofacies 9
storm layers &
tubular tempestites
tubular tempestites
bioturbated
current activity
degree of bioturbation
sedimentation rate

Figure 4.5.

(A) Lithofacies 9: metre thick, wackestones separated by thin shaly/marl layers. (Barry Island).

(B) Overturned *Syringopora*, occurring within a Lithofacies 9 bed. (Middle Hope).

(C) *Thalassinoides*-type burrows, occurring within a Lithofacies 9 bed. (Halecombe Quarry, Mendip Hills).

(D) Coarse crinoidal sediment fill of burrows (T), within a Lithofacies 9 bed. (Tears Point, near Rhossili).

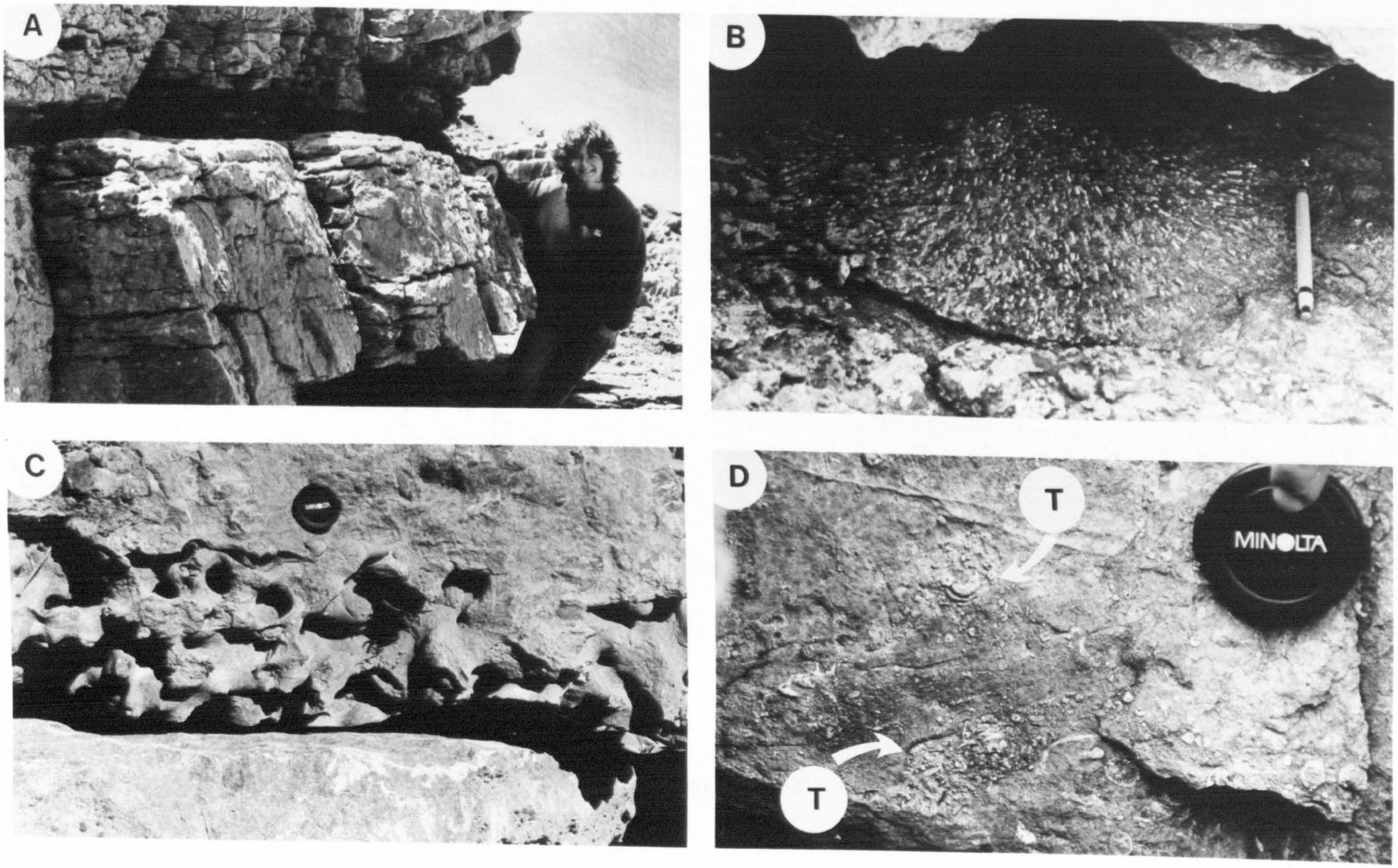
A
B
C
D
T
T
MINOLTA

overturned *Syringopora* colonies show notable inflexions in the growth directions of the corallites, passing along their length from being bedding-parallel to bedding-perpendicular. Overall, there is a tendency for the crinoid stems to have a wider diameter (up to 1cm) than those seen in the underlying facies (e.g. Lithofacies 8). Measurements of the orientation of crinoid stems and zaphrentoid corals on bedding plane surfaces at Barry Island, Rhossili and Middle Hope revealed either a poorly defined N-S trend or random arrangement (Figures 4.3 & 4.6 denoted by c).

Both the fissile units and the hard limestones are extensively bioturbated. The majority of the burrow systems are either infilled with micrite or fine grained crinoidal debris. Locally, coarser-grained bioclastic burrow fills can be observed within the wackestone layers (Figure 4.5D). The identification of such features was extremely difficult in the compacted shale units. Where developed, the coarse crinoidal burrow fills occur restricted within thin bands (<10cm thick) which are laterally extensive and parallel to bedding (Figure 4.5D).

The trace fossils identified include simple horizontal and vertical burrows, *Zoophycos*, *Planolites*, *Chondrites*, and *Thalassinoides*-type burrows. Within the Halecombe quarry (Appendix Q) in the Mendip Hills, *Zoophycos* is particularly prominent (up to 30cm across) and the intricate network of the *Thalassinoides*-type burrows are locally preserved in their original three dimensional form by chert (Figure 4.5C).

Chert is common in Lithofacies 9 and occurs both as discrete nodules and bedding-parallel sheets. On bedding plane surfaces, the latter commonly consists of a network of nodules (up to ten's of centrimetres thick) joined by thin layers of chert (usually less than 3cm in thickness).

Figure 4.6. Graphic sedimentary logs of the Friars Point Limestone (including Middle Hope volcanics) in SW England. In addition there are rose diagram plots of the orientation of crinoid stems (denoted by c) and cross-bed palaeocurrent vectors (denoted by e). Key to lithofacies symbols is shown in Figure 4.3)

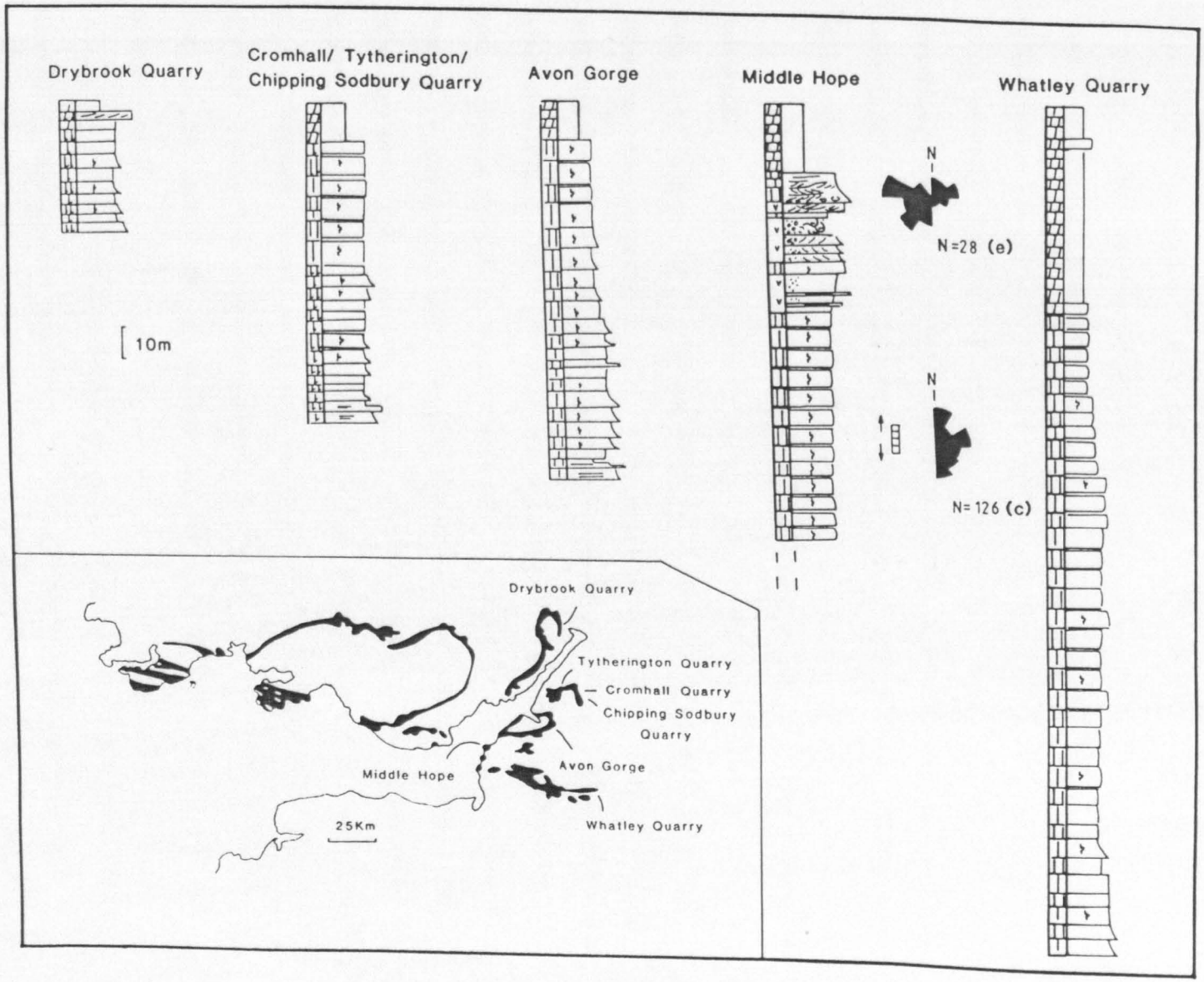
Drybrook Quarry
Cromhall/ Tytherington/
Chipping Sodbury Quarry
Avon Gorge
Middle Hope
Whatley Quarry
10m
N
N=28 (e)
N
N=126 (c)
Drybrook Quarry
Tytherington Quarry
Cromhall Quarry
Chipping Sodbury
Quarry
Avon Gorge
Middle Hope
25Km
Whatley Quarry

Interpretation: The diverse fauna, and array of biogenic structures contained within this fine grained, extensively bioturbated lithofacies is indicative of deposition in a low energy, open marine, offshore environment. The formation of the shaly layers containing abundant dissolution seams occurred as a result of compaction. The alternation of hard limestones separated by shaly layers is a common feature of slightly argillaceous platform and ramp limestones (Bathurst 1987). Bathurst (1987) proposed that the early cementation of the hard limestones caused the intense compaction of those layers which are poorly cemented.

The paucity of storm-related sedimentary structures would suggest deposition in an environment well *beneath* storm wave-base (Figure 4.4). The affects of (storm-related ?) currents operating below wave-base are recorded by the rare tubular tempestites. The restricted occurrence of the coarse-grained crinoidal burrow fills within bedding-parallel bands would seem to support a storm-related origin, rather than a biogenic process sorting the sediment such as described by Rhoads & Stanley (1965), Rhoads (1967) and Tudhope & Scoffin (1984). Other possible indicators of current activity include the overturned *Syringopora* colonies (Figure 4.5B) and the poorly defined N-S trend shown by the crinoid stems and zaphrentoid corals (Figures 4.3 & 4.6 denoted by c). The geniculate growth pattern in some of the *Syringopora* colonies is indicative of corallites growing upwards after being overturned.

The absence of event-beds is thought to be due to the homogenizing process of bioturbation which both obliterates sedimentary structures and mixes the deposits laid-down during 'foul-' and 'fair'-weather (Figure 4.4). In modern offshore shelf settings, the destruction of storm-related sedimentary structures by biogenic processes can occur within a

relatively short period after the passage of the storm. Resampling of the deposits laid-down by cyclone Winifred, one year after it impinged upon the Great Barrier Reef shelf, showed that there had been a complete obliteration of those features characteristic of storm sedimentation in the offshore environment (water depths exceeding 30m) (e.g. Gagan *et al.* 1988).

4.3.3 *Lithofacies 10:* Crinoidal stem-rich packstone

This pale grey packstone of decimetre-thick beds is dominated by bedding-parallel crinoid stems (up to 30cm in length) (Figures 4.1C & 4.7A). The matrix surrounding the crinoid stems includes crinoid ossicles (up to 2cm in diameter), plates of disarticulated calyxes, brachiopod valves and fragments of bryozoans. Lithofacies 10 forms the uppermost part of the section at Barry Island (Appendix H) and overlies the Berry Slade Formation at Castlemartin (Appendix B) (Figure 4.3).

Measurements of the orientation of crinoid stems, taken at Barry Island, show a random arrangment (Figure 4.3 denoted by d). At the same locality, the brachiopods are locally observed in layers, closely stacked upon one another in a convex-upward orientation (Figure 4.7B). Very few biogenic structures were recorded, where developed they tend to consist of simple short vertical or horizontal burrows. Chert nodules are rare and usually less than 5cm in diameter.

Interpretation: Poor sorting and preservation of abundant crinoid stems in a random orientation (Figure 4.7A), would suggest that they were deposited in an open marine subtidal environment. The origin of the skeletal elements is likely to be autochthonous. Evidence of currents is recorded by the rare stacked accumulation of convex-upward brachiopod valves at Barry Island (Figure 4.7B).

Tabular bedded sequences comprising a concentration of generally

Figure 4.7

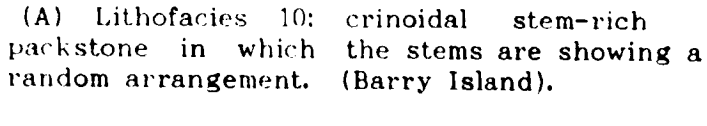

(A) Lithofacies 10: crinoidal stem-rich packstone in which the stems are showing a random arrangement. (Barry Island).

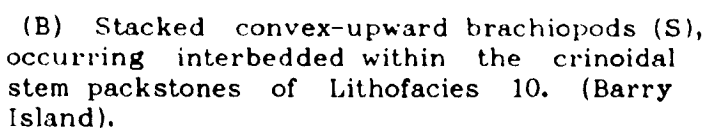

(B) Stacked convex-upward brachiopods (S), occurring interbedded within the crinoidal stem packstones of Lithofacies 10. (Barry Island).

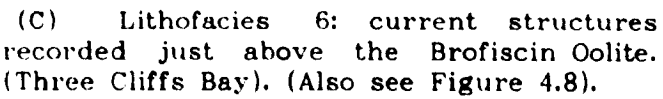

(C) Lithofacies 6: current structures recorded just above the Brofiscin Oolite. (Three Cliffs Bay). (Also see Figure 4.8).

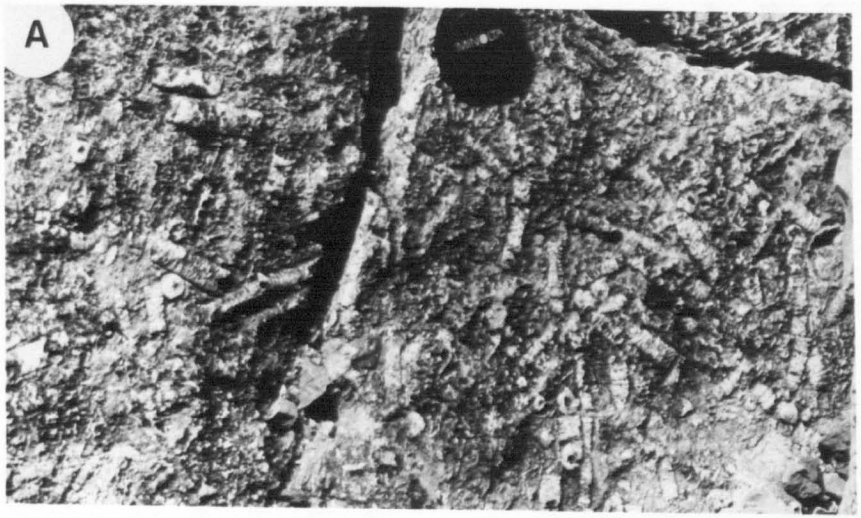
A

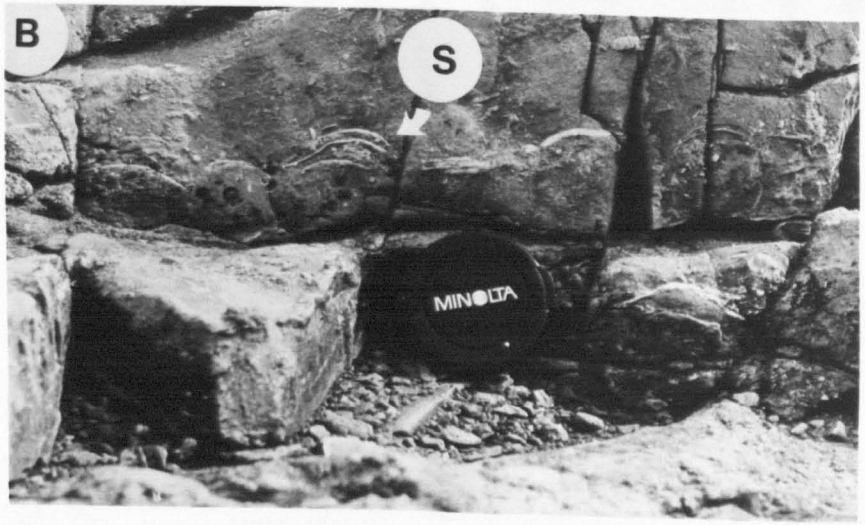
B
S
MINOLTA

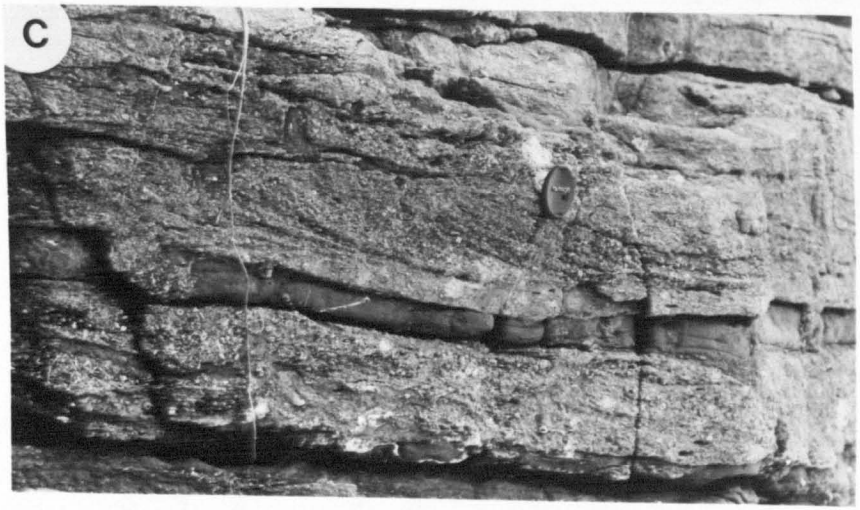
C

in-place carbonate skeletons are known as biostromes (James 1983). These localised occurrences of abundant crinoid stems are interpreted as crinoidal biostromes.

4.3.4 Black Rock Dolomite

Overall, the Black Rock Dolomite consists of massive, decimetre beds of slightly argillaceous, reddish-brown, saccharoidal dolomite in which pods of partially dolomitized crinoidal packstones and wackestones occur. The latter consist of disarticulated crinoid ossicles and show signs of bioturbation. The regular identification of burrow types is impossible owing to the replacive dolomite which has only left isolated relics of individual burrows.

Interpretation: Deposition of the bioturbated, crinoidal packstones and wackestones is thought to have been in a low energy, probably subtidal environment. Unfortunately, any further evaluation of the depositional environment is hampered by the lack of relict sedimentary features preserved within the replacive dolomite. However, the overall appearance of the crinoidal packstone/wackestone pods is similar to Lithofacies 9. In the absence of storm-related sedimentary structures deposition beneath the storm-wave base is suggested. If such a comparison between the above is valid then the environment of deposition was likely to have been mainly subtidal, and probably beneath 'storm wave-base'.

4.4 Temporal and spatial distribution of the lithofacies

The Friars Point Limestone Formation shows ca. a 7 fold increase in thickness from the thinnest measured development at Drybrook Quarry (ca. 40m) to the thickest development at Castlemartin (280m) (Figures 4.3 & 4.6). A summary of the distribution of the different lithofacies is shown in Figure 4.8. The lower part of the succession comprises a sequence of

Figure 4.8 Temporal and lateral distribution of the lithofacies recognized within the Friars Point Limestone.

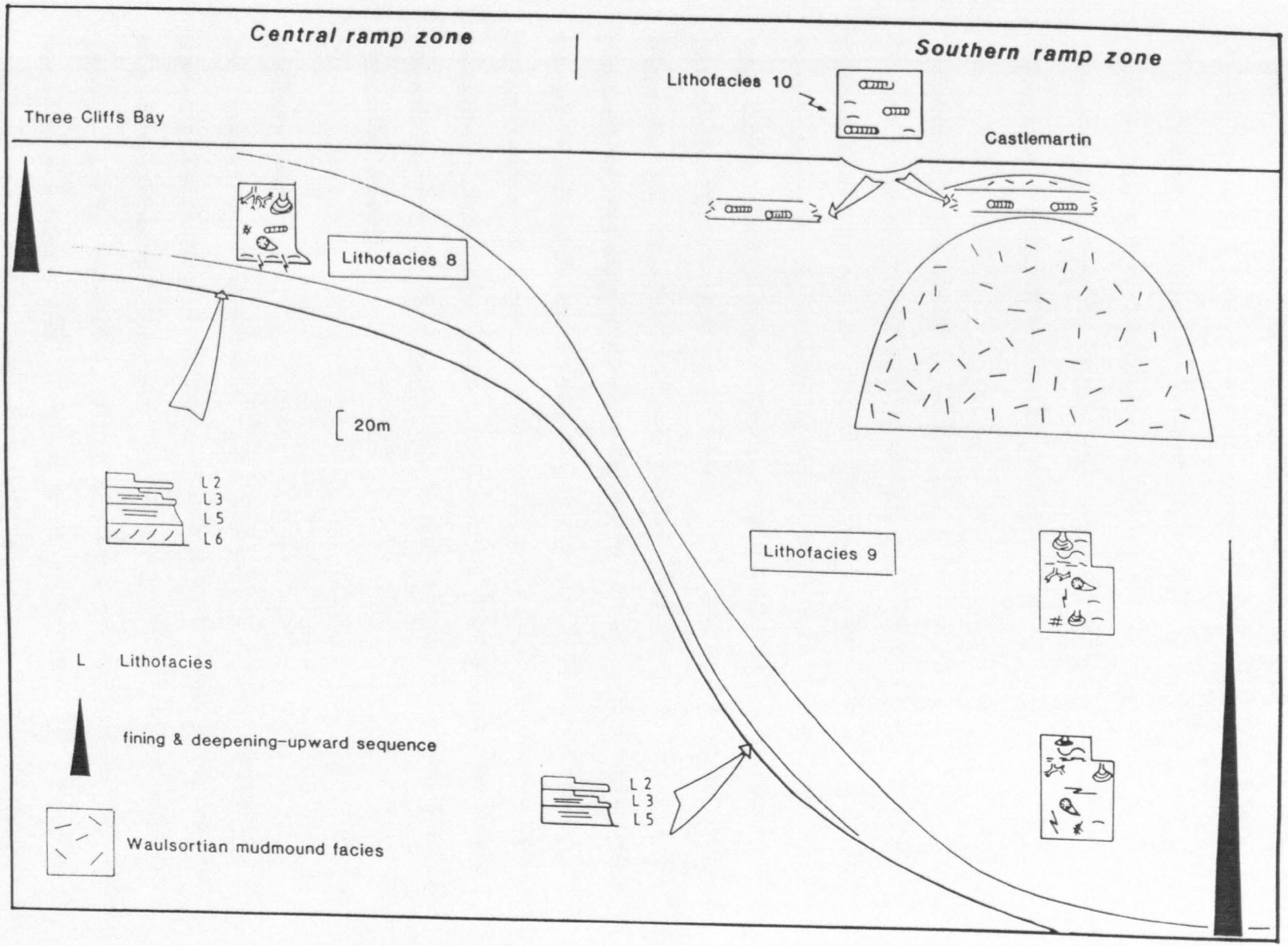
Central ramp zone
Southern ramp zone
Three Cliffs Bay
Lithofacies 10
Castlemartin
Lithofacies 8
20m
L 2
L 3
L 5
L 6
Lithofacies 9
L Lithofacies
fining & deepening-upward sequence
Waulsortian mudmound facies
L 2
L 3
L 5

bioclastic limestones. In stratigraphic order they are represented by Lithofacies 6, 5, 3 & 2 (previously described in Chapter 3), above which the thickest developments of Lithofacies 8 occur in the northern and central ramp zones. Lithofacies 9 dominates the successions of the southern ramp zone in which the minor Lithofacies 10 and the rare Waulsortian mudmounds occur (Figure 4.8).

Northern & Central Zones

Decimetre bedded, bioturbated packstones and shelly lags (Lithofacies 8) dominate the sections at Three Cliffs Bay (Appendix F) and Caldey Island (Appendix D). Here, Lithofacies 8 can locally be found interbedded with ungraded sedimentary couplets (Lithofacies 2) and rare, graded beds (Lithofacies 3). In Tytherington Quarry (Appendix J), Cromhall Quarry (Appendix K), Chipping Sodbury Quarry (Appendix L) and the Avon Gorge (Appendix M) the skeletal lags of Lithofacies 8 can be identifed even though the fresh fracture surfaces reveal few sedimentary features. Much of the section at Drybrook Quarry (Appendix I) has been extensively dolomitized but relict skeletal lags (up to 5cm thick) can be found. Towards the top of the succession a low-angle cross-bed was identified within the dolomite.

Southern Zone

The extensively bioturbated wackestones/packstones (Lithofacies 9) dominate the sections at Middle Hope (Appendix O), Barry Island (Appendix H) and Castlemartin (Appendix B). Unfortunately, very few sedimentary features can be observed in the fresh fracture surfaces of the quarry faces in the Mendip Hills at Halecombe (Appendix Q) and Whatley (Appendix R). However, towards the uppermost part of both successions there are rare crinoidal lags (up to 4cm thick). Occurring within the

uppermost parts of the Barry Island and Castlemartin successions are the crinoidal stem-rich packstones of Lithofacies 10 (Figure 4.8).

4.5 Discussion

The main purpose of this discussion is to evaluate the offshore, depth-related facies trend in the main part of the Friars Point Limestone, overlying the basal transgressive sequence. In addition, the subsidence history of the basin and its effect upon the distribution of the lithofacies will be assessed using the biostratigraphic zones as viable time-lines.

4.5.1 Basal Transgressive Sequence

The basal part of the Friars Point Limestone Formation forms a fining- and deepening upward sequence (5-15m thick) (Figure 4.8). In the central ramp zone, the sequence commences with cross-bedded bioclastic limestones (Lithofacies 6, Figure 4.7C) representing deposition in above fairweather-wave base environment. It passes transitionally upward into the subtidal storm-dominated facies of amalgamated and graded storm beds (Lithofacies 5 & 3) which are overlain by the below mean wave base facies of ungraded sedimentary couplets (Lithofacies 2) (Figure 4.8). The transition upward into Lithofacies 8 is recorded by the decrease in the abundance of the storm layers, partly as a result of their obliteration by biogenic processes. The transgressive sequence in the southern zone is comparable but commences from amalgamated and graded storm beds (Lithofacies 5 & 3) and passes upward, over a short vertical distance of less than 20m, into the below storm-wave base facies of Lithofacies 9 (Figure 4.8).

The overall upward decrease in current energy as a result of the transgression, is reflected in the alignment of the crinoid stems. Those

measurements taken from skeletal lags, where Lithofacies 8 occurs interbedded with Lithofacies 2 and 3, show a prefered orientation towards the NE-SW (Figures 4.3 denoted by a & b). Whereas in the main part of the Friars Point Limestone succession in the southern ramp zone (Lithofacies 9) the orientation of the crinoid stems is either random or shows a poorly defined N-S alignment (Figures 4.3 & 4.6 denoted by c).

4.5.2 Proximality Trend

The three lithofacies types described, conspicuously lack those sedimentary structures characteristic of sedimentation from tractional currents, and record deposition in a below storm-wave base environment. From an analysis of the distribution of the lithofacies two major ramp facies belts can be recognized. The more proximal, inner facies belt, includes those sequences of the northern and central ramp zone which record the affects of storm-related currents operating in the below wave base environment (i.e. Lithofacies 8). The outer facies belt contains few current related features and consists of extensively bioturbated limestones (Lithofacies 9), rare crinoidal biostromes (Lithofacies 10) and Waulsortian mudmounds. The preservation of the effects of current activity within Lithofacies 10 is thought to be due to the low degree of biogenic activity. Presumably, the substrate of coarse crinoidal debris was unsuitable for extensive infaunal colonization and biogenic reworking.

The distribution and nature of the tubular tempestites also conforms to the proximality trend (Figure 4.4). Within Lithofacies 8, they are connected to a recognizable storm layer (Figure 4.2C). This is in marked contrast to those found in the lower parts of of the sequence of Lithofacies 9, where the tubular tempestites are not associated with any recognizable skeletal lag (Figure 4.5D). This could either be due to an

insufficient supply of coarse skeletal material to produce a skeletal lag, or the storm layers were thin enough to be subsequently obliterated by biogenic reworking. Nevertheless, the presence of tubular tempestites records the effects of current activity. Within the main part of the Lithofacies 9 succession, there is a conspicuous absence of tubular tempestites which is considered to represent deposition in a more distal setting (Figure 4.4).

In conclusion, the dipartite distribution of Lithofacies 8 and 9 conforms to two depth-related facies belts (Figure 4.4) which were most probably arranged parallel to the palaeo-shoreline, located further to the north.

4.5.3 Biofacies

The environmental gradient across the ramp may well have had an effect upon the distribution of the fauna. Basic field observations reveal that the abundance of the corals is conspicuously greater in the southern ramp sequences. A study of the stratigraphic distribution of corals and conodonts against the sedimentary facies shows that the former is clearly facies related whereas the latter is only partly facies controlled (Figures 4.9 & 4.10).

Coral biozones

The base of the *Zaphrentites delanouei* Zone occurs in close-proximity to the lithological contact between the Lower Limestone Shale and Black Rock Limestone (Mitchell 1980). From a comparison of the coral assemblages with the lithofacies assemblages, it is apparent that the zaphrentoid corals have a wide facies distribution (Figure 4.9). They are present both within the shallow water succession of the Barry Harbour Limestone and the deeper water facies of the Friars Point Limestone (Figure 4.9). Whereas the

Figure 4.9. The relationship between the lithostratigraphy of the Black Rock Limestone Group, the sedimentary lithofacies recognized and the distribution of zaphrentoid and caninioid corals. Key to lithofacies symbols are shown in Figure 4.3.

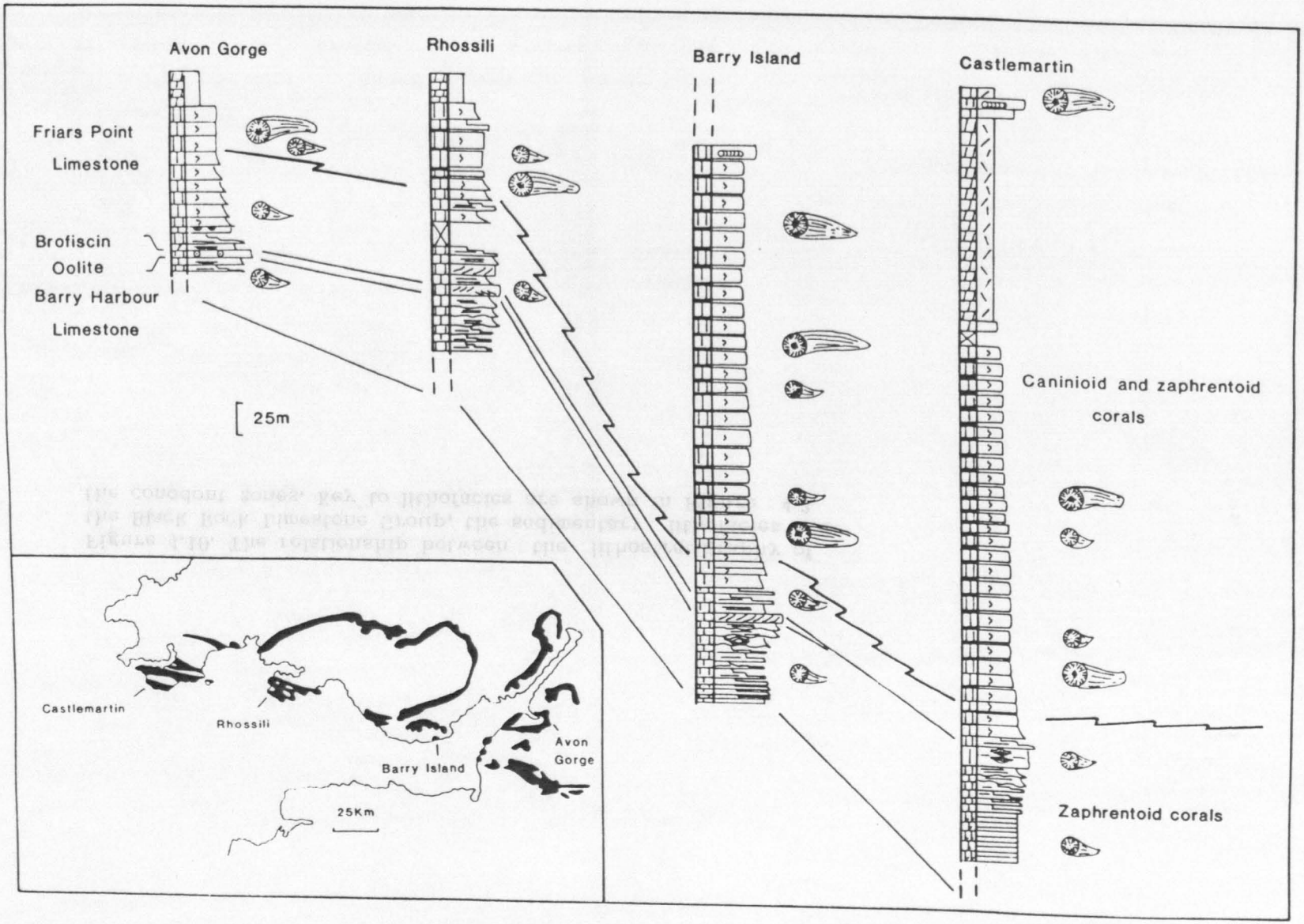
Avon Gorge
Rhossili
Barry Island
Castlemartin
Friars Point
Limestone
Brofiscin
Oolite
Barry Harbour
Limestone
25m
Caninioid and zaphrentoid
corals
Zaphrentoid corals
Castlemartin
Rhossili
Barry Island
Avon
Gorge
25Km

Figure 4.10. The relationship between the lithostratigraphy of the Black Rock Limestone Group, the sedimentary lithofacies and the conodont zones. Key to lithofacies are shown in Figure 4.3.

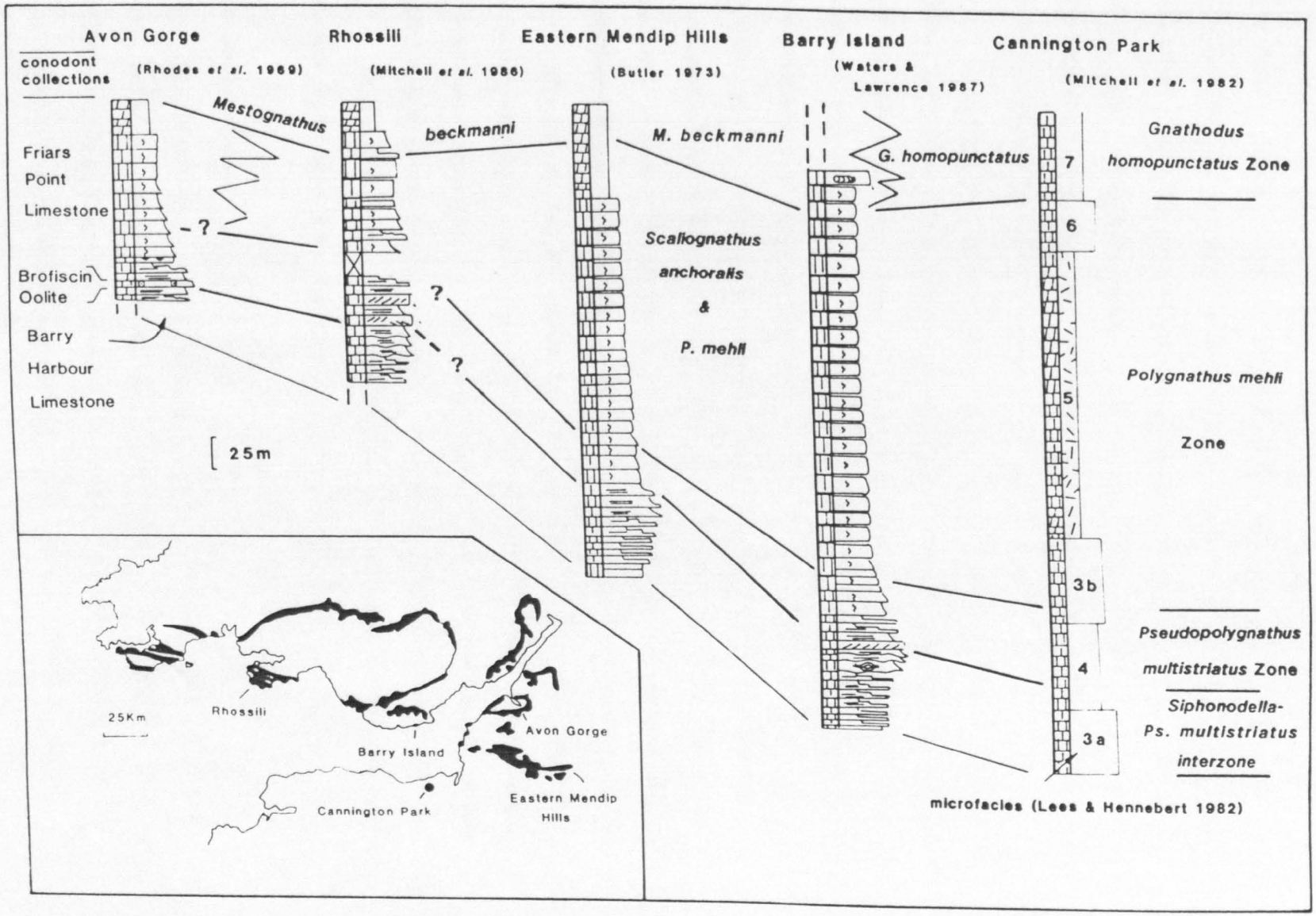
Avon Gorge
Rhossili
Eastern Mendip Hills
Barry Island
Cannington Park
conodont collections
(Rhodes et al. 1969)
(Mitchell et al. 1986)
(Butler 1973)
(Waters & Lawrence 1987)
(Mitchell et al. 1982)
Mestognathus
beckmanni
M. beckmanni
G. homopunctatus
Friars Point Limestone
Brofiscin Oolite
Barry Harbour Limestone
Scalognathus anchoralis & P. mehli
25m
7
6
5
3b
4
3a
Gnathodus homopunctatus Zone
Polygnathus mehli Zone
Pseudopolygnathus multistriatus Zone
Siphonodella-Ps. multistriatus interzone
microfacies (Lees & Hennebert 1982)
25Km
Rhossili
Barry Island
Avon Gorge
Cannington Park
Eastern Mendip Hills

caninioid corals (e.g. *Caninophyllum patulum* and *Siphonophyllia cylindrica*) are restricted to the deeper water facies. The northward migration of the caninioid corals, from the southern to central ramp zone, was seemingly related to the prolonged Friars Point Limestone transgression, causing the shoreward migration of the deeper water facies belt of Lithofacies 9 (Figures 4.8 & 4.9).

A variety of depth-related fossil communities have been described from the Lower Carboniferous of Britain by Ramsbottom (1978) and Beus (1984). Unfortunately, none of the associations described by the above authors are readily comparable to the shallow-water zaphrentoid and brachiopod assemblages of the lower part of the Black Rock Group. The shallow water communities of post-Courceyan age contain caninioid corals (Ramsbottom 1978; Beus 1984). The caninioid corals that lived in shallow water environments tended to be large to withstand the turbulent waters (Ramsbottom 1978).

The faunal association in the upper part of the Black Rock Group includes abundant small caninioids corals and smooth shelled brachiopods, which are comparable to the deep water *Rhipidomella* association of Beus (1984) and the brachiopod calcarenite community of Ramsbottom (1978).

In conclusion the incoming of the zaphrentoid and caninoid corals appears to be strongly influenced by sedimentary facies.

Conodont biozones

A plot of the conodont zones against the lithological formations of the Black Rock Group are shown in Figure 4.10. The base of the *Ps. multistriatus* Zone does not appear to be facies controlled as it occurs in a large variety of different ramp facies types, including: oolitic,

bioclastic and micritic limestones (Waters & Lawrence 1987; Mitchell *et al.* 1982; Lees & Hennebert 1982). A regional study of the base of *Ps. multistriatus* in Ireland and Britain by Sevastopulo & Nudds (1987) concluded that it is not strongly facies controlled, and is a viable zone with regard to time correlation.

The base of the *Polygnathus mehli* Zone does not appear to be facies controlled. However, as the main part of the Friars Point Limestones consists of deep water ramp facies it is extremely difficult to certify such an interpretation solely from a study of its occurrence in SW Britain. A regional investigation in Ireland by Sevastopulo & Nudds (1987) noted that the base of the *P. mehli* Zone does not appear to be associated with any consistent lithological change, and as a result it is considered not to be facies controlled.

The uppermost part of the Friars Point Limestone contains two zones which are clearly facies related. *Mestognathus beckmanni* tends to be associated with shallow-water facies while *Gnathodus homopunctatus* is more abundant in distal ramp facies (Austin & Davies 1984) (Figure 4.10).

4.5.4 Biostratigraphic Time-Lines

An assessment of the effect of differential subsidence across an area is relient upon subdividing the succession into isochronous units. Ideally, faunal zones are time equivalents. Regional plots of the thickness variation of each zone should permit an evaluation as to the relative timing and effects of differential subsidence.

A synthesis of the isochroneity of the upper Courceyan coral and conodont zones of SW Britain and Ireland has been published by Sevastopulo & Nudds (1987). This revealed that the bases of the coral zones do not consistently appear at the same relative positions as the conodont zones. For example, in those sections in a more distal setting the first

appearance of the caninioid corals is within the *Ps. multistriatus* Zone (e.g. Cannington Park & Barry) (Lees & Hennebert 1982; Waters & Lawrence 1987). Whereas in the more proximal sections the caninioid corals first appear towards the end of the overlying *P. mehli* Zone (e.g. Rhossili) (compare Figures 4.9 & 4.10). Sevastopulo & Nudds (1987) went on to suggest that the conodont zones represent a more accurate guide to time correlation because they are evolutionary lineages and are not linked to lithology. The basis of the coral zones reflect the occurrences of cryptogenic taxa (unknown phyletic origin), whose distributions were judged by the above authors to be strongly controlled by facies - a point which they did not elaborate upon.

It would seem that conodont zones offer the best means by which to subdivide the Courceyan into seemingly isochronous biostratigraphic units. Although it must be appreciated that those faunas characteristic of a zone may well be partly facies controlled e.g. *Mestognathus beckmanni* (Austin & Davies 1984).

Using the conodont zones and lithostratigraphy, the Friars Point Limestone can be subdivided into three units. For convenience the lower unit is taken as that part of the *Ps. multistriatus* Zone above the Brofiscin Oolite and Barry Harbour Limestone (Figures 4.10 & 4.11). This seems a viable proposition, since the base of the *Ps. multistriatus* Zone consistently occurs in close-proximity to this regionally significant facies boundary (Waters & Lawrence 1987). The middle unit consists of the *P. mehli* Zone which is bounded by the base of the overlying *Mestognathus beckmanni* Zone (Figures 4.10 & 4.12). The upper unit includes that part of the *Mestognathus beckmanni* Zone beneath the Gully Oolite (Figures 4.10 & 4.12). Unfortunately, the upper surface of this unit cannot be delineated in the southern ramp zone, as the Black Rock Group passes transitionally upward into the

Figure 4.11 Plots of the thickness variation of the Friars Point Limestone within the *Ps. multistriatus* Zone and a facies model of the transgressive sequence (Also see Figure 4.10).

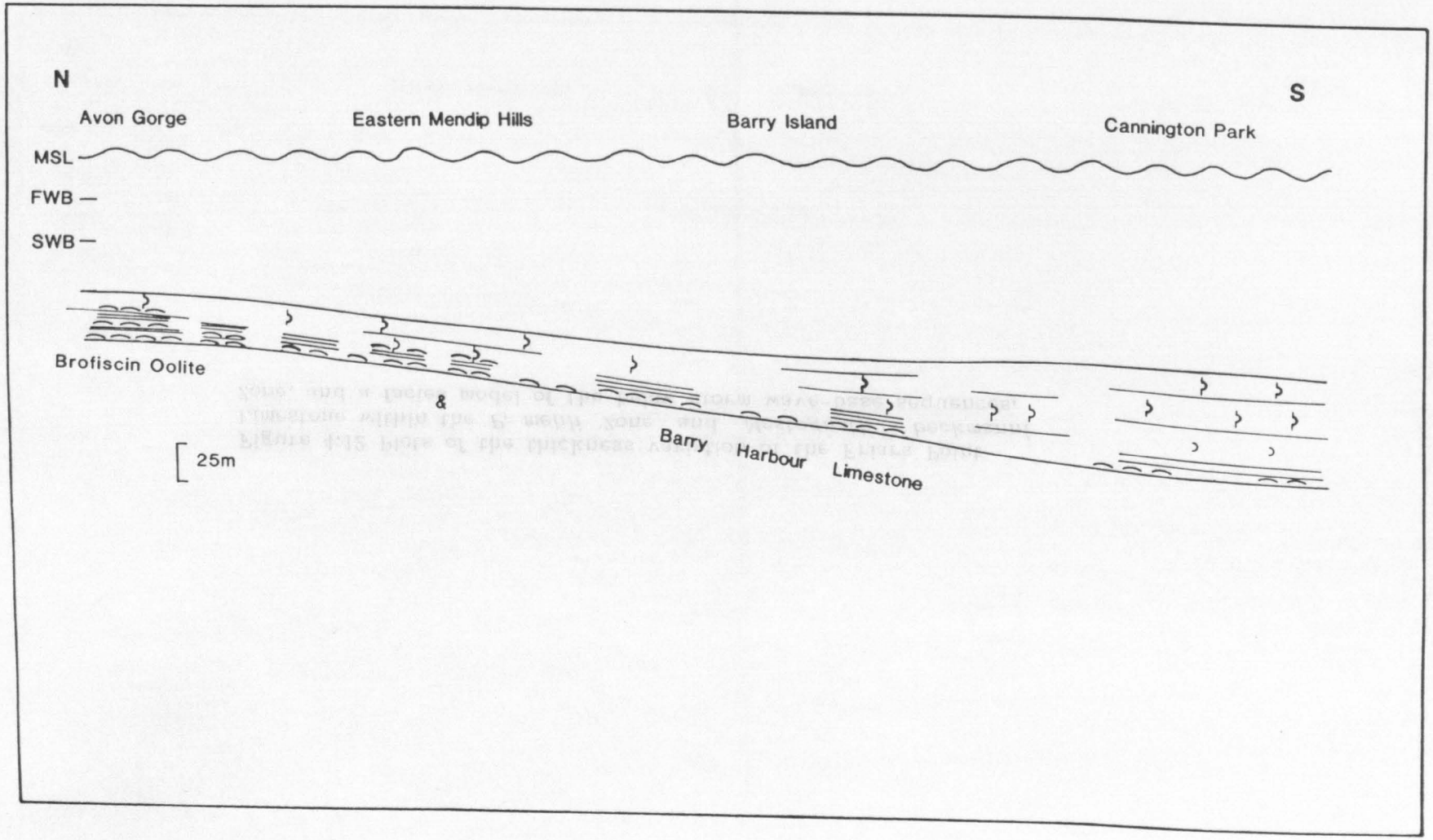
N
S
Avon Gorge
Eastern Mendip Hills
Barry Island
Cannington Park
MSL
FWB
SWB
Brofiscin Oolite
&
Barry Harbour Limestone
25m

Figure 4.12 Plots of the thickness variation of the Friars Point Limestone within the *P. mehli* Zone and *Mestognathus beckmanni* Zone, and a facies model of the below storm wave-base sequences.

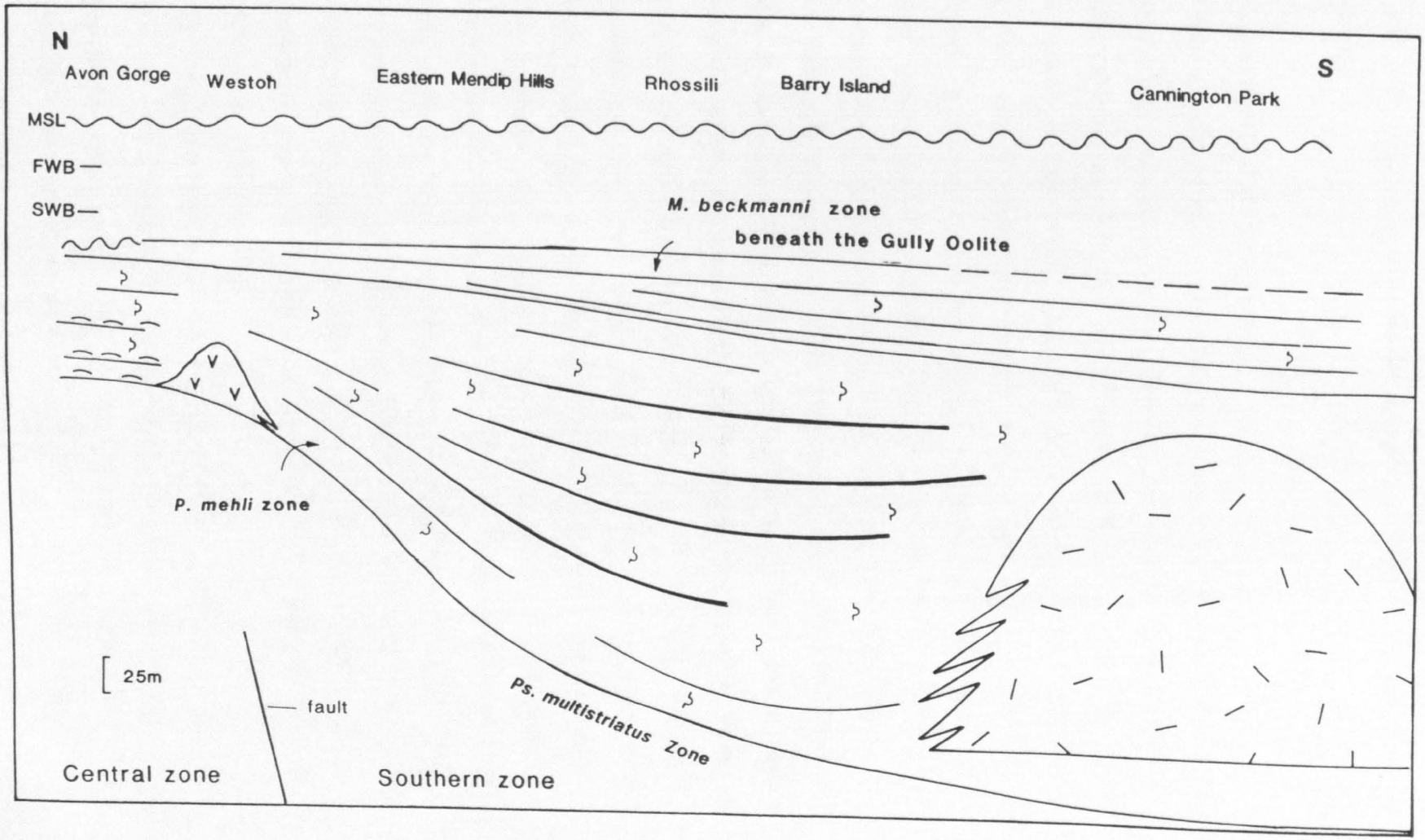
N
S
Avon Gorge
Westoh
Eastern Mendip Hills
Rhossili
Barry Island
Cannington Park
MSL
FWB
SWB
M. beckmanni zone
beneath the Gully Oolite
P. mehli zone
25m
fault
Ps. multistriatus Zone
Central zone
Southern zone

overlying mid-Chadian succession of crinoidal limestones without a change in lithology.

4.5.5 Sedimentation and Tectonics

To develop a thick (>100m) succession of below wave base facies, requires a relative rise in sea level to be greater or equal to the net rate of carbonate production (Kendall & Schlager 1981). In addition to the relative rise in sea level, carbonate sedimentation across SW Britain during the upper Courceyan period was influenced by differential subsidence. A marked increase in the thickness of the Friars Point Limestone occurs to the south of an east-west line between Weston-super-Mare, Cardiff, Cowbridge and Three Cliffs Bay (Waters 1984; Waters & Lawrence 1987; Wilson *et al.* 1988; Wright 1984a; Wright 1986). To the north of this line, the Friars Point Limestone of the central ramp zone has a relatively uniform thickness, most probably forming part of the stable Welsh-Brabant Massif (Figures 4.3 & 4.6). Overall, sedimentation across the basin kept pace with the differential subsidence to maintain a shallowly inclined carbonate ramp configuration.

To evaluate the relative timing and effect of differential subsidence requires the use of the isochronous units established in the preceding section 4.5.4. Contained within the lower unit is the basal transgressive sequence of the Friars Point Limestone which culminates in the establishment of below storm-wave base facies across the study area. The geometry of this unit is that of a southerly thickening uniform wedge (up to 90m thick) (Figure 4.11).

The overlying middle unit (*P. mehli* Zone) consists of a montonous succession of thickly-bedded, bioturbated limestones (Lithofacies 9); rare Waulsortian mudmounds (Mitchell *et al.* 1982) as well as the Middle Hope volcanics - Weston-super-Mare (Whittaker & Green 1983) (Figure 4.12).

This middle unit also forms a southerly thickening wedge but shows a pronounced thickening of the succession to the south of Caldey Island, Rhossili, Cardiff-Cowbridge, and Weston-super-Mare (Figure 4.12). This is considered to be in response to the vertical movement of a major hinge-line, most probably a fault at depth, which is locally known as the Vale of Glamorgan axis (Waters 1984; Waters & Lawrence 1987; Wilson *et al.* 1988). The upper unit forms a uniformly southward thickening wedge (Figure 4.12) consisting mainly of the Black Rock Dolomite and Lithofacies 10 (Figure 4.10).

In conclusion, the timing for the main phase of differential subsidence occurred early during the *P. mehli* Zone, the onset of which was signified by volcanic activity in the Weston-super-Mare area. The tectonic evolution of the Friars Point Limestone is analogous to the structurally controlled block and basin configuration that occurred north of the Welsh-Brabant Massif during the Lower Carboniferous. Here, extensional faulting in the underlying basement produced a series of NE to SW orientated blocks separated by areas of high subsidence which formed the basins (Bott 1967 & 1987; Johnson 1967; Leeder 1976, 1982 & 1987; Miller & Grayson 1982; Grayson & Oldham 1987).

Differential subsidence played an important role in the distribution of the facies within the main part of the Friars Point Limestone. Those successions to the north of the tectonic hinge-line typically contain sedimentary features indicative of storm-related currents influencing sedimentation (e.g. Lithofacies 8). Whereas, the thicker successions in the southern ramp zone, are dominated by the deepest water facies (Lithofacies 9, 10 and Waulsortian mudmounds) which lack evidence of current activity.

4.6 Conclusions

1) The Friars Point Limestone records a basinwide transgression above the the locally exposed Brofiscin Oolite and subtidal facies of the Barry Harbour Limestone.

2) Two distinct offshore ramp facies belts are recognized. The more proximal inner facies belt was influenced by storm-related currents. It contains tubular tempestites (storm sediment-filled burrows) which are connected to thin shelly lags. The finer-grained, outer facies belt is extensively bioturbated and preserves fewer features indicative of deposition from storm-related currents.

3) The pronounced differential subsidence to the south of the Vale of Glamorgan axis commenced early during the *P. mehli* Zone, the onset of which was signified by volcanic activity at Middle Hope (Weston-super-Mare).

4) Differential subsidence was instrumental in maintaining the temporal and spatial configuration of the proximal (mid-ramp) and distal (outer ramp) facies belts.

Chapter 5 - The Middle Hope volcanics of Weston-super-Mare: Development and demise of an offshore volcanic high

5.1 Introduction

During the Dinantian there was a widespread and prolonged period of volcanic activity over what is now Britain. Those areas which were affected by volcanism include the Scottish Midland Valley, the Northumberland Trough, the Isle of Man, the Derbyshire Block, the English Midlands, SW Britain (Upton 1982). Generally, the vents from which the tuffs and lavas erupted were relatively small and short-lived, even during the period of maximum activity in the Courceyan (Upton 1982). The lavas and pyroclastics lie interbedded with marine and non-marine deposits. The sedimentary structures preserved in such deposits record the buildup of the volcanic centres and their subsidence histories subsequent to the cessation of volcanic activity.

The Lower Carboniferous Middle Hope volcanics, just north of Weston-super-Mare, contains a diverse range of sedimentary structures which record the aggradation of a volcanic high in an offshore setting, on deposits of a carbonate ramp. Analysis of the sedimentary facies allows the detailed nature of volcanic buildup to be determined. This study of the Middle Hope volcanics forms the basis of Faulkner (1989). In addition, this chapter contains a pilot geochemical study of pillow basalt in an attempt to evaluate their tectonic significance.

5.2 Background

Extrusive igneous rocks have long been recognized in the Weston district (see historical summary of Morgan & Reynolds 1904) and were shown to occur at two distinct stratigraphic levels (Sibly 1905) (Figure 5.1). The older volcanics occur within the Black Rock Limestone at Middle Hope (Appendix O), whereas the younger development occurs east of Birnbeck Pier in the lower Birnbeck Limestone (Figure 5.1) at Spring Cove

Figure 5.1. Cross-section of the lower Lower Carboniferous Limestone in the Bristol - Weston-super-Mare district. Taken from Whittaker & Green (1983).

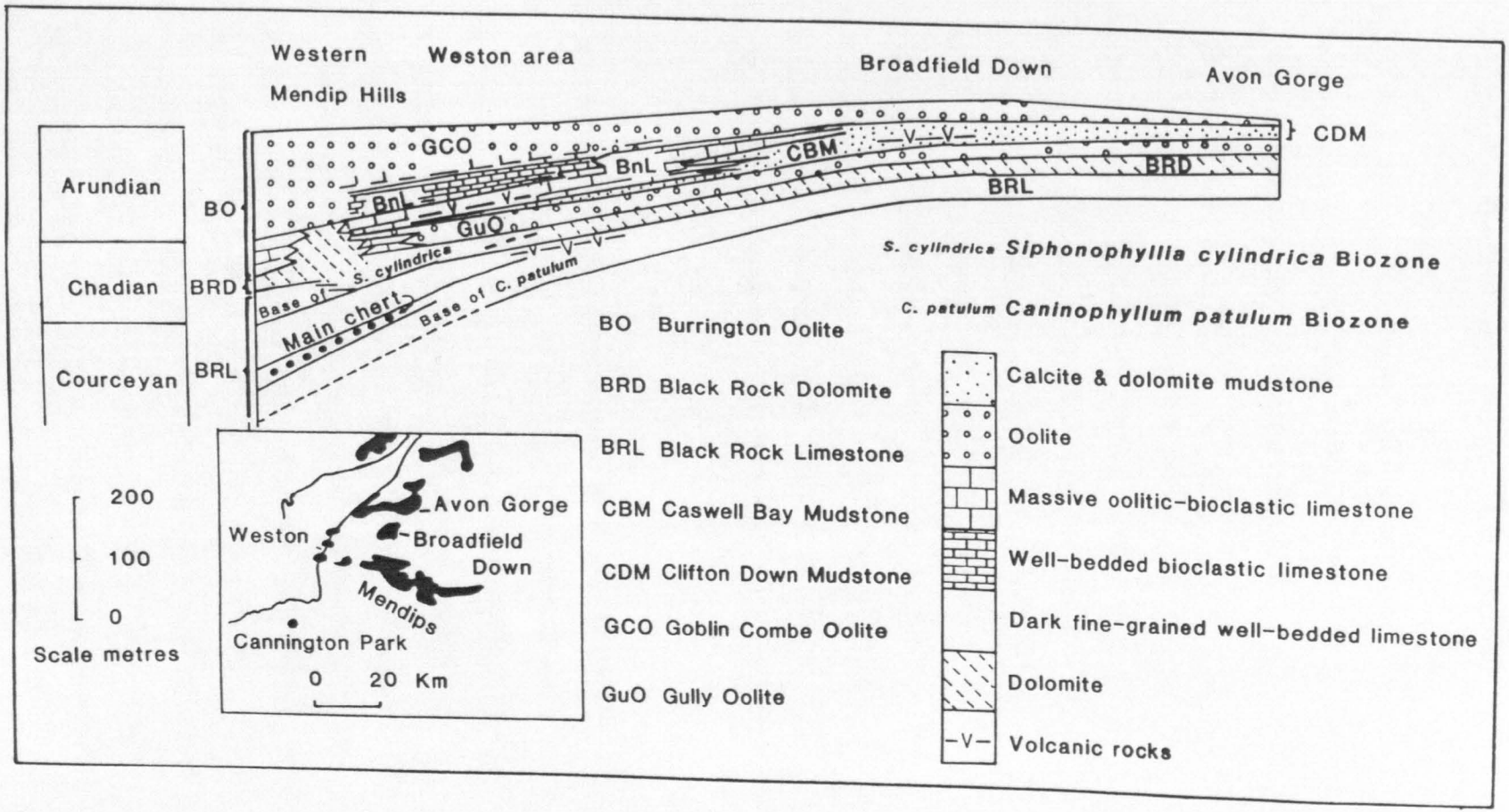
Western Mendip Hills
Weston area
Broadfield Down
Avon Gorge
CDM
GCO
BnL
CBM
BRD
BRL
Bnl
GuO
S. cylindrica
Base of
Main chert
Base of C. patulum
Arundian
Chadian
Courceyan
BO
BRD
BRL
S. cylindrica Siphonophyllia cylindrica Biozone
C. patulum Caninophyllum patulum Biozone
BO Burrington Oolite
BRD Black Rock Dolomite
BRL Black Rock Limestone
CBM Caswell Bay Mudstone
CDM Clifton Down Mudstone
GCO Goblin Combe Oolite
GuO Gully Oolite
Calcite & dolomite mudstone
Oolite
Massive oolitic-bioclastic limestone
Well-bedded bioclastic limestone
Dark fine-grained well-bedded limestone
Dolomite
Volcanic rocks
200
100
0
Scale metres
Avon Gorge
Weston
Broadfield Down
Mendips
Cannington Park
0 20 Km

(Speedyman 1977; Jeffreys 1979; Jeffreys & Aigner 1982; Whittaker & Green 1983).

The volcanic deposits at Middle Hope are seen in four exposures along the north coast of the peninsula (Figure 5.2) and were numbered 1 to 4 by Morgan & Reynolds (1904). Their lithostratigraphic position is above the main cherts of the Black Rock Limestone and beneath the Black Rock Dolomite (Figure 5.1). Situated in the *Caninophyllum patulum* Assemblage Biozone (Mitchell 1980) and the *P. mehli* conodont Biozone. The Middle Hope volcanics are immediately overlain by a cross-bedded bioclastic limestone which is not seen in equivalent sections to the north (e.g. in the Avon Gorge) and the south (e.g. in the western Mendip Hills).

The main phases of volcanic activity in the Cornubian Basin occurred during Chadian to Arundian times (Selwood & Thomas 1987). This postdates the first phase of volcanic activity in the Bristol district but coincides with the second development.

5.3 Correlation

The Middle Hope volcanics thin from 37.5m in the west at exposure 1 to less than 4m in the east at exposure 4 (Figure 5.3). Correlating horizons within the volcanic series between exposures is made more difficult owing to faulting and variation in lateral thickness and facies (Figure 5.3). Three limestone marker bands are recognized but for the reasons above, lithostratigraphic correlations are unfortunately only reliable between exposures 1 and 2. The sequence at exposure 3 has been extensively folded and faulted and is incomplete (Figure 5.3). The lower marker horizon, a crinoidal packstone, is however thought to be correlateable from exposure 1 to 3 (Figure 5.3). The middle marker horizon is a 3m thick crinoidal limestone containing zaphrentoid corals (Figure 5.3). The upper marker horizon is a dark grey, bioturbated crinoidal limestone with lines of

Figure 5.2. Locality map and the geology of the Middle Hope Peninsula.

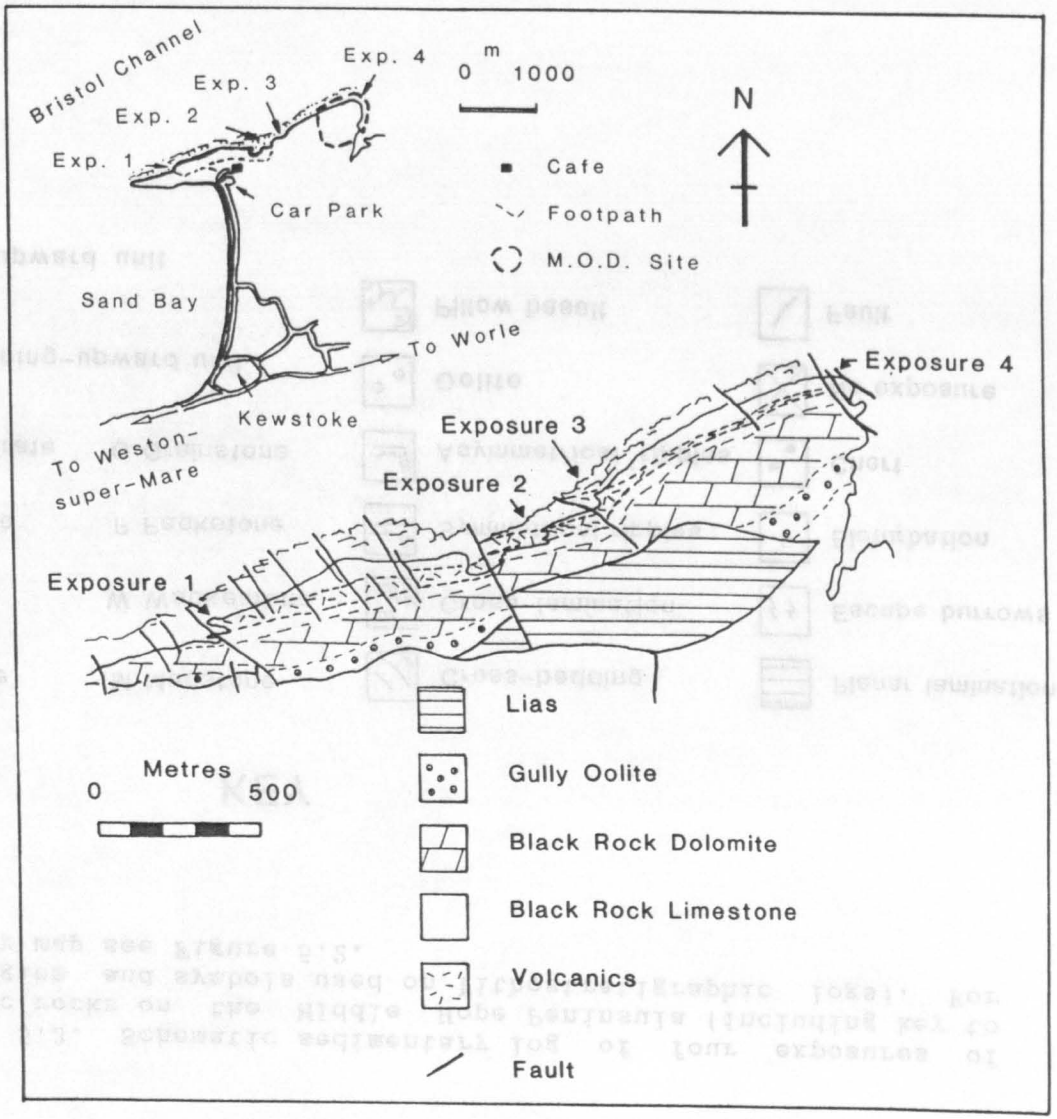
Bristol Channel
Exp. 4
Exp. 3
Exp. 2
Exp. 1
0 m 1000
N
Cafe
Footpath
M.O.D. Site
Car Park
Sand Bay
To Worle
Kewstoke
To Weston-super-Mare
Exposure 4
Exposure 3
Exposure 2
Exposure 1
Lias
Gully Oolite
Black Rock Dolomite
Black Rock Limestone
Volcanics
Fault
Metres
0 500

Figure 5.3. Schematic sedimentary log of four exposures of volcanic rocks on the Middle Hope Peninsula (including key to lithologies and symbols used on lithostratigraphic logs). For locality map see Figure 5.2.

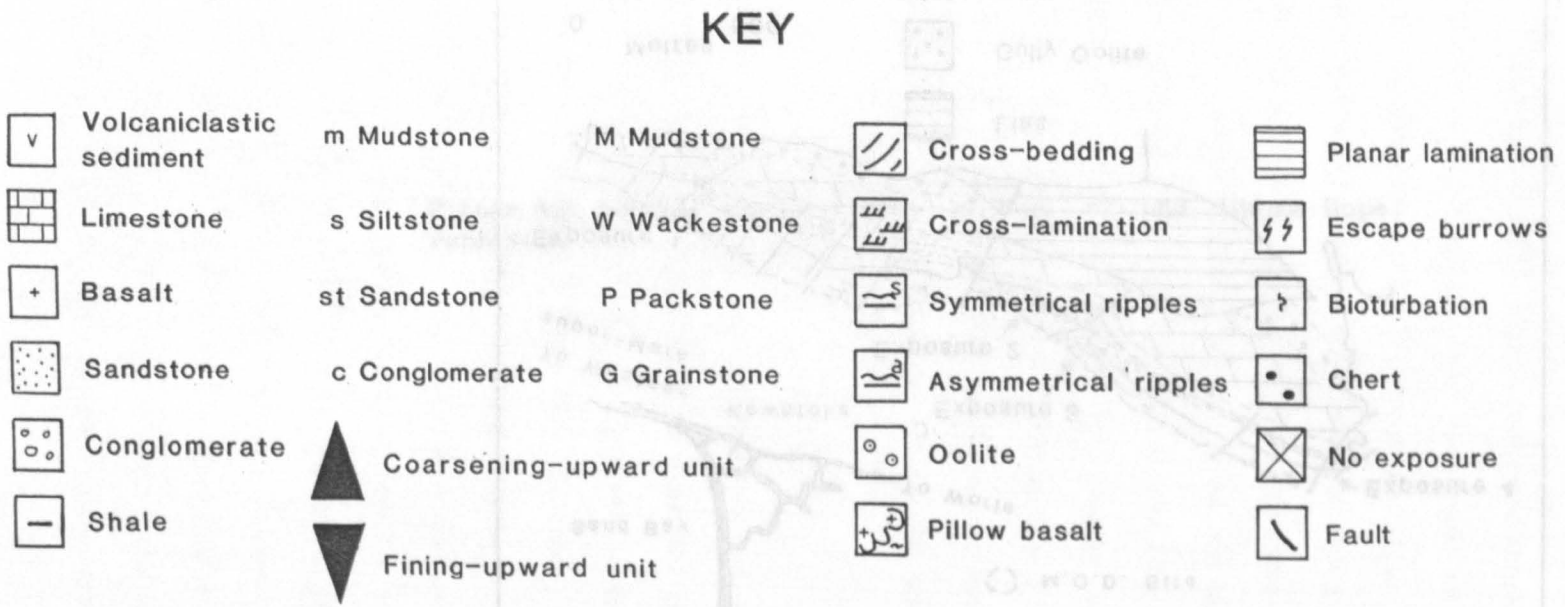

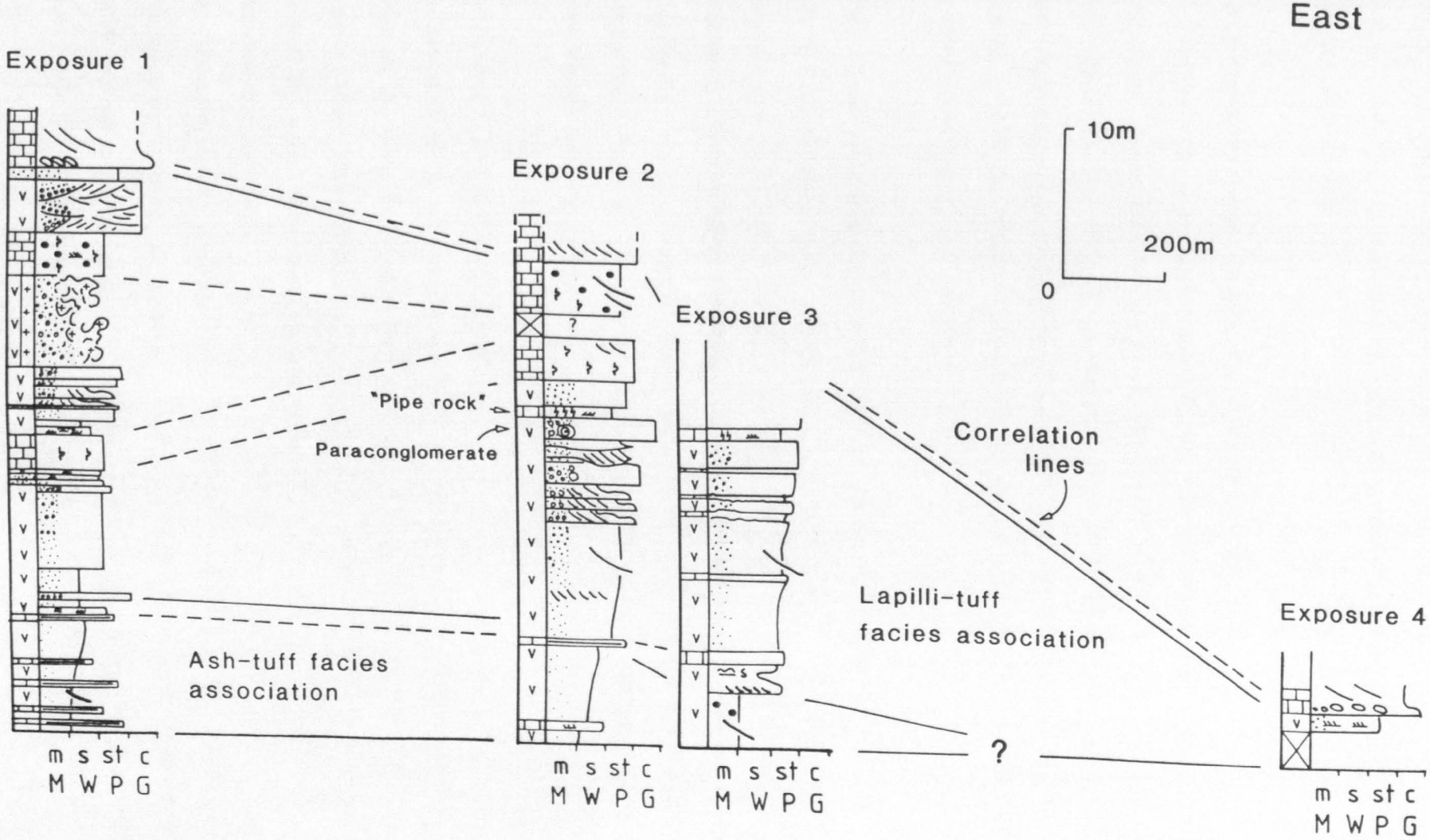
West
East
Exposure 1
Exposure 2
Exposure 3
Exposure 4
10m
200m
0
"Pipe rock"
Paraconglomerate
Correlation lines
Ash-tuff facies association
Lapilli-tuff facies association
?
m s st c
M W P G

cherty nodules. It outcrops at exposure 1 immediately above the pillow basalts (Figure 5.3).

5.4 Sedimentary facies description and interpretation

To simplify the sedimentary descriptions, the succession can be separated into four facies associations (A-D) (Faulkner 1989). In stratigraphic order they are as follows: argillaceous bioturbated limestone, ash-tuff, lapilli-tuff and cross-bedded bioclastic limestone (Figure 5.4). To save repetition of facies descriptions where necessary the reader is referred to relevant sections in Chapters 3 & 4.

5.4.1. *Facies Association A* : Bioturbated argillaceous limestone

This is exposed along the foreshore at Middle Hope and underlying the volcanics is a 51m thick succession of decimetre-bedded, extensively bioturbated, wackestones and packstones separated by shaly/marl layers (Figure 5.5A). Such features are characteristic of Lithofacies 9 which is described in section 4.3.2 and is interpreted as below storm wave-base facies.

5.4.2. *Facies Association B* : Ash-tuff

The ash-tuff facies association dominates the lower part of the volcanic series at the first three exposures but is not present at the fourth (Figure 5.3). The dominant subfacies is an ash-tuff (Ba) which occurs interbedded with thin-bedded limestones (Bb).

Subfacies Ba: Ash-tuff

The structureless, multi-coloured ash-tuff subfacies is slightly calcareous and forms a broadly upward-coarsening unit, from coarse ash to medium grained ash-tuff. Present within it are maroon and pale green lapilli which tend to concentrate in layers (3-5cm thick). From the

Figure 5.4. Schematic sedimentary log of exposure 1 on the Middle Hope Peninsula. The lower rose diagram is a plot of crinoid stem orientations; the upper rose diagram is a plot of the accretion direction of the cross-bed foresets. Symbols as for Figure 5.3.

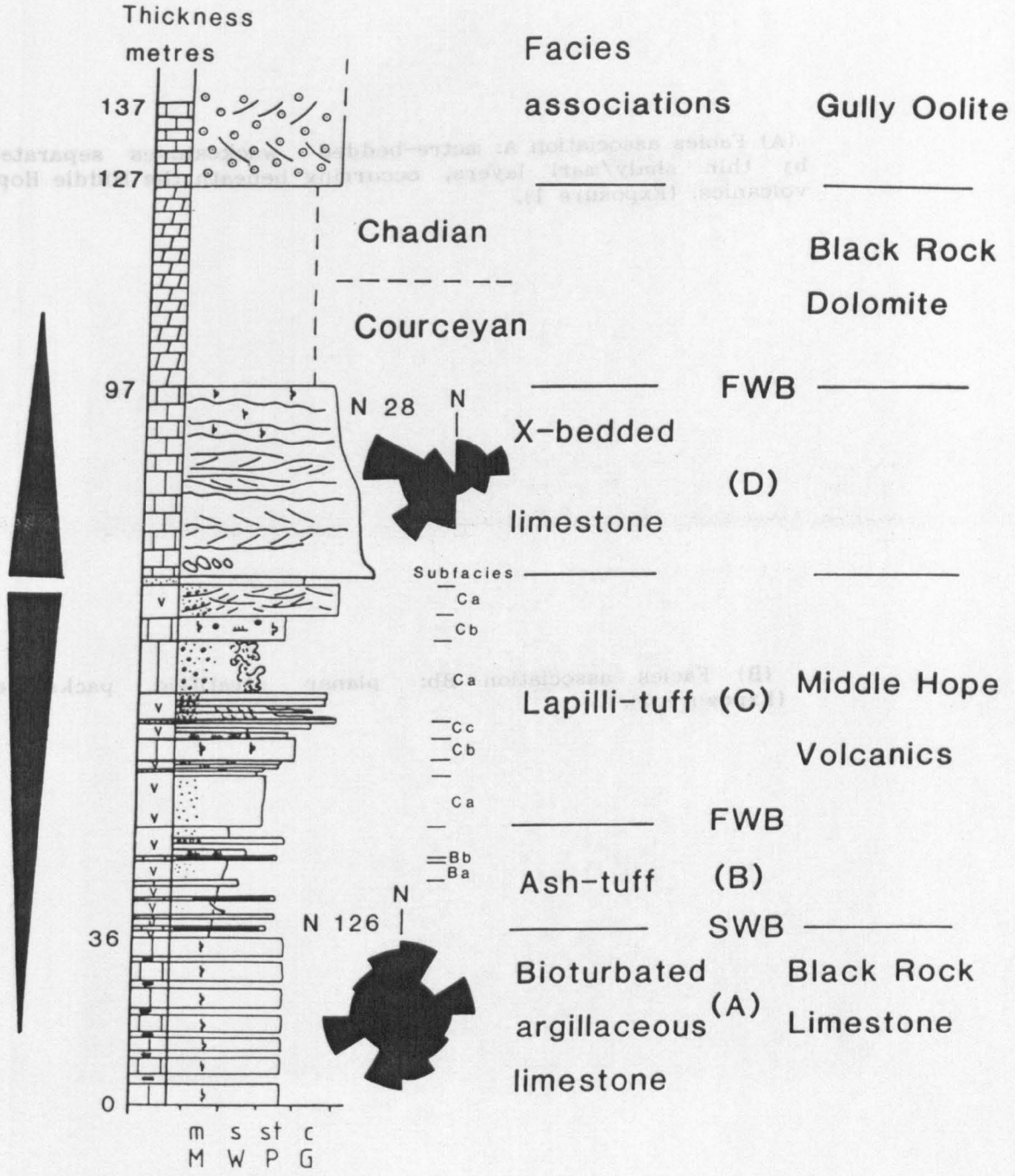
Thickness
metres
137
127
97
36
0
m s st c
M W P G
Facies
associations
Gully Oolite
Chadian
Courceyan
Black Rock
Dolomite
FWB
N 28
N
X-bedded
limestone
(D)
Subfacies
Ca
Cb
Ca
Cc
Cb
Ca
Bb
Ba
Lapilli-tuff
(C)
Middle Hope
Volcanics
FWB
Ash-tuff
(B)
N
N 126
SWB
Bioturbated
argillaceous
limestone
(A)
Black Rock
Limestone

Figure 5.5

(A) Facies association A: metre-bedded wackestones separated by thin shaly/marl layers, occurring beneath the Middle Hope volcanics. (Exposure 1).

(B) Facies association Bb: planar stratified packstone (Exposure 1).

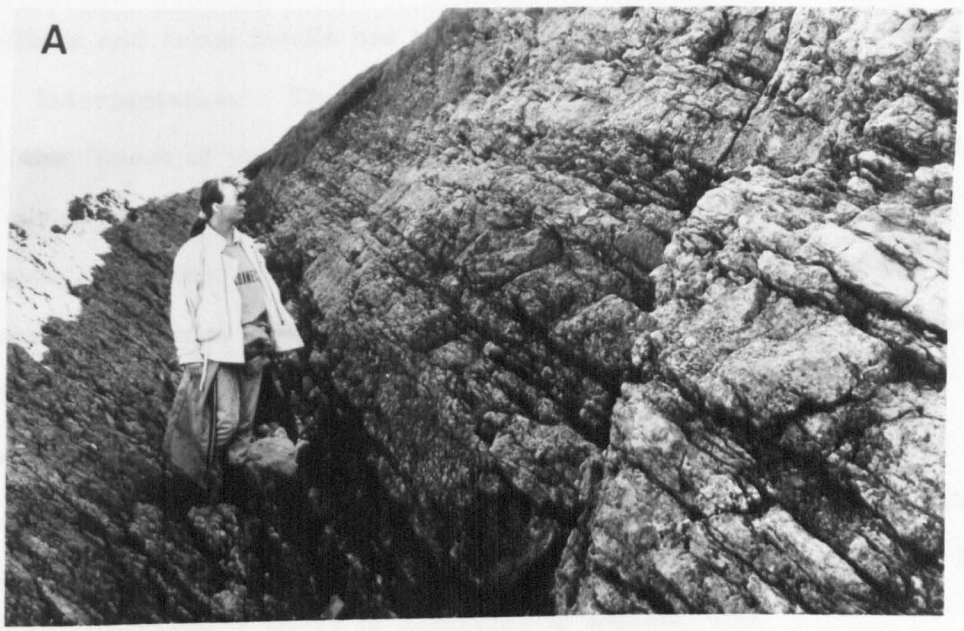
A

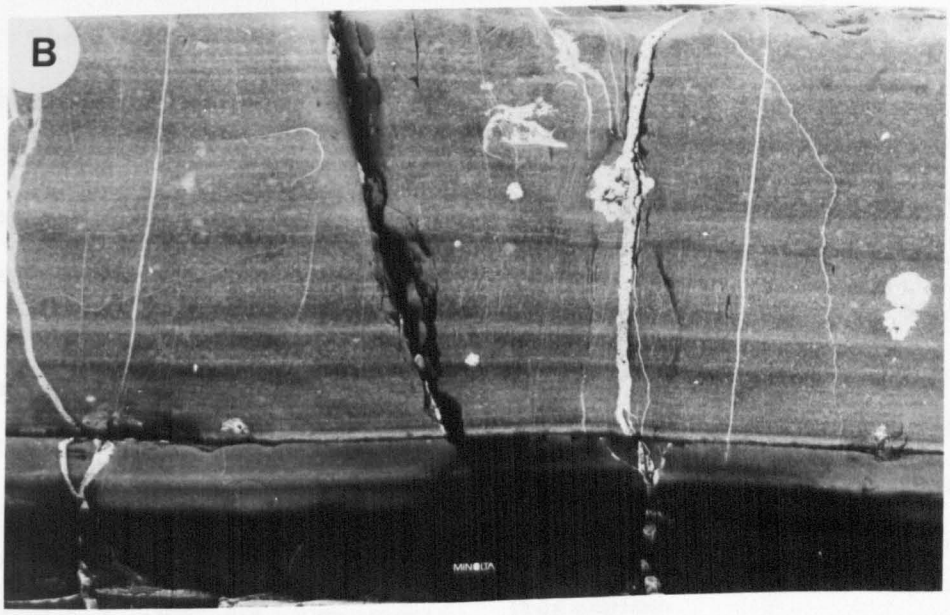
B

base, there is an upward increase in both the abundance of lapilli layers and their average grain size, which increases from 2mm to 0.5cm in diameter. The lapilli are rounded to subrounded and altered to chlorite. Disarticulated crinoid ossicles, brachiopods, and occasional corals are ubiquitous and trace fossils are rare.

Interpretation: The coarsening-upward volcaniclastic unit records both the onset of volcanic activity and its increase in intensity with time. The lapilli-rich horizons, are thought to be the product of the more energetic volcanic eruptions. The calcareous ash-tuff was deposited in a marine environment, in which the supply of volcaniclastic material was sufficient to dilute the supply of carbonate.

Subfacies Bb: Thin-bedded limestones

The thin-bedded limestones (2-20cm thick) are either finely planar-stratified or structureless (Figure 5.5B). The former is similar to Lithofacies 1 which is described in section 3.2.1.

The sharp based structureless packstones consist of disarticulated crinoids and convex-upward bivalve and brachiopod valves. Invariably these beds are moderately bioturbated and contain discontinuous lenses of tuffaceous material (5-30cm long). Small clusters of brachiopods and bivalves are found on the upper surface of the bioclastic limestone beds.

Interpretation: Lithofacies 1 records sedimentation from low energy current flows operating beneath mean wave-base (see section 3.2.1). The structureless, ungraded, sharp-based bioclastic packstones were probably also formed by storm-related processes. These deposits represent sedimentary lags of winnowed sediment because the bioclasts are generally disarticulated and not extensively fragmented.

5.4.3 *Facies association C* : Lapilli tuffs

The lapilli tuff facies association forms the upper part of the volcanics (Figure 5.3). It contains three subfacies: (Ca) graded and ungraded lapilli tuffs, (Cb) thickly-bedded bioclastic limestones and (Cc) laminated and cross-laminated sandstones. In addition, it includes the pillow basalts at exposure 1 (Figure 5.3).

Subfacies Ca: Graded and ungraded lapilli tuffs

This subfacies predominates in the upper part of the volcanics at the first three exposures and is not found at exposure 4 (Figure 5.3). Bedded on a decimetre scale, the granular green lapilli tuffs range from being poorly to moderately well sorted. The stratified and unstratified, angular to rounded lapilli clasts (2mm to 15cm in diamter) are set within a finer grained tuff matrix. The tuffs consist of devitrified amygdaloidal basalt and unidentifiable chloritized clasts. Additional sedimentary components include quartz grains, crinoid ossicles, and bivalve and brachiopod valves. The lapilli tuffs are cemented by sparry calcite which locally dissects the rock with a network of veins (Whittaker & Green 1983 page 13 plate 5). This feature is particularly well developed at exposure 1 beneath the pillow basalts.

The graded beds usually fine upwards but rare inverse to normally graded beds are to be found. The fining upward beds commonly display high-angle trough cross-stratification and form both sets and cosets separated by finer grained tuff layers (Figure 5.6A). It is notable that the cosets concentrate towards the top of the volcanic succession (Figure 5.4). Invariably both the sets (5-30cm thick) and cross-sets (1 to 5cm thick) are graded and fine upwards. Some sets display reactivation surfaces (spaced on a 1-3m scale) above which the grain size decreases both vertically and laterally.

The ungraded lapilli tuffs are either matrix or clast

Figure 5.6

(A) Facies association Ca: cross-bedded bioclastic lapilli tuff. (Exposure 2).

(B) Facies association Ca: paraconglomerate lapilli-tuff. The two large cobble clasts, denoted by 'T' and 'O' are stratified tuff and oolite respectively. (Exposure 2).

(C) Photomicrograph of the ooids of the oolite cobble clast, shown in Figure 5.6B. Scale bar 0.5mm. (Exposure 2).

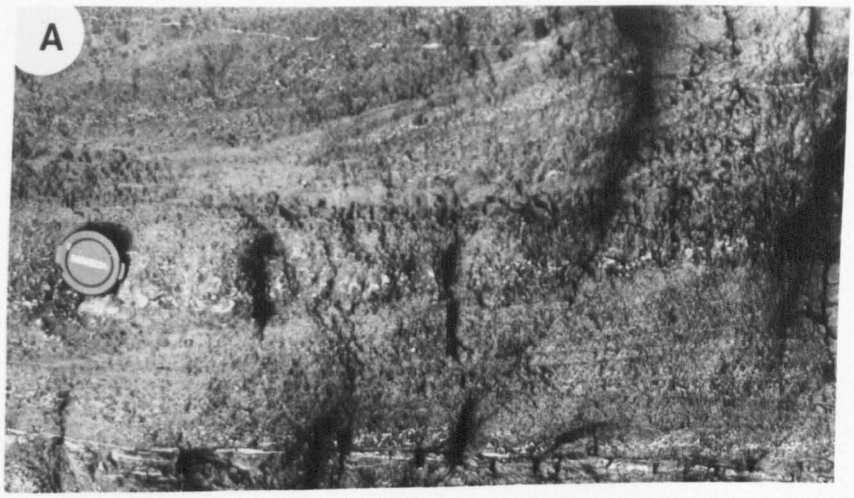
A

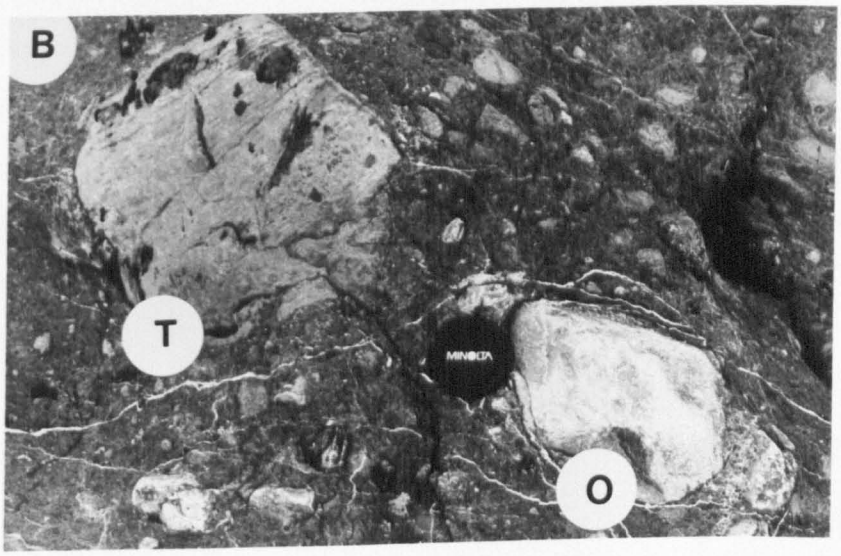
B
T
O

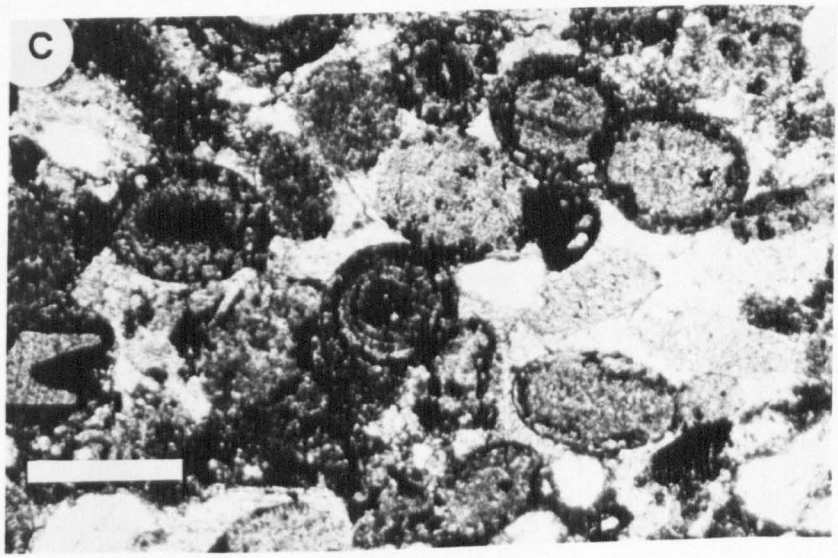
C

supported, and the former is particularly well developed at exposure 2, just beneath the 'pipe-rock' (Figures 5.3 & 5.6B). Additional clasts identified in paraconglomerate beds include chert nodules and limestones clasts containing the coral *Michelinia*. A single large cobble of oolitic limestone which lacks internal stratification, also occurs (Figure 5.6B). The ooid nuclei consist of subrounded echinoderm, bivalve and coral bioclasts, and angular quartz grains (silt to medium sand sized in diameter). Set within sparite cement, the ooids commonly show a poorly developed concentric cortex due to their partial replacement by microspar (Figure 5.6C) and more rarely by pyrite. The latter also occurs as crystal aggregates within the microspar cement.

Interpretation: Since the lapilli tuffs contain crinoids and brachiopods, it seems likely that deposition was in a shallow-marine environment. The coarse grain size and sedimentary features of the lapilli tuffs suggest deposition from high-energy currents. Grading between reactivation surfaces, spaced on a metre scale, indicates punctuated phases of deposition. The grading of the cross-sets is most probably due to the episodic avalanching of ripples down the slip-face of dunes.

The high-energy currents could either be due to subaqueous eruption-related gravity flows and/or normal shallow-marine processes. 'Cold' pyroclastic flows are known to develop in subaqueous environments and form non-welded turbidite-like sequences (Carey & Siguardsson 1980). Owing to the dominance of medium-scale cross-bedding much of the Middle Hope volcanics is interpreted as having been ultimately laid-down by shallow-marine processes. The paraconglomerate containing intraformational cobble clasts was interpreted, by Jeffreys (1979), as a pyroclastic debris-flow or lahar. Moving down the palaeoslope the debris-flow entrained intraformational clasts of chert, coralliferous limestone and

oolitic limestone.

Subfacies Cb: Thickly-bedded bioclastic limestone

This subfacies consists of decimetre to metre thick beds of fine- to medium-grained crinoidal bioclasts with zaphrentoid and caninioid corals. There are two developments (Figure 5.4), both are approximately 3m thick, which range from being moderately to extensively bioturbated and are thought to be correlatable between exposures 1 and 2 (Figure 5.3). The lower, pale grey limestone is better sorted and exhibits poorly-developed cross-bedding at exposure 2. The overlying, sandy blue-grey crinoidal limestone contains lines of chert nodules, and has partings of fine grained tuff with abundant lapilli of basaltic pumice (Whittaker & Green 1983). In addition, rare ripple cross-laminated layers and *Chondrites* burrows occur.

Interpretation: These two limestone beds are significant because they mark major breaks in volcanic activity and the establishment of an indigenous shallow marine fauna across the volcanic apron. Owing to the preservation of relict current-produced sedimentary structures the shallow-marine coralliferous crinoidal limestones have probably been reworked. However the net rate of sedimentation was relatively slow since both beds were bioturbated.

Subfacies Cc: Cross-laminated sandstone subfacies

The laminated and cross-laminated sandstone subfacies is thinly bedded on a 1-10cm scale. The medium- to coarse-grained quartzose and calcarenite beds appear creamy-white and are better sorted than the purple- or green-tinted immature, tuffaceous sandstone layers. Separating the sets and cosets are finer grained, structureless layers of tuffaceous sandstones and siltstones. The cross-laminae form predominantly westward dipping sets, the height of which varies between 0.5cm to 3.0cm and the ripple wavelength between 10 to 21cm. The bases of the rippled horizons

are sharp, slightly sinuous and commonly erosive. Beneath the limestone marker horizon at exposure 1 (Figures 5.3 & 5.4) partially onlapping climbing ripples are to be found. At the same locality but above the limestone marker bed, slightly sinuously crested current ripples occur.

Morgan & Reynolds (1904) ascribed the name 'pipe-rock' to the thinly-bedded tuffaceous calcarenite (ca. 75cm thick) at exposure 2 containing close-packed, near-vertical 'pipe-like' burrows in its central portion (Figure 5.7A). Immediately enclosing the laminated unit containing the 'pipe-like' burrows, is a ripple cross-laminated unit (13-15cm thick), and above it is an extensively bioturbated unit (ca. 23cm thick).

The lower part of the ripple cross-laminated unit includes symmetrical wave ripples with 'pointed' crests and rounded troughs and bidirectional, cross-laminated bundled lenses (Figure 5.7B). The latter sedimentary structure is similar to the wave generated structures described by de Raaf *et al.* (1977) from the Lower Carboniferous of County Cork, Ireland. The upper, ripple cross-laminated unit is dominated by westward dipping convex-upward sets. Observations of the profile of those ripples which initially have convex-upward lee slope, reveal progressive development towards the more usual, concave-upward attitude.

Within the ripple cross-laminated unit there is paucity of biogenic structures. Low diversity ichnofauna includes short spreiten-filled burrows (2-4cm in height) and thin vertical burrows (5-10cm in height) which are similar in appearance to the 'pipe-burrows'.

Passing transitionally from the ripple cross-laminated unit to the middle planar laminated unit, the calcarenite layers become thinner. The high concentration of 'pipe-like' burrows commence from a particularly tuffaceous horizon 27cm above the base of the cross-laminated unit. From the tuffaceous horizon, individual burrows may be traced upwards through as much as 12-15cm of sediment; Hardy (pers. comm.) has estimated a

Figure 5.7

(A) Facies association Cc: 'Pipe-rock' (as defined by Morgan & Reynolds 1904). The subvertical 'pipe-like' burrows pass transitionally into the overlying bioturbated unit. (Exposure 2).

(B) Facies association Cc: Wave-ripples outcropping in the unit immediately beneath the 'pipe-rock' burrows (Figure 5.7A). (Exposure 2).

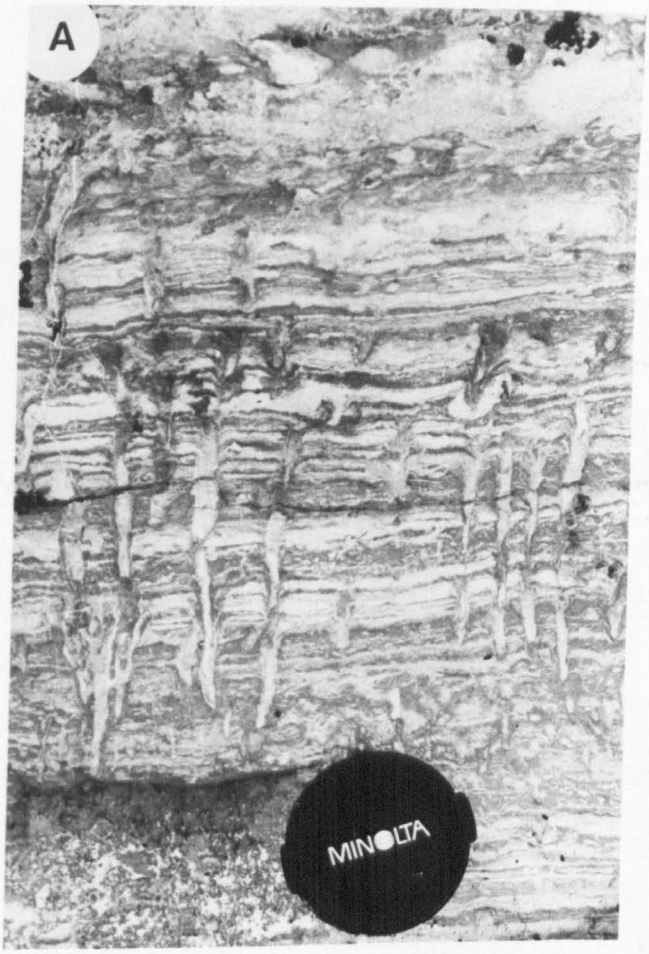
A
MINOLTA

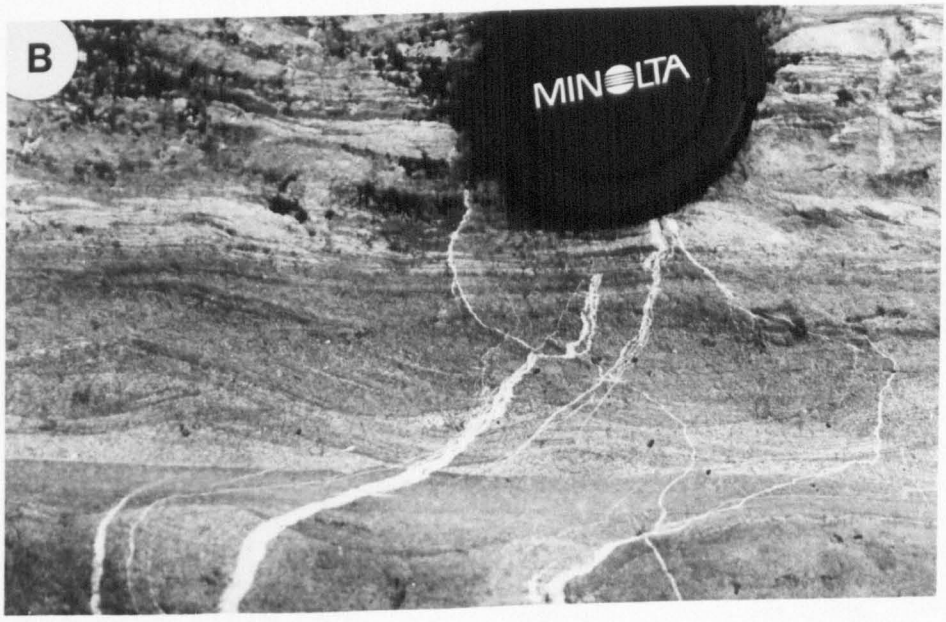
B
MINOLTA

maximum length of 25cm. The shape of the 'pipe' burrows is an elongated cone which diverges upwards (a width of 1-2mm at the base and 6-8mm at the top) with an ellipsoidal cross-section (Hardy pers. comm.). Hardy recorded *Lingula mytiloides* Sowerby in the 'pipe-like' burrows and along bedding plane surfaces. The overlying, extensively bioturbated unit has a mottled appearance and contains a high density of cylindrical (?*Thalassinoides*) burrows. Some of these burrows penetrate downwards into the upper part of the underlying 'pipe-rock' unit.

Interpretation: Rhythmic alternation of thin beds consisting of wave or current ripples overlain by finer-grained, immature tuffaceous drapes suggests deposition was by fairweather processes, above wave-base. Hardy (pers. comm.) concluded from his analysis of cross-sectional shape of the burrows and the inarticulate brachiopod that they had similar dimensions and, as such, the occurrence of *Lingula* within the burrows was not fortuitous, *Lingula* probably occupied and passed through the burrows. In addition, he noted the upward increase of the diameters of the 'pipe-like' burrows (Figure 5.7A) and suggested this reflects the establishment of the *Lingula* larvae and their progressive ontogeny and upward movement through the accreting sediment to maintain contact with the sediment/water interface. The progressive upward diminishing density of burrows clearly demonstrates the animal population of the 'pipe-like' burrows was 'escaping' from the accreting sediments (Hardy pers. comm.; cf. Broadhurst *et al.* 1980). The upward transition into the overlying extensively bioturbated unit probably reflects a change of ichnofauna probably due to a decrease in the rate of sedimentation.

5.4.4 *Facies Association D* : Cross-bedded bioclastic limestone

Facies association D outcrops at beach level at exposure 4 but forms the lower part of the inaccessible cliffs at the other three localities. The

cross-bedded bioclastic limestone has a sharp basal erosive contact with the underlying volcanics but passes gradationally upwards into the overlying Black Rock Dolomite. Above a basal conglomerate, the crinoidal limestone sequence (24m thick) progressively fines upward from granular to medium-sand sized bioclasts.

The conglomerate bed is accessible at exposures 1 and 4 where the oval, granular and cobble clasts of red tuffaceous sandstones, wackestones and packstones occur in a crinoidal matrix (Figure 5.8A) . In thin section the red tuffaceous sandstones consist of recrystallized and occasionally partially chertified ostracod, bivalve, brachiopod, coral and echinoderm bioclasts as well as devitrified amygdoidal basalt clasts, set in red ash. Petrographically, the sandstone clasts are similar to the red tuffaceous sandstone beds at the top of the volcanic succession at exposure 1. The packstone and wackestone cobble clasts have contrasting faunal constituents. The former contains echinoderm, coral (*Michelinia*), gastropod, ostracod, brachiopod and bivalve fragments within a matrix of sparite. In contrast the latter contains the microproblematicum *Uraloporella*, thin-valved bivalves, ostracods, multilocular forams, occasional echinoderm fragments and peloids within a matrix of micrite and neomorphic spar.

Passing upward from the base of facies association D there is not only a reduction in grain-size and bed thickness, but also a corresponding increase in the degree of micritization of grains and bioturbation. The lower part consists of compacted, 'well-washed' echinoderm bioclasts with thin micritized margins. In contrast, the upper part consists of rounded to subrounded bioclasts (1-2mm in diameter) of echinoderms, bivalves and brachiopods; cemented by a syntaxial blocky sparite and microspar. Towards the top of the facies association D zaphrentoid corals are to be found in life position.

Figure 5.8

(A) Basal conglomerate of the Middle Hope Limestone; Facies assocation D. The letter 'R' denotes clasts of red tuffaceous sandstone and 'W' the wackestone clast containing the microproblematicum *Uraloporella*. (Exposure 1).

(B) Pillow basalt. (Exposure 1).

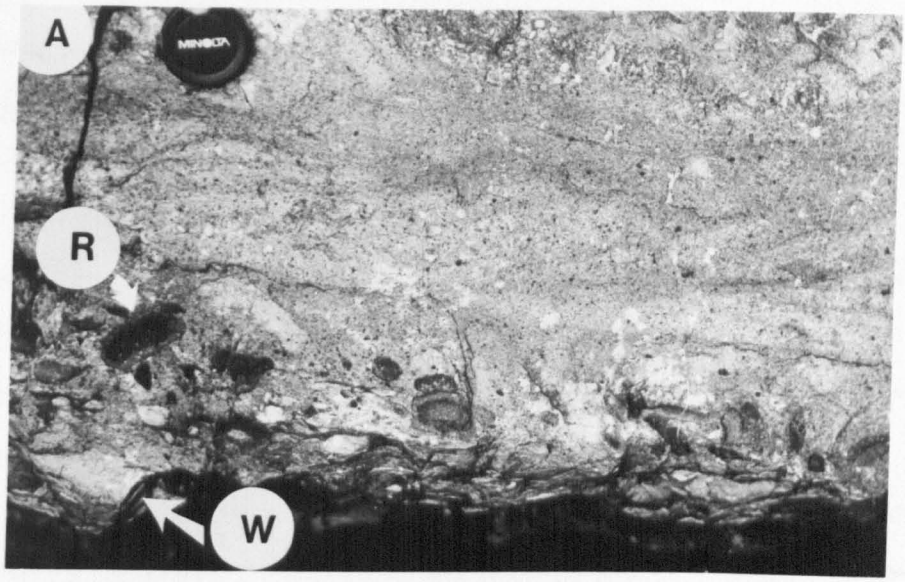
A
MINOLTA
R
W

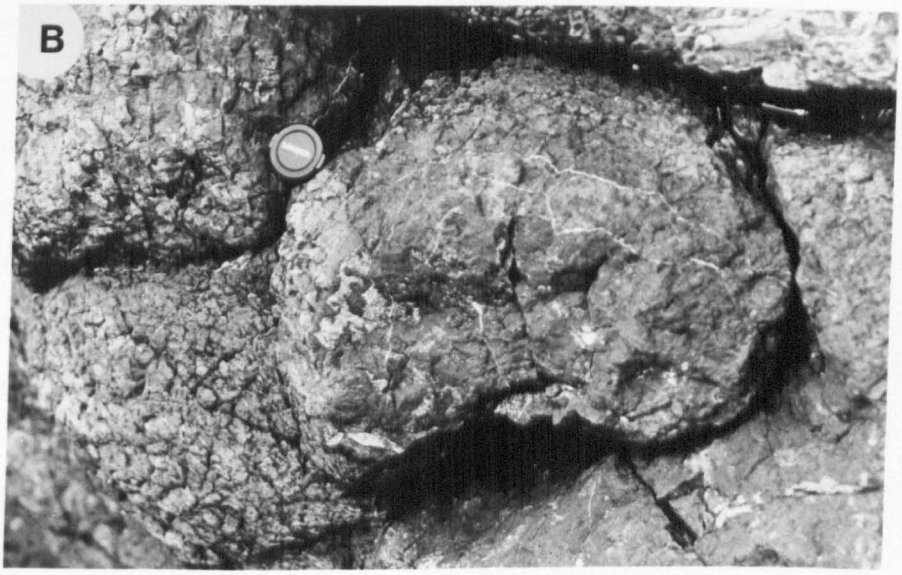
B

Bedded on a decimetre scale are the sharp, planar or undulatory erosively-based crinoidal-limestones. Short crinoid stems, when present, tend to concentrate along the base of the beds as a lag deposit. The planar and trough cross-sets form both cosets and sets separated by structureless crinoidal limestones. The latter exhibit rare reactivation surfaces and erosive asymmetric dish-like troughs (5m wide and 25cm deep) filled by the lateral accretion of sets. The dominant palaeocurrent vector is toward the west with a corresponding reverse current flow toward the east (Figure 5.4).

Interpretation: The erosively-based crinoidal unit was laid-down upon the poorly sorted, sedimentologically immature deposits of the volcanics. The well-washed appearance of the cross-bedded crinoidal grainstone records deposition in a shallow marine environment. High energy currents are thought to be responsible for forming the erosive-based granular crinoidal-limestone beds which exhibit dune-like structures, reactiviation surfaces and large asymmetric (channel?) scours. The east - west palaeocurrents parallel the inferred orientation of palaeo-shoreline to the north (cf. Wright 1986). From the base of the sequence, the upward decrease in bed-thickness, grain-size and corresponding increase in degree of micritization, biogenic structures and occurrence of zaphrentoids in growth position suggest an overall decrease in current energy and the rate of sedimentation. Modern studies of degree of grain micritization, by marine endolithic algae, show it increases with residence time on the sea floor (Kobluk & Risk 1977). Overall, sedimentary evidence suggests the cross-bedded limestone is a transgressive sequence and records progressive deepening of the water column above a crinoidal gravel sandbank.

The occurrence in the basal conglomerate of the wackestone clast containing *Uraloporella* indicates localised development of low energy

(protected?) environments on the upper surface of the volcanics, prior to the establishment of the crinoidal sandbank.

5.5 Discussion

The aim of this discussion is to assess the significance of the facies associations which record the evolution of a geologically transient, offshore volcanic-high. The Middle Hope volcanics occur within the upper part of the Black Rock Limestone offshore outer-ramp facies. The coarsening- and shallowing-upward volcanic sequence (facies association B & C) records the buildup of the localised volcanic submarine-high (Figure 5.9). The source of the volcanic material is thought to have been from the west, since the volcanic pile thins notably towards the east (Whittaker & Green 1983). Thus the volcanic wedge probably forms part of an apron which flanks a volcanic centre (Figure 5.9). Subsequent to the cessation of volcanic activity a crinoidal sandbank developed upon the upper surface of the volcanic high. The decline of the submarine-high to beneath wave-base is recorded by the upward-fining, transgressive, bioclastic limestone (facies association D).

The four facies associations (A-D) were laid-down in a subaqueous environment because there is a conspicuous absence of subaerial exposure features (Jeffreys 1979). The volcanics were initially deposited over the outer ramp facies of bioturbated, argillaceous limestones (facies association A). The regressive sequence records deposition from below storm wave-base to above fairweather wave-base. The ash-tuff facies association B contains stratified, thin-bedded storm-related deposits characteristic of a depositional environment above storm wave-base. Facies association C consists of a diverse range of lithologies which reflects the variability of above fairweather wave-base sedimentary environments.

Figure 5.9. Idealised, three dimensional, composite model of the volcanic high showing sedimentary features upon its upper surface.

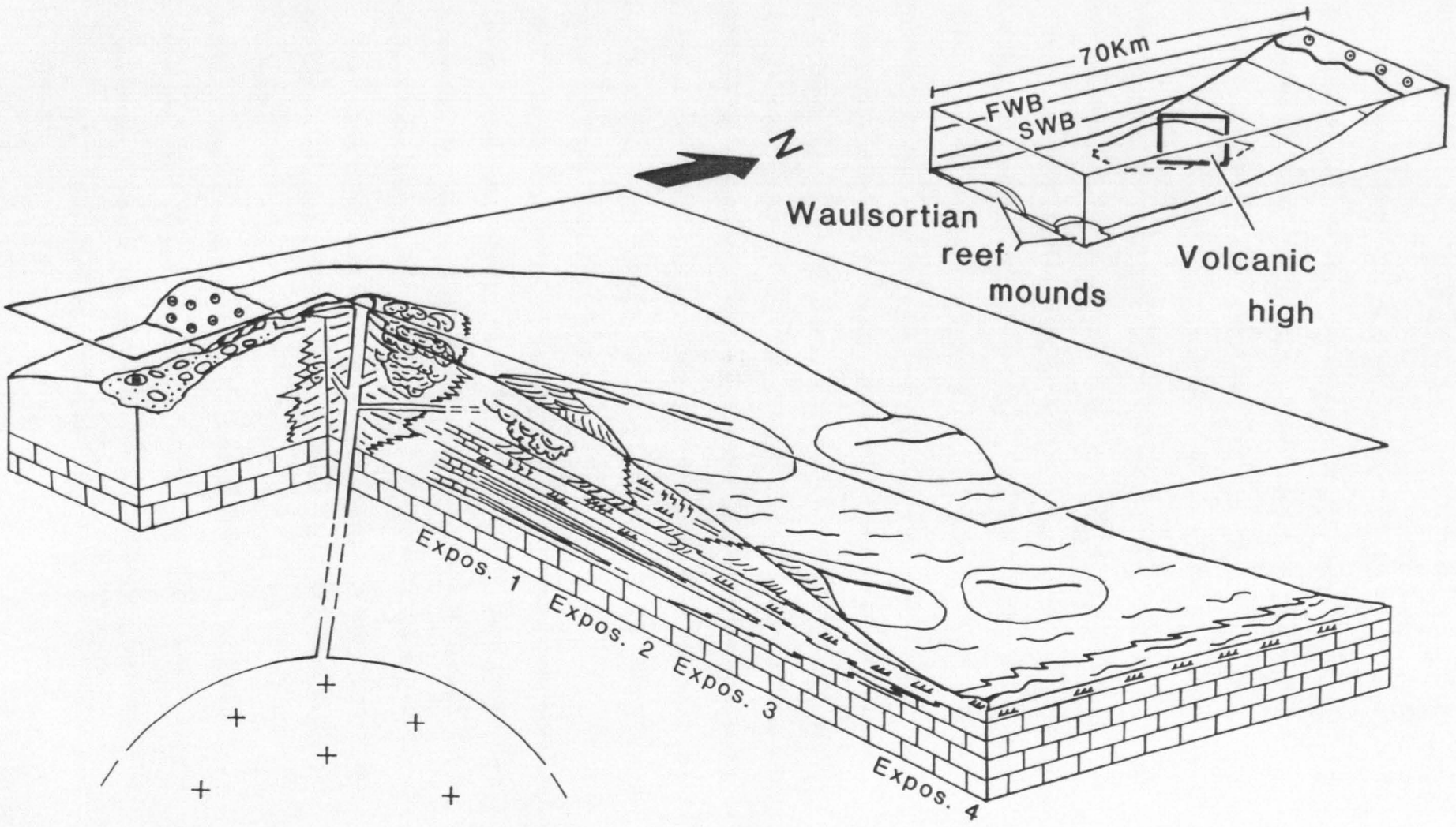
70Km
FWB
SWB
N
Waulsortian
reef
mounds
Volcanic
high
Expos. 1
Expos. 2
Expos. 3
Expos. 4

Contained within facies association C are a number of palaeontological and sedimentary palaeo-depth indicators which suggest that the volcanic high shallowed to within close proximity of sea level. They include clasts with the microproblematicum *Uraloporella*, the oolite cobble clast and wave and current ripples associated with *Lingula* burrows. *Uraloporella* occurs preferentially in restricted environments: such as lagoonal deposits (Riding & Jansa 1974 & 1976; Kazmierczak & Goldring 1978; Faber & Riding 1979) and the surf zone deposits of the Lower Carboniferous (Arundian?) Llanelly Formation of South Wales (Wright 1982). The low diversity fauna within the *wackestone* clast containing *Uraloporella* suggests deposition in a protected marine environment.

The oolite cobble clast could have had three potential sources. Firstly, it could be a volcanic bomb, derived from the underlying country rock which was ejected onto the volcanic apron during an eruption. Alternatively, it could have formed within a nearshore oolite shoal complex, from which it was transported offshore onto the volcanic pile. Thirdly, it could have formed *in situ* as part of the volcanic and sedimentary offshore shoal complex.

Oolite sandbodies are to be found in the underlying Lower Limestone Shale Group (Burchette 1987) and within the lower part of the Black Rock Limestone in the region. These however, do not occur in the Weston-super-Mare area, but predominate in the Forest of Dean area further north. The absence of volcanic activity in those areas where the oolite sandbodies developed, also militates against the oolite clast being a volcanic bomb.

During the deposition of the Middle Hope volcanics the palaeo-shoreline was situated at least 30-40km northward of the Weston-super-Mare - Bristol exposures of the Carboniferous Limestone (cf. Wright 1986). The bioturbated thickly-bedded deposits of the upper part

of the Black Rock Limestone record deposition beneath storm wave-base in an offshore environment (Wright 1986). Thus it would seem unlikely that the oolite cobble was derived from a nearshore environment, transported across the ramp and onto the volcanic high. Therefore the most likely origin for the oolite clast is from an oolite shoal which developed upon the upper slopes of the volcanic high.

Oolite production is known to be significantly reduced at depths greater than 10m. Thus, that part of the volcanic high from which the oolite cobble was derived, seemingly shallowed to within close proximity of sea level. There is no evidence that the oolite clast was subaerially exposed and cemented in a vadose zone.

Recent lingulids commonly occur in intertidal sediments and are usually found at depths of less than 40m (Craig 1952; Paine 1970) but they have been recorded as deep as the bathyal and abyssal zones (Mileikovsky 1971). Fossil lingulids, by analogy with modern forms, are often inferred to have lived in shallow water but appear to have had a wide depth range in the geological past (Cherns 1979). Boucot (1975) noted that the simple occurrence of linguloids does not unequivocally indicate shallow water conditions, as it is necessary to have a knowledge of the associated lithofacies before reaching this conclusion. The high density of *Lingula* burrows passing through a series of wave and current ripples, interpreted as being produced within fairweather wave-base, seems strong evidence in favour of shallow marine conditions. The notable absence of subaerial exposure features militates against deposition in an intertidal zone.

Following the cessation of volcanic activity, an open-marine crinoidal sandbank (Facies association D) developed over the volcanic apron. The upward-fining crinoidal-limestone sequence records the progressive increase in depth of the water column above the volcanic high, to beneath wave-base. The demise of the volcanic high could either

be due to eustatic rise in sea level and/or slow subsidence of the extinct volcanic centre.

During the deposition of the Courceyan Black Rock Limestone there was differential subsidence across SW Britain and the sea level is thought to have risen until the end of the Courceyan when there was a marked regression (Ramsbottom 1973; Lees & Hennebert 1982; Ross & Ross 1985). As yet, there is no evidence of a major basin-wide net change in the rate of subsidence and/or sea level rise during the period of the accumulation of the volcanics.

The geological processes capable of building a localised volcanic high to within close proximity of sea level, include volcanic updoming and aggradation of the sedimentary pile due to the supply of pyroclastic material. Determining whether volcanic updoming or aggradation was the major factor in the evolution of the volcanic high is dependent upon separating the effect that sediment accretion had upon its development. The Middle Hope volcanic sedimentary wedge thins from 37.5m at exposure 1 to less than a postulated 4m at exposure 4 (Figure 5.3). At exposure 4 the above fairweather wave-base deposits of facies association C are seen to directly overlie the below storm wave-base deposits of facies assocation A, without any deposits of the intervening facies association B (Figure 5.3). Regardless of whether facies association B accumulated and was then eroded or not, the incongruous juxtaposition of depth-related facies and the thinness of the volcanic sediments suggest updoming was a significant factor in the development of the volcanic high.

5.6 Geochemistry of the pillow basalts (locality 1)

In recent years sophisticated geochemical techniques have been developed to identify ancient tectonic settings even when they cannot be deduced from the field relationships. The principle is based upon the recognition

that there is a close link between the rare earth element composition of modern basic rocks and their tectonic setting (Figures 5.10 & 5.11), against which analyses of ancient rocks are readily comparable (Pearce & Cann 1973; Pearce 1983).

The aim of this study is to characterise the geochemical traits of the pillow basalts at Middle Hope, in order to evaluate their tectonic significance. The results of the analyses were compared against more comprehensive geochemical studies undertaken to the south, in Rheno-Hercynian zone by Floyd (1982), and along the northern margin of Welsh-Brabant Massif, by Macdonald *et al.* (1984).

5.6.1 Pillow basalt

The greenish amygdaloidal basalt of exposure 1 exhibits a four fold increase in thickness, over a lateral distance of 15m, from 2 metres in the east to c. 8m in the west. Within the basal part of the flow there are well developed pillows (c. 50cm in diameter) (Figure 5.8B).

The petrography of the basalt from Swallow Cliff (Locality 1) has been described in considerable detail in the Geological Memoir (Whittaker & Green 1983). The sparsely amygdaloidal, porphyritic, olivine-basalt has undergone extensive alteration and apart from the texture, there are very few relicts of the original minerals. Identifying the primary mineralogical phases has mainly been achieved by identifying the alteration products and utilising information of the form of the minerals from their relict texture. The primary phases include olivine, albite, K-feldspar, pyroxenes and opaque ore (Whittaker & Green 1983). The sparse ovoid amygdales are lined with sparry calcite or opaque ore and are filled with pale green clay.

5.6.2 Methods

Two samples of the basalt were taken for geochemical study of major and trace elements (using X-ray fluorescence using U.S.G.S standard rocks).

Figure 5.10. Discrimination diagram using Ti, Zr and Y. (Pearce & Cann 1973).

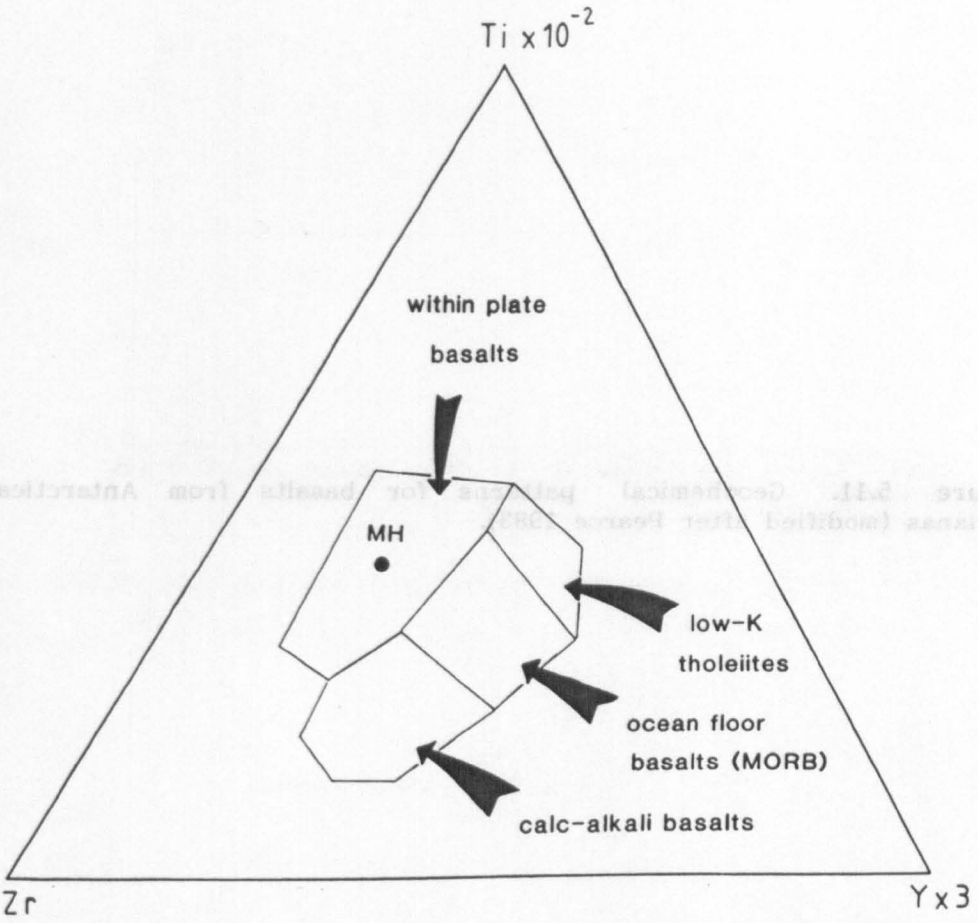

MH Middle Hope

Figure 5.11. Geochemical patterns for basalts from Antarctica & Marianas (modified after Pearce 1983).

Within plate basalts

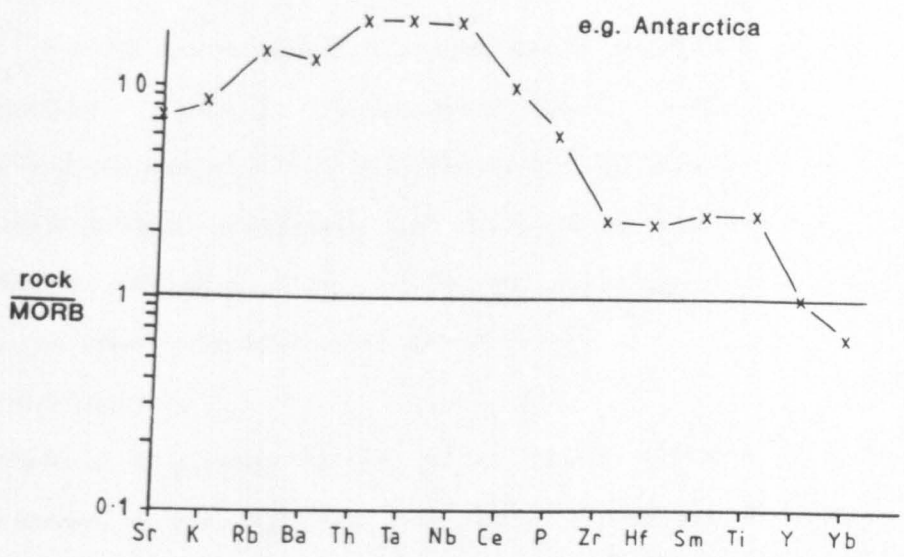

Oceanic calc-alkali basalts

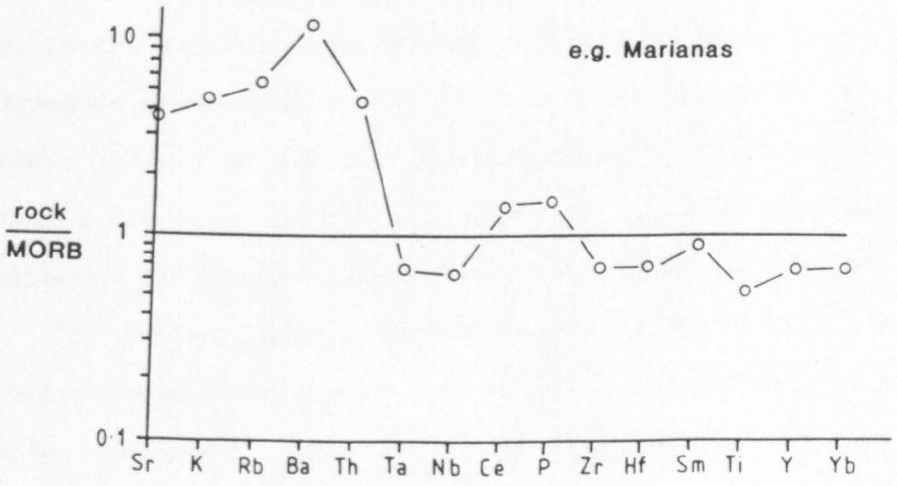

Both the preparation and analyses were undertaken by M. Widdowson (Oxford University) (Appendix S). The former required the removal of the amygdales, by slicing samples into thin slabs and breaking off the secondary void filling phases.

Basalts are commonly classified solely upon their bulk chemical composition into: silica-oversaturated, silica-saturated and silica-undersaturated. This is achieved by calculating the C.I.P.W. norm: the hypothetical assemblage of standard minerals (Cross *et al.* 1903; modified by Cox *et al.* 1979). This was calculated on a volatile free basis and with Fe_2O_3 arbitrarily set at 1.5wt%.

5.6.3 Geochemistry

The chemical composition of the pillow basalt is silica-undersaturated, alkali basalt, as revealed from the norm calculation (Table 5.1). From the available information, the bulk chemical composition of the rock (Table 5.1) does not seem to have been notably changed, even though the majority of the primary mineralogical phases are highly altered.

Magmatic affinity

Two trace element plots have been used to delimit the tectonic environment of the pillow basalts: Ti, Zr and Y triangular diagram and trace element geochemistry patterns (Figures 5.10 & 5.12). The stable incompatible elements Ti, Zr and Y are particularly useful in assessing magmatic affinity in that they are assumed to be unaffected by alteration processes. The use of the Ti, Zr and Y triangular diagram is implicit whereas the geochemical pattern diagram requires some explanation.

To produce smooth, readily comparable geochemical patterns the samples are normalized against the trace element composition of an average tholeiitic mid-ocean ridge basalt (MORB) (Pearce *et al.* 1981) (Figure 5.11). The patterns characterisitic of calc-alkali basalts show selective enrichment of Sr, K, Rb, Ba and Th; Ta, Nb, Zr, Hf, Ti, Y and Yb

Table 5.1. Geochemistry of the pillow basalt at Middle Hope. Or orthoclase, ab albite, an anorthite, ne nephline, di diopside (wo wollastonite, en enstatite, fs ferrosilite), ol olivine (fo forsterite, fa fayalite), mt magnetite, cm cummingtonite, il illmenite.

	wt%
SiO_2	45·86
TiO_2	3·10
Al_2O_3	13·95
Cr_2O_3	0·06
Fe_2O_3	10·70
MnO	0·07
MgO	8·65
CaO	8·87
Na_2O	1·80
K_2O	4·30
P_2O_5	0·57
Total	97·93

NORM		
or	25·41	
ab	5·55	
an	17·28	
ne	5·24	
di	18·52	(wo 9·60) (en 6·33) (fs 2·59)
ol	15·47	(fo10·66) (fa 4·81)
mt	2·33	
cm	0·09	
il	5·89	
	97·11	

	ppm
Zn	189·8
Cu	39·0
Ni	236·5
Co	48·2
Cr	410·9
V	231·5
Ba	524·6
Ga	19·7
Rb	54·4
Sr	285·9
Y	26·0
Zr	204·5
Nb	42·2
Pb	13·2
Th	2·8
U	1·4

Analysis of

Middle Hope Basalt

Figure 5.12. Geochemical pattern for the pillow basalt at Middle Hope.

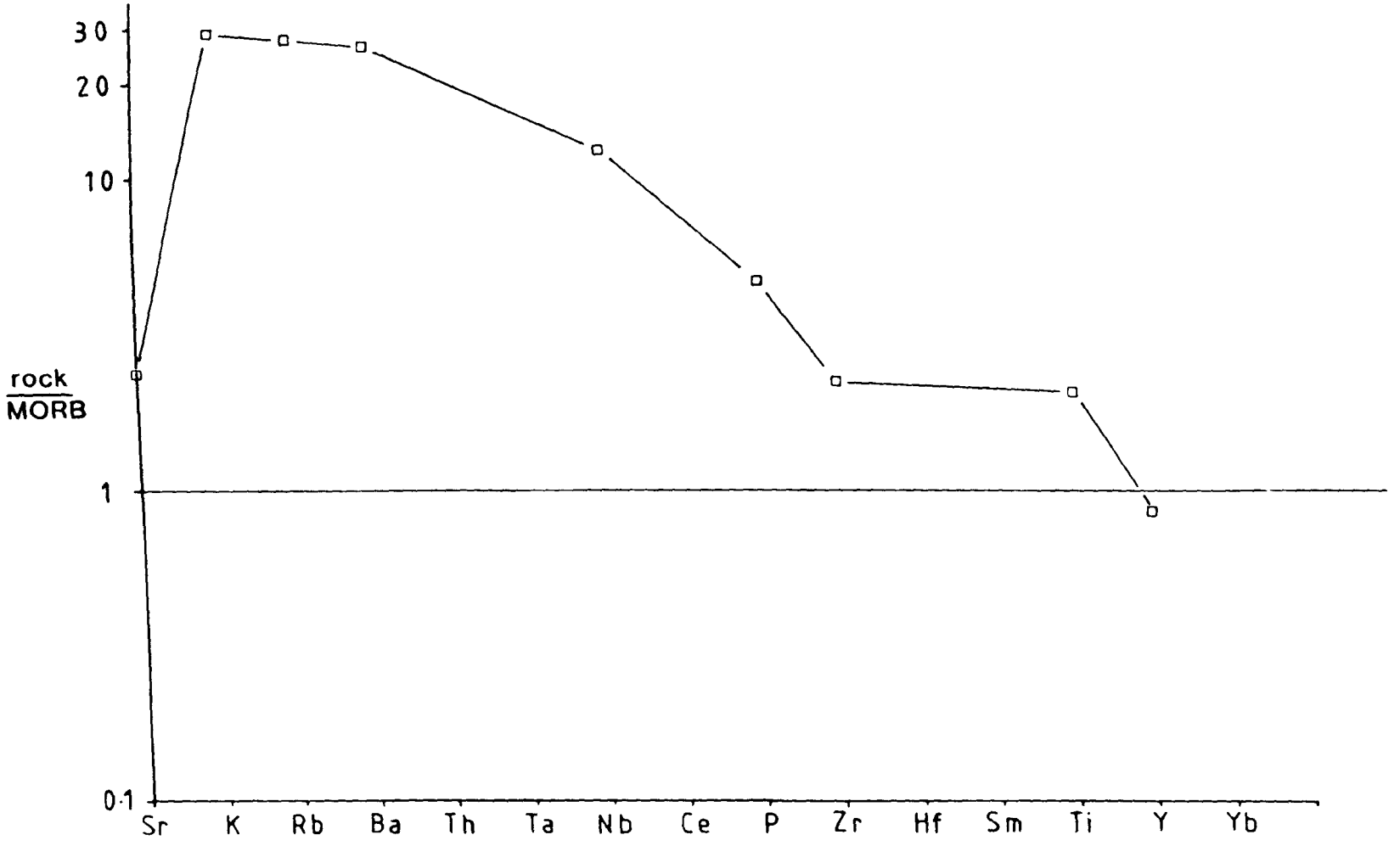
30
20
10
1
0·1
rock
MORB
Sr
K
Rb
Ba
Th
Ta
Nb
Ce
P
Zr
Hf
Sm
Ti
Y
Yb

form a flat trend which lies parallel to the tholeiitic MORB pattern but at a lower level (Pearce & Cann 1973). Apart from the least incompatible elements Y and Yb, within plate basalts show enrichment relative to MORB. The most incompatible elements, Ba, Th, Ta and Nb show the greatest enrichment. As a result, the 'humped' pattern is characteristic for within plate basalts.

The pillow basalt at Middle Hope shows the geochemical traits of a within plate basalt by having "humped" geochemical pattern (compare Figures 5.11 against 5.12) and plotting within the "within plate basalt" field on the Ti, Zr and Y triangular diagram (Figure 5.10). Such characteristics are consistent with the geochemical analyses of other Hercynian basalts of the Rheno-Hercynian Zone (Floyd 1982) as well as those just to the north of Welsh-Brabant Massif in the N Derbyshire area (Macdonald *et al.* 1984). The above show a mild to moderate light rare earth element enrichment and are of intra-plate in aspect. Their origin is considered to be subsidence related (Leeder 1982; Macdonald *et al.* 1984). The cause of the tensional regime across Britain, is considered to have been the result of northward subduction occurring some considerable distance to the south of Welsh-Brabant Massif (Leeder 1974, 1982 & 1987).

The geographical siting of Hercynian volcanic activity does in part seem to have been influenced by the position of tectonic hinge lines (Leeder 1974), particularly when coincidental with ancient (Caledonide) lines of weakness which were most probably reactiviated e.g. the Midland Valley (Upton 1982). These ancient basement lineaments most probably facilitated easier access through the lithosphere for the melts (Upton 1982; Macdonald *et al.* 1984). The siting of volcanics in the Weston-super-Mare region overlies the Mendip axis, interpreted as a probable hinge-line at depth (Green & Welch 1965; Wilson *et al.* 1988). The timing of the Middle Hope volcanics is seemingly related to movement

along a hinge-line, early during the *P. mehli* Zone, causing subsidence to the south of the Mendip and Vale of Glamorgan axis (Figure 5.12). Although in the vicinity of the area of volcanic activity localised uplifted occurs (section 5.5).

5.7 Conclusions

1) The Dinantian (Courceyan) Middle Hope volcanics (near Weston-super-Mare) form a coarsening- and shallowing-upward sequence which records the buildup of a localised, offshore volcanic high upon the below storm wave-base (outer carbonate ramp zone) deposits of the upper Black Rock Limestone.

2) Combined palaeontological and sedimentary depth indicators suggest the volcanic high developed from below mean wave-base to above fairweather wave-base and shallowed to within close proximity of sea level. No subaerial exposure features were identified.

3) Comparative study of the sedimentary facies, developed down the volcanic apron slope, revealed that volcanic updoming was a significant factor in the development of the volcanic high.

4) The submergence of the topographic high, to below wave base, is recorded by the succeeding erosively-based cross-bedded bioclastic limestone which forms a fining- and deepening-upward sequence.

5) The geochemistry of the pillow basalt is of intra-plate character. The timing for volcanic activity is seemingly related to major subsidence to the south of the Vale of Glamorgan and Mendip axis, and as a consequence of tensional regime set-up across Britain during the Lower Carboniferous.

Chapter 6 - Facies and dolomite geochemistry of the Castlemartin Waulsortian buildups

6.1 Introduction

Mudmounds are typically large reef-like buildups dominated by a fine grained matrix and lacking any prominent skeletal framework. They are a special category of reef mound in which carbonate mud exceeds bioclastic debris in volume (Wright 1989). Such reefs are common in the Palaeozoic. The term Waulsortian was originally reserved for the sparry calcite "veines bleues" lithology which makes up a considerable proportion of the buildups of Waulsort, in Belgium (Lees *et al.* 1977). The present use of the term has been modified to include all those mudmounds which show comparable faunal assemblages and sedimentary fabrics to the Waulsortian buildups of Belgium (Miller & Grayson 1982; Lees *et al.* 1977). The reef mounds described in this chapter are Waulsortian mounds, but notably lack the "veines bleues" lithology.

Dixon (1921) was the first to describe the dolomitized mounds at Berry Slade and Wind Bay (100-130m thick) as well as the undolomitized mudmound at Hanging Tar (11m thick) (Figure 6.1). He proposed that these mounds were of Waulsortian aspect; a conclusion later supported by Sullivan (1960) and more recently confirmed by Lees & Hennebert (1982). The aim of the first part of this chapter is to describe the Castlemartin buildups and compare their evolution to other Waulsortian mound complexes, situated along the southern margin of Welsh-Brabant Massif, at Cannington Park (Lees & Hennebert 1982) and in Belgium (Lees *et al.* 1985) (Figure 1.1).

In the second part of this chapter there is a full petrographic description of the Waulsortian dolomites and their geochemistry, including stable isotope analyses. Constraints from the geochemistry and distribution of the dolomite permit an evaluation as to the most likely subsurface hydrological system to have caused dolomitization.

Figure 6.1 Stratigraphy of the coastline at Castlemartin between the Pole and Pen-y-Holt Bay, showing the position of the Waulsortian mounds and the approximate position of the Bullslaughter Bay syncline.

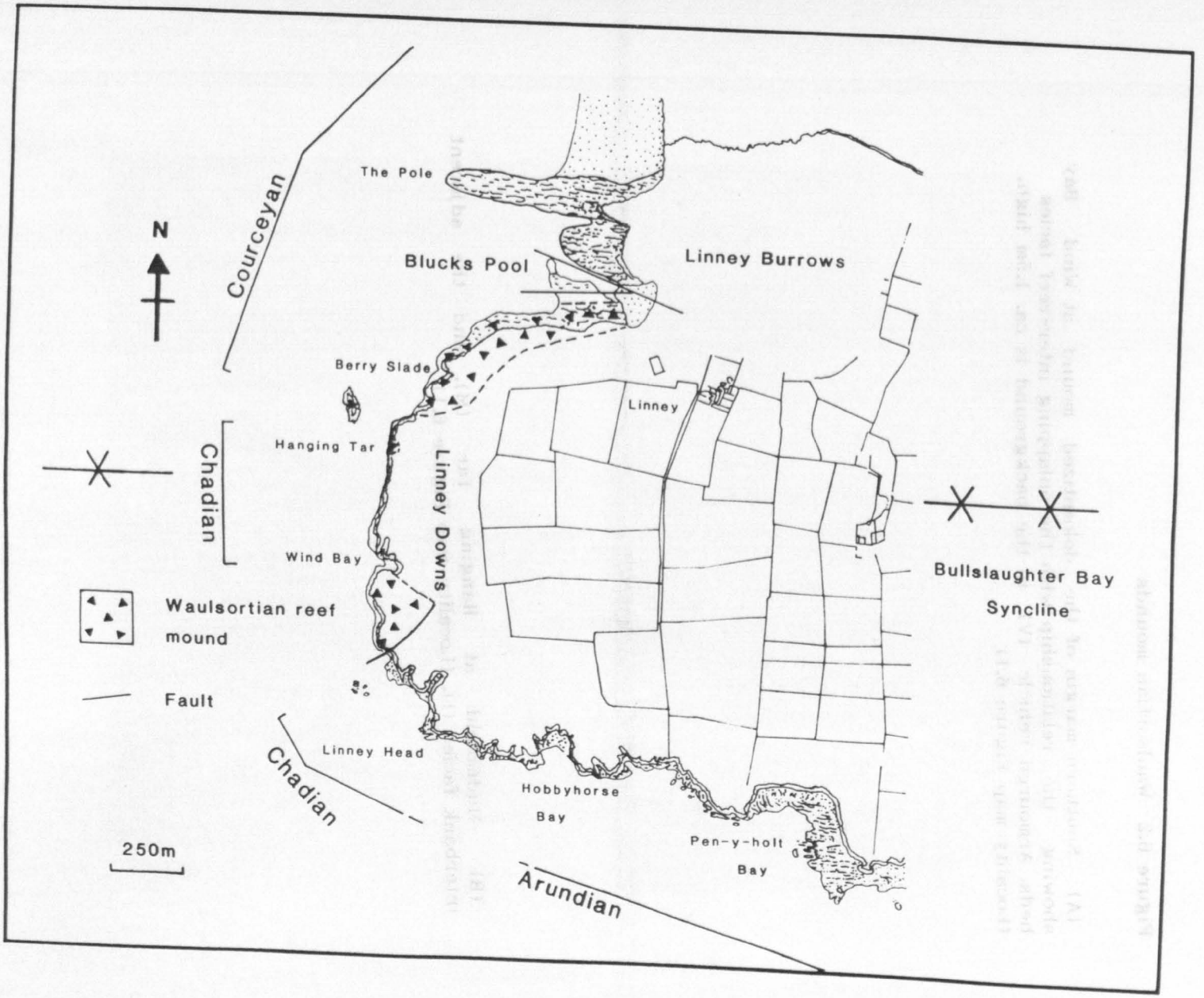
N
Courceyan
The Pole
Blucks Pool
Linney Burrows
Berry Slade
Linney
Hanging Tar
Chadian
Linney Downs
Wind Bay
Bullslaughter Bay
Syncline
Waulsortian reef
mound
Fault
Linney Head
Chadian
Hobbyhorse
Bay
Pen-y-holt
Bay
250m
Arundian

Figure 6.2 Waulsortian mounds

(A) Southern margin of the dolomitized mound at Wind Bay showing the relationship with the onlapping inter-reef facies beds. Armoured vehicle (V) in the background is ca. 1.5m high. (Locality map Figure 6.1)

(B) Mudmound at Hanging Tar (M), and the adjacent interbank facies (I). (Locality map Figure 6.1).

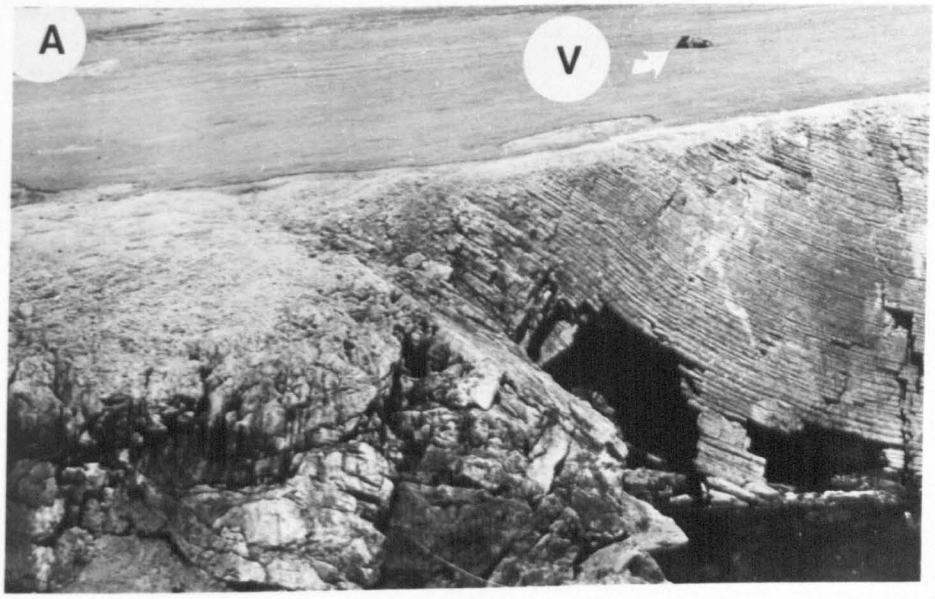
A
V

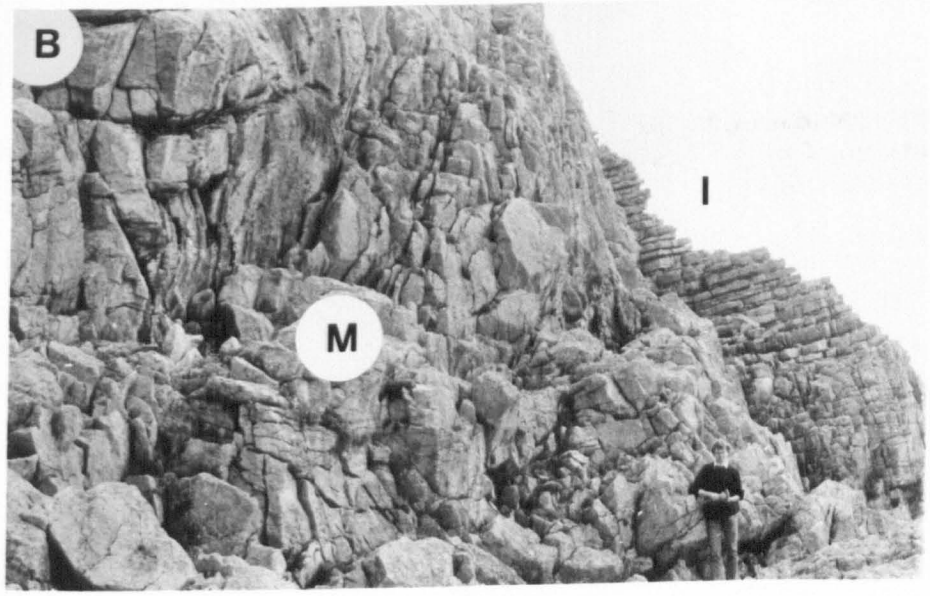
B
I
M

6.2 Waulsortian buildups of Castlemartin

The two extensively dolomitized mounds at Berry Slade and Wind Bay are thought to be lateral equivalents because they outcrop at a similar stratigraphic position either side of the axis of the Bull Slaughter Bay syncline (Dixon 1921) (Figures 6.1 & 6.2A). Stratigraphically, they are overlain by the minor buildup at Hanging Tar (Figures 6.1 & 6.2B) (Appendix B). All three developments occur within below storm wave-base facies of late Courceyan to early Chadian age (see Chapter 4).

In SW Britain, the main period of the mudmound formation occurred during upper Courceyan times within the *S. anchoralis* Zone (Mitchell *et al.* 1982). The only development that has an early Chadian age is the minor buildup at Hanging Tar which occurs within the *Gnathodus homopunctatus* Zone (Mitchell *et al.* 1982) (Figure 6.3).

6.2.1 Berry Slade and Wind Bay Mounds

The Berry Slade and Wind Bay dolomite mounds are both ca. 100-130m thick (Mitchell *et al.* 1982) and occur within a succession of pseudo-bedded packstones separated by shaly/marly layers (Lithofacies 9; previously described in Chapter 4) (Figure 6.2A). The Berry Slade mound has a gradational contact with the underlying succession which consists of abundant disarticulated crinoids, sponge spicules, and fenestellid bryozoans, set within micrite. The junction between the mounds and the overlying bedded limestones is sharp. The high angle dips (up to 55 °) recorded in the inter-reef facies at Wind Bay, appear to have been enhanced tectonically as well as by differential compaction (Figure 6.2A).

The pale white dolomite mounds are characterised by a striking lack of recognizable bedding-planes (Figure 6.2A). Unfortunately, they contain few calcite relics which consist of crinoid and bryozoan debris. Two ghost plurilocular foraminifera were identified within the dolomite, towards the

Figure 6.3 Schematic diagram of the sedimentary phases within the mounds at Castlemartin. Biostratigraphy taken from Mitchell *et al.* (1982).

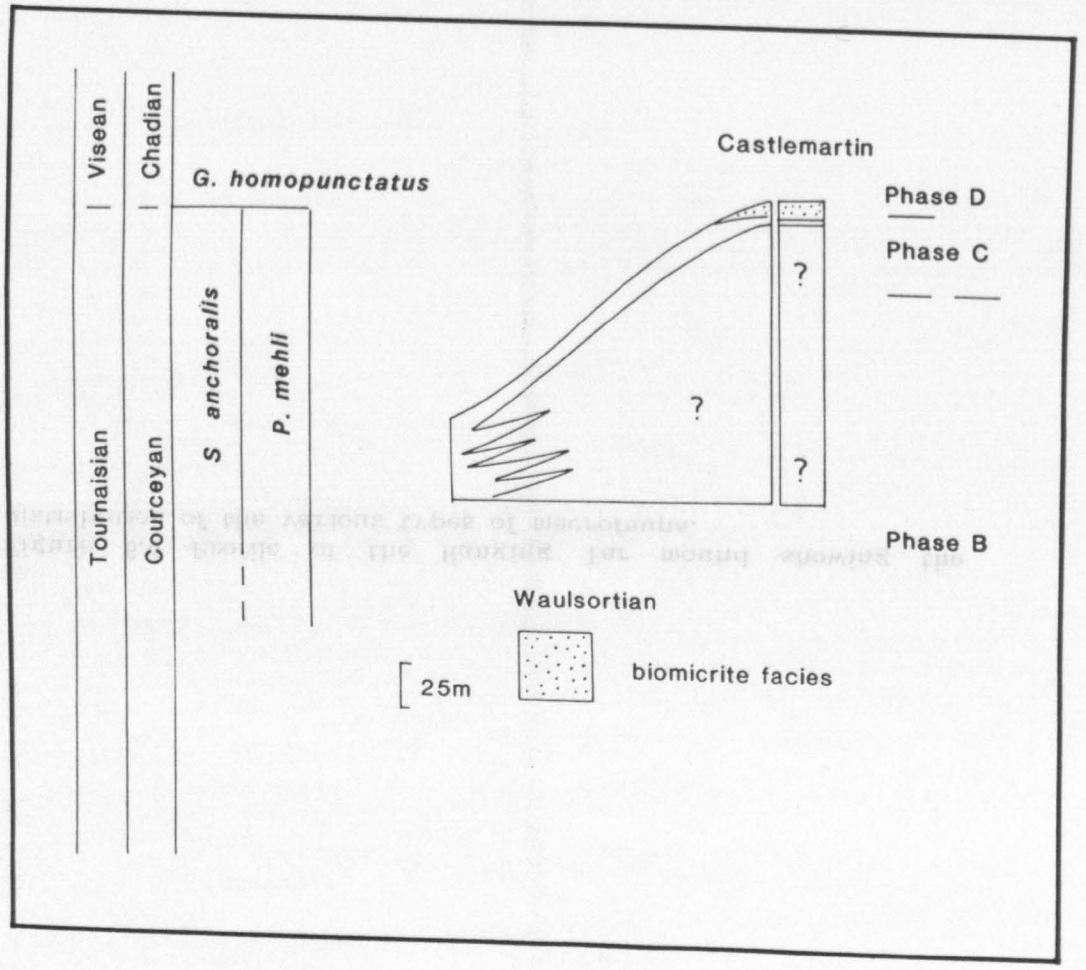
Tournaisian
Visean
Courceyan
Chadian
G. homopunctatus
S anchoralis
P. mehli
Castlemartin
Phase D
Phase C
Phase B
?
?
?
Waulsortian
25m
biomicrite facies

Figure 6.4 Profile of the Hanging Tar mound showing the distribution of the various types of macrofauna.

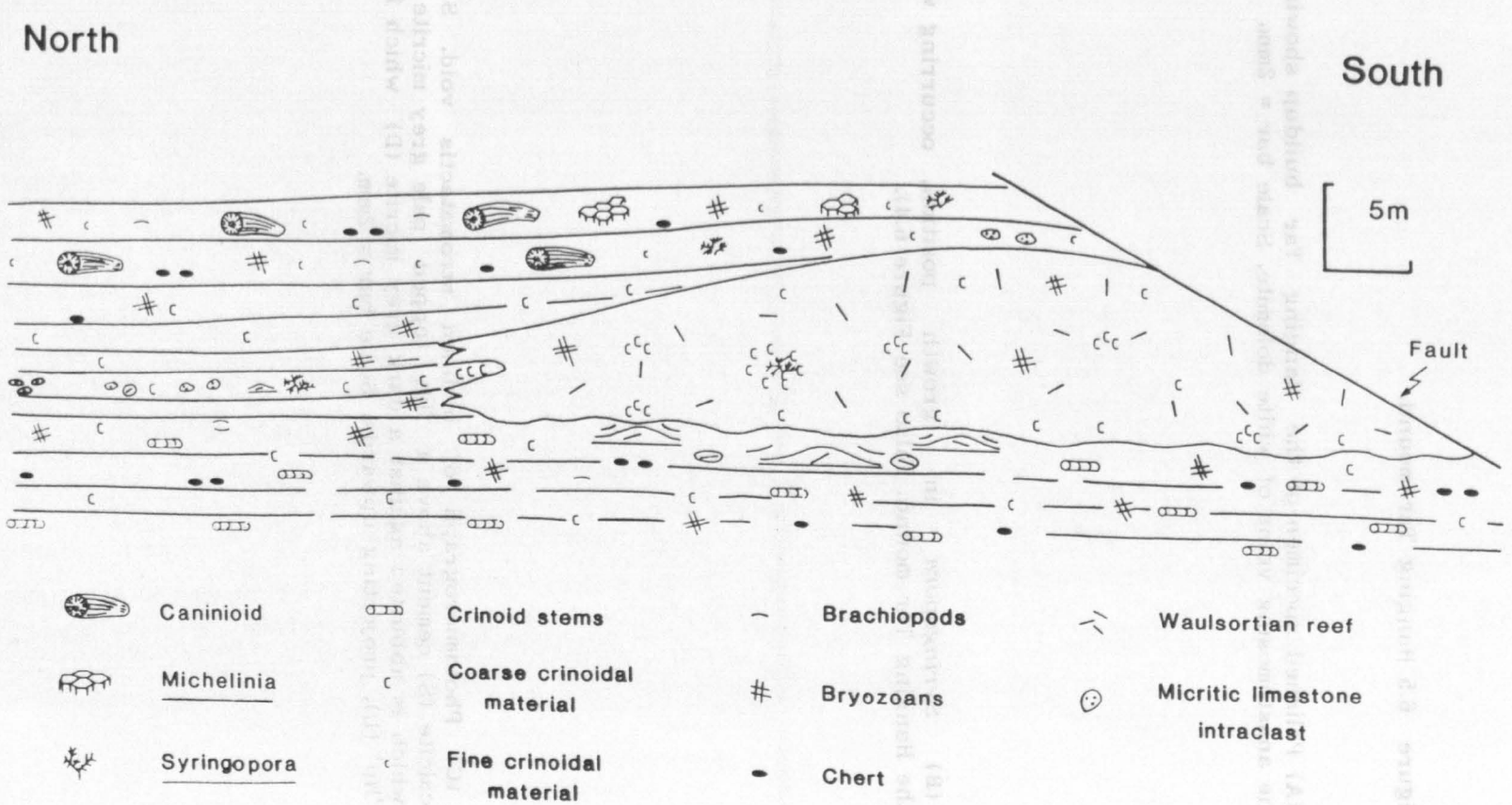
North
South
5m
Fault
Caninioid
Michelinia
Syringopora
Crinoid stems
Coarse crinoidal material
Fine crinoidal material
Brachiopods
Bryozoans
Chert
Waulsortian reef
Micritic limestone intraclast

Figure 6.5 Hanging Tar mound.

(A) Polished specimen of the Hanging Tar buildup showing the the anastomosing veins of white dolomite. Scale bar = 2mm.

(B) *Syringopora* in growth position, occurring within the Hanging Tar mound. (Also see Figure 6.4).

(C) Photomicrograph of inclined stromatactis void. Sparry calcite (S) cement above a flat topped pale grey micrite (P), which is abbutted against a dark grey micrite (D) which forms a 'lip' (L), projecting upwards. Scale bar = 2mm.

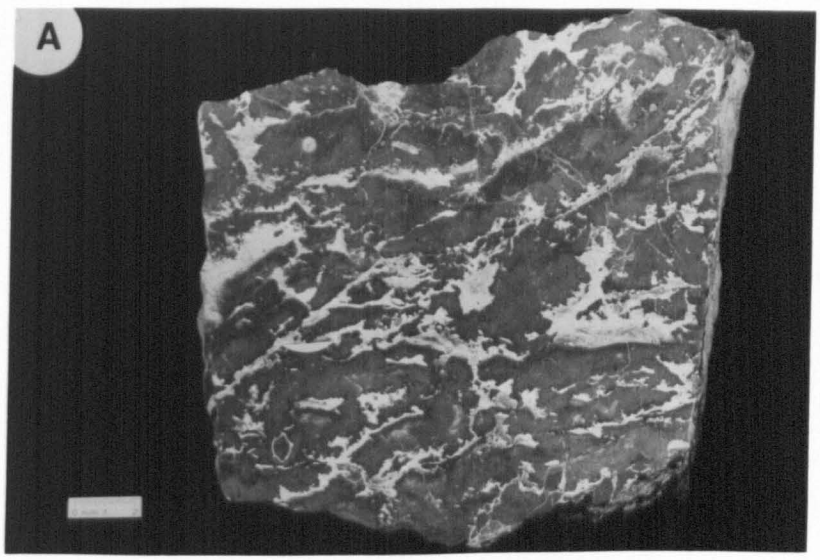
A


B

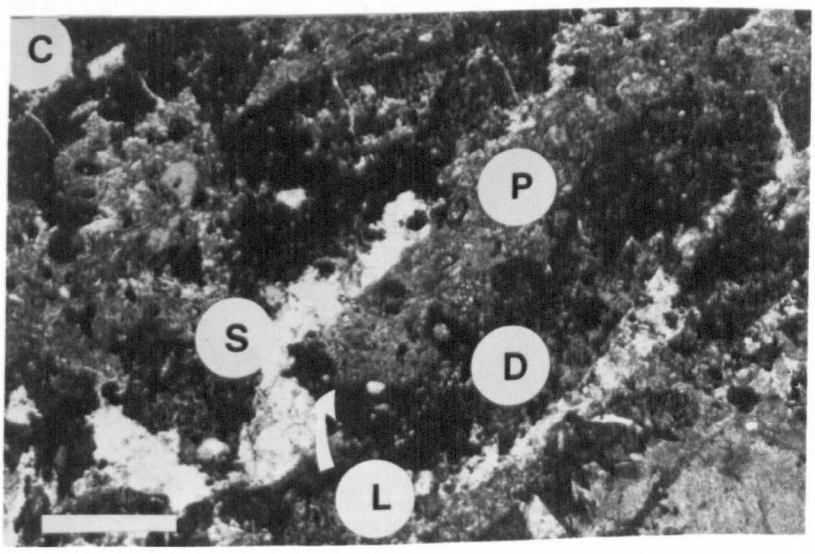
C
P
S
D
L

top of the Berry Slade mound.

Interpretation: The scarcity of relict primary features hampers any meaningful interpretation of the development of the Berry Slade and Wind Bay mounds. Even though they form sizeable buildups and are onlapped by the surrounding bedded succession, there is no evidence as to the topographic height developed above the surrounding sea floor surface.

6.2.2 Hanging Tar Mound

The mudmound at Hanging Tar is ca. 11m thick and bedded on a 0.5m-2m scale (Figures 6.2B & 6.4). It possesses an irregular, gradational contact with the underlying crinoidal stem-rich packstone (Lithofacies 10; previously described in Chapter 4). The interdigitating of the reef and inter-reef crinoidal packstones (bedded on 10-30cm scale) can be observed along the northern margin of the buildup, as the southern margin is fault bounded (Figure 6.4). The convex-upward mound exhibits a sharp boundary with the overlying bioturbated packstones which contain large caninioid corals.

The reef facies is dominated by a pale grey micrite (Figure 6.5A) in which occurs a macrofauna of fenestellid bryozoans, crinoids, and rare brachiopod valves (Figure 6.4). Fenestellid sheets are present but not abundant. The crinoidal debris is locally clustered to form packstone pods (up to 40cm in diameter) within which *Syringopora* can be found in growth position (Figure 6.5B).

A microfacies analysis revealed that the reef contains a diverse fauna in which two componental assemblages were recognized (Figure 6.6). Contained within the lower part of the reef are crinoids, fenestellid bryozoans, ostracods, unilocular and plurilocular foraminifera (Figure 6.7A) (such as *Earlandia* and lituotubellids), aoujgaliidas, sponge spicules (e.g. hyalosteliids), peloids and

Figure 6.6 Microfacies of the Hanging Tar mound showing the distribution of the allochems and micritisation. The key to the different types of macrofauna is as shown in Figure 6.4.

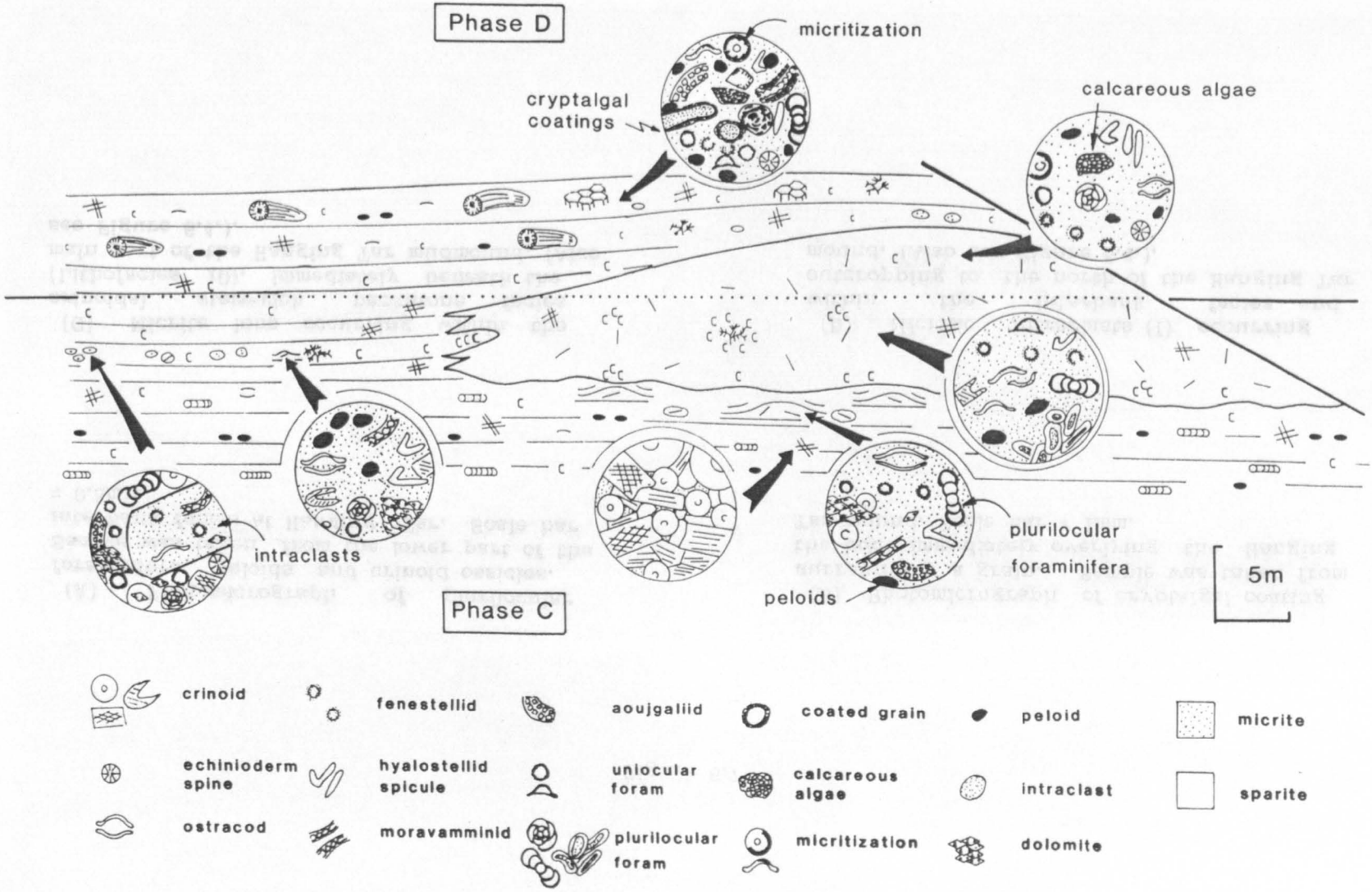
Phase D
micritization
cryptalgal coatings
calcareous algae
intraclasts
plurilocular foraminifera
peloids
5m
Phase C
crinoid
fenestellid
aoujgaliid
coated grain
peloid
micrite
echinioderm spine
hyalostellid spicule
uniocular foram
calcareous algae
intraclast
sparite
ostracod
moravamminid
plurilocular foram
micritization
dolomite

Figure 6.7

(A) Photomicrograph of plurilocular foraminfera, peloids and crinoid ossicles. Sample was taken from the lower part of the interbank facies at Hanging Tar. Scale bar = 0.5mm.

(B) Photomicrograph of cryptalgal coating surrounding a grain. Sample was taken from the beds immediately overlying the Hanging Tar mound. Scale bar = 1mm.

(C) Micrite lens occurring within the crinoidal stem-rich packstone facies (Lithofacies 10), immediately beneath the main part of the Hanging Tar mudmound. (Also see Figure 6.4.).

(D) Micritic intraclasts (I) occurring within the interbank facies and outcropping to the north of the Hanging Tar mound. (Also see Figure 6.4.).

A
B
C
D
MINOLTA

filaments. The filaments are particularly abundant in the pale grey micrites where they form tubular structures, 30-40μm in diameter, without calcareous sheaths or wall structures. Overall, the plurilocular foraminifera are not particularly abundant in the reef facies.

In addition to the above mentioned components, the upper part of the reef includes calcareous algae (e.g. *Koninckopora*) and cryptalgal coatings around grains (Figure 6.7B). Notably, many of the allochems have been extensively bored and exhibit micrite rims. The transitional boundary between the lower and upper reef assemblages occurs just above the centre of the mound and can traced laterally into the inter-reef facies (Figure 6.6).

The stromatactis structures consists of sparry calcite cement infilling the void, above a flat topped pale grey micrite which has a sharp and irregular basal contact with the underlying darker grey micrite (Figure 6.5C). Generally, the stromatactis voids tend to be small (<3cm in length) (Figure 6.5C). The void filling sparry calcites are commonly replaced by the veins of white dolomite. The dips of the stromatactis structures along the northern margin of the reef facies are approximately 6-8° greater than bedding.

Convex-upward lenses of micritic limestones are to be found both within the beds underlying the reef and in the inter-reef facies (Figures 6.4 & 6.7C). Less than a metre thick, and up to several metres wide, the lenses commonly exhibit a gradational contact with the surrounding lithology. Their internal microstructure is comparable in its organisation to the main reef facies e.g. they contain stromatactis cavities.

Also occurring with the inter-reef facies are intraclasts of micritic limestone and *Syringopora* corals in growth position. The intraclasts are usually less than 5cm in diameter and have a sharp contact

with the surrounding crinoidal packstones (Figure 6.7D). They consist of dark grey, dense micrite and lack those microstructural features characteristic of the reef facies. Overall, there is no tendency for the larger intraclasts to predominate in closer-proximity to the reef facies.

Interpretation: The reef development at Hanging Tar represents a minor buildup of Waulsortian facies. The low-angle primary depositional dips recorded by the stromatactis (8-10°) suggest the buildup had a low relief, of perhaps only a few metres above the surrounding sea floor surface. Overall, current activity is likely to have been of relatively low intensity because *Syringopora* is found within growth position. However, there are likely to have been periods of more intense current activity which have been recorded by the presence of micritic intraclasts (up to 5cm in diameter). There is no evidence of erosional surfaces within the Hanging Tar mound which would indicate that the intraclasts and micritic lenses represent detached clasts from the reef facies. The former are most likely derived from the erosion of the sea floor surface surrounding the Waulsortian facies. A similar conclusion was also reached by Miller (1986) in his study of the mound complex at Hill 707 (Ireland). The micritic lenses are likely to have a similar origin to the mound because they exhibit comparable sedimentary fabrics (e.g. stromatactis).

There has been considerable debate as to the origin of Waulsortian buildups. Many authors have regarded them as having been due to the baffling effect of organisms, such as fenestellids and crinoids (Wilson 1975; Philcox 1971). This would seem an unlikely mode of origin for the Hanging Tar mound which contains relatively low abundances of the above mentioned faunas. A study of the Waulsortian buildups of Belgium by Lees *et al.* (1977) has show there is no direct correlation between the volume

of micrite and the abundance of fenestellids and crinoids.

In 1982 Pratt suggested that microbial mats may have trapped and bounded (and lithified) the micrite which form Waulsortian mounds. This is inconsistent with the observations of Lees & Miller (1985) who noted that the micrite mud in the mounds is texturally and compositionally different from the mud of the surrounding lithologies. The microbial trapping and binding mechanism of Pratt (1982) would require selective exclusion of argillaceous material which is more abundant in the inter-mound deposits e.g. at Hanging Tar. Such a mechanism for mound formation would have had to have been extremely efficient to form the huge buildups of Belgium, with 100-200m of relief (Lees *et al.* 1985).

Lees & Miller (1985) proposed that the mound mud must have been locally produced, associated with a probable mucilaginous surface cover, and were probably microbially precipitated. They described abundant filaments (comparable to those described above) occurring within certain parts of Waulsortian buildups as well as 'clotted' textures of a type commonly referred to as 'cryptalgal'. As yet, there is no direct evidence of the role of microbial activity in producing the bulk of the mound-building carbonate mud (Lees & Miller 1985).

6.3 Sedimentary Phases

The study of the Waulsortian buildups of Belgium by Lees *et al.* (1985) culminated in a composite model of a Mid-Dinantian Waulsortian buildup. Four componental assemblages in order A, B, C & D were recognized (Figure 6.8) and related to water-depth, based on palaeontological data (Lees *et al.* 1985) (Figure 6.9).

Assemblage (A): fenestellids + crinoids + ostracods

Assemblage (B): as (A) + hyalosteliid sponge spicules

Assemblage (C): as (B) + plurilocular foraminifera

Assemblage (D): as (C) + cryptalgal coating, micritisation of grains and cavity walls and calcareous algae.

The phases (A-D) were later shown to be of more general application to other Waulsortian buildups in Europe and the United States (Lees & Miller 1985; Bridges & Chapman 1988). The latter authors showed that the four phases were consistent and not sporadic in their distribution, and express increasing faunal diversity of components in associations, rather than stratigraphic position.

The four Phases (A-D) record a range of marine environments from Phase A (most probably more than 300m) to Phase D in the photic zone, about 120m or shallower (Lees *et al.* 1985) (Figure 6.9). The phase with which a Waulsortian complex is initiated in a given basin should reflect water depth at that time and place (Lees & Miller 1985). Subsequent major changes in the depth of the water column should be reflected by the bathymetric assemblages (Lees *et al.* 1985; Lees & Miller 1985).

6.3.1 Sedimentary Phases at Castlemartin

Even though the Berry Slade and Wind Bay mounds have been extensively dolomitized it is still possible to deduce which of the phases they are most likely to contain. Constraints from the phases that immediately underlie and overlie a buildup can, in some instances, be confirmed by the identification of the relict components preserved within the dolomite.

Those constituents contained within the beds that immediately underlie the Berry Slade mound include fenestellids, crinoids and hyalosteliid sponge spicules (section 6.2.1) which are characteristic of

Figure 6.8 Schematic representation of the composition of the sediments associated with the four Waulsortian bathymetric assemblages proposed by Lees *et al.* (1985). Modified after Bridges & Chapman 1988.

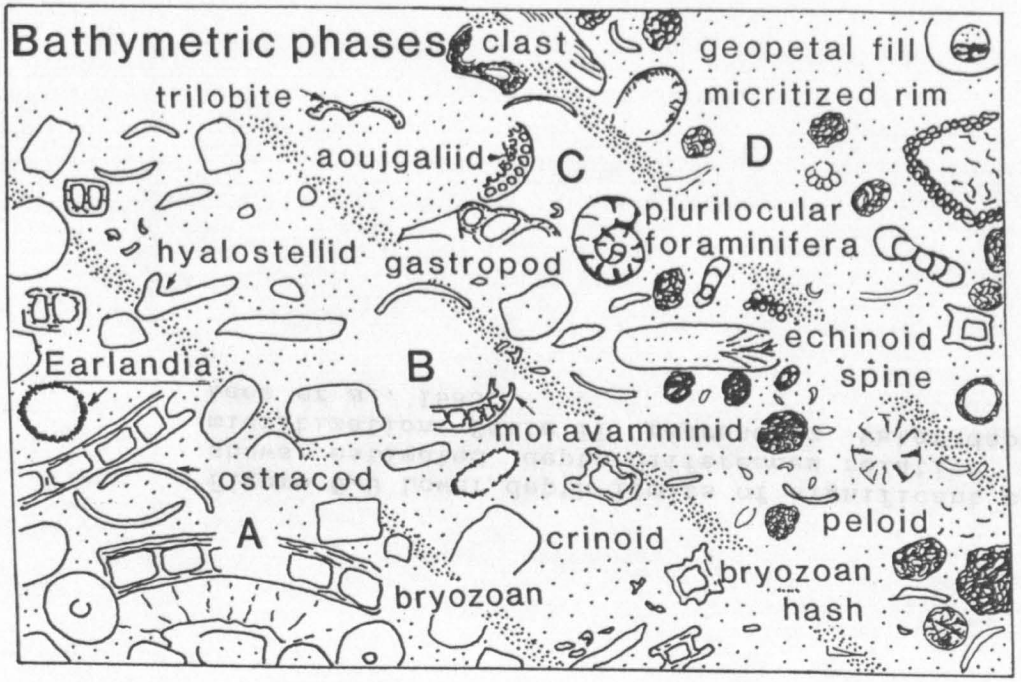

Assemblage (A)

fenestellids
crinoids
ostracods

Assemblage (B)

as (A) &
hyalosteliid sponge spicules

Assemblage (C)

as (B) &
plurilocular foraminifera

Assemblage (D)

as (C) &
cryptalgal coating
micritization of grains
calcareous algae

Figure 6.9 Lower depth limits of significant components. Scale I shows estimated depth differences relative to the level of micritization. Scale II represents water depth. Modified after Lees *et al.* 1985.

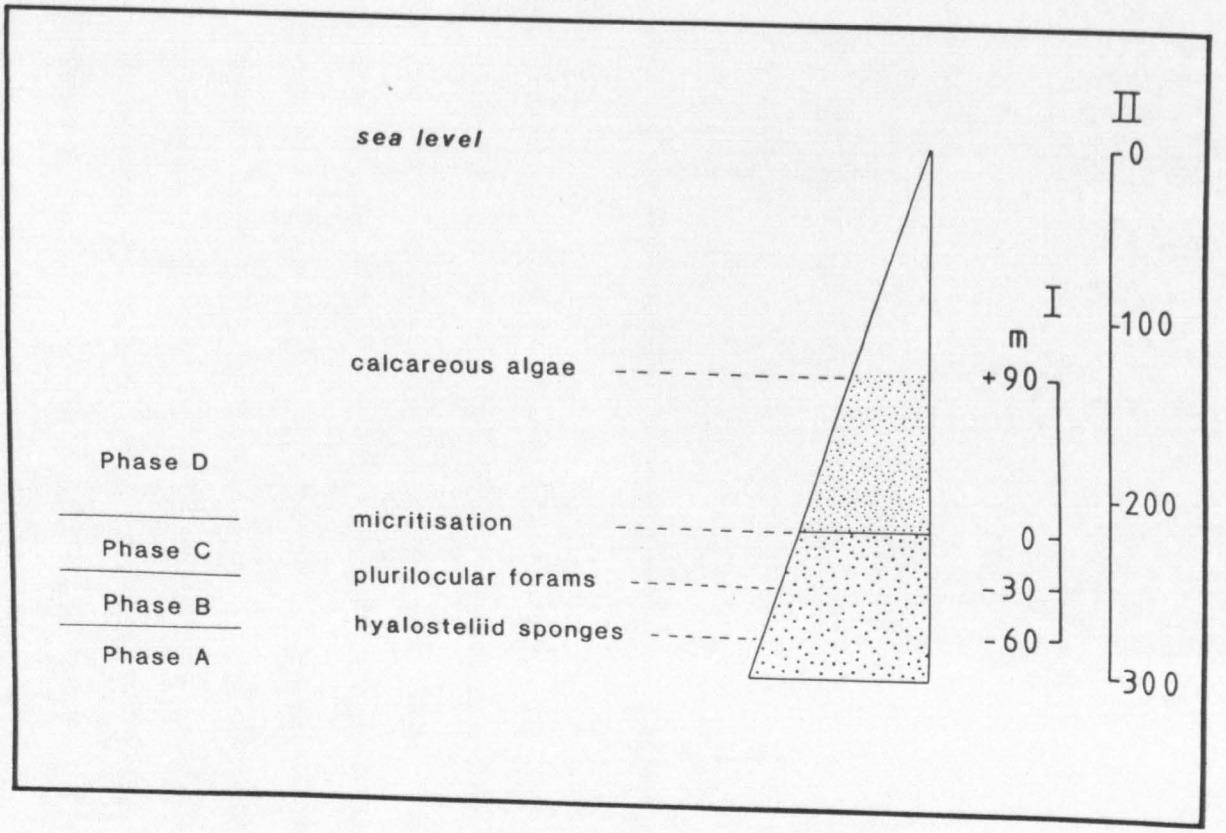
sea level
calcareous algae
micritisation
plurilocular forams
hyalosteliid sponges
Phase D
Phase C
Phase B
Phase A
I
m
+90
0
-30
-60
II
0
100
200
300

Phase B. In addition, the beds that immediately overlie the Berry Slade and Wind Bay mounds contain plurilocular foraminifera which are characteristic of Phase C.

Unfortunately, no relict hyalosteliid sponge spicules were identified within the dolomite mounds. However, two relict ghost plurilocular foraminifera (diagnostic of Phase C) were found in the upper part of the Berry Slade mound. From the available evidence, it would seem the dolomitized mound at Berry Slade, and its lateral equivalent at Wind Bay, both contain Phases B and C, although the exact position of the boundary is unknown.

Phases C and D are readily identifiable within the Hanging Tar mound, where the boundary occurs within the upper part of the buildup (Figure 6.6). A similar conclusion was reached by Lees & Miller (1985). The base of Phase D is denoted by the incoming of cryptalgal coatings, calcareous algae and micritised grains all at approximately the same level (Figure 6.6).

Interpretation: The initiation of the Berry Slade and Wind Bay mounds was within Phase B, a subphotic environment, most probably representative of water depths between 250m and 280m. Using the depth-related scale of Lees *et al.* (1985) (Figure 6.9), the three phases recognized within the Waulsortian mounds at Castlemartin record a regression passing upward from Phases B to D (Figure 6.3). The incoming of micritisation and calcareous algae together, most probably represents a marked relative fall in sea level during early Chadian times (compare Figures 6.6 & 6.9). In the absence of wave formed features, it would seem that the southern ramp zone remained beneath storm wave-base. The preservation of the effects of currents operating beneath wave-base are not, however, conspicuous until the uppermost parts of Phase C, and the appearance of abundant micritic intraclasts (up to 5cm in diameter) in

the inter-reef facies at Hanging Tar.

6.4 Discussion

The Waulsortian phases provide a new tool for basin analysis (Lees & Miller 1985). A record of the phase changes within Waulsortian facies and good biostratigraphic controls provide the means by which local tectonic effects and regional eustatic events can be distinguished. The aim of the first part of this discussion is to evaluate the significance of the phase changes recorded within the Waulsortian mounds of SW Britain. A comparison of the evolution of the buildups of SW Britain with those of Belgium allows an assessment to be made of the effects of tectonics and eustacy upon mound development along the southern margin of the Welsh-Brabant Massif (Figure 1.1).

All four of the depth-related sedimentary Phases (A to D), as described by Lees *et al.* (1985) from the buildups in Belgium, are present within the Waulsortian facies of SW Britain (Figures 6.10 & 6.11). The deepest water assemblage of Phase A has only been identified at Cannington Park (Lees & Hennebert 1982). Here, the lower part of the mound complex consists of sparry calcite facies readily comparable to the "veines bleues" of Belgium. The upper part of the Cannington Park mound complex consists of a biomicrite facies which contains a Phase B assemblage (Lees & Hennebert 1982). The incoming of plurilocular foraminifera (Phase C) occurs within the uppermost part of the Cannington Reef Limestone. The decline of the Cannington Park mound complex occurred prior to the end of the Courceyan (Mitchell *et al.* 1982; Lees & Hennebert 1982). Development of the Waulsortian facies during the uppermost Courceyan and early Chadian times is recorded at Castlemartin (Figures 6.3, 6.10 & 6.11). Here, Phases B, C and D have been

Figure 6.10 Schematic cross-sectional model of the carbonate ramp of SW Britain and the Waulsortian facies of Belgium for the upper Courceyan (Tournaisian) to early Chadian (Visean) period. The sedimentary phases for the mudmound complex of Cannington Park are taken from Lees & Hennebert (1982), while information for the mound complexes of Belgium is taken from Lees *et al.* (1985).

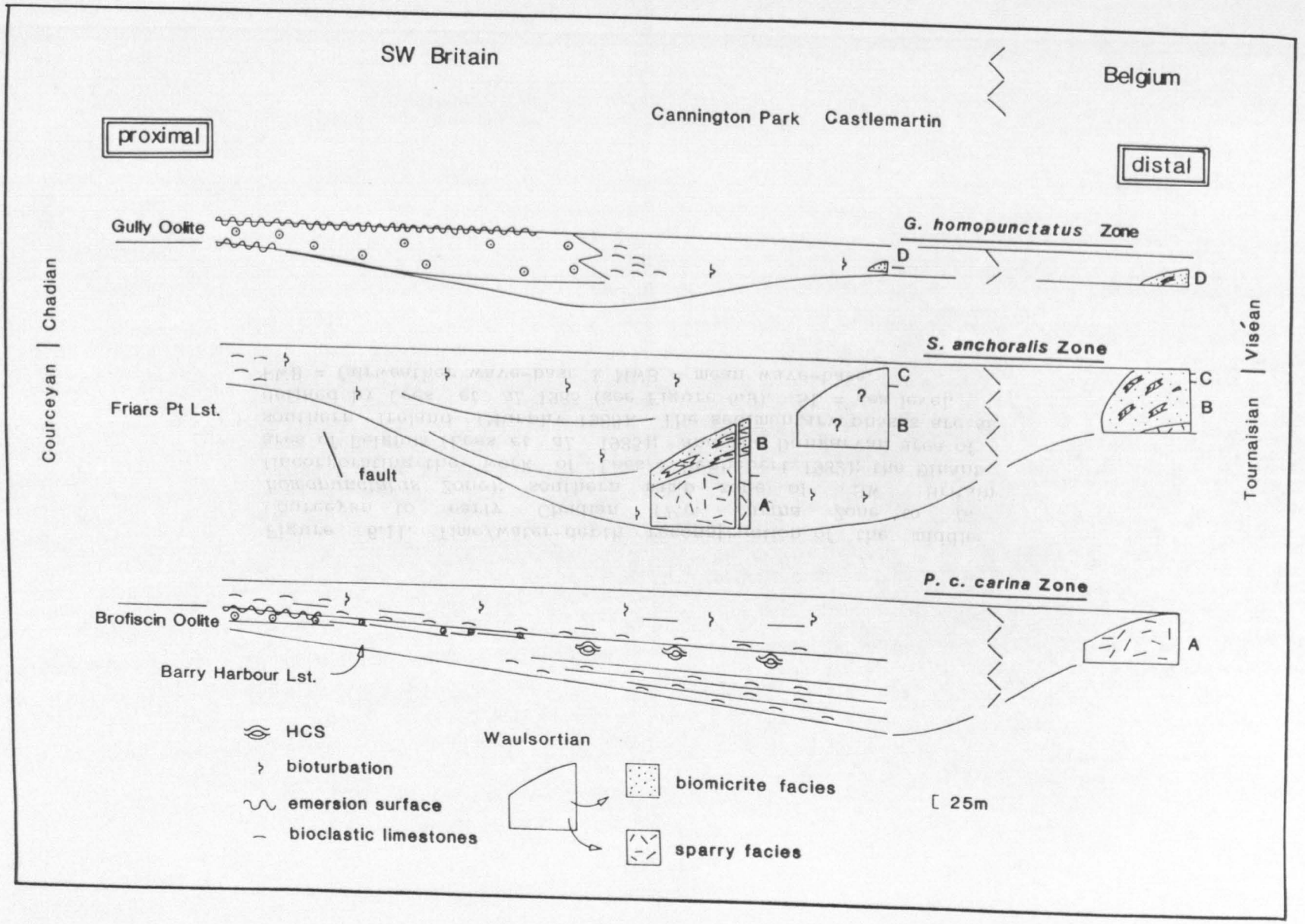
SW Britain
Belgium
Cannington Park
Castlemartin
proximal
distal
Courceyan | Chadian
Tournaisian | Viséan
Gully Oolite
G. homopunctatus Zone
D
D
S. anchoralis Zone
Friars Pt Lst.
C
?
?
B
C
B
B
fault
A
P. c. carina Zone
Brofiscin Oolite
Barry Harbour Lst.
A
HCS
bioturbation
emersion surface
bioclastic limestones
Waulsortian
biomicrite facies
sparry facies
25m

Figure 6.11. Time/water-depth reconstruction of the middle Courceyan to early Chadian (*P.c. carina* Zone to *G. homopunctatus* Zone): southern ramp zone of SW Britain (incorporating the work of Lees & Hennebert 1982); the Dinant area of Belgium (Lees *et al.* 1985); and the Dungarvan area of southern Ireland (Murphy 1988). The sedimentary phases are as defined by Lees *et al.* 1985 (see Figure 6.9). SL = sea level, FWB = fairweather wave-base & MWB = mean wave-base.

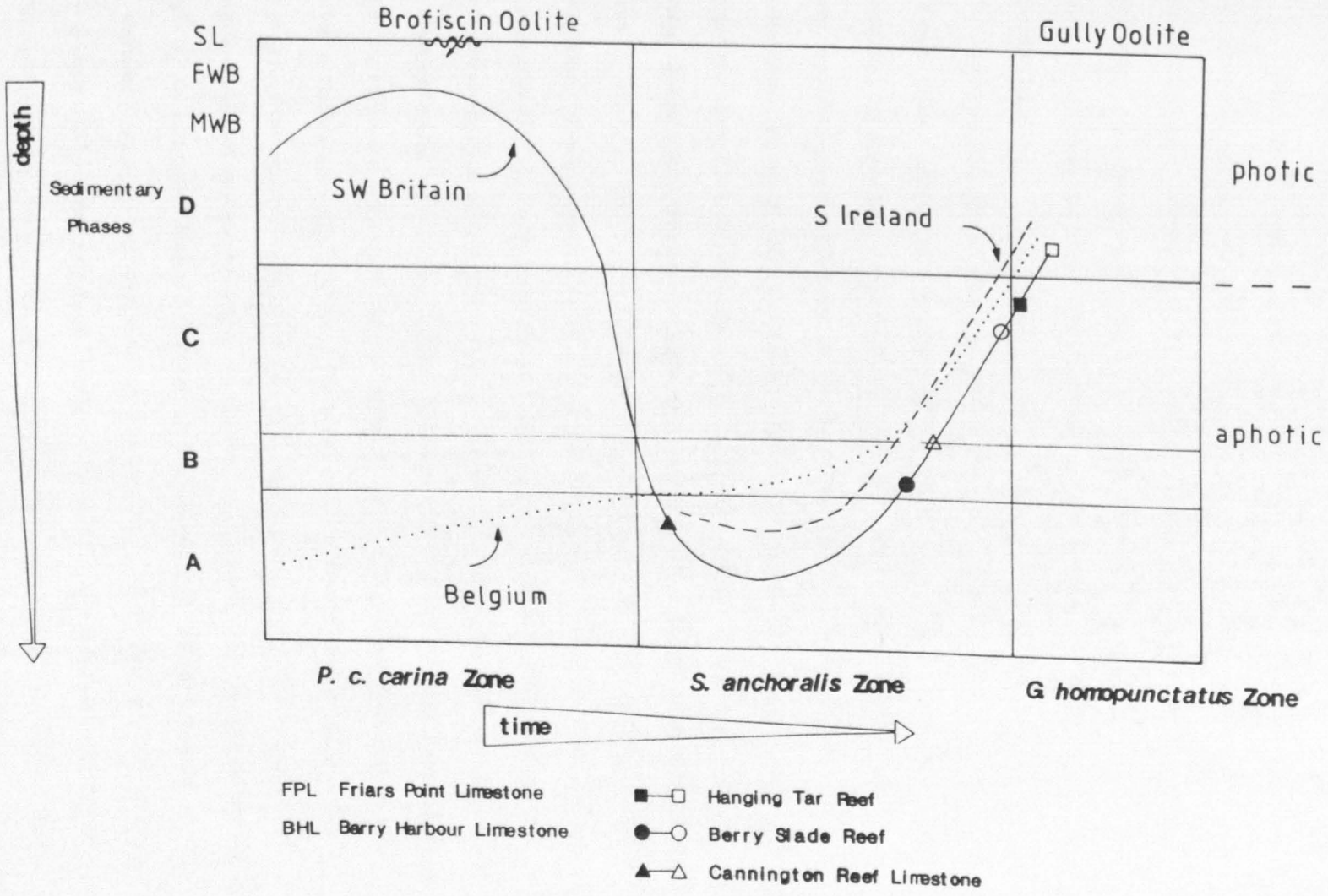
Brofiscin Oolite
Gully Oolite
SL
FWB
MWB
depth
Sedimentary
Phases
D
C
B
A
SW Britain
S Ireland
Belgium
photic
aphotic
P. c. carina Zone
S. anchoralis Zone
G. homopunctatus Zone
time
FPL Friars Point Limestone
BHL Berry Harbour Limestone
Hanging Tar Reef
Berry Slade Reef
Cannington Reef Limestone

identified within the buildups (section 6.2.3). The incoming of Phase D was during early Chadian times.

The four phases (A-D) record a shallowing-upward succession during the late Courceyan to early Chadian times (Figures 6.9, 6.10 & 6.11). The presence of Phase A at Cannington Park represents water depths most probably in excess of 300m. The subsequent relative fall of sea level was likely to have been within close-proximity of 100m by early Chadian times.

A comparison of the evolution of the Waulsortian buildups of SW Britain with those of Belgium show that the initiation of the mound complexes is strongly diachronous whereas their subsequent evolution is more synchronous (Figures 6.10 & 6.11). The development of the Waulsortian facies of Belgium commenced with the deepest water assemblage (Phase A) near the base of the *P. c. carina* Zone. Throughout the *P. c. carina* Zone, SW Britain was dominated by notably shallower water facies, such as the Barry Harbour Limestone (Figures 6.10 & 6.11). The establishment of the Waulsortian facies of SW Britain did not occur until the *S. anchoralis* Zone (Figures 6.10 & 6.11). Initation of the Waulsortian facies commenced with Phase A at Cannington Park and Phase B at Castlemartin. The formation of these deep water phases represents a major relative rise in sea level above the shallow water facies of the Brofiscin Oolite and the Barry Harbour Limestone (Figures 6.10 & 6.11). The magnitude of this sea level rise is likely to be in the order of several hundred metres. If such a facies change was as a result of eustacy then it is highly likely to be represented by phase changes in the Waulsortian mounds of Belgium. In actual fact, the buildups of Belgium show a relative shallowing from Phase A to Phase B, from the uppermost *P. c. carina* Zone to the lower part of the *S. anchoralis* Zone (Figures 6.10 & 6.11). This would suggest that the main control upon the

establishment of Waulsortian facies in SW Britain was regional tectonic subsidence.

The tectonic setting for the Waulsortian mounds of Castlemartin and Cannington Park is within the southern ramp zone which underwent the greatest subsidence (see Chapter 4). Their occurrence is comparable to the Waulsortian developments of Northern England (Miller & Grayson 1982). Here, the Waulsortian mounds occur in distal ramp settings in rapidly subsiding basins, which contrast with the adjacent slowly subsiding blocks, dominated by shallow water facies.

Subsequent to the initiation of Waulsortian mounds in SW Britain, their evolution is comparable to the buildups of Belgium which record a major change of environment during the upper Courceyan (Tournaisian) times (Lees *et al.* 1985; Lees & Hennebert 1982). Throughout the early part of this period, the Waulsortian buildups of both regions continued to form and develop but then suffered a sharp decline from which the mound complex at Cannington Park did not recover, while those in Belgium (Lees & Hennebert 1982) and Castlemartin persisted only into the early part of the Viséan (Chadian) (Figures 6.10 & 6.11).

Towards the end of the Courceyan (Tournaisian) period there was a sharp, 'take-over' in the main faunal constituents of the buildups, from crinoids and bryozoans to moravamminids and plurilocular foraminifera (Lees & Hennebert 1982; Lees *et al.* 1985). This marked facies change preceded the expansion of the area effected by micritisation. The incoming of calcareous algae occurred during the late Courceyan (Tournaisian) to early Chadian (Viséan) times. These phenomenon have been attributed by Lees *et al.* (1985) and Lees & Hennebert (1982) to the passage of the buildups and their flanking beds up into the photic zone and as a consequence of a marked fall in sea level (Figures 6.9, 6.10 & 6.11). A study of the buildups of Castlemartin would support this

interpretation.

Correlative evidence for a sea level fall at the end of the Courceyan has come from the study of the Waulsortian Limestone Formation of the (Dungarvan Syncline) Munster Basin, southern Ireland by Murphy (1988) (Figure 6.11). Initiation and growth of the reef commenced with Phase A during the *S. anchoralis* Zone; the incoming of Phase D was occurred during the late Courceyan; and the eventual demise of the mound complex occurred during early Chadian times (Figure 6.11).

In conclusion, suitable conditions for the initiation of the Waulsortian reefs of SW Britain developed after a major phase of differential subsidence, following which relatively deep water environments prevailed over the southern ramp zone. Three sedimentary phases, comparable to the sedimentary Phases B-D of Lees *et al.*, can be identified within the Waulsortian mounds at Castlemartin. They support the interpretation by Lees *et al.* (1985) for a pronounced change of environment, most probably as a result of a marked eustatic sea level fall, at the end of the Courceyan and during early Chadian times.

6.5 Petrography and Geochemistry of the Castlemartin Waulsortian Dolomites

There is a marked contrast between the pale white, almost completely dolomitized Waulsortian mounds of Berry Slade and Wind Bay, and the surrounding dark grey, stratified inter-reef limestones (Figure 6.2A). These "peculiar reef dolomites" lacking bedding, were proclaimed by Dixon (1921) to be without analogue in SW Britain and comparable to dolomites he observed in the Waulsortian buildups of northern England (Clitheroe) and Belgium.

Even though many Waulsortian buildups have been partially to extensively dolomitized (Dixon 1921; Cotter 1966; Miller 1986; Lees & Hennebert 1982; Philcox 1971; Lees *et al.* 1977) there have been few studies into the origin of the dolomite. Cotter (1966) proposed that the buildups of central Montana (USA) were dolomitized by near-surface hypersaline fluids, by means of seepage reflux. Whereas Miller (1986) favoured a burial origin for the dolomites within the mound complex at Hill 707 (Ireland).

Characterisation of the Waulsortian dolomites at Castlemartin is aided by making comparisons with the other major dolomite types occurring within the Dinantian of South Wales (Bhatt 1973 & 1976; Hird *et al.* 1987; Wright & Robinson 1988; Searl 1988). These mainly outcrop in the northern and central ramp zones and include: penecontemporaneous peritidal and pedogenic dolomicrites, pervasive stratal dolomites of shallow-burial mixing zone origin, and cross-cutting 'vein' or 'dyke' dolomites of burial origin.

6.6 Burial History

The buildups of Castlemartin underlie a thick limestone succession, mainly consisting of below storm wave-base facies (Wright 1986; Simpson 1987). The post-Dinantian sediments are predominantly sandstones, reflecting the establishment of fluvio-deltaic environments within the Hercynian fore-deep of SW Britain (Kelling 1988). The original thickness of the Namurian and Westphalian strata is unknown because of uplift and erosion during the Stephanian(?) and the Permian. However, the thickness of Namurian and Westphalian sediments in the adjacent area of Swansea indicates burial of the Dinantian sequence to a depth of at least 7Km by late Carboniferous times (Dickson 1985, Jones 1974; Thomas 1974; George 1970) (Figure 6.12). The Hercynian orogeny deformed and raised the Carboniferous Limestone which became subaerially exposed. Subsequent burial occurred during the Mesozoic (Figure 6.12) and up to 1.5Km of Jurassic and Cretaceous sediments were deposited but later removed by the Oligocene (George 1974; Dickson 1985).

6.7 Methods

Twenty representative samples of the Waulsortian dolomites at Castlemartin were taken for analysis. The thin sections and thirty acetate peels were stained with Alizarin Red S and potasium ferricyanide using the modified technique described by Dickson (1965). Cathodoluminescence (CL) was undertaken using a Technosyn (Model 8200) MkII cold cathode luminescope. The following elements were analysed using atomic absorption spectrophotometer (AAS): Ca, Mg, Sr, Fe, Mn and Na (Appendix T). Operation of the AA was undertaken by A. Kemp (Bristol University). Carbon and oxygen stable isotope analyses were carried out by M.T. Burchell (Oxford University) at BP Research Centre, Sunbury (Appendix U).

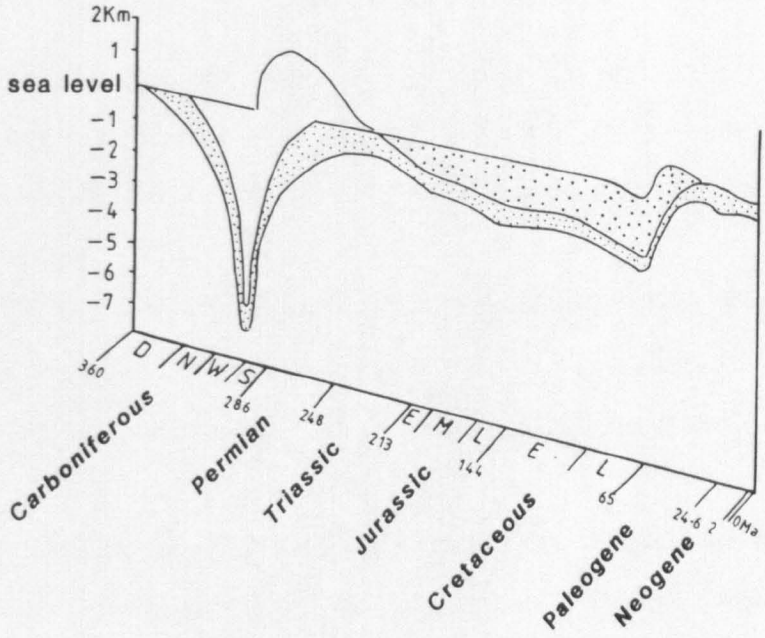

Figure 6.12. Time-depth reconstruction to show the history of South Wales sediments from their deposition, through burial to their present position. Dinantian sediments are shown in fine stipple. Modified after Dickson 1985.

6.8 Diagenetic relationships

In addition to replacing the mounds at Wind Bay and Berry Slade, the pale dolomites also form rare stratabound units in the inter-reef facies at Wind Bay (Figure 6.13A) and anastomosing veins in the buildup at Hanging Tar (Figure 6.5A). Overall, dolomitization was a selective process, more commonly replacing lime mud. Its timing postdated the void filling calcite cements in the Hanging Tar mound, which it both replaced (Figure 6.13B & C) and cross-cut in veins. Three void filling calcite cement phases have been identified within the Hanging Tar mound (Figure 6.13B).

Cement stage I consists of clear, non-ferroan, prismatic calcite crystals which are non-luminescent under CL (Figure 6.13B). The crystals are generally euhedral with rhombohedral terminations and are usually less than 500μm in length.

Cement stage II comprises several alternating bright yellow-orange and non-luminescent zones (Figure 6.13B). The individual zones are usually less than 10μm thick. Cement stage II is syntaxial with the stage I prisms (Figure 6.13B).

Cement stage III consists of blocky ferroan, calcite crystals which are orange-brown to dull brown luminescent under CL. Cement stage III also occurs in veins.

The cement stages I-III record precipitation in oxidising to reducing conditions. This is thought to reflect the decreasing redox potential of pore fluids with time and burial. A comparable sequence of cements (Stages 2-4) has been described by Miller (1986) in the mound complex at Hill 707 Co. Galway Ireland. The cement Stages 2-4 are also interpreted as representing the progressive change in the chemistry of the pore fluids during burial.

Figure 6.13

(A) Stratabound pale dolomites (D), approximately 5m thick, within the interbank facies at Wind Bay.

(B) Photomicrograph of a CL image of void cements, showing Stages I, II & III. See text. Scale bar = 0.25mm

(C) Photomicrograph of a CL image of a void infilled by a Stage III (III) calcite cement that has in part been replaced by a zoned dolomite (Z). Scale bar = 0.25mm.

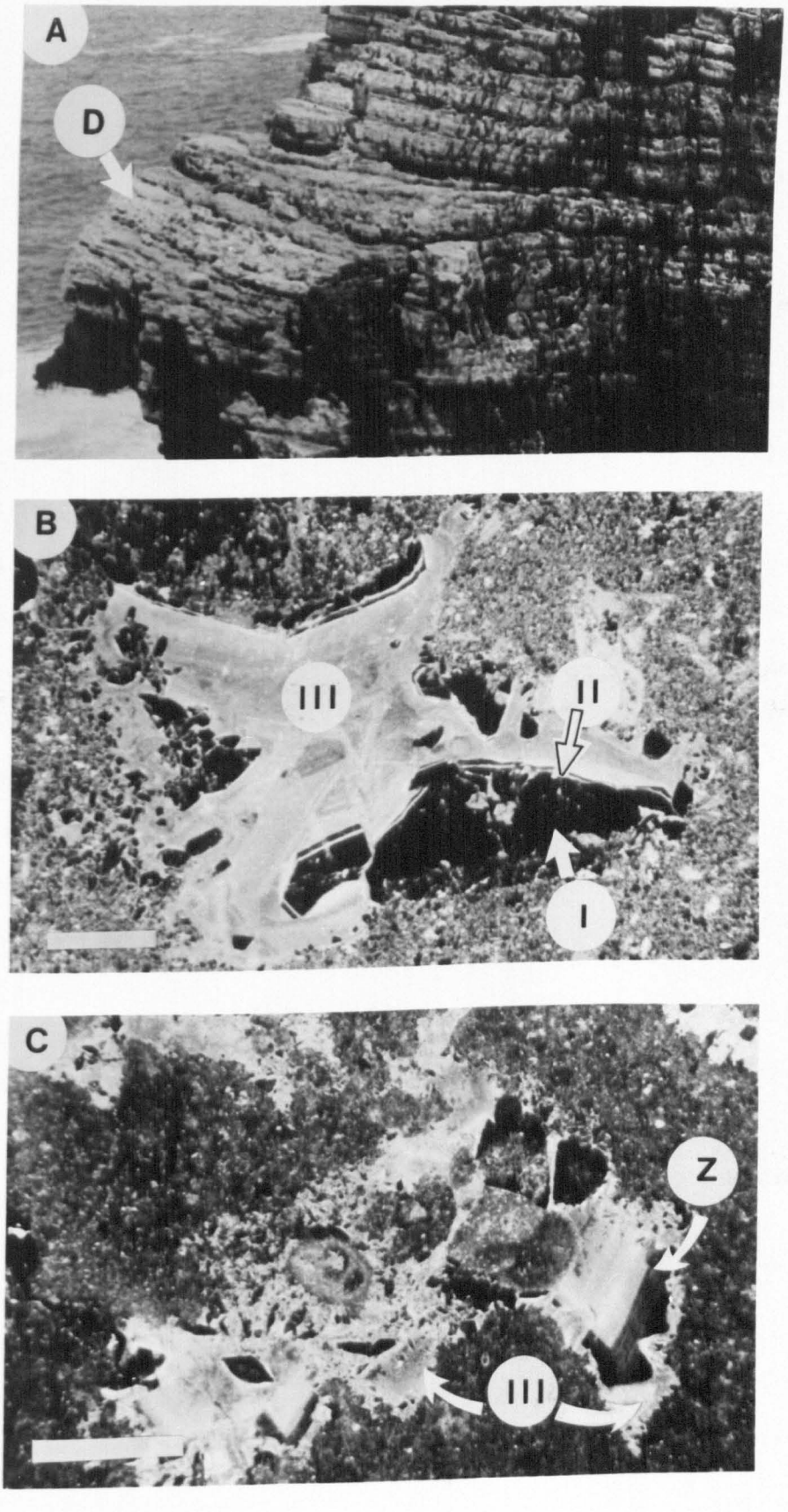
A
D
B
III
II
I
C
Z
III

The relative timing of the dolomite diagenesis of the Waulsortian mounds postdates the burial cement stages I-III but predates tectonic jointing. Both the Berry Slade and the Wind Bay dolomite mounds are extensively fractured. Occurring within the fractures are veins of hematite, goethite and non-ferroan calcites that display a bright orange luminescence when observed under CL.

Tectonic fracturing of the Waulsortian mounds is interpreted as having been related to the Hercynian orogeny which uplifted the mounds during the late Carboniferous to early Permian times (Figure 6.12). The non-ferroan calcites, hematite and goethite were precipitated from oxidising fluids, most probably groundwater. A comparable mineralogical association and occurrence has been recorded in the Lower Carboniferous limestone of Llanharry (South Wales) by Rankin & Criddle (1985). They proposed that the source of the iron came from descending groudwaters which acquired a high salinity and iron content from the overlying Permo-Triassic red beds.

In conclusion the diagenetic relationships and burial history of the Waulsortian mounds indicate that the timing for the formation of the pale dolomites was during burial.

6.9 Dolomite types & their geochemistry

Two main morphological types of dolomite have been recognized, (1) mosaic dolomite and (2) saddle dolomite.

6.9.1 Type 1-Mosaic dolomite

This style of dolomite is volumetrically dominant in the two mounds at Berry Slade and Wind Bay (replacing more than 95% of the reefs), and forms rare stratabound units in the inter-reef facies (Figure 6.13A). It also occurs in the Hanging Tar mound within veins (Figure 6.5A), voids and more

rarely occurs along stylolites. The dolomite veins define a 'net-like fabric' enclosing centrimetre-sized 'cells' of micrite (Figure 6.5A).

The dolomite crystal size distribution is polymodal and ranges from 25μm to 600μm in diameter. The dolomite crystals locally exhibit an inclusion-rich core and limpid surround. Two styles of mosaic dolomite can be recognized based on the nature of the intercrystalline boundaries (Figure 6.14A). **Idiotopic mosaics** comprise euhedral rhombs that have planar intercrystalline boundaries. The rhombs show unit extinction under crossed polars. The intercrystalline area is either filled with non-ferroan calcite, clay minerals or hematite. The intercrystalline boundaries of the **xenotopic mosaics** are generally irregular and lobate. They are commonly more coarsely crystalline, with crystal sizes varying from 100-600μm in diameter. Individual crystals have an anhedral form and show sweeping extinction to varying degrees.

Using cathodoluminescence two phases of dolomite have been identified. The first phase is dominant and has a uniform bright red luminescence (Type-1A). In contrast, the second phase (Type-1B) is finely zoned and typically exhibits alternating bright red and dull luminescence (Figure 6.14B). Volumetrically Type-1B is less significant than Type-1A which it cross-cuts in minor veins. Another important occurrence for Type-1B is as a void fill. The term void filling is used in the sense of Sibley & Gregg (1987) and includes dolomite cement as well as dolomite that has replaced a precursor cement. Type-1B replaces the sparry calcite within stromatactis at Hanging Tar and also occurs as a void-fill within fossil allochems, such as ostracods.

6.9.2. Type 2-Saddle dolomite

Associated with the mosaic dolomites are sparry crystals, 250μm to 1cm in size. These have curved cleavage traces and crystal faces, and show

Figure 6.14.

(A) Photomicrograph of the xenotopic mosaic dolomite characterized by by anhedral crystals (A) of dolomite with irregular intercrystalline boundaries and euhedral crystals (E) with planar intercrystalline boundaries. Scale bar = 0.5mm.

(B) Photomicrograph of a CL image showing the uniform luminescent Type-1A (1A) dolomite and the zoned bright red and dull luminescent Type-1B (1B) dolomite. Scale bar = 0.5mm.

(C) Photomicrograph of a CL image of saddle dolomite showing well developed curved crystal faces. The non-luminescent anhedral crystals are of geothite and hematite, and the cross-cutting bright luminescent veins are of non-ferroan calcite. Scale bar = 0.25mm.

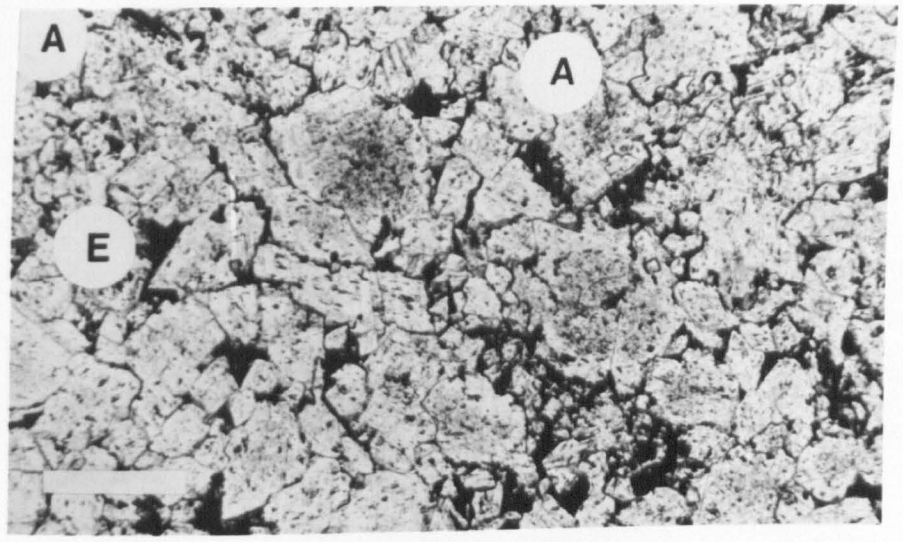
A
A
E

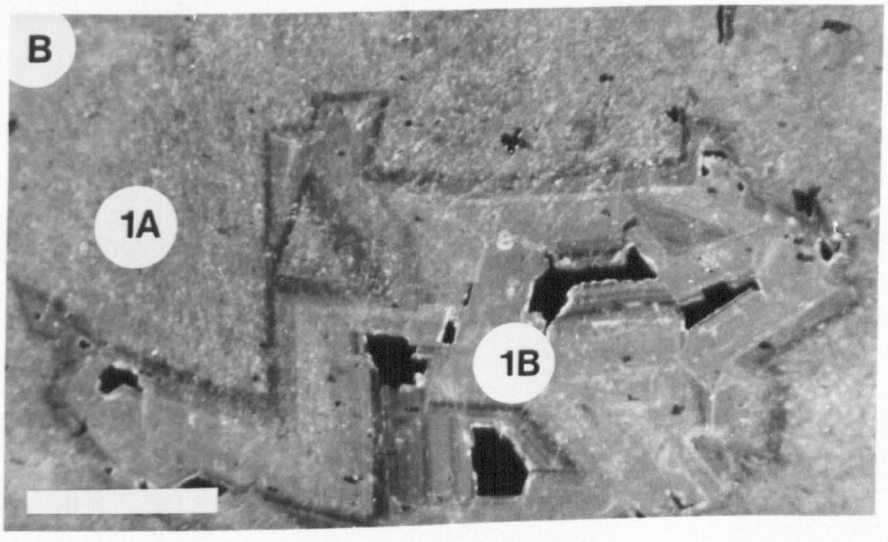
B
1A
1B

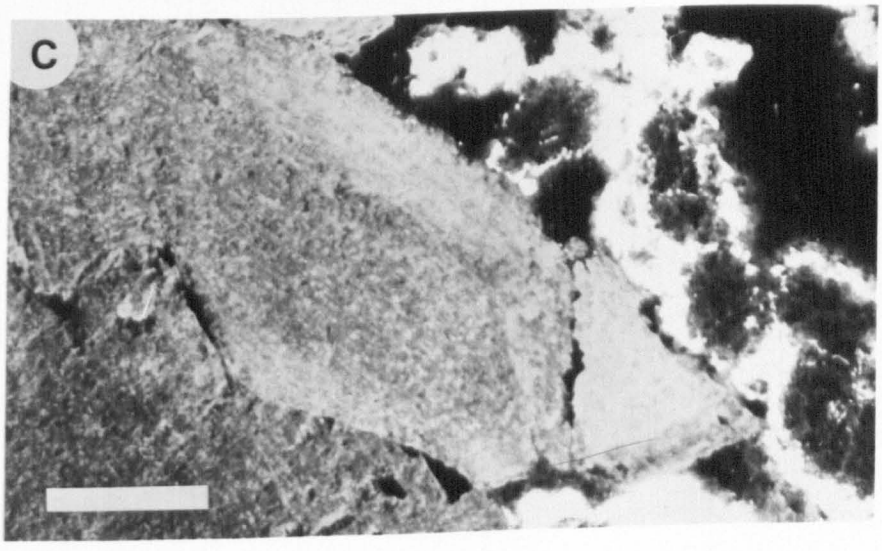
C

sweeping extinction when viewed under crossed polars. Each crystal commonly exhibits an inclusion-rich core and limpid surround (Figure 6.14C). This particular type of dolomite is mainly restricted to the Berry Slade and Wind Bay mounds, where it occurs within veins. The crystals commonly occur in a palisade arrangement orientated perpendicular to the surface from which they grew; a feature described as 'laminae' by Dixon (1921).

These pore-filling dolomites are saddle dolomites (in the sense of Radke & Mathis 1980; or 'baroque dolomite' Zenger 1983; or 'white-sparry dolomite' Beales 1971) and have an anhedral to euhedral form. Under CL they exhibit a uniform red-brick luminescence. The saddle dolomite is thought to postdate the Type-1A mosaic dolomite upon which they grew. The relationship to the Type-1B mosaic dolomite is unclear.

6.9.3. Geochemistry

Only Type-1A (mosaic) dolomite and Type-2 (saddle) dolomite have been analysed (Table 6.1). The occurrences of Type-1B dolomite are too small to be extracted successfully.

The trace element compositions are remarkably consistent (Table 6.1). The Mg/Ca ratios are approximately 1:2 and show a high degree of ordering typically 49:51, respectively. The average concentrations of Mn (82ppm), Fe (165ppm) and Sr (76ppm) are low compared with many other examples from the geologic record (summary see Mattes & Mountjoy 1980). Similar values for Mn (35-95), Fe (200ppm) and Sr (50ppm) have been recorded by Mattes & Mountjoy (1980) for the burial dolomites of the Upper Devonian Miette reefs of Cananda.

Isotope data for the Waulsortian reef dolomites from 12 analyses is presented in Table 6.1. Carbon and oxygen values are presented relative to the PDB standard. The samples are bulk rock analyses since individual

Table 6.1. Data from atomic absorption and stable isotope analyses of the Waulsortian dolomites at Castlemartin. (Sample BS13A is of saddle dolomite).

	wt %		ppm				δ	
	Ca	Mg	Fe	Na	Mn	Sr	13C (PBD)	18O (PBD)
BS1	21·41	12·15	280	777	132	79	+3·87	-5·86
BS2	21·63	12·82	182	583	60	75	+3·55	-8·39
BS3	21·82	12·34	89	444	89	91	+3·63	-6·09
BS4	22·13	12·74	138	601	87	78	+3·70	-7·65
BS5	21·85	12·53	134	509	50	75	+3·65	-6·39
BS6	21·65	12·76	199	499	73	77	+3·79	-7·92
BS7	21·98	12·72	199	450	64	56	---	---
BS9	21·35	11·91	75	586	148	74	---	---
BS13A	21·67	12·21	96	640	49	75	+3·14	-9·39
BS13B	21·38	8·34	216	446	65	86	+3·51	-7·63
WB1	21·98	12·37	166	584	63	53	---	---
WB3	21·76	12·15	187	574	80	76	+3·74	-7·11
WB4	21·17	11·76	132	582	72	65	+3·73	-7·41
WB6	21·59	11·96	136	561	191	94	+3·67	-7·19
HT10	21·79	12·20	247	583	101	81	+3·85	-7·25

individual crystals could not be isolated.

The $\delta^{13}C$ compositions of both the mosaic (Type-1A) and the saddle (Type-2) dolomite fall within a narrow range (+3.14‰ to +3.87‰.) (Table 6.1 & Figure 6.15). The Type-1A mosaic dolomite is uniformly enriched in $\delta^{18}O$ ranging from -5.86‰.. to -7.63‰.. Notably, it is the saddle dolomite (BS13A; Table 6.1) which is the most $\delta^{18}O$-depleted (Figure 6.15).

Interpretation: The types of dolomite and their geochemistry provide constraints as to their origin. The warped crystal lattice of saddle dolomites has been attributed to a number of factors (Radke & Mathis 1980), among which elevated temperature (>60°C) appears to be one of the most important. Integration of experimental data and field examples by Gregg & Sibley (1984), suggests that xenotopic dolomite textures are the result of growth at elevated temperatures in excess of 50°C. The association of idiotopic and xenotopic mosaic dolomite within the Waulsortian mounds can be explained in terms of increasing temperature during progressive burial.

The $\delta^{18}O$ composition of dolomite is influenced by 1) the composition of the precursor carbonates and 2) the composition of the dolomitizing fluids (Land 1980). At increased temperatures the composition of the dolomitizing fluids is likely to alter as a result of the fractionation of $\delta^{18}O$, so that higher temperature dolomites are relatively ^{18}O-depleted (Land 1980). The wide range of negative values shown by the $\delta^{18}O$ composition in the reef dolomites at Castlemartin would support the petrographic evidence of increasing temperatures of dolomite formation, most probably as a result of progressive burial. It is significant that the most depleted $\delta^{18}O$ dolomite type is the saddle dolomite (Figure 6.15; Table 6.1, sample BS13A) which most probably formed

Figure 6.15. Isotopic composition of the Waulsortian dolomites of Castlemartin.

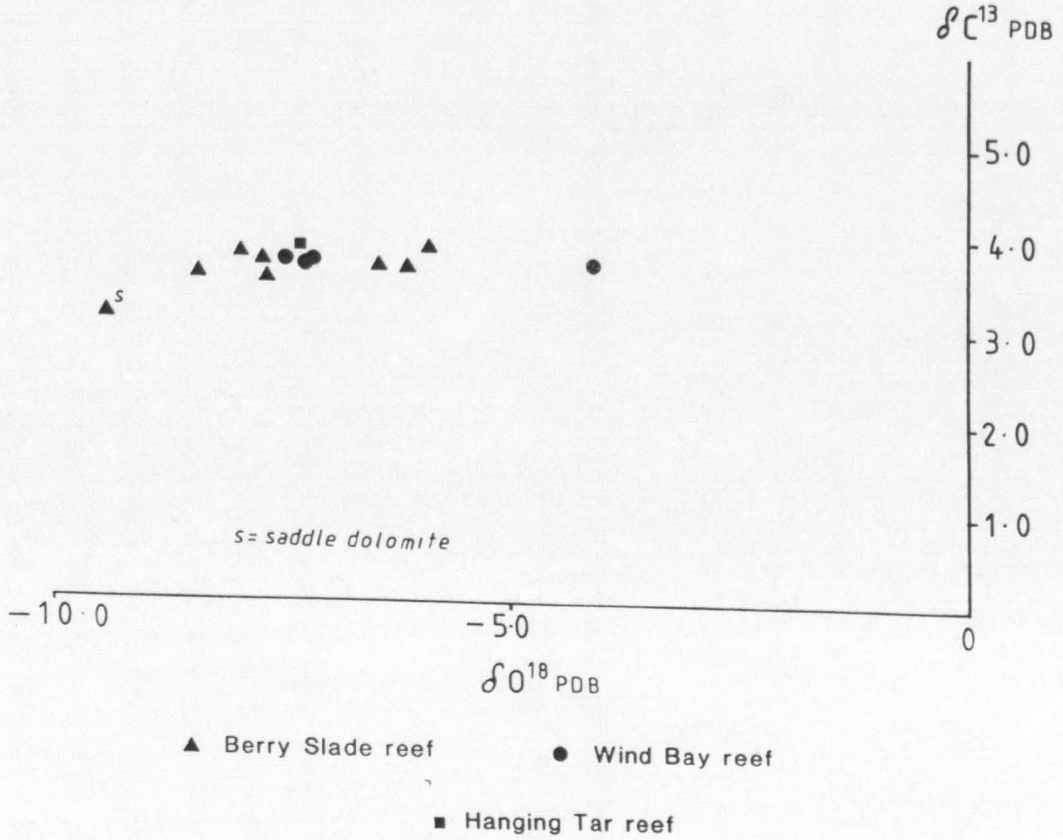
δC13 PDB
5·0
4·0
3·0
2·0
1·0
0
s
s = saddle dolomite
−10·0
−5·0
δO18 PDB
▲ Berry Slade reef
● Wind Bay reef
■ Hanging Tar reef

under the highest temperatures.

Because of the relative insolubility of CO^2, it is very difficult to markedly alter the carbon isotopic composition of carbonate sediment from its initial value (Land 1980). The $\delta^{13}C$ of modern carbonate sediment ranges between about +4.0‰ and -2.0‰ on the PDB scale (Gross 1964) and most platform dolomites fall within this range (Land 1980). The narrow isotopic composition of the Castlemartin reef dolomites falls within that for marine dolomites (+4.0 to -2.0PDB) (Figure 6.15).

There are many difficulties in interpreting dolomite trace element geochemistry data (Land 1980; Hardie 1987). However, it is significant that the dolomites have a low iron content. A low total iron concentration reflects the quantity of iron delivered to a site during deposition and diagenesis. This can have important constraints upon the nature of the dolomitizing fluids.

In conclusion the petrographic observations and geochemical data suggests the dolomites formed under increasing temperature conditions, during burial.

6.10 Other Dinantian dolomites of South Wales

Petrographically, the Waulsortian dolomites at Castlemartin show some similarity to the burial 'vein' dolomites described from the Gully Oolite (Chadian) and Hunts Bay Oolite (Holkerian) by Hird *et al.* (1987). The 'vein' dolomites consist of dolomite mosaics, mainly of anhedral cloudy crystals and saddle dolomite (Hird *et al.* 1987). Chemically, however, the Waulsortian dolomites are distinct from the other major dolomite types documented in the Dinantian of South Wales (Hird *et al.* 1987; Searl 1988). The concentration of manganese and iron (average 88ppm and 165ppm respectively) within the Waulsortian dolomites is notably less than the results from the other dolomite types. For example, the 'vein' dolomites

show an average of 3074ppm for manganese and 1.81wt% for iron (Hird *et al.* 1987). Isotopically the Waulsortian dolomites define their own 'field', showing no overlap with other dolomite types, as they have a significantly higher $\delta^{13}C$ value (average +3.65) (Figure 6.16). The $\delta^{18}O$ value shows a similar spread of data points to that of the 'vein' dolomites which are also interpreted as having formed during burial (Hird *et al.* 1987).

6.11 Discussion

It is well established that Waulsortian mudmounds form in water depths greater than 100m and occur in distal ramp settings (Miller & Grayson 1982; Lees *et al.* 1985; Lees & Miller 1985; op. cit. Bridges & Chapman 1988). This places a major constraint upon dolomitization by near-surface processes (the reflux of hypersaline brines and the mixing of seawater and meteoric water) which require a marked fall in sea level to allow the infilltration of near-surface fluids into the reef mounds. Therefore, the fluids most likely to dolomitize Waulsortian facies are sea water and burial connate water.

Important constraints on the origin of the pale dolomites at Castlemartin include: (1) the relative timing of dolomitization, (2) the dolomite types, (3) their distribution and (4) geochemistry. The diagenetic relationships show the dolomites are of burial origin (section 6.8) and this is consistent with the types of dolomite identified and their geochemistry (section 6.9). At elevated temperatures, there are fewer thermodynamic and kinetic constraints on dolomite formation than are required at surface temperatures (Usdowski 1968; Lovering 1969; Lippmann 1973; Mattes & Mountjoy 1980; Zenger 1983; Hardie 1987; Machel & Mountjoy 1986). This both hastens the reaction rates and permits dolomitization at lower Mg/Ca ratios.

Figure 6.16. A diagram showing the range of stable isotope data of the four main dolomite types in the Dinantian of South Wales (excluding pedogenic dolomites). Modified after Hird *et al.* 1987.

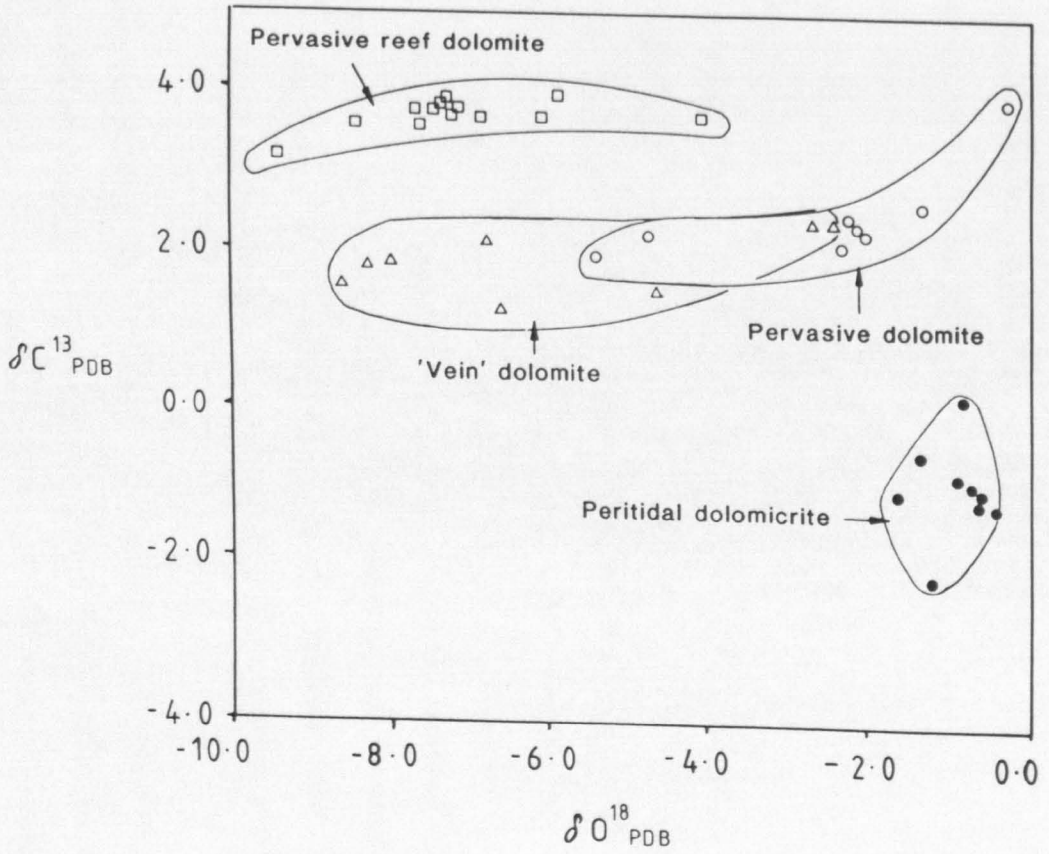
Pervasive reef dolomite
Pervasive dolomite
'Vein' dolomite
Peritidal dolomicrite
4·0
2·0
0·0
-2·0
-4·0
-10·0
-8·0
-6·0
-4·0
-2·0
0·0
δC13PDB
δO18PDB

In order to dolomitize the Waulsortian mounds at Castlemartin, two basic conditions must have been fulfilled: 1) the source of ions must have been sufficiently large to replace the mounds at Wind Bay and Berry Slade; and 2) a mechanism for transporting the ions from their source to the site of dolomitization must have existed.

There are three main models in the literature which explain dolomitization in the subsurface. These include: cellular thermal convection, regional topography-driven flow, and compactional flow (Figure 6.17). Thermal convection requires the establishment of a 'half-cell' between the platform interior and seawater, which acts as an infinite reservoir for magnesium (Kohout *et al.* 1977; Simms 1984). It is believed to originate from the density gradient that exists between the warmer (geothermally heated) waters of the platform interior and the cold surrounding seawater (Simms 1984) (Figure 6.17A). Cellular thermal convection has only been proven for the Florida platform where the supply of sea water is from the adjacent cold, deep water straits (Kohout *et al.* 1977; Simms 1984) (Figure 1.7A). The low angle configuration shown by carbonate ramps is in marked contrast to the platform geometries which are most likely to establish cellular thermal convection. Therefore, it is considered highly unlikely that the Waulsortian reefs at Castlemartin were dolomitized by cellular thermal convection.

Topography-driven flow (Garven & Freeze 1984; Garven 1985), otherwise known as gravity driven flow, of groundwater water is reliant upon the hydraulic head established in a site of elevation, known as the recharge area (e.g. hills and mountains) (Figure 6.17B). A topography driven flow is a regional flow and its diagenetic effects are liable to be recognizable throughtout a region, rather than localised within certain facies type. As a result it is also considered to be an unlikely

Figure 6.17. Models for dolomitization within the subsurface: (A) cellular thermal convection as recorded in Florida (after Kohout *et al.* 1977); (B) conceptual model of topography -gravity- driven flow in the subsurface of sedimentary basins (after Garven & Freeze 1984); (C) model of fluid flow during compaction (modified after Jodry 1969, Mattes & Mountjoy 1980).

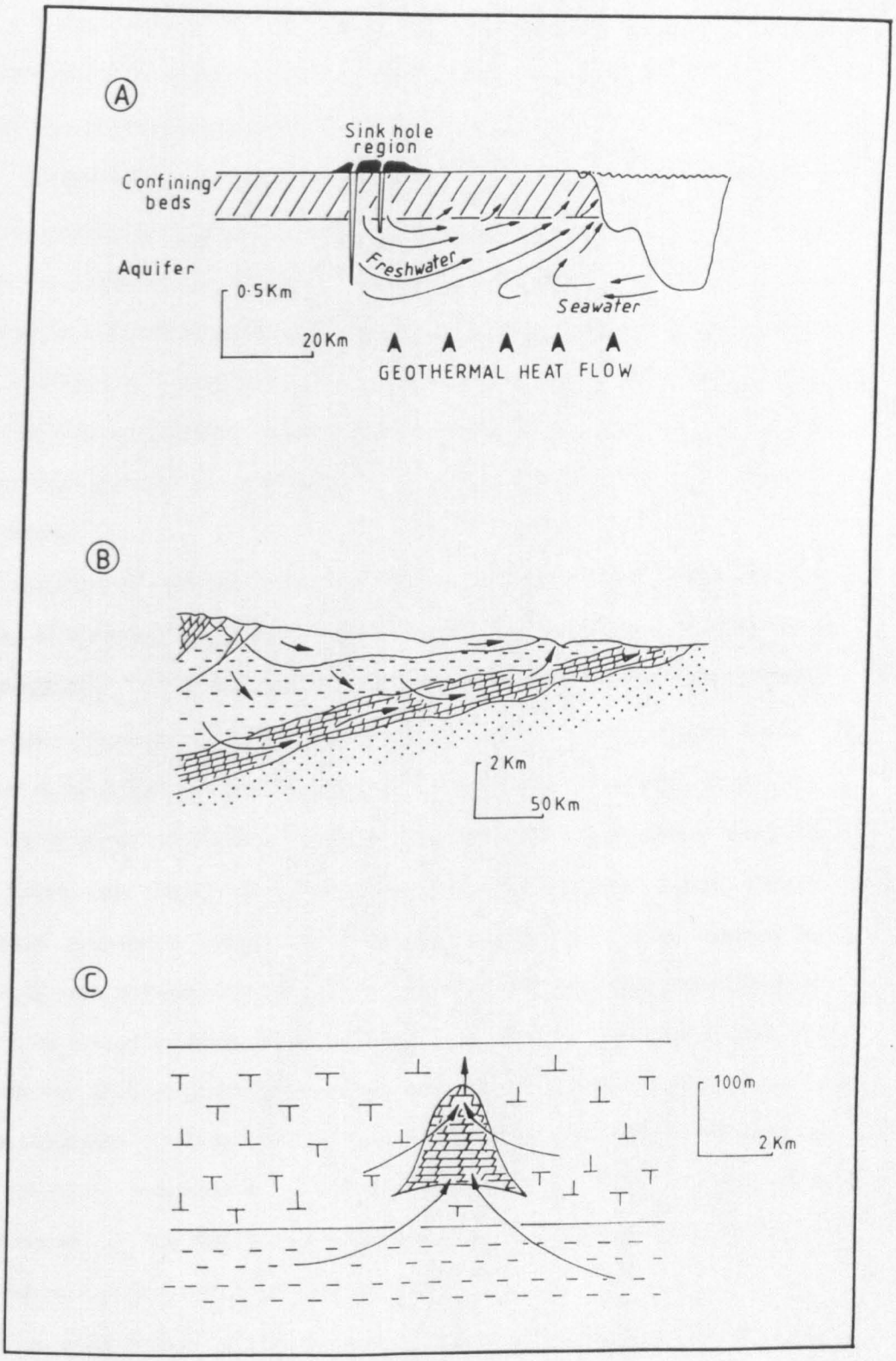
A
Sink hole region
Confining beds
Aquifer
Freshwater
Seawater
0·5Km
20Km
GEOTHERMAL HEAT FLOW
B
2Km
50Km
C
100m
2Km

mechanism for dolomitizing the Waulsortian reefs at Castlemartin.

Dolomitization by means of burial compaction can occur either as a result of a supply of ions from an internal source (Wanless 1979) or from an external source (Jodry 1969; Mattes & Mountjoy 1980; Gawthorpe 1987; Machel 1984; Schofield & Adams 1986). Wanless (1979) proposed an internal mechanism whereby magnesium for dolomitization is released by pervasive pressure-solution of magnesian calcites. A commonly invoked external source for magnesium ions is marine shales (Mattes & Mountjoy 1980; Schofield & Adams 1986). Marine shales are capable of both releasing large volumes of connate water (Figure 6.17C) and supplying magnesium ions from certain mineral transformations e.g. smectite to illite (Mac-Hargue & Price 1982).

Extensive dolomitization of the mounds at Castlemartin would require an external source to supply the large volumes of ions necessary for alteration. The limited distribution of the dolomite within the Waulsortian mounds and rare stratabound beds would seem to imply a localised source for the dolomitizing fluids and not a regional flow.

It is apparent from the field observations that both the Friars Point Limestone Formation and the Lower Limestone Shale Group have undergone extensive compaction which is likely to have released large volumes of connate water with the potential for causing dolomitization. However, at present there is insufficient evidence to determine the most likely source of supply for the magnesium. The low concentrations of iron and manganese within the Waulsortian dolomites militate against the origin of the magnesium being derived from clay mineral transformations. The latter process typically produces ferroan dolomites (Mac-Hargue & Price 1982; Gawthorpe 1987).

The distribution of the dolomite reflects the permeability of the rocks during burial. It is not surprising that many Waulsortian mounds

have been extensively dolomitized because they contain numerous cavities, such as stromatactis. The limited amount of dolomite within the Hanging Tar mound is considered to be a result of the occlusion of many of the voids prior to dolomitization. The dolomite preferentially 'picked-out' relict porosity within the spar filled cavities (Figure 6.13C) by means of veins which cross-cut the mound facies (Figure 6.5A). This would seem to indicate that the fluids permeated through the rock under pressure. Extensive dolomitization of the Wind Bay and Berry Slade mounds would suggest a more open network of interconnected voids, through which large volumes of connate water could be funnelled. The off-reef compaction exceeding the reefal compaction caused the expelled fluids to be funnelled towards and through the reefs. A similar process has been invoked by Jodry (1969) for the dolomitized reefs of St. Clair County Michigan (USA) and Mattes & Mountjoy (1980) for the Devonian Miette Reef Complex (Canada).

6.12 Conclusions

1) The establishment of deep water facies including Waulsortian facies across SW Britain during *S. anchoralis* times was strongly influenced by regional subsidence.

2) Recognition that the temporal distribution of shallow and deep water facies in SW Britain was influenced by tectonic subsidence would explain the diachronous initiation of Waulsortian mudmounds to the south of St George's Land.

3) Three sedimentary phases, comparable to sedimentary Phases B-D of Lees *et al.* (1985), can be identified within the Waulsortian mounds at Castlemartin. They support the interpretation by Lees *et al.* (1985) for a pronounced change of environment, most probably as a result of a marked eustatic sea level fall at the end of the Courceyan and during

early Chadian times.

4) The Waulsortian dolomites of Castlemartin originated during burial diagenesis.

5) The most likely source of magnesium was from connate waters from the surrounding limestones and/or the underlying Lower Limestone Shale Group.

Chapter 7 - Cryptic exposure horizons in the Carboniferous Limestone of Portishead

7.1 Introduction

Two subaerial exposure units, containing fibrous columnar calcites, have been discovered at Portishead (Black Rock Quarry, Appendix N), near Bristol (Figure 1.2). These horizons are significant because similar developments of approximately the same age, have been recorded within other sequences located along the southern margin of the Welsh-Brabant Massif (Figure 1.1). These horizons occur in South Wales (Searl 1989; Raven 1983), southern Germany (Kasig 1980) and Belgium (Swennen *et al.* 1981) (Figure 1.1).

The aim of this chapter (which forms the basis of Faulkner *et al. submitted*) is to describe these paleosols, record their significant petrographic features, and stress their apparent remarkable stratigraphic continuity along the southern margin of the Welsh-Brabant Massif (Figure 1.1). It also includes a discussion of the nature of the stratigraphic contact between the Black Rock Limestone and the Gully Oolite across SW Britain.

7.2 Succession

Stratigraphically, the two paleosol beds (here named the Portishead Paleosol Beds) containing the columnar calcites occur above and below the Sub-Oolite Bed which separates the Black Rock Dolomite from the overlying Gully Oolite at Portishead (Figures 7.1). For a full evaluation of the significance of the paleosols it is important that the beds immediately underlying and overlying them are also described and interpreted. This is followed by a detailed field and petrographic description of the Portishead Paleosol Beds (section 7.3).

7.2.1 The Black Rock Dolomite

The relict sedimentary features preserved within the Black Rock Dolomite have previously been described in Chapter 4 (section 4.3.4) and

Figure 7.1. Sedimentary log of the uppermost Black Rock Dolomite, the Portishead Paleosol Beds, the Sub-Oolite Bed and the Gully Oolite. (Black Rock Quarry; locality map is shown in Appendix N.)

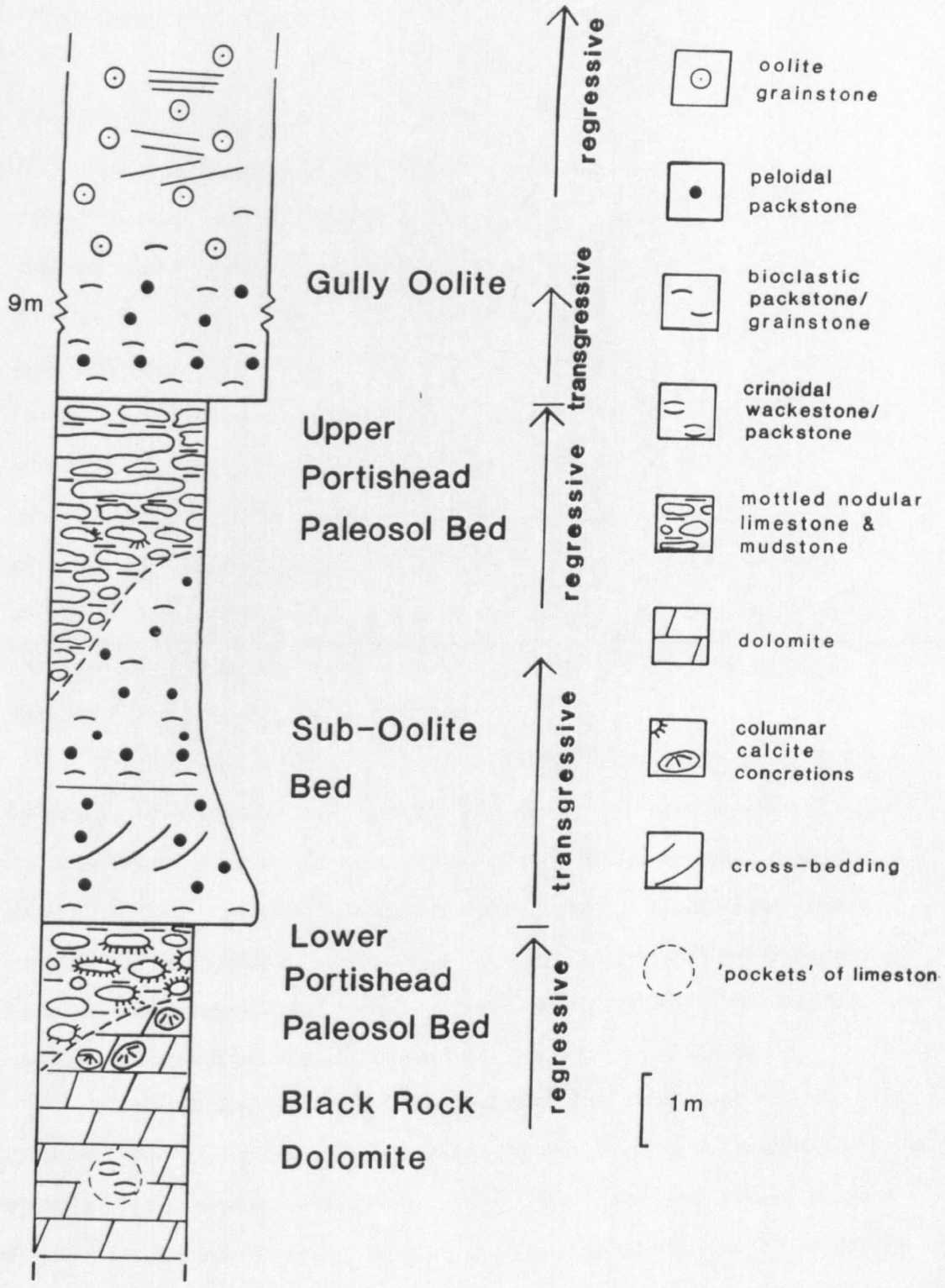
9m
Gully Oolite
Upper
Portishead
Paleosol Bed
Sub-Oolite
Bed
Lower
Portishead
Paleosol Bed
Black Rock
Dolomite
regressive
transgressive
regressive
transgressive
regressive
oolite grainstone
peloidal packstone
bioclastic packstone/ grainstone
crinoidal wackestone/ packstone
mottled nodular limestone & mudstone
dolomite
columnar calcite concretions
cross-bedding
'pockets' of limeston
1m

interpreted as having been laid-down in a subtidal, probably beneath storm wave-base environment.

7.2.2 The Sub-Oolite Bed

The packstone/grainstone Sub-Oolite Bed (0.5m to 3.0m thick) has a sharp planar contact with the Lower Portishead Paleosol Bed and a gradational contact with Upper Portishead Paleosol Bed (Figure 7.1). Upward from the base of the unit there is an overall grain size decrease from granular grade to coarse sand-grade. The sedimentary features include graded beds (5-10cm thick) and medium scale trough cross-sets, laterally persistent for up to 2m. The base of the graded beds consists of a crinoidal lag (1-2cm thick) overlain by a bioturbated, peloidal-rich layer of coarse sand-grade. Biogenic structures are more noticeable in the upper part of the unit and their appearance is similar to *Thalassinoides*-type burrows occurring as circular tubular burrows (ca. 3cm in diameter) both parallel and perpendicular to bedding.

The Sub-Oolite Bed has a low diversity fauna, and consists of the following constituents in decreasing order of abundance:- peloids; disarticulated crinoid ossicles with thin micritized margins; composite grains of micrite-coated bioclasts; disarticulated brachiopod valves; angular silt to medium sand grade quartz grains; and rare microfossils such as moravamminids. The ovoid peloids, 1-4mm in diameter, are commonly amalgamated due to compaction prior to cementation.

Interpretation: Deposition of the Sub-Oolite Bed was mainly from currents which reworked and deposited the allochems into graded beds and laterally impersistent cross-beds. The dominance of coarse peloidal allochems and a low diversity fauna suggest deposition not in an active shoal environment but perhaps a more restricted, either back-shoal or inter-shoal environment.

7.2.3 The Gully Oolite

At Black Rock Quarry, the Gully Oolite (ca. 30m thick) has a sharp planar contact with the underlying Upper Portishead Paleosol Bed. The basal 10m of the Gully Oolite consists of a poorly sorted, granular-sized, peloidal and bioclastic packstone/grainstone that passes gradationally into the overlying oolitic grainstone unit.

The peloidal limestone shows signs of bioturbation and include thin layers (less than 5cm thick) of disarticulated, convex-upward brachiopod valves. Overall, the relative abundance and types of allochems are similar to that recorded in the Sub-Oolite Bed (section 7.2.2).

Above the peloidal limestone, the ooids have a well developed concentric structure (up to 0.5mm in diameter) around a nucleus of crinoid, brachiopod and echinoderm spine fragments. Locally observed within the oolite grainstone are cosets of low angle, planar cross-beds (5-10cm thick).

Interpretation: The similarity between the lower part of the Gully Oolite and the Sub-Oolite Bed suggests that the latter was also deposited in a subtidal environment. The thin layers of disarticulated, convex-upward brachiopod valves are interpreted as representing deposition from higher energy (storm-related?) currents. The upward passage from the subtidal peloidal packstone/grainstone into the overlying low angle cross-bedded oolite grainstone is interpreted as a shallowing-upward sequence, perhaps into an upper shoreface environment. Similar shallowing-upward successions have been recorded in the Gully Oolite of South Wales by Waters (1984), Wright (1986), Ramsay (1987), and Waters & Lawrence (1987).

7.3 The Portishead Paleosol Beds

Lithologically the Portishead Palaeosol Beds (1-4m thick) consist of 1) carbonate nodules, 2) columnar calcite crystals, 3) siltstones and 4) variegated clays. The base of each paleosol bed is gradational with the underlying beds, and exhibits a relief of 1-2m over a short lateral distance of only a few metres. The top of the beds is sharp and planar.

7.3.1 Carbonate nodules

Both the paleosol beds have a strongly nodular appearance. The nodules commonly either consist of crinoidal limestone (Figure 7.2) or dolomite depending on which unit they overlie, the Sub-Oolite Bed or the Black Rock Dolomite respectively. The nodules are round, irregular to ovoid, and vary from 3cm to 40cm in diameter. Locally they exhibit irregular, internal cavities (up to 1cm in diameter), and cuspate embayments particularly on the upper surface (up to 5cm deep). Occluding the intra-nodular cavities is a clear microspar which consists of rhombic and sub-rhombic crystals (4μm in diameter). When viewed under cathodoluminescence (CL) the latter comprises numerous thin alternating bright orange and dull zones, outlining a rhombic shape, commonly with internal crenulated crystal faces (Figure 7.3A).

The surface embayments are a dissolution feature because they cross-cut fossil allochems (e.g. crinoid ossicles) and the matrix of the rock (e.g. micrite and its neomorphic microspar replacement). Locally, infilling the embayments are layered micrites which are either sub-concordant or disconcordant to the cavity wall (Figure 7.2). It is common for the layered micrites to be subsequently replaced by either a fine grained (25-50 μm in diameter) xenotopic dolomite or neomorphic microspar. Significantly, simple burrow forms have been observed within a layered dolomite (Figure 7.2), just beneath the sharp contact with the

Figure 7.2. Schematic diagram of a section through a crinoidal limestone encrusted with columnar calcite crystals.

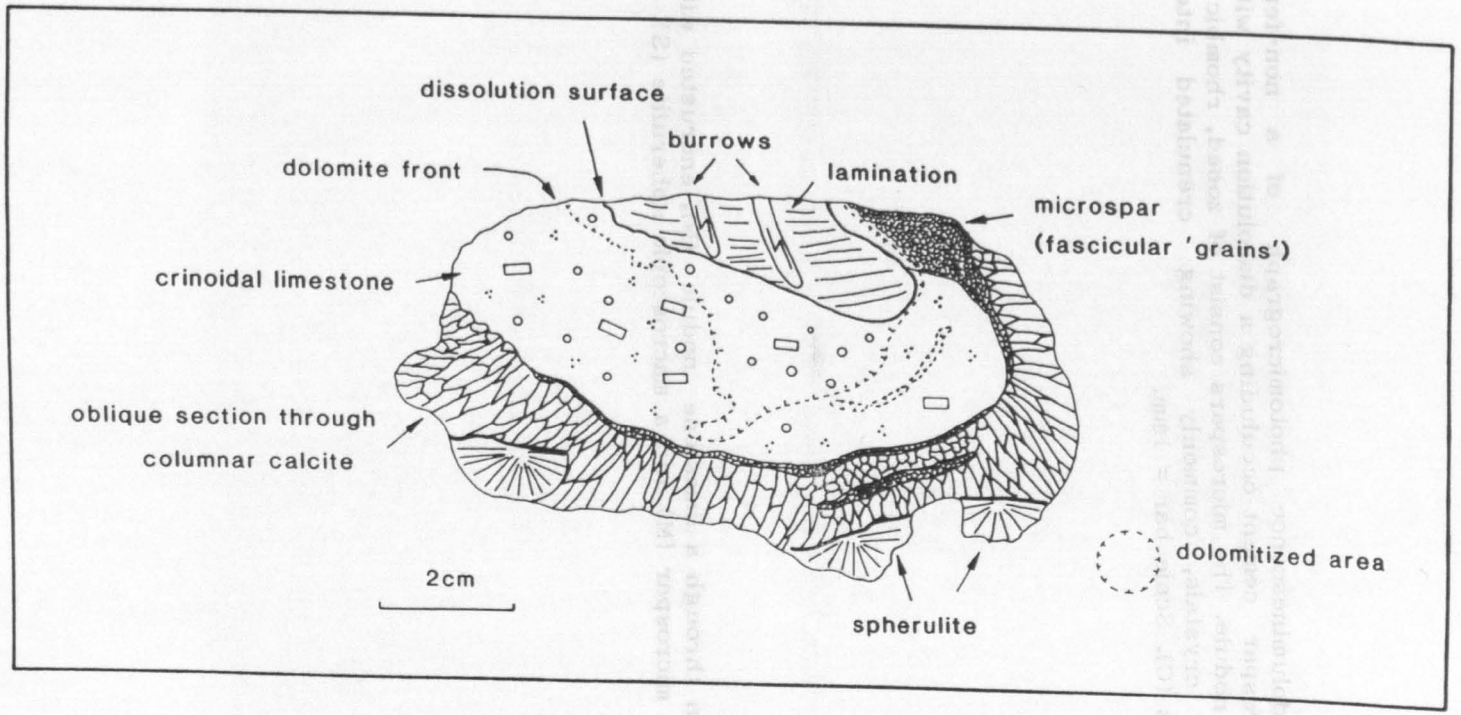
dissolution surface
burrows
dolomite front
lamination
microspar
(fascicular 'grains')
crinoidal limestone
oblique section through
columnar calcite
2cm
spherulite
dolomitized area

Figure 7.3

(A) Cathodoluminescence photomicrograph of a non-ferroan rhombic microspar cement occuluding a dissolution cavity within a carbonate nodule. The microspars consist of zoned, rhombic and sub-rhombic crystals, commonly showing crenulated internal crystal faces (C). Scale bar = 1mm.

(B) Section through a limestone nodule (N), encrusted with a non-ferroan microspar (M) and a macroscopic spherulite (S).

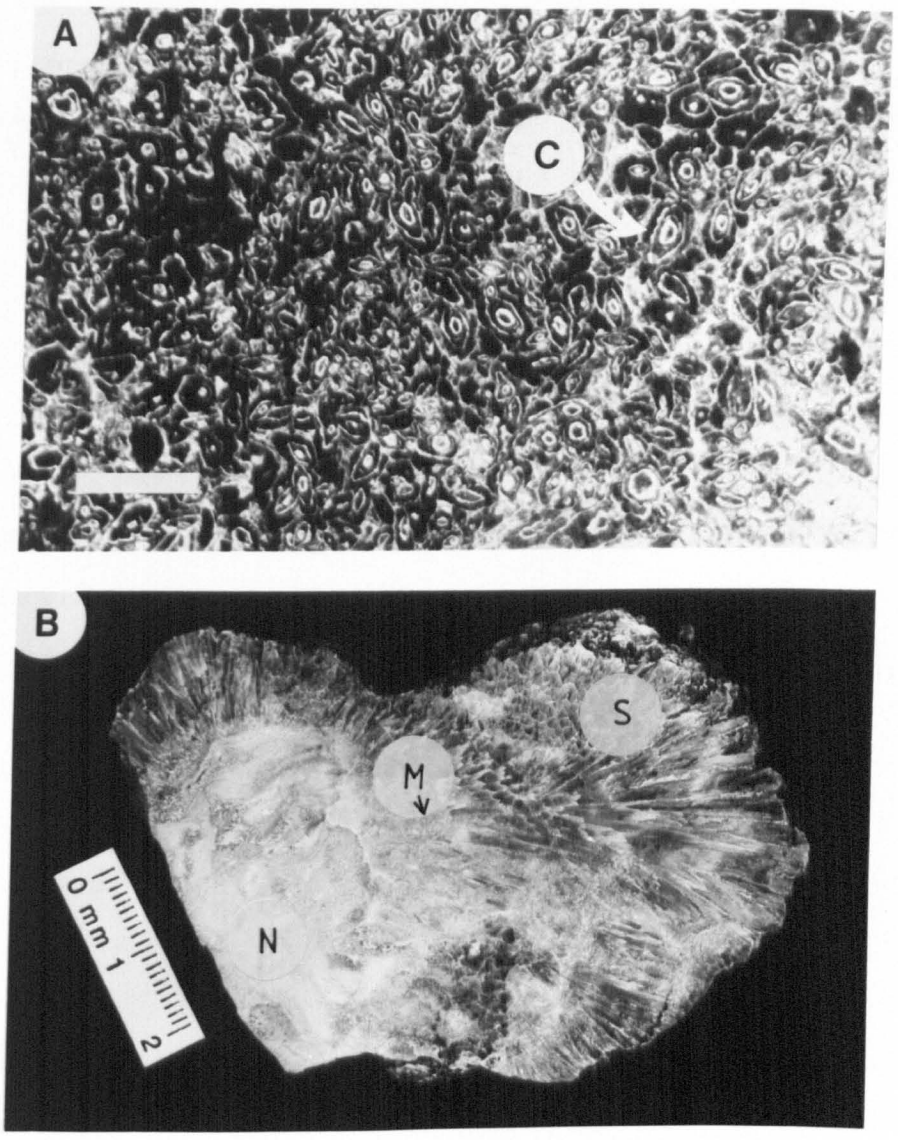
A
C
B
S
M
N
0 mm 1 2

overlying Sub-Oolite Bed.

7.3.2 Columnar calcite crystals

Encrusting the nodules are concentric layers of radiating, outward thickening columnar calcite crytals, up to 5cm in length (Figure 7.3B). Up to three phases of columnar calcite crystal growth have been recorded. Each phase either nucleated directly onto an earlier one or is separated by a layer of non-ferroan microspar. The columnar calcites show no prefered orientation. Locally, whole cavities are found lined with a layer of spherulites (1-5cm in diameter). Generally the larger columnar calcite crystals are associated with the larger cavities.

The microstructure of the spherulites is highly variable, with two types of calcite (Figure 7.4): inclusion-rich calcite and clear sparry calcite. The contact between these two types is commonly irregular with crenulated and feathery margins (Figure 7.4) and they possess differing crystallographic orientations.

The inclusion-rich calcite display a relict fibrous structure (Figures 7.5A & B) which is commonly pseudopleochroic (pale brown to colourless). Individual fibres are a few microns wide and up to several hundred microns long, and are arranged in densely packed bundles (Figure 7.5) in which the fibres range from a parallel to a radiating arrangement (Figure 7.4). Occasionally the bundles define a plumose type structure, the central axis of which is parallel to the elongate crystal axis. The pseudopleochroic fibrous calcite crystals occur as two main forms: a) fascicular 'grains' and b) columnar fascicular growths (Figure 7.4).

a) fascicular 'grains' : these are sub-spherical to oblate 'grains' from 20 um to several hundred μm in size (Figure 7.5B), found as layers between and as substrates for, the columnar growths. These grains occur in millimetre to centrimetre-sized clusters which have distinct

Figure 7.4. Schematic diagram of a section through a macroscopic spherulite showing both the microstructure of the bladed calcites and the fascicular grains. (Also see Figure 7.5).

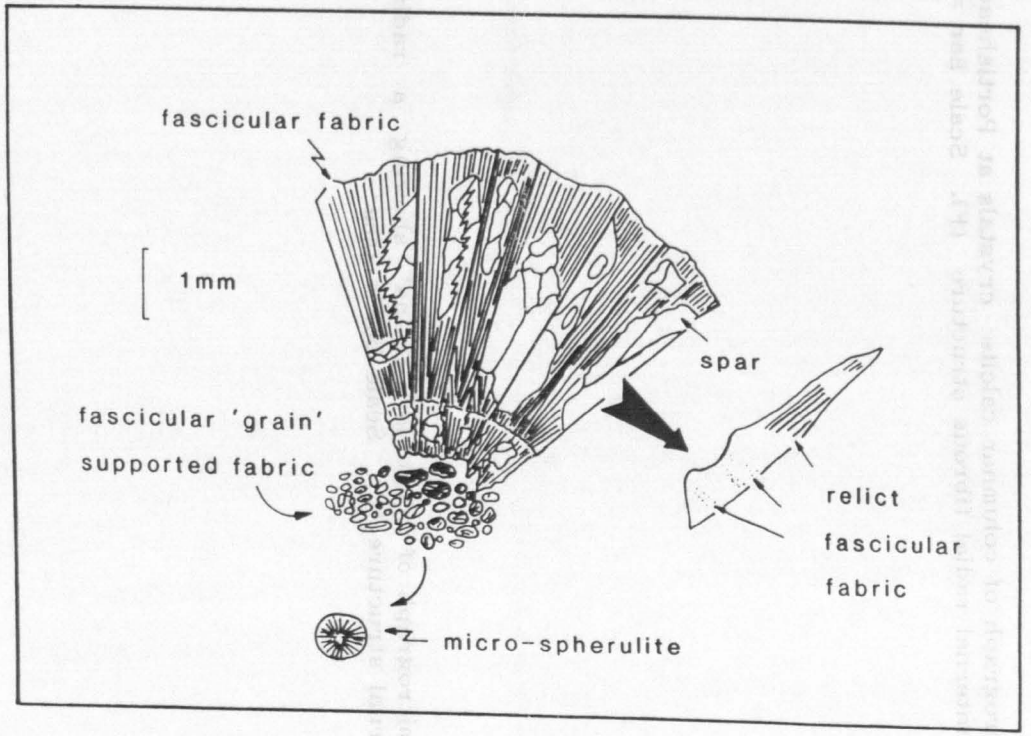
fascicular fabric
1mm
spar
fascicular 'grain'
supported fabric
relict
fascicular
fabric
micro-spherulite

Figure 7.5.

(A) Photomicrograph of columnar calcite crystals at Portishead showing the internal radial fibrous structure (F). Scale Bar = 1mm.

(B) Photomicrograph of fascicular 'grains' showing a radial fibrous internal structure (F). Scale bar = 1mm.

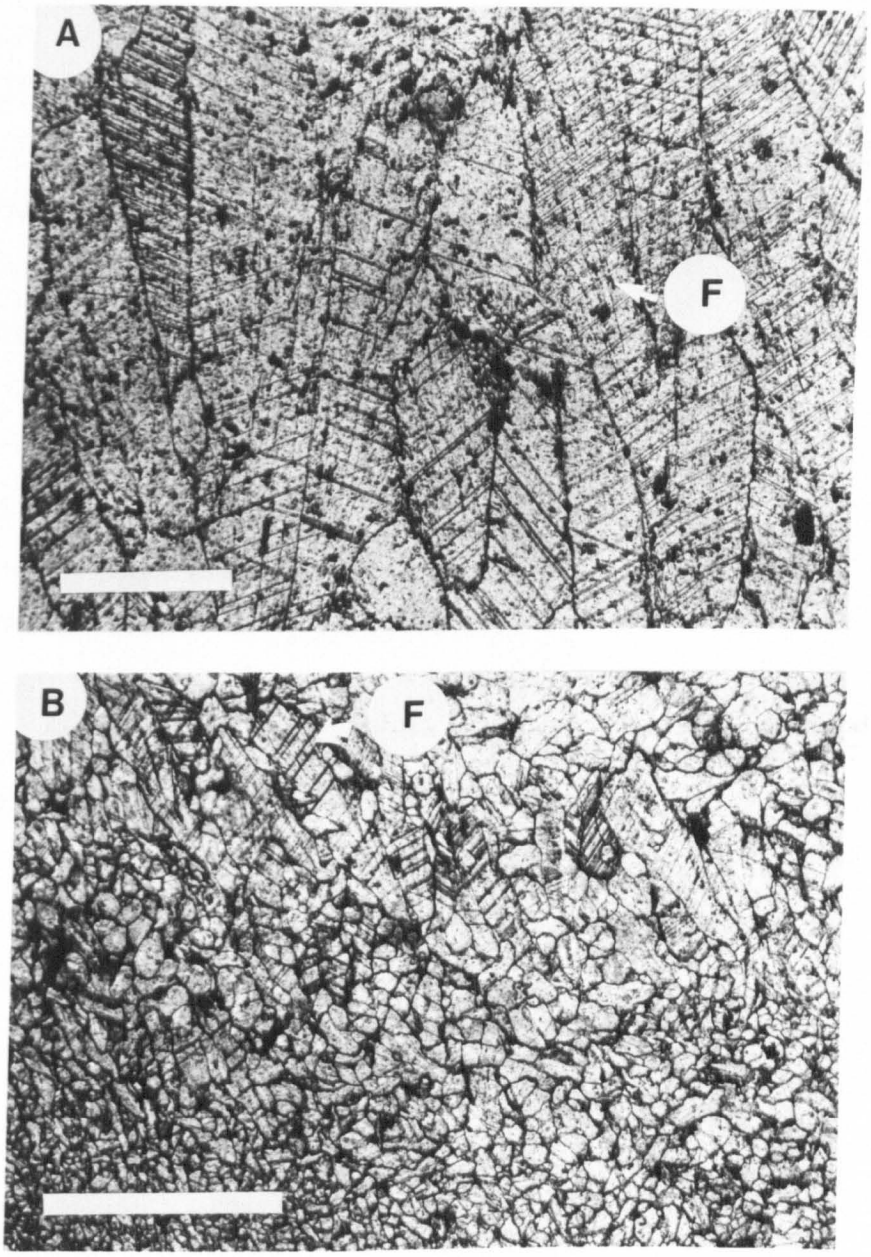
A
F
B
F

boundaries with adjacent populations of coarser or finer grains (Figure 7.5B). Thin veneers of argillaceous material (<1mm thick) are commonly found enclosing individual crystals. There is no prefered orientation to the component fibres between each grain, but within each the fibres vary from a parallel to radial arrangement (Figure 7.4).

b) columnar fascicular growths : these are centimetre-long crystals which form the macroscopic spherulites (Figure 7.3B) but also include transitional forms with the fascicular oblate grains (Figure 7.4). The crystal terminations commonly consist of a series of pointed fibres, particularly along the outer margin of the spherulites. The crystals with relict fibres exhibit uniform extinction, straight cleavage/twin planes and uniform dull luminescence under cathodoluminescence. The optical properties of the fibrous spar are thus not comparable with radiaxial fibrous or fascicular optic calcite (cf. Kendall 1985), but are comparable to classical radial fibrous calcites (cf. Bathurst 1975). The fibres are defined by lines of clay inclusions (Figure 7.5). Etching and SEM examination has revealed neither microdolomites or aragonite relicts, which suggests formation from either high Mg calcite or aragonite precursors.

7.3.3 Clays and siltstones

Infilling the areas (up to 15cm in diameter) between the nodules and the spherulites are quartz siltstones and mottled, variegated (typically purple and green) clays. The quartz siltstones form bedding-parallel, laterally discontinuous layers (0.3mm to 10mm thick) and lenses (0.5cm to 3cm wide) whose lower bounding surfaces are commonly convex-downward. Layering is picked-out by colour variation: the thinner, pale white layers (1-5mm thick) are more quartz-rich (up to 70%) than the pale orange layers (1-2cm thick), in which the quartz grains occur floating in

micrite or neomorphic microspar.

Clay mineralogical determinations were undertaken by L. Garvie at Bristol University (Appendix V). The clay mineralogy of the two paleosol beds is essentially the same. The clay fraction is dominated, in decreasing order of abundance, by: interstratified illite/smectite (I/S), kaolinite, discrete illite and probably some chlorite. Comparison of the observed I/S peaks with the computer calculated patterns for I/S (Reynolds 1984) indicated that the interstratified I/S contains approximately 80% illite with an ordering of R=1.

Interpretation: The crinoidal sediments of the Black Rock Limestone and Sub-Oolite Bed were laid-down, cemented and underwent neomorphic microspar replacement, prior to dissolution. The irregular, gradational base of the nodular units, suggests that dissolution took place *in situ*. It was within the dissolution cavities that the layered micrites, the clays and the silts were deposited; and that the rhombic calcites and the fibrous calcite crystals were precipitated.

The presence of biogenic structures in the layered micrites suggests deposition occurred in close-proximity to the surface (Figure 7.2). Unfortunately, the clays do not possess any obvious pedogenic signature (e.g. Robinson & Wright 1987). The estimated burial depth from the clay mineralogy of the Portishead Paleosol Beds is not incompatible with the known burial history of the region. The abundance of interstratified illite/smectite and kaolinite, and the paucity of discrete illite and chlorite indicates a relatively low grade of diagenesis (e.g. depth of ca. 4000m, Temperature ca. 120°C) (Eslinger & Pevear 1988). Robinson & Wright (1987) invoked a pedogenic explanation for the clays in the Arundian paleosols of South Wales because of the discrepancy between the high degree of illitisation and the shallow burial history of the area.

The appearance of the rhombic calcites in the intra-nodular cavities (Figure 7.3A) are comparable to calcrete fabrics described from the Lower Carboniferous of South Wales by Wright (1982b). Rhombic habit is a typical calcrete feature and the crenulated growth zones (Figure 7.3A) indicate phases of dissolution between phases of precipitation (Wright & Peeters *submitted*).

The origin of the columnar calcites is problematic. They show some similarites with both speleothems (cf. Heckel 1983; Assereto & Folk 1976; Kendall & Broughton 1978) and selenitic gypsum as described by Vai & Ricci-Lucchi (1977) from the thick evaporites of the Mediterranean Messinian. Similar columnar calcite horizons in the Lower Carboniferous of Britain have been described by Dixon & Wright (1983) and Searl (1989) and interpreted as speleothems. Swennen *et al.* (1981) suggested the developments in the Vesder Basin (Belgium) represent replacement after gypsum, owing to the dominant upward growth direction of the spherulites and their occurrence beneath known evaporitic collapse breccias (Jacobs *et al.* 1982). However, it is unlikely that the replacement of gypsum would have resulted in the development of pseudomorph crystals with a regular fabric. Similarily the very fine relict fibre bundles do not have an obvious analogue in gypsum crystal fabrics.

Dixon & Wright (1983) described similar spherulites and palisade fabrics from an Arundian paleosol in the Llanelly Formation of the Tredegar area, South Wales. They interpreted the fibrous calcites as probable fossil speleothems, because they only occur in association with palaeokarsts and paleosols, and are absent from associated limestones which lack clear evidence of subaerial exposure. Such an interpretation is consistent with the developments at Portishead where the columnar crystals grew within subaerial exposure horizons. The use of the term speleothem seems inappropriate in the absence of a cave system. However,

the term is applied here because the columnar calcite crystals are known to have grown into cavities and clearly show affinity with other known speleothems in their mode of formation and petrographic attributes.

7.4 Other Columnar Calcites

Other subaerial exposure surfaces containing columnar calcites have been documented at a similar stratigraphic level to the Portishead development, along the southern margin of the Welsh-Brabant Massif (Figure 1.1). To date they have been recorded from South Wales (Raven 1983; Searl 1989), Belgium (Swennen *et al.* 1981) and southern Germany (Kasig 1980). Their occurrence in mainland Europe is consistent with Lees' (1982) conclusions that there are striking geological similarities between the two areas.

Two columnar calcite units (each ca. 1m thick) have been documented in the Daren Ddu Beds (ca. 5m thick) of the Oolite Group which outcrops between Cwar-yr-Ystrad and Daren Cilau in South Wales (Raven 1983; Searl 1989) (Figures 7.6 & 7.7A). They occur, separated by a bioclastic peloidal and oolitic limestone (up to 3m thick), stratigraphically sandwiched between the Pwll-y-Cwm Oolite (8m thick) and the overlying Blaen Onnen Oolite (5-14m thick) (Figures 7.6 & 7.7A).

Unfortunately, the age of the Daren Ddu Beds and the position of the Courceyan-Chadian boundary in the Oolite Group, has yet to be accurately determined. On account of its stratigraphic position, the Daren Ddu Beds are thought to have a late Courceyan to early Chadian age. They occur sandwiched between the Courceyan Lower Limestone Shale Group, and beneath the Arundian Coral Bed (George *et al.* 1976) which immediately overlies the Blaen Onnen Oolite. However, it is still necessary to verify the age of the columnar calcite beds as well as the position of Courceyan-Chadian boundary.

Figure 7.6. Sedimentary logs showing the position of the columnar calcite developments at Daren Cilau (1) and Portishead (2), as well as the occurrence of a possible clay paleosol at Taff's Well (3) separating the Black Rock Dolomite from the Gully Oolite. Inset map shows the location of the sections and the approximate position of the Vale of Glamorgan axis.

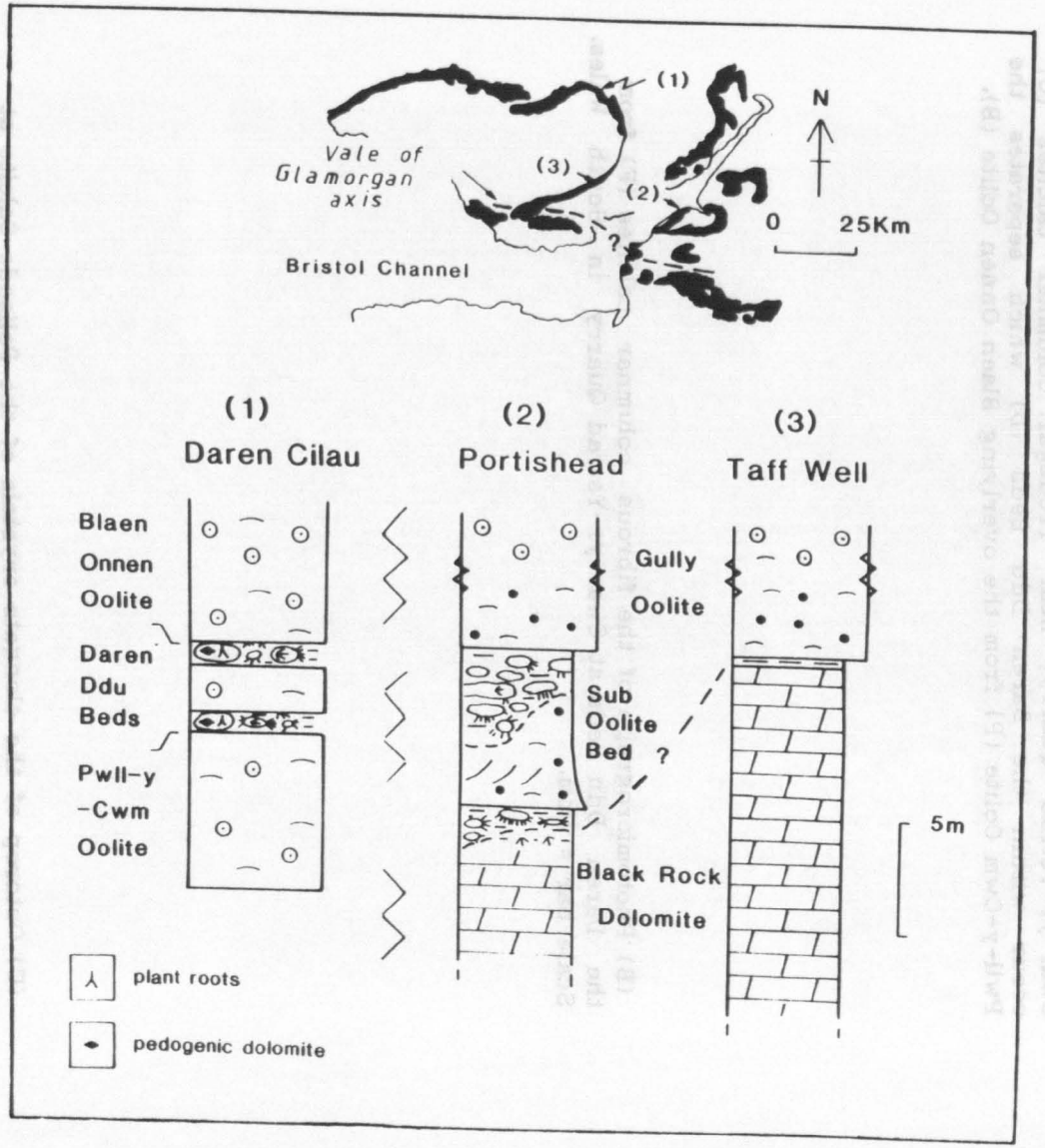
(1)
(2)
(3)
N
Vale of
Glamorgan
axis
Bristol Channel
0
25Km
?
(1)
Daren Cilau
(2)
Portishead
(3)
Taff Well
Blaen
Onnen
Oolite
Daren
Ddu
Beds
Pwll-y
-Cwm
Oolite
Gully
Oolite
Sub
Oolite
Bed ?
Black Rock
Dolomite
5m
plant roots
pedogenic dolomite

Figure 7.7

(A) Outcrop of the Daren Ddu Beds (Oolite Group) at Cwar-yr-Ystrad Quarry, near Tredegar. Columnar calcites (C) occur within the Daren Ddu Beds (D) which separates the Pwll-y-Cwm Oolite (P) from the overlying Blaen Onnen Oolite (B).

(B) Photomicrograph of the fibrous columnar calcites (F) from the Daren Ddu Beds at Cwar-yr-Ystrad Quarry in South Wales. Scale bar = 1mm.

(C) Outcrop of the elongate crystals of the Palisade Calcite at Engihoul (E-Namur basin) in Belgium.

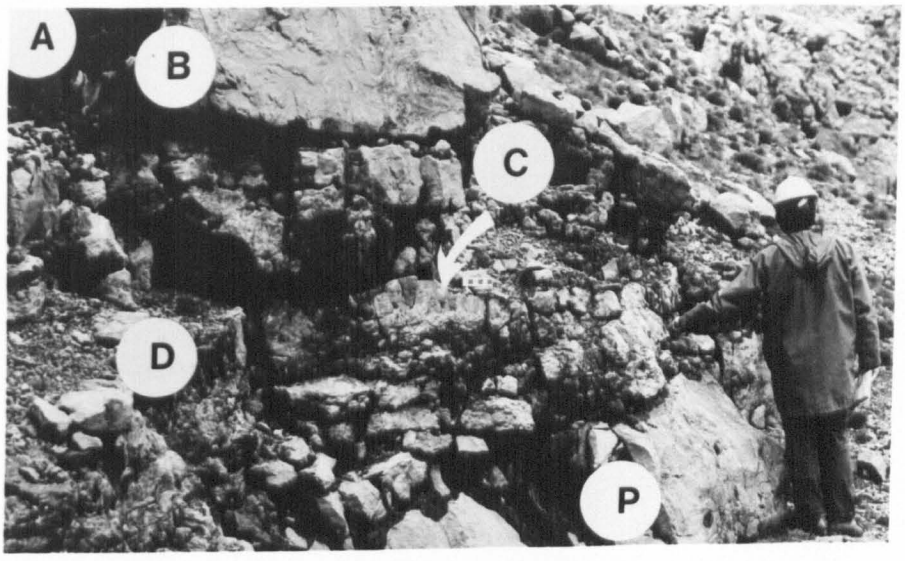
A
B
C
D
P

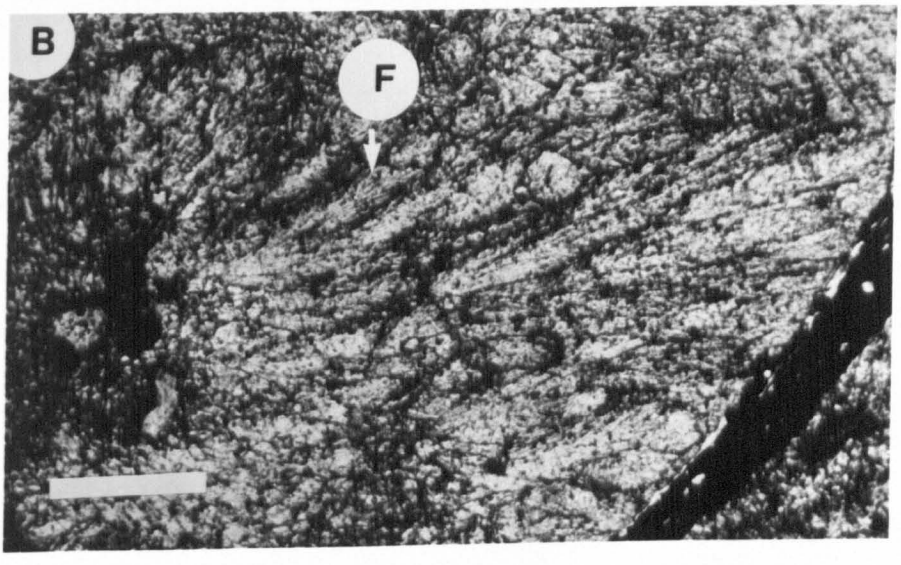
B
F

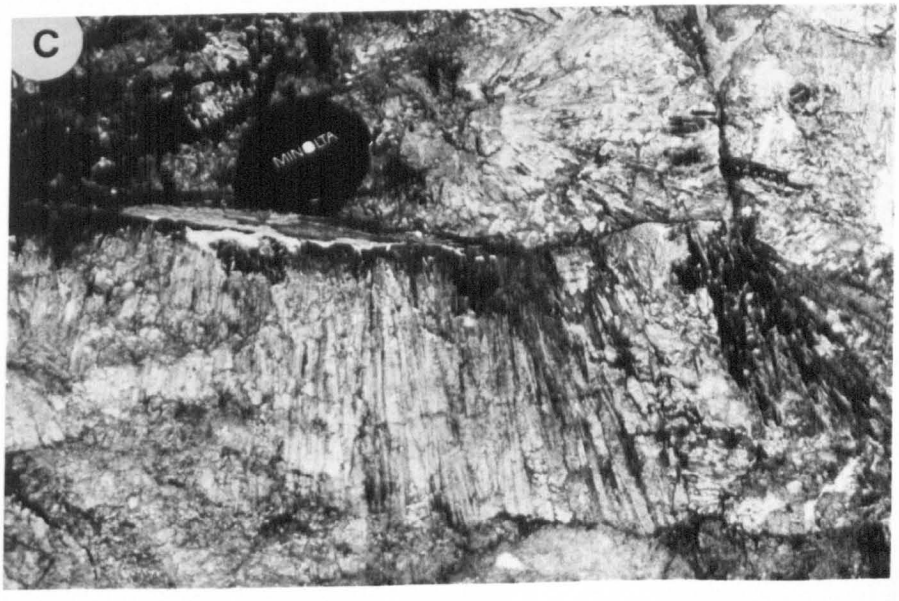
C
MINOLTA

The overall appearance of the nodular units in the Daren Ddu Beds is similar to the developments at Portishead. The skeletal limestone nodules, upon which the columnar calcites nucleated and grew, occur interbedded with a variety of different lithologies including clays and silts as well as stratiform concretions of dolomite (Searl 1988) (Figure 7.7A). Contained within the dolomite concretions (up to 1m thick) are thin coals, plant roots and organic-rich shales which locally pick-out fine scale lamination and simple burrows (Searl 1988).

The columnar calcite crystals are fibrous, pseudopleochroic and usually less than 10cm in length and taper towards their point of nucleation (Figure 7.7B). Predominantly, they are non-luminsecent, unzoned and exhibit straight extinction. The fibres are defined by clay inclusions (Figure 7.7B) and locally the fibrous bundles have a plumose appearance, the long axis of which is subparallel to that of the crystal. The crystal terminations are commonly finely fibrous but locally they are syntaxially overgrown by clear sparry calcites that exhibit well developed rhombohedral form. The columnar calcites show no prefered orientation. Locally, within the nodular beds, there are areas dominated by elongate fence-like layers of (palisade) calcite up to 50cm in length.

Searl (1989) interprets the columnar calcite as speleothem deposits owing to their similarity with such preciptates as described in the literature (cf. Heckel 1983; Folk & Assereto 1976; and Kendall & Broughton 1978). The presence of fine scale primary crystal growth zones revealed by cathodoluminescence precludes a secondary origin, such as the replacement after evaporites (Searl pers comm.). The stratiform dolomites are thought to have a pedogenic origin (Searl 1988) and formed within swamps by the replacement of calcite sediments, derived by washing in by storms. Similar dolomites occur in the Llanelly Formation of South Wales and have also been interpreted as marsh deposits (Wright & Robinson 1988).

Searl (1988) accounted for the close spatial and stratigraphic association of the nodular dolomites and columnar calcites by regarding the former as representing the coastal pedogenic equivalent of the latter, which developed in more fully emergent conditions.

Within the Vesder region (Belgium) the Palisade Calcite Member (ca. 5m thick) is laterally extensive (Jacobs *et al.* 1982) and is thought to be early Viséan in age (Figure 7.7C & 7.8) (it is sandwiched between the Vesder Dolostone Formation of late Tournaisaian to early Viséan in age, and the overlying lower Viséan Terwagne Formation). Thus the age of the columnar calcites in the Vesder basin is approximately the same as the development at Portishead.

Similar horizons to the Palisade Calcite Member have been recorded in the east Namur basin (Swennen *et al.* 1982), and the continuation of the Vesder Basin in southern Germany (Kasig 1980) (Figure 7.8). All the developments overlie dolomitized crinoidal limestones interpreted as having accumulated in a subtidal environment (Swennen *et al.* 1982) (Figure 7.8). Evidence of a regression has been recorded at Walhorn, in the eastern part of the Vesder Basin, where inter-tidal, finely laminated dolomites, with birdseye structures occur at the top of the Vesder Dolostone Formation, directly beneath the Palisade Calcite Member (Swennen *et al.* 1982).

There are two distinct geological occurrences and habits for the columnar calcites. The developments in the Namur Basin (Belgium) and at Aachen (Germany) are similar to those of Britain: the columnar crystals occur in cavities, associated with karstic horizons, and exhibit a wide range of lengths from 1 to 30cm. The columnar calcite crystals exhibit straight extinction and mainly show a uniform dull luminescence under CL, but locally there are fine scale primary crystal growth zones. The crystals are different from those of SW Britain in that they do not

Figure 7.8. Stratigraphic log of the uppermost Tournaisian and lower Viséan sequences of E-Namur, Vesder and Aachen (modified after Jacobs *et al.* 1982), showing the stratigraphic position of the Palisade Calcite Member.

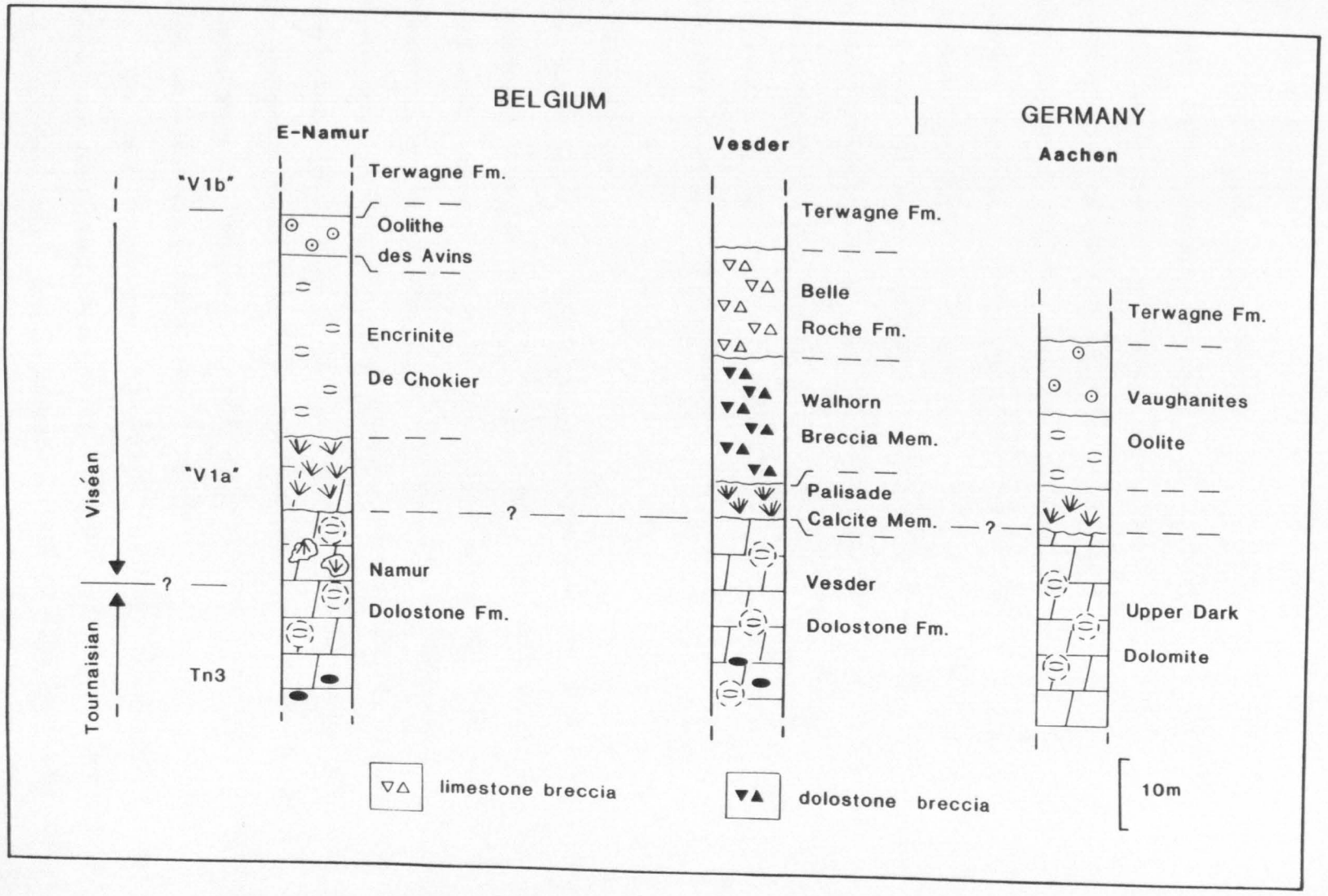
BELGIUM
GERMANY
E-Namur
Vesder
Aachen
"V1b"
"V1a"
Viséan
Tournaisian
Tn3
Terwagne Fm.
Oolithe
des Avins
Encrinite
De Chokier
Namur
Dolostone Fm.
Belle
Roche Fm.
Walhorn
Breccia Mem.
Palisade
Calcite Mem.
Vesder
Dolostone Fm.
Vaughanites
Oolite
Upper Dark
Dolomite
limestone breccia
dolostone breccia
10m

show an internal fibrous microstructure. This is likely to be a manifestation of the paucity of clay material within the Palisade Calcite Member.

The second variety, described by Swennen *et al.* (1981) from the Vesder Basin, consists of layers or clusters of conical calcite spherulites (1-2cm in length), predominantly facing upwards in a unidirectional growth pattern (Figure 7.9). The layers occur interbedded with peloidal, micritic limestones containing birdseye structures, calcrete textures, and reworked conglomerates of columnar calcite crystals. The depth of formation of the columnar calcite crystals must have been in close proximity to the surface and diagenetically early to allow reworking. Based on the undirectional growth of the spherulites, the formation of growth rhythms and the presence of sulphate traces, Swennen *et al.* (1981) proposed a selenite precursor for this particular type of columnar calcite.

7.5 Discussion

The preservation of subaerial exposure surfaces, as with many other sedimentary deposits, is very much reliant upon early burial to inhibit removal by erosion. It is particularly unfortunate that subaerial exposure features, which can provide unique information on early terrestrial environments and climates, are so readily removed by weathering and erosion on land, and during shoreline retreat. The aim of this discussion is to evaluate the regional signficance of the Portishead Paleosol Beds and the contact between the Black Rock Dolomite and the Gully Oolite/Sub-Oolite Bed (where developed).

In 1973 Ramsbottom proposed that a major non-sequence existed between the Black Rock Limestone and the Gully Oolite. His interpretation was based upon the reputed evidence of faunal breaks above and below the

Figure 7.9 A model of the sediment cycles within the palisade calcites of Belgium. Modified after Swennen *et al.* 1981.

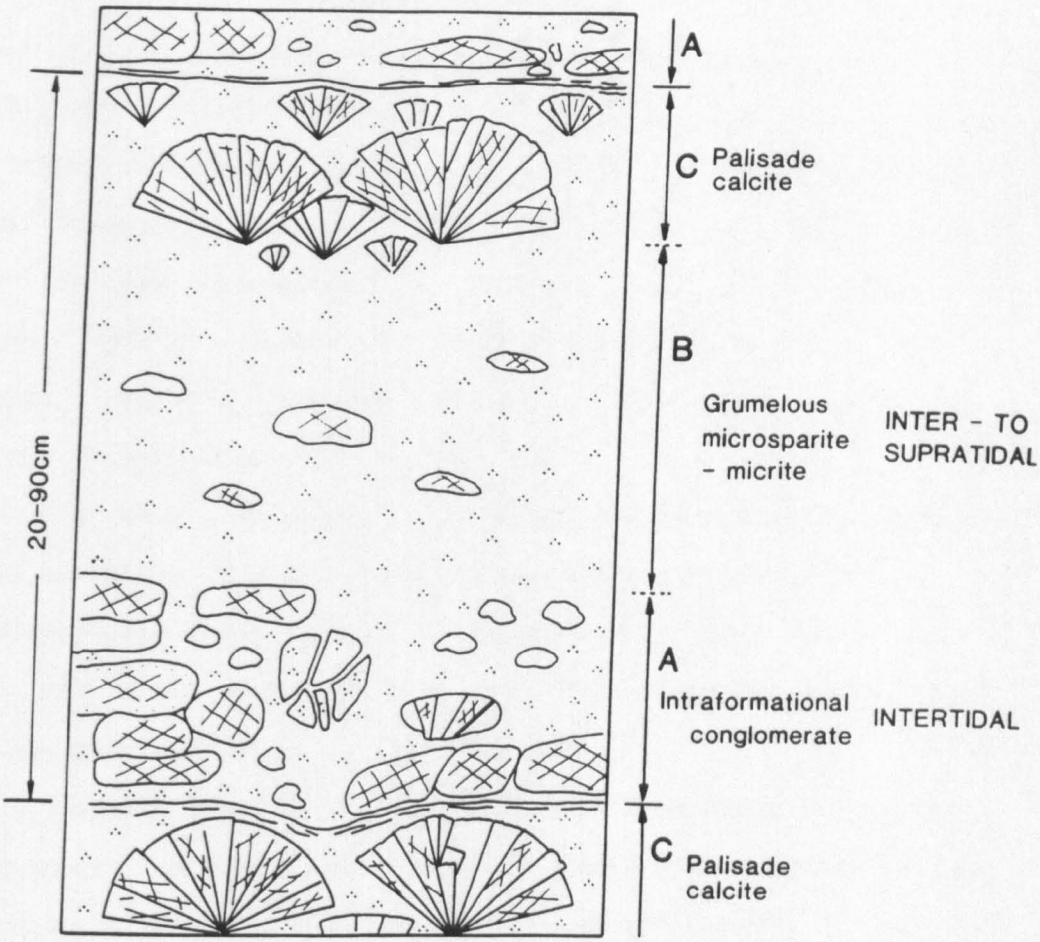
A
C Palisade calcite
B
Grumelous microsparite - micrite
INTER - TO SUPRATIDAL
A
Intraformational conglomerate
INTERTIDAL
C Palisade calcite
20-90cm

Sub-Oolite Bed (Mitchell 1971 & 1972). More recently, the evidence for the faunal breaks has been called into doubt (Waters & Lawrence 1987) and as a result cannot be used to substantiate the sedimentary evidence for this non-sequence.

Apart from the Portishead Paleosol Beds, the only other direct evidence for a subaerial exposure surface separating the Black Rock Limestone from the Gully Oolite has been recorded at Taff's Well in South Wales (Figure 7.6). Here a possible clay paleosol (up to 15cm thick) and a shallowing-upward sequence have been documented by Waters & Lawrence (1987). The latter unit consists of shoreface facies of fine grained dolomites, lacking crinoid debris, and exhibiting faint low-angle lamination, overlying crinoidal limestones representing the below wave-base facies (Waters & Lawrence 1987).

On a more regional scale, the widespread development of exposure surfaces containing columnar calcite crystals along the southern margin of the Welsh-Brabant Massif (section 7.4), supports the case for a major eustatic fall in sea level at the end of the Courceyan (Tournaisian) and during the early part of the Chadian (Viséan).

In addition compelling evidence for a sea level fall at the end of the Courceyan (Tournaisian) and during the early Chadian (Viséan) has come from a study of those sequences in a more basinward setting. Studies of the Waulsortian facies of Belgium (Lees *et al.* 1977; Lees *et al.* 1985) and in SW Britain (Lees 1982; Lees & Hennebert 1982) have revealed much evidence to show that a change of environment occurred during upper Courceyan (Tournaisian) times, most probably as a result of a marked fall in sea level (*v.* Chapter 6). From a synthesis of the Lower Carboniferous successions of northwest Europe, the Mississippi Valley (USA) and the Russian Platform, Ross & Ross (1985 & 1987) concluded there was a marked eustatic sea level fall at the end of the

Figure 7.10. Sea level curves for the lower part of the Carboniferous (modified from Ross & Ross 1985).

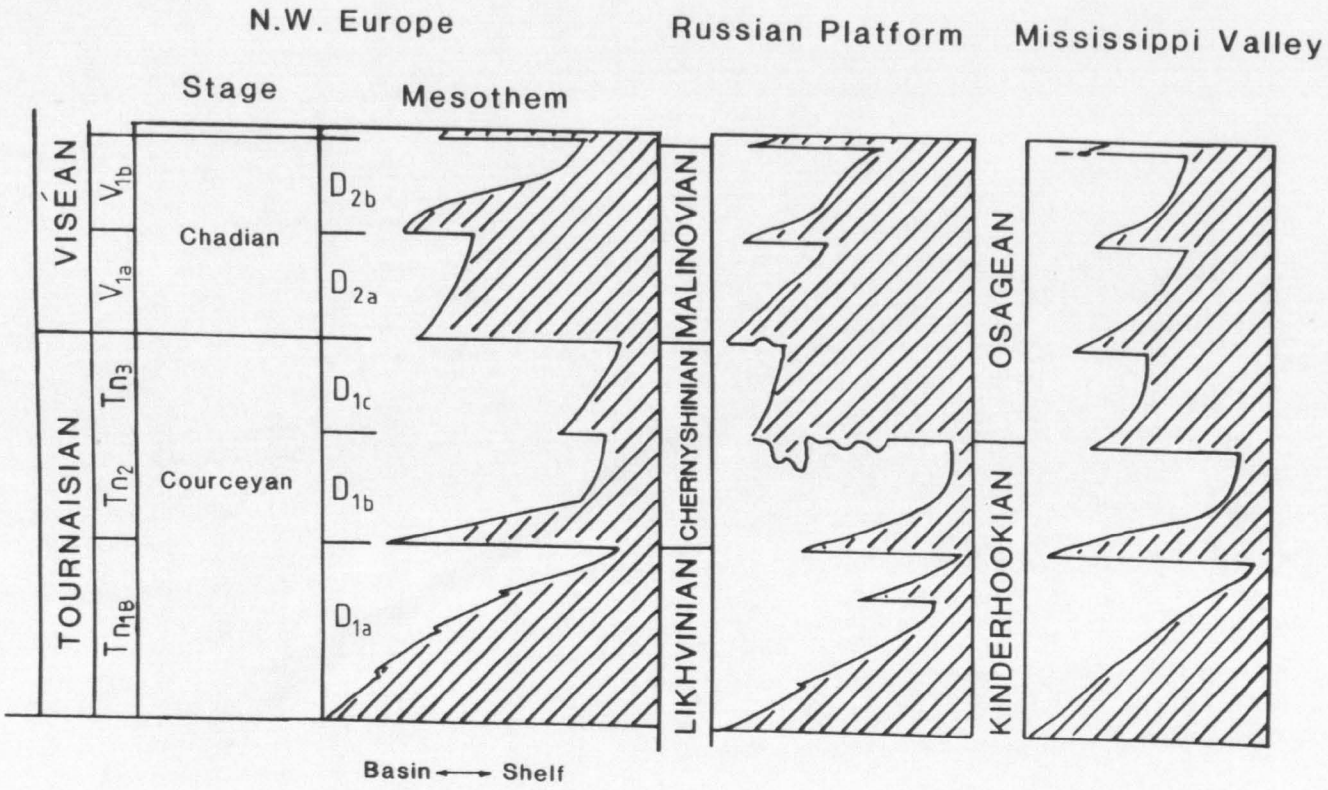
N.W. Europe
Russian Platform
Mississippi Valley
Stage
Mesothem
VISÉAN
TOURNAISIAN
V1b
V1a
Tn3
Tn2
Tn1B
Chadian
Courceyan
D2b
D2a
D1c
D1b
D1a
LIKHVINIAN
CHERNYSHINIAN
MALINOVIAN
KINDERHOOKIAN
OSAGEAN
Basin ⟷ Shelf

Courceyan (Tournaisian) (Figure 7.10).

If the sedimentary break beneath the Gully Oolite (Sub-Oolite Bed in the Bristol district) represents a significant global sea level fall then the apparent rarity of subaerial exposure features at the top of the Black Rock Limestone requires an explanation. Within the Daren Ddu Beds, a major control affecting the lateral extent of such horizons is thought to have been local topography because westward (over a distance of 13Km) they can be correlated with thin-bedded dolomites displaying algal lamination (Raven 1983). Other, more likely mechanisms by which regionally significant exposure features could be destroyed include erosional removal and obliteration of the textures by dolomite. However, as yet, no occurrence of the reworked clasts of the subaerial exposure horizons have been found in the overlying beds.

It is significant that the Black Rock Dolomite is regionally extensive and contains few relict sedimentary features. However, dolomitizing fluids are incapable of obliterating the non-carbonate features associated with the paleosols e.g. siltstones and clays. It is for this reason that the loss of the emergent features is thought to be a result of both erosional and diagenetic processes.

In conclusion, the evidence strongly suggests that the Black Rock Limestone at Portishead, and presumably also at Taff's Well, underwent a period of subaerial exposure. It would seem highly unlikely that these developments represent major isolated topographic highs whilst the surrounding area remained submerged. Following this line of reasoning, large areas along the southern flanks of the Welsh-Brabant Massif in SW Britain, are likely to have become subaerially exposed during early Chadian times.

It is tempting to correlate the southward extent of the subaerial break with the outer limits of the central ramp zone which extends as far

Figure 7.11. Idealized block models of the evolution of southwest Britain during the late Courceyan - late Chadian period. (FWB = fairweather wave-base; SWB = storm wave-base).

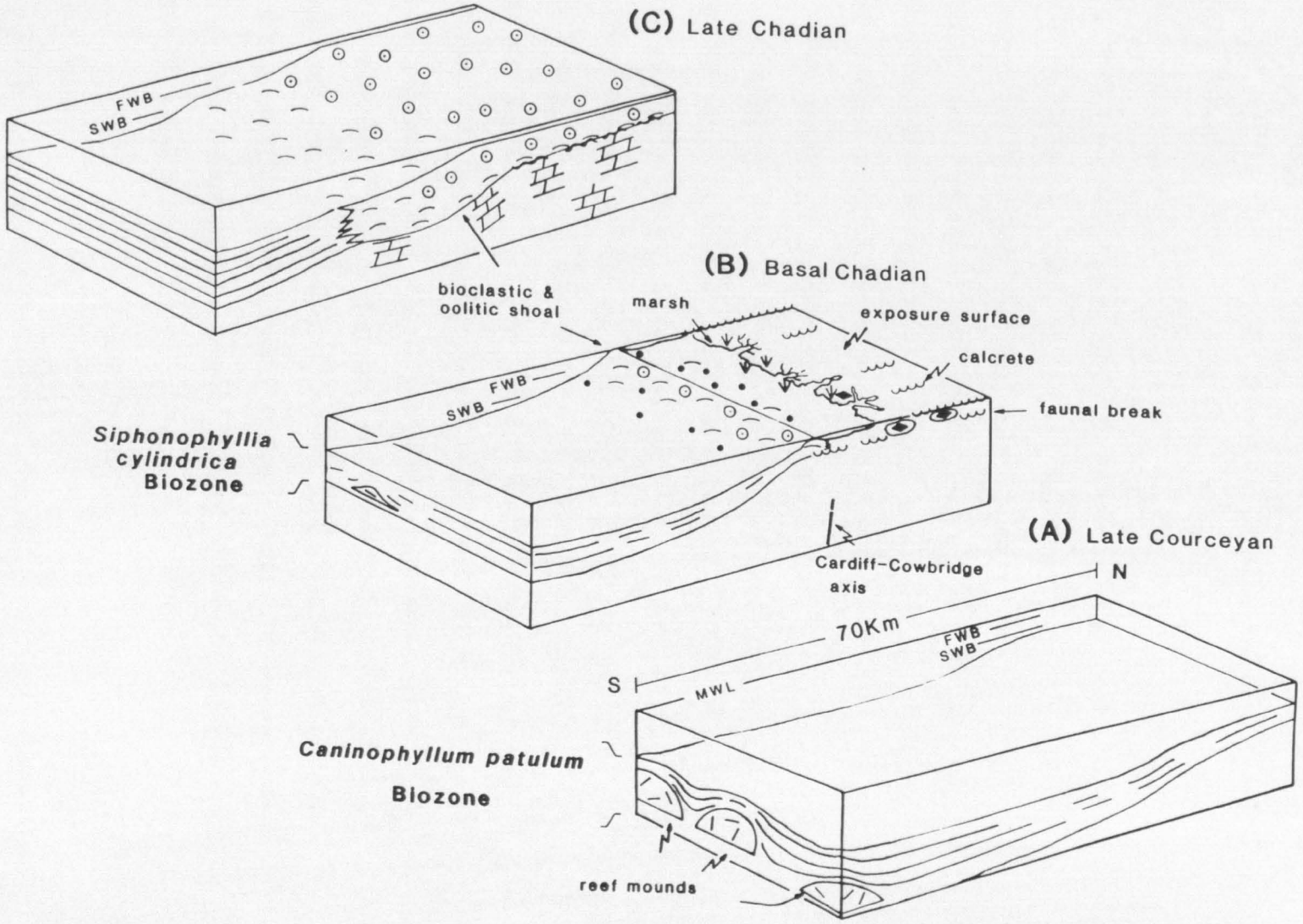
(C) Late Chadian
FWB
SWB
(B) Basal Chadian
bioclastic &
oolitic shoal
marsh
exposure surface
calcrete
faunal break
FWB
SWB
Siphonophyllia
cylindrica
Biozone
(A) Late Courceyan
Cardiff-Cowbridge
axis
N
70Km
FWB
SWB
S
MWL
Caninophyllum patulum
Biozone
reef mounds

south as Cardiff, Cowbridge and Weston (Figure 7.6). To the south of this line, the Black Rock Dolomite passes apparently gradationally, upwards into the overlying Gully Oolite (Waters & Lawrence 1987). While in the central ramp zone the contact between the Black Rock Limestone and the Gully Oolite is predominantly sharp and planar, although locally it may be slightly undulatory, such as at Weston (Mitchell 1980). This would suggest that apart from sea level changes, sedimentation was also influenced by differential subsidence (Waters 1984; Waters & Lawrence 1987; Wright 1984a; Wilson *et al.* 1988; Chapter 4). The rate of subsidence in the southern ramp zone was greater than the rate of sea level fall and as a result, continuous deposition took place.

A model for the development of the carbonate ramp of SW Britain during the upper Courceyan to late Chadian period is shown in Figure 7.11. During the upper Courceyan, below wave-base facies and rare Waulsortian reefs dominated the area south of the Forest of Dean (Chapter 4) (Figure 7.11A). The late Courceyan eustatic sea level fall is thought to have caused the decline of the reef mounds and the periodic emergence of an area at least as far south as Cardiff and Bristol (Figure 7.11B). The low relief emergence surfaces were suseptible to drowning by even a minor rise in sea level. The manifestation of this was the establishment of subtidal (e.g. Sub-Oolite Bed) and active shoal facies upon the emergent surface (Figure 7.11C). The shallowing-upward cycles in the Gully Oolite represent the progradation of beach fronted shorelines (Wright 1986; Waters & Lawrence 1987).

7.6 Conclusions

1) The Black Rock Limestone and the Sub-Oolite Bed at Portishead are capped by exposure surfaces with palaeokarst features, calcrete and unusual columnar calcite 'speleothem'. The emergent features formed as a

result of a major eustatic sea level fall at the end of the Courceyan and during the early part of the Chadian.

2) Further confirmation of a eustatic sea level fall at the end of the Courceyan has come from the recognition that other subaerial exposure horizons containing columnar calcites documented in South Wales, Belgium and Germany occur at a similar stratigraphic level to the development at Portishead.

3) In SW Britain, the Black Rock Dolomite - Gully Oolite (Sub-Oolite bed where developed) contact is interpreted as a subaerial exposure horizon. Subsequent geological processes (erosion, removal and dolomitization) are thought to have partly obscured the evidence for exposure. This exposure surface probably reached as far south as the present day Cowbridge, Cardiff and Weston areas. Its southerly extent is thought to have been controlled by differential subsidence.

Chapter 8 - Ramp longevity & summary

8.1 Introduction

The Black Rock Limestone forms a major component of the early Carboniferous to late Arundian ramp succession of SW Britain (Wright 1987). In this chapter the development of this ramp sequence is discussed, especially the tectonic controls. The ramp history is compared with other Dinantian ramp sequences. Those other basins under consideration include: the Craven Basin, Northern England; the Munster Basin, southern Ireland; the Shannon Basin, western Ireland; and the Dublin Basin, eastern Ireland (Figure 8.1B).

Ramps are typical features of the early stages in the development of carbonate build-ups and form soon after the drowning of the continental areas (Wilson 1975; Read 1982 & 1985). They are considered to be relatively short-lived phenomenon because they readily evolve into rimmed carbonate shelves or platforms (Figure 8.1A) once carbonate sedimentation is established (Read 1982 & 1985). Read (1985) proposed that this process is a result of high carbonate production in the nearshore environment and sediment starving of off-shelf environments. The persistence of the Dinantian ramps of England, Ireland and Wales, from the early Courceyan to Arundian period or later (up to 25 million years, George *et al.* 1976) requires explanation.

8.2 Ramp to shelf evolution

Five stages of basin development are recognized (Figure 8.2). It is important to note that the stages are not intended to represent regional correlatable 'events'. They reflect the comparable evolution of each basin: from a carbonate ramp to a shelf.

Figure 8.1

(A) The three major geomorphological settings of shallow-marine carbonates: ramp, shelf and platform (modified after Tucker 1985).

(B) The approximate positions of the Carboniferous basins of the British Isles and Ireland. The major depocentres discussed in the text are labelled.

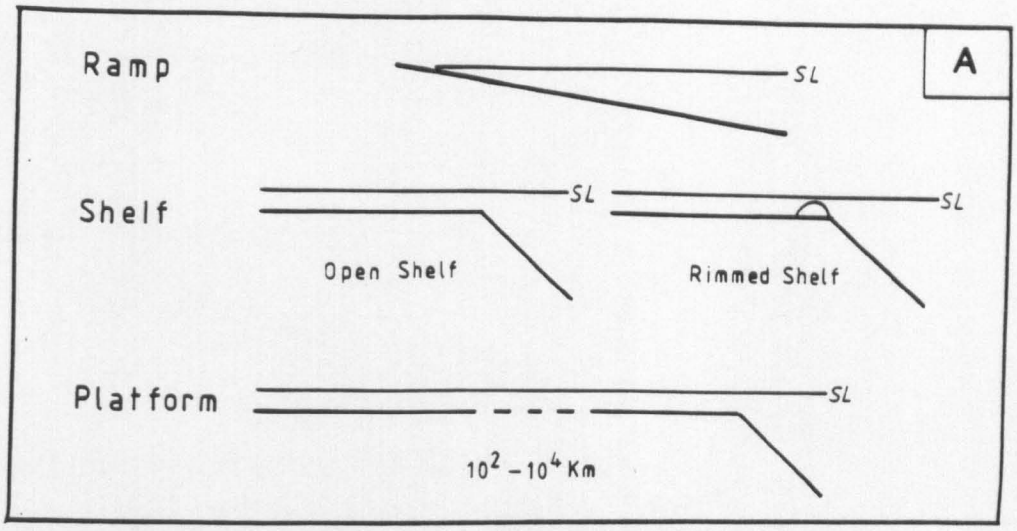
A
Ramp
SL
Shelf
SL
SL
Open Shelf
Rimmed Shelf
Platform
SL
$10^2 - 10^4$ Km

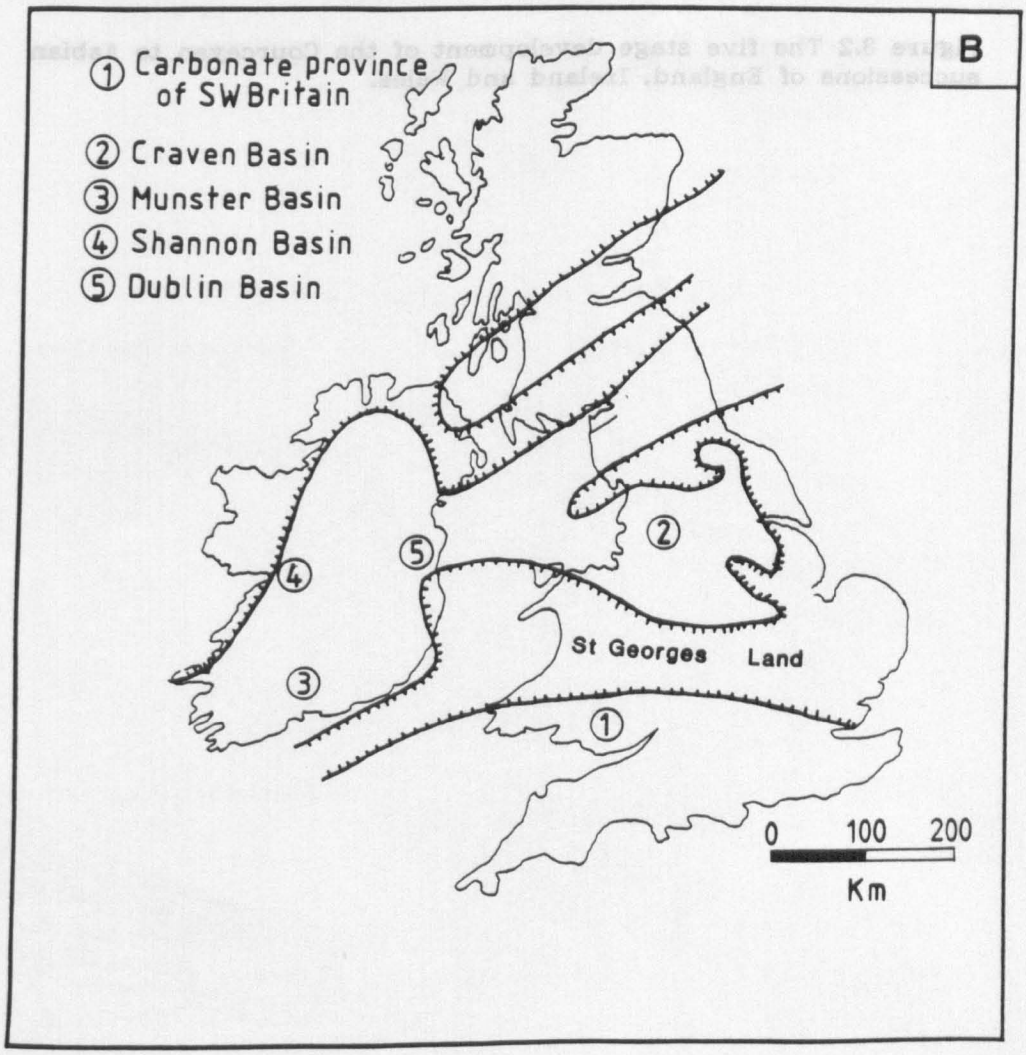
B
① Carbonate province of SW Britain
② Craven Basin
③ Munster Basin
④ Shannon Basin
⑤ Dublin Basin
St Georges Land
0 100 200
Km

Figure 8.2 The five stage development of the Courceyan to Asbian successions of England, Ireland and Wales.

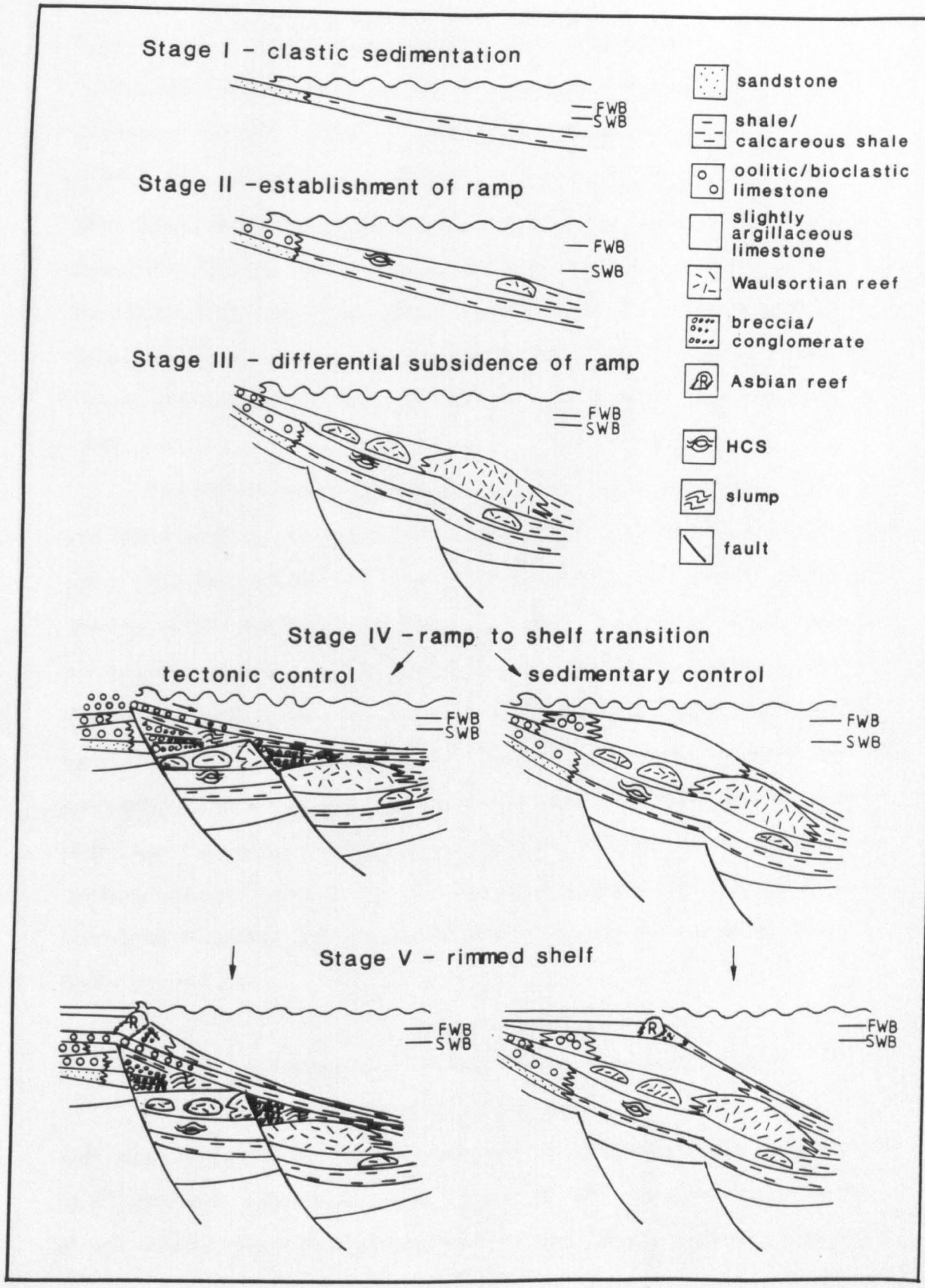
Stage I - clastic sedimentation
FWB
SWB
Stage II -establishment of ramp
FWB
SWB
Stage III - differential subsidence of ramp
FWB
SWB
sandstone
shale/
calcareous shale
oolitic/bioclastic
limestone
slightly
argillaceous
limestone
Waulsortian reef
breccia/
conglomerate
Asbian reef
HCS
slump
fault
Stage IV - ramp to shelf transition
tectonic control
sedimentary control
FWB
SWB
FWB
SWB
Stage V - rimmed shelf
FWB
SWB
FWB
SWB

8.2.1 Stage I - Clastic sedimentation ('lower' Courceyan)

During the lower Dinantian a major transgression flooded the Old Red Sandstone alluvial plains (Johnson 1982). The depositional units which record this transgression include: the Lower Limestone Shale Group (100-120m) of SW Britain (Burchette 1987) (Figure 8.3); the Kinsale Formation (1600m) of the Munster Basin (MaCarthy & Gardiner 1987; MacCarthy 1987); the Mellon House Formation (38m) and the Ringmoylan Shale Formation (31m) of the Shannon Basin (Somerville & Jones 1985); and the 'Lower Limestone Shale' unit (>30m) of the Dublin Basin (Jones *et al.* 1988).

The above sequences mainly consist of shales/calcareous shales and are interpreted as representing offshore muddy facies. The transgressive units typically culminate in very extensive mudrock deposition (George 1972; MacCarthy & Gardiner 1987; MacCarthy 1987). Detailed sedimentary studies by Burchette (1987), MacCarthy & Gardiner (1987) and MacCarthy (1987) reveal that the overall transgression was locally pulsed by several minor, wave and storm dominated, coarsening and shallowing-upward (progradational) sedimentary cycles. Overall, during this stage the basins underwent a regional subsidence by flexure (a gradual, linear increase in the rate of subsidence into the basin) but there was no marked differential subsidence, along tectonic hinge-lines or faults (Figure 8.2).

8.2.2 Stage II - Establishment of the muddy carbonate ramps ('middle' Courceyan)

This stage is marked by the predominance of carbonate sediments deposited as a uniformly thickening wedge. Some of the sequences representative of this stage of basin development include: the Barry Harbour Limestone

Figure 8.3 Summary of the eustatic and tectonic evolution of the Lower Limestone Shale, the Black Rock Limestone and the Gully Oolite.

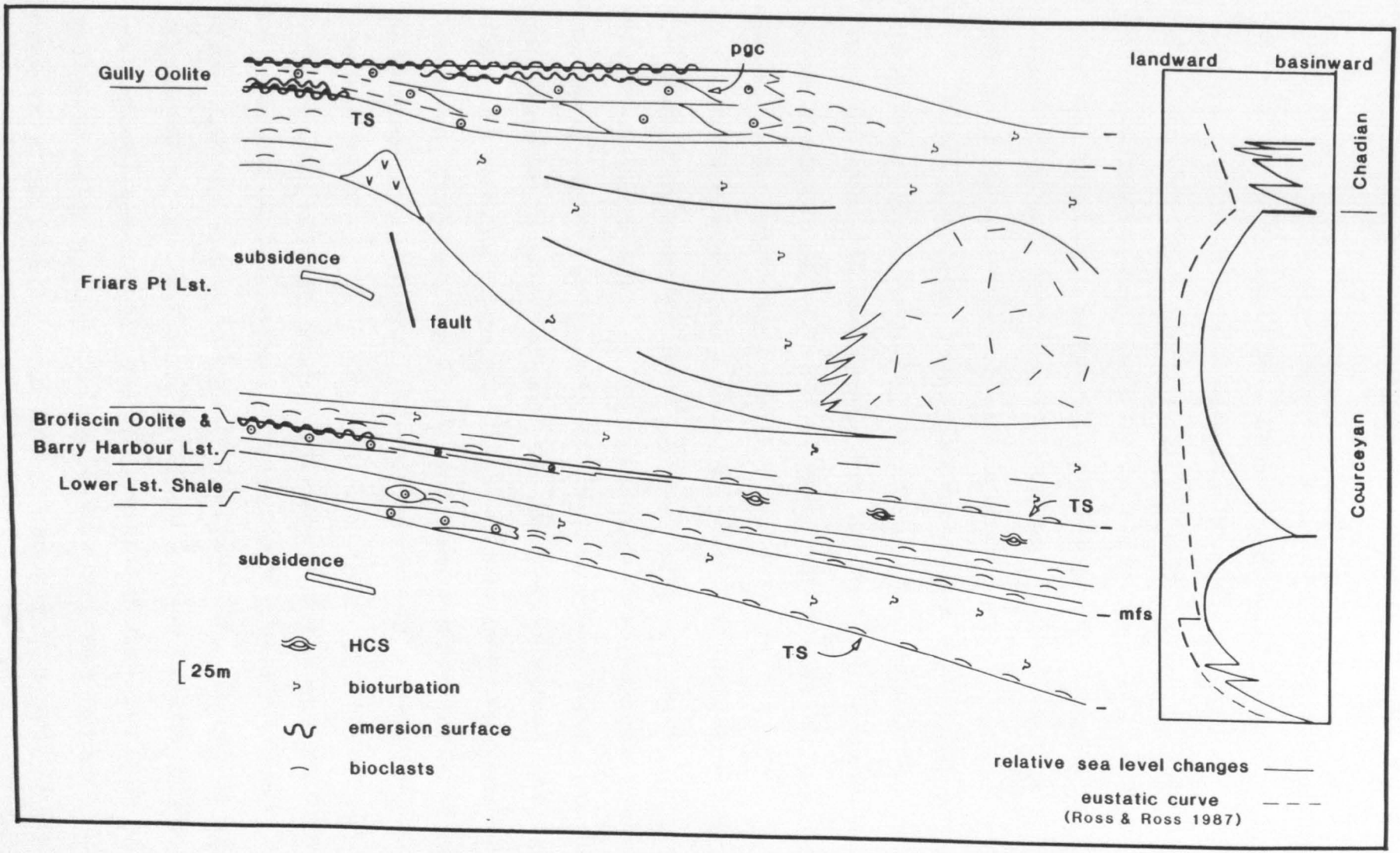
Gully Oolite
pgc
TS
subsidence
Friars Pt Lst.
fault
Brofiscin Oolite &
Barry Harbour Lst.
Lower Lst. Shale
TS
subsidence
mfs
TS
HCS
[25m
bioturbation
emersion surface
bioclasts
landward
basinward
Chadian
Courceyan
relative sea level changes
eustatic curve
(Ross & Ross 1987)

(>90m) and the Brofiscin Oolite (up to 16m thick) of SW Britain (Figure 8.3); the Haw Bank Limestone (>300m) of the Craven Basin (Miller & Grayson 1982); the Ballysteen Limestone Formation and equivalent part of the Lower Cork 'Reef' Limestone Formation of the Munster Basin (MacCarthy & Gardiner 1987; Murphy 1988); the Ballymartin Limestone Formation (46m) and the Ballysteen Limestone Formation (190m) of the Shannon Basin (Somerville & Jones 1985); and the Malahide Limestone Formation (MLF) (1200m) of the Dublin Basin (Jones *et al.* 1988).

Three sedimentary depth-related facies zones are recognized. The inner ramp, above fairweather wave-base, facies comprise oolitic and coarse bioclastic grainstones and peritidal complexes (e.g. the Brofiscin Oolite Formation, the Huntstown Laminated Member (MLF) and the Turvey Micrite Member (MLF), respectively).

The mid-ramp facies, between fairweather and storm wave-base, are represented by muddy bioclastic limestones containing a variety of event beds (e.g. Barry Harbour Limestone Formation and Ballymartin Limestone Formation). The outer-ramp, below storm wave-base, facies comprises bioturbated, argillaceous limestones (e.g. Haw Bank Limestone and the Ballysteen Limestone Formation), rare Waulsortian reefs and calcareous mudstones. The development of the Waulsortian reefs was only in the most distal to shoreline of settings e.g. the Munster Basin (MacCarthy & Gardiner 1987).

Stage II witnessed the continued regional subsidence of the basins as a result of flexure (defined in section 8.2.1). Similar to Stage I there was no marked differential subsidence. The contrast in the thicknesses of the successions in different basins reflects the varying rates of subsidence and the length of duration of Stage II. The 'lower' to 'middle' Courceyan Malahide Limestone Formation (Dublin Basin) is up to 1200m thick, and records a high rate of subsidence. It consists of a

succession of coarsening- and shallowing-upward sedimentary cycles (each 30-80m thick) (Jones *et al.* 1988). Stage II is represented in SW Britain by the 'middle' Courceyan Barry Harbour Limestone and Brofiscin Oolite shallowing-upward succession which has a maximum measured thickness of 90m (Figure 8.3).

8.2.3 Stage III - Differential subsidence ('upper' Courceyan to Arundian)

This stage is marked by a predominance of carbonate sediments deposited as a markedly thickening wedge into the basin (Figure 8.2). Some of the sedimentary sequences typical of Stage III include: the Friars Point Limestone (340m) and the Cannington Reef Limestone (222m) of SW Britain (Figure 8.3); the Chatburn Limestone, the Thornton Limestone and the Peach Quarry Limestone of the Craven Basin (Miller & Grayson 1982; Gawthorpe 1986); the Waulsortian Limestone Formation (up to 600m) of the Munster Basin (Murphy 1988); the Waulsortian Limestone Formation (up to 900m) of the Shannon Basin (Somerville & Jones 1985); and the Feltrim Limestone Formation (187m) of the Dublin Basin (Jones *et al.* 1988).

Throughout Stage III the carbonate ramp configuration was maintained (Figure 8.2). All three ramp facies types (inner, mid- and outer ramp) can be identified (e.g. Miller & Grayson 1982; Gawthorpe 1986; Wright 1986). In South Wales, the late Courceyan to Arundian North Crop sequence of the Carboniferous Limestone forms an attenuated succession (only 70m thick) of mainly oolitic and peritidal limestones with fluvial intercalations (Wright 1986). Along the most southerly outcrops, in Dyfed and Cannington Park, the time equivalent sequence reaches over 800m and consists of a monotonous succession of below storm wave-base argillaceous limestones (e.g. Friars Point Limestone) which contain Waulsortian reefs (e.g. Berry Slade reef). In the distal ramp setting of the Munster Basin the Waulsortian reefs pass seaward into basinal shales and thin-bedded

limestones (e.g. Ringabella Limestone Member) (MacCarthy & Gardiner 1987).

Stage III is identified by an overall deepening of the carbonate succession. It records the widespread accumulation of below storm wave-base facies. In the Munster Basin the Waulsortian reefs developed in both mound and sheet-like form (Lees 1964) and 'prograded' shoreward, presumably in response to the progressive deepening (MacCarthy & Gardiner 1987). Sevastopulo (1982) estimated that at their acme the Waulsortian complexes extended over an area of 20,000 square kilometres over what is now central and southern Ireland. The deepening was strongly influenced by differential subsidence as testified by the marked thickness differences occurring between the inner ramp and outer ramp sequences (see above). Significantly, pronounced thickness variations have also been documented in the outer ramp successions by Miller & Grayson (1982), Grayson & Oldham (1987), Strogen (1988), and Jones *et al.* (1988). Along the southern limb of the Limerick Syncline (Shannon Basin), Strogen (1988) identified a 160m increase in thickness of the Waulsortian facies (ca. 290m to 450m thick) over a distance of 10km.

These marked thickness changes have been attributed to movement along fault bounded, tilt blocks forming either graben or half-graben basins (Miller & Grayson 1982; Wright 1984; Grayson & Oldham 1987; Gawthorpe 1986; Wright 1987; Jones *et al.* 1988; Wilson *et al.* 1988; Strogen 1988) (Figures 8.2 & 8.3). During Stage III carbonate production was sufficient to maintain a gentle sea floor slope (ramp). The tilt-block faults did not achieve a surface expression i.e. create significant topographic gradients.

Overall, the tectonic setting of Stage III is distinct from Stages I & II (regional flexure) because of sedimentation was influenced by movement along linear basement structures (e.g. hinge-lines and faults) across which there was marked differential subsidence.

8.2.4 Stage IV - Ramp-to-shelf transition

Two styles of ramp-to-shelf transition have been recognized: accretionary model and tectonic model (Figure 8.2).

Accretionary model (Holkerian)

The accretionary model is characterised by the widespread deposition of shallow water-carbonates e.g. SW Britain, NE Wales and Derbyshire (Northern England) (Wright 1987, Somerville *et al.* 1989; Schofield & Adams 1985, respectively). Typically behind the shoal complex of crinoidal and oolitic packstone/grainstone is a thick succession of open lagoonal, oolitic and peritidal carbonates represented by the Dowlais Limestone of South Wales and the Clifton Down Limestone of SW England (Murray & Wright 1971; Wright 1982c; Wright 1987). Seaward of the shoal complex, bioclastic limestones accumulated (e.g. Stackpole Limestone, Wright 1987). It has been suggested by Somerville *et al.* (1989) that in NE Wales the bioclastic limestone deposits pass seaward with a gently inclined slope (ramp) into deeper water basinal facies e.g. shales.

To permit the thick accumulation of barrier and back-barrier facies there must have been a net rise in sea level. It is significant that there was a major basinward shift of the loci of the shoal facies during this stage of basin development (Wright 1987). Wright (1987) proposed that this may have been influenced by local tectonic changes as a result of a reduction in the rate of subsidence. Regardless of the cause, shallow-water carbonate supply was able to keep pace with the rise in sea level and build-up as a regionally extensive flat-topped sediment wedge (Figure 8.2).

Tectonic model (late Chadian to Holkerian)

During the late Chadian to Holkerian period, both the Craven Basin and the Dublin Basin were dominated by terrigenous mudstones in which occur beccia/conglomerates and fining-upward calcarenites (Miller & Grayson 1982; Gawthorpe 1986; Jones *et al.* 1988). The limestone breccias/conglomerates (are up to tens of metres in diameter) are often of reef facies (Miller & Grayson 1972; Gawthorpe 1986). Associated with the breccias/conglomerates in the Craven Basin are sedimentary slide and slump structures (Gawthorpe 1986).

The breccia/conglomerate horizons have been interpreted as debris flow deposits and the fining-upward calcarenites as having a turbiditic-type origin (Gawthorpe 1986; Jones *et al.* 1988). The graded calcarenite beds suggest an offshore transport of carbonate material by storm surges and turbidity flows from shelf areas into the mud-dominated basins (Nolan 1987; Jones *et al.* 1988).

The cessation of local carbonate production was replaced by an increased influx of terrigenous material. The reworking of the underlying succession and the formation of slump and slide structures must have had a tectonic origin, requiring steep gradients, suggesting the basin edge faults were surfacing to have a significant topographic expression (Gawthorpe 1986; Jones *et al.* 1988). The shallow water carbonates accumulated landward of the developing shelf edge, most probably within the hanging-wall dip-slope of a half-graben (Nolan 1987) (Figure 8.2).

Overall, tectonic controls played a major role in the development of the shelf edge in the Dublin Basin and Craven Basin (Miller & Grayson 1982; Gawthorpe 1986; Jones *et al.* 1988).

In conclusion the Dinantian ramp-to-shelf transition occurred either by 1) the progradation of shallow water carbonate facies to form a flat-topped sediment wedge (accretionary model) or 2) the surfacing of

basement faults to create steep gradients and a shelf edge (tectonic model) (Figure 8.2).

8.2.5 Stage V - shelf/rimmed shelf (Asbian)

The palaeogeography during the Asbian is characterised by shallow water shelf facies, commonly delineated from the basin by reefs along the shelf-edge (Broadhurst & Simpson 1973; Somerville 1979; Walkden 1987; Miller & Grayson 1982; Gawthorpe 1986; Grayson & Oldham 1987). The shallow water facies comprise decimetre-thick, fossiliferous, bioclastic and peloidal limestones (Somerville 1979; Walkden 1974 & 1987; Wright 1987). The sequences are typically bounded by palaeokarstic surfaces, or calcareous laminated crusts, or paleosols (Somerville 1979; Walkden 1974 & 1987). Each minor cycle suggests an alternation of transgressive and regressive periods which culminates in widespread emergence (Ramsbottom 1973 & 1979; Walkden 1974 & 1987; Somerville 1979). Overall, the style of sedimentation suggests a uniform, shallow, relatively flat, shelf configuration (Walkden 1987; Wright 1987).

The shelf edge reefs have rich and diverse faunas, often showing depth-related ecological zonation (Ramsbottom 1978). They commonly have a stromatolitic algal wall from which fore-reef talus slopes extend basinwards, into deep water shales (Broadhurst & Simpson 1973; Ramsbottom 1978; Miller & Grayson 1982; Grayson & Oldham 1987).

8.3 Discussion

The aim of this discussion is to evaluate the factors which enabled the Dinantian ramps to persist. Those parameters which affect the geomorphology of carbonate settings include: (a) sediment supply and (b) sea level changes.

8.3.1 Sediment supply

In modern carbonate settings the supply of sediment is highly localised, mainly within shallow water environment (<30m) and typically negligible in the aphotic zone (Kendall & Schlager 1981). Excess sediment supply in the shallow-water environment and sediment starvation in the basin will eventually cause the aggrading sedimentary pile to over-steepen along the seaward margin (Read 1982 & 1985). On a seismic scale the low-angle ramp clinoforms (few metres per kilometre, Chatellier 1988) progressively steepen in the central ramp zone to form a 'shelf-like' configuration (Figure 8.4A).

Significantly, carbonate supply during the the Dinantian was locally produced and over a wide range of environments, including the aphotic zone. The thick accumulations of aphotic deposits, locally in excess of 1500m, comprise crinoids, bryozoans, hyalosteliid sponge spicules, plurilocular foraminifera and Waulsortian reefs (Lees *et al.* 1985).

It was the nature of the supply of sediment during the Dinantian which enabled the ramps to persist. During high sea level stands, a plentiful supply of sediment in a wide range of environments results in seafloor aggradation and inhibits lateral accretion (progradation). Progradation represents an excess sediment supply, it causes a sedimentary pile to locally over-steepen and ultimately results in the development of a carbonate shelf or platform configuration (Figure 8.4A).

8.3.2 Sea level changes

A plentiful supply of sediment in a wide range of environments is a necessary but insufficient criterion by which to maintain a carbonate ramp. The supply of sediment needs to be accomodated by a rise in sea level (e.g. eustatic rise in sea level or subsidence) otherwise progradation of

Figure 8.4

(A) Ramp-to-shelf transition (note, a negligible *in situ* carbonate supply in the aphotic zone).

(B) The persistence of carbonate ramps during a eustatic rise in sea level (note, a plentiful supply of material in the aphotic zone).

(C) The persistence of carbonate ramps during differential subsidence (note, a plentiful supply of material in the aphotic zone).

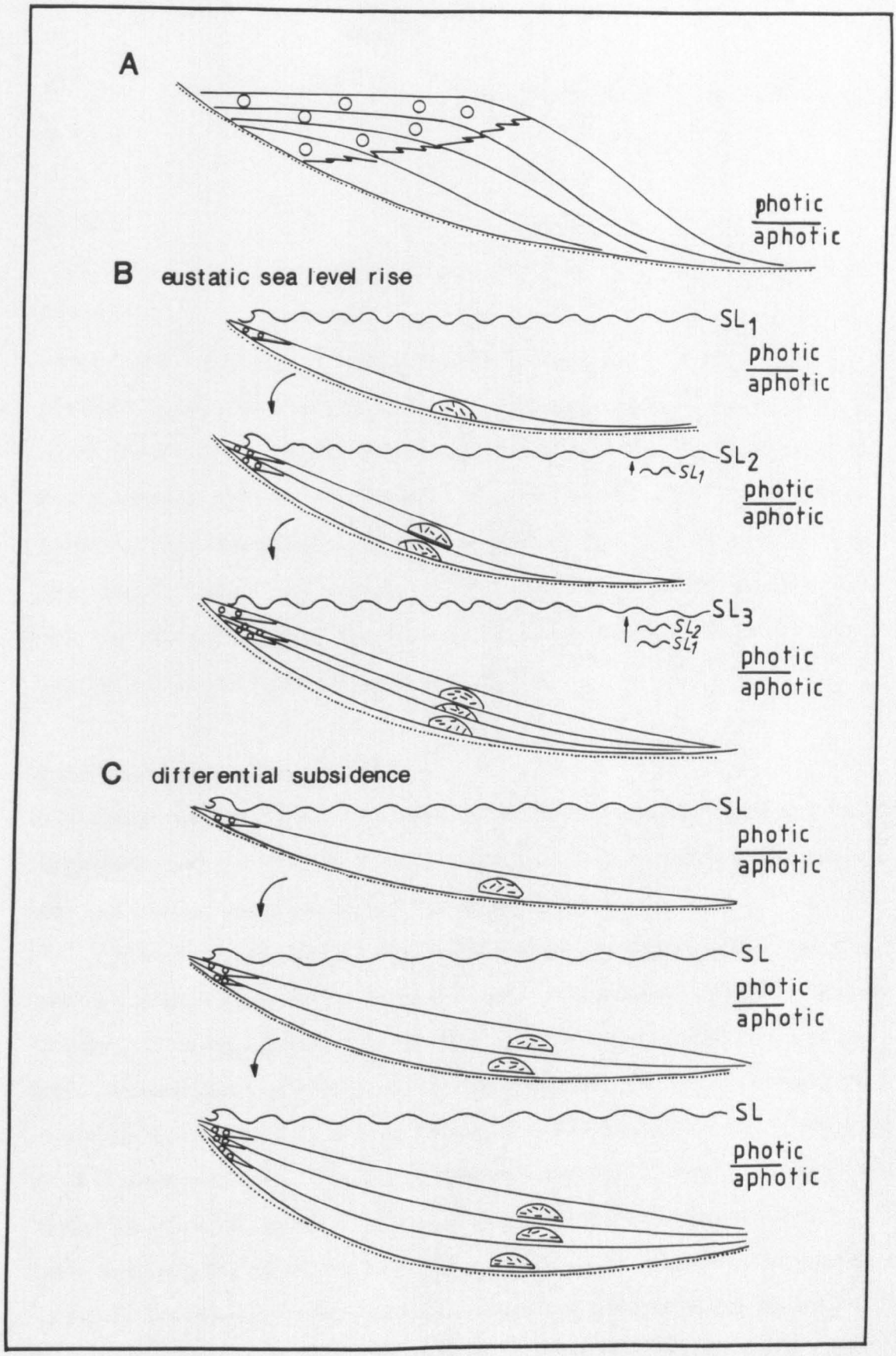
A
photic
aphotic
B eustatic sea level rise
SL1
photic
aphotic
SL2
SL1
photic
aphotic
SL3
SL2
SL1
photic
aphotic
C differential subsidence
SL
photic
aphotic
SL
photic
aphotic
SL
photic
aphotic

the inner ramp zone causes the ramp-to-shelf/platform transition (Figure 8.4A).

Eustacy

Carbonate ramps are typically considered to be untenable if solely effected by a progressive eustatic rise in sea level (no differential subsidence) (Wilson 1975; Read 1982 & 1985). However, provided there is a plentiful supply of locally produced sediment over a wide range of environments it is possible, under certain cirumstances (i.e. a balance between the rate of sea level rise and sediment supply), for a carbonate ramp to be maintained during a eustatic sea level rise (Figure 8.4B). Unfortunately, there is no suitable example of this in the Dinantian of the British Isles because typically subsidence has played an important role in sedimentation.

Differential subsidence

Differential subsidence can provide the available space by which sediment aggradation can occur without over-steepening of the accreting sedimentary pile and causing lateral accretion (progradation).

During the Dinantian two distinct styles of subsidence are known to have occurred during the period of ramp development: regional flexure (Stages I & II) and pronounced differential subsidence (Stage III) (Figure 8.2). A good example of regional flexure maintaining a carbonate ramp is shown by the Malahide Limestone Formation (Dublin Basin) which is composed of a sequence of stacked shallowing-upward cycles (in excess of 1200m) (Jones *et al.* 1988). Increasing differential subsidence into the basin provides the space for sediment aggradation to dominate over lateral accretion (progradation) (Figure 8.4C). The minor progradational phases of the shallow-water shoal facies, peter-out basinward (Figure 8.4C). The

latter feature is shown by the Brofiscin Oolite (SW Britain) which can be traced down the depositional slope into the subtidal facies of the Barry Harbour Limestone (Figure 8.3). The progressive basinward increase in the rate of subsidence (regional flexure) is thought to be a major factor in limiting the seaward extent of the progradational shoal facies (section 3.4.5).

Ramps can persist during periods of marked differential subsidence depending upon the nature of the sediment supply and the rates of subsidence. A plentiful supply of sediment smooths out any topographic expression created by the activity of the underlying tectonic hinge-lines or faults (Stage III, Figures 8.2 & 8.3). During the Dinantian, differential subsidence had a marked effect upon both the shallow water facies (e.g. Gully Oolite, Waters & Lawrence 1987) and the deep water (aphotic) facies (e.g. Waulsortian reefs, Miller & Grayson 1982; Strogen 1982) (Figure 8.2, Stage III). Without the blanketing effect of the *in situ* sediment supply in a wide range of environments (including the aphotic zone) it is considered less likely that the Dinantian ramps would have persisted for so long.

The longevity of a carbonate ramp is dependent upon a balance between the nature and the rate of supply of the sediment and relative rise in sea level. In SW Britain, North Wales and Derbyshire the ramp-to-shelf transition is thought to have been caused by a slowing in the rate of subsidence which enabled carbonate production to catch-up with sea level and prograde basinward (accretionary model) (Figure 8.2, Stage IV). Development of the shelf-edge in the Craven Basin and the Dublin Basin was as a result of the surfacing of fault scarps (tectonic model). Sedimentation was unable to keep pace with the rate of differential subsidence which caused the ramp-to-shelf transition.

8.4 Conclusions

1) To maintain a carbonate ramp requires sediment aggradation to be the dominant mode of sediment accumlation, rather than progradation.

2) The persistence of the Dinantian ramps of England, Ireland and Wales was mainly as a result of differential subsidence and a plentiful supply of sediment over a wide range of environments, including the aphotic zone.

3) Under certain conditions (i.e. balance between the nature and supply of sediment, and the relative rise in sea level) carbonate ramps are tenable both during a eustatic sea level rise and differential subsidence.

8.5 Summary

The Lower Carboniferous ('mid'-Courceyan to early Chadian) Black Rock Limestone ramp succession of SW Britain accumulated along the southern margin of the Welsh-Brabant Massif, during the early stage in the development of the SW European foreland basin. Two depositional cycles which culminate with the subaerial exposure of those sequences in a more landward setting are recognized.

The lower depositional cycle includes the Barry Harbour Limestone Formation which contains a variety of storm-related sedimentary structures including hummocky cross-stratification (Figure 8.3). Conformably overlying the Barry Harbour Limestone is the tidally influenced, cross-stratified Brofiscin Oolite Formation which locally displays evidence of subaerial exposure. These two formations record a distal to proximal, shallowing-upward trend that passes from beneath mean wave-base to above fairweather wave-base (Figure 8.3). The Barry Harbour Limestone and the Brofiscin Oolite record the first major basin-wide shallowing-upward phase, subsequent to the early Carboniferous transgression (Figure 8.3).

The upper depositional cycle of the Friars Point Limestone Formation includes the volcanics at Middle Hope, the Waulsortian facies at Castlemartin and Cannington Park, and is capped by the Portishead Paleosol Beds (near Bristol) (Figure 8.3). Above the basal transgressive sequence, the Friars Point Limestone consists of two distinct offshore ramp facies belts. The more proximal inner ramp facies belt was more strongly influenced by storm-related currents (Figure 8.3) and exhibits tubular tempestites (storm sediment-filled burrows). The finer-grained, outer ramp facies belt is extensively bioturbated and preserves few features indicative of deposition from storm-related currents (Figure 8.3). The effects and relative timing of differential subsidence was elucidated by using the well documented biostratigraphy to separate the succession into isochronous units. The onset of pronounced differential subsidence was signified by volcanic activity at Middle Hope (Weston-super-Mare) (Figure 8.3). The volcanics form a coarsening and shallowing-upward sequence which records the development of a localised, probably non-emergent, offshore-volcanic high. Recognition of a major eustatic sea level fall at the end of the Courceyan and during the early part of the Chadian is revealed by studying the decline of the Waulsortian reefs in an offshore ramp setting and evaluating the regional significance of the Portishead Paleosol Beds.

The Barry Harbour Limestone and the Brofiscin Oolite represents a classical shallowing-upward cycle during which time sediment supply was able to catch-up with sea level (no eustatic fall in sea level) (Figure 8.3). In contrast, the identification of a eustatic sea level fall between the deposition of the Friars Point Limestone and the overlying Gully Oolite/Sub-Oolite Bed (where developed) is more cryptic in nature. Evidence of subaerial exposure of the Black Rock Dolomite in the central ramp zone has only been locally preserved. Significantly, only one well

defined shallowing-upward sequence has been identified in the uppermost part of the Black Rock Limestone (Waters & Lawrence 1987).

This case study shows that the recognition of eustatic sea level changes requires a good understanding of basin development to separate the effects of subsidence and sediment supply from eustacy.

REFERENCES

Ahr, W. 1973. The carbonate ramp; an alternative to the shelf model. *Transactions of the Gulf Coast Association of Geologists, Twenty-Third Annual Convention*, 221-225.

Aigner, T. 1984. Dynamic stratigraphy of epicontinental carbonates, Upper Muschelkalk (M. Triassic) South-German Basin. *Neues Jb. Geol. Paläont. Abhandlungen*, 169, 127-159.

Aigner, T. 1985. Storm depositional systems: dynamic stratigraphy in modern and ancient shallow marine sequences. In: *Lecture notes in Earth Sciences* (Eds G.M. Friedman, H.J. Neugebauer & A. Seilacher) 1-174. Springer-Verlag (Berlin).

Aigner, T. & Reineck, H. -E. 1982. Proximality trends in modern storm sands from the Helgoland Bight (North Sea) and their implications for basin analysis. *Senckenbergiana Maritima*, 14, 183-215.

Allen, P.A. 1985. Hummocky cross-stratification is not produced purely under progressive gravity waves. *Nature*, 313, 562-564.

Anderton, R., Bridges, P.H., Leeder, M.R. & Sellwood, B.W. 1979. *A Dynamic Stratigraphy of the British Isles.* George Allen & Unwin.

Assereto, R.A.M. & Folk, R.L. 1976. Brick-like texture and radial rays in Triassic Pisolites of Lombardy, Italy: a clue to distinguish ancient aragonite pisolites. *Sedimentary Geology*, 16, 295-322.

Austin, R.L. 1973. Modifications of the British Avonian conodont zonation and a reappraisal of European Dinantian conodont zonation and correlation. *Extrait des Annales de la Societé Geologique de Belgique*, 96, 523-532.

Austin, R.L. & Davies, R.B. 1984. Problems of recognition and implications of Dinantian conodont biofacies in the British Isles. In: *Conodont Biofacies and Provincialism* (Ed. D.L. Clark). Special Paper Geological Society of America, 196, 195-228.

Bathurst, R.G.C. 1975. *Carbonate sediments and their diagenesis:* second enlarged edition. Elsevier, Amsterdam.

Bathurst, R.G.C. 1987. Diagenetically enhanced bedding in argillaceous platform limestones: stratified cementation and selective compaction. *Sedimentology*, 34, 749-778.

Beales, F.W. 1971. Cementation by white sparry dolomite. In: *Carbonate cements* (Ed. O.P. Bricker), 339-346. John Hopkins University Press, Baltimore, Maryland.

Berner, R.A. 1971. Diagenesis of iron minerals. In: *Principles of chemical sedimentology.* (Ed. R.A. Berner). International Series in Earth & Planetary Scieneces. McGraw-Hill.

Beus, S.S. 1984. Fossil associations in the High Tor Limestone (Lower Carboniferous) of South Wales. *Journal of Paleontology*, 58, 651-667.

Bhatt, J.J. 1973. Ca/Mg ratio classification of Main Limestones (Mississippian) in South Wales, U.K. *Sedimentary Geology*, 10, 225-231.

Bhatt, J.J. 1976. Geochemistry and petrology of the Main Limestone Series (Lower Carboniferous), South Wales, U.K. *Sedimentary Geology*, 15, 55-86.

Blyth Cain, J.D. 1968. Aspects of the depositional environment and palaeoecology of crinoidal limestones. *Scottish Journal Geology*, 4, 191-208.

Bott, M.P. 1967. Geophysical investigations of the northern Pennine basement rocks. *Proceedings of the Yorkshire Geological Society*, 36, 139-168.

Bott, M.P. 1987. Subsidence mechanisms of Carboniferous basins in northern England. In: *European Dinantian Environments* (Eds J. Miller, A.E. Adams & V.P. Wright), 21-32. Geological Journal Special Issue No. 12. John-Wiley (Chicester).

Boucot, A.J. 1975. Evolution and extinction rate controls. In: *Developments in Palaeontology and Stratigraphy 1*. Elsevier.

Bourgeois, J. 1980. A transgressive shelf sequence exhibiting hummocky cross-stratification. The Cape Sebastian Sandstone (Upper Cretaceous), southwestern Oregon. *Journal of Sedimentary Petrology*, 50, 681-702.

Brenchley, P.J. 1985. Storm influenced sandstone beds. *Modern Geology*, 9, 369-396.

Brenchley, P.J., Newall, G. & Stanistreet, I.G. 1979. A storm surge origin for sandstone beds in an epicontinental platform sequence, Ordovician, Norway. *Sedimentary Geology*, 33, 185-217.

Brett, C.E. 1983. Sedimentology, facies and depositional environments of the Rochester Shale (Silurian; Wenlockian) in western New York and Ontario. *Journal of Sedimentary Petrology*, 53, 947-971.

Bridges, P.H. & Chapman A.J. 1988. The anatomy of a deep water mud-mound complex to the southwest of the Dinantian platform in Derbyshire, UK. *Sedimentology*, 35, 139-162.

Brindley, G.W. & Brown, G. *Crystal structures of clay minerals and their x-ray identification*. Mineralogical Society of London, Monograph 5.

Broadhurst, F.M., Simpson, I.M. & Hardy, P.G. 1980. Seasonal sedimentation in the Upper Carboniferous of England. *Journal of Geology*, 88, 639-651.

Broadhurst, F.M. & Simpson, I.M. 1973. Bathymetry on a Carboniferous reef. *Lethaia*, 6, 367-381.

Burchette, T.P. 1987. Carbonate-barrier shorelines during the basal Carboniferous transgression: the Lower Limestone Shale Group, South Wales and Western England. In: *European Dinantian Environments* (Eds J. Miller A.E. Adams, and V.P. Wright), 239-263. Special Issue Geological Journal No. 12. John Wiley (Chichester).

Burchette, T.P., Wright, V.P. & Faulkner, T.J. *submitted.* Oolitic sandbody geometries and sequences, Mississippian of South West Britain: implications for petroleum exploration in carbonate ramp settings. *Sedimentary Geology.*

Butler, M. 1972. *Conodont faunas and stratigraphy of certain Tournaisian sections in the Bristol-Mendip area.* Unpublished thesis University of Bristol, England.

Butler, M. 1973. Lower Carboniferous conodont faunas from the Eastern Mendips, England. *Palaeontology*, 16, 477-517.

Calvet, F. & Tucker, M.E. 1988. Outer ramp cycles in the Upper Muschelkalk of the Catalan Basin, northeast Spain. *Sedimentary Geology*, 57, 185-198.

Carey, S.N. & Sigurdsson, H. 1980. The Roseau Ash: deep-sea tephra deposits from a major eruption on Dominica, Lesser Antilles Arc. *Journal Volcanology Geotherm. Res.*, 7, 67-86.

Channon, R.D. & Hamilton, D. 1976. Wave and tidal current sorting of shelf sediment southwest of England. *Sedimentology*, 23, 17-42.

Chatellier, J.Y. 1988. Carboniferous carbonate ramp, the Banff Formation, Alberta, Canada. *Bulletin des Centres de Recherches Exploration-Production, Elf-Aquitaine*, 12, 569-599.

Cherns, L. 1979. The environmental significance of *Lingula* in the Ludlow Series of the Welsh Borderland and Wales. *Lethaia*, 12, 35-46.

Cotter, E. 1966. Limestone diagenesis and dolomitization in Mississippian carbonate banks in Montana. *Journal of Sedimentary Petrology*, 36, 764-774.

Cox, K. G., Bell, J.D. & Pankhurst, R.J. 1979. *The interpretation of igneous rocks*, 408-414. George Allen & Unwin.

Craig, G.Y. 1952. A comparative study of the ecology and palaeoecology of Lingula. *Transactions of the Geological Society of London*, 124, 213-238.

Craig, M. 1957. Isotopic standards for carbon and oxygen and correction factors for mass spectrometric analysis of carbon dioxide. *Geochim. et Cosmochimica Acta*, 12, 133-149.

Cross, W., Iddings, J.P., Pirrson, L.V. & Washington, H.S. 1903. *Quantitative classification of igneous rocks.* University of Chicago Press.

Deines, P. 1970. Mass spectrometer correction factors for the determination of small isotopic composition variations of carbon and oxygen. *Int. Journal Mass Spectrometry Ion. Phys.*, 4, 283-295.

Devey, C.W. 1986. *Stratigraphy and geochemistry of the Deccan Trap lavas, Western India.* Unpublished D. Phil. thesis University of Oxford.

Dickson, J.A.D. 1965. A modified staining technique for carbonates in thin section. *Nature*, 205, 587.

Dickson, J.A.D. 1985. Diagenesis of shallow-marine carbonates. In: *Sedimentology: Recent Developments and Applied Aspects*, (Eds P.J. Brenchley & B.P.J. Williams) Geological Society Special Publication, 18, 173-189. Blackwells.

Dixey, F. & Sibly, T.F. 1918. The Carboniferous Limestone Series on the south-eastern margin of the S. Wales Coalfield. *Quarterly Journal of the Geological Society, London*, 73, 111-164.

Dixon, E.E.L. 1921. *The Geology of the South Wales Coalfield.* Part XIII. The country around Pembroke and Tenby. Memoir of the Geological Survey of Great Britain, Sheet 244, 245. H.M.S.O. (London).

Dixon, E.E.L. & Vaughan, A. 1911. The Carboniferous succession in Gower. *Quarterly Journal of the Geological Society of London*, 67, 477-571.

Dixon J. & Wright V.P. 1983. Burial diagenesis and crystal diminution. The origin of crystal diminution in some limestones from South Wales. *Sedimentology*, 30, 537-546.

Dodd, R., Carter, P., Fara, D., Feldman, H., Hill, J., Malvia, R., Maples, C., Petricca, A. & Thompson, T. 1987. Ramp Creek and Harrodsburg Limestones: a shallowing-upward sequence with storm-produced features in southern Indiana, U.S.A.. *Sedimentary Geology*, 52, 207-226.

Donato, J.A. 1988. Possible Variscan thrusting beneath the Somerton anticline, Somerset. *Journal of the Geological Society of London*, 145, 431-438.

Dott, R.H. Jr & Bourgeois, J. 1982. Hummocky stratification: significance of its variable bedding sequences. *Bulletin of the Geological Society America*, 93, 663-680.

Duff, B. 1980. The palaeomagnetism of Jersey volcanics and dykes, and the Lower Palaeozoic apparent polar wander path for Europe. *Geophys. J. R. Astr. Soc.*, 60, 355-375.

Duke, W.L. 1985. Hummocky cross-stratification, tropical hurricanes, and intense winter storms. *Sedimentology*, 32, 167-194.

Duke, W.L. 1987. Hummocky cross-stratification, tropical hurricanes, and intense winter storms: reply. *Sedimentology*, 34, 344-359.

Dunne, W.D. 1983. Tectonic evolution of SW Wales during the Upper Palaeozoic. *Journal of Geological Society of London*, 140, 257-265.

Eslinger, E. & Peavear, D. 1988. Clay minerals for petroleum geologists and engineers. *Society of Economic Paleontologists and Mineralogists* Short course notes, 22, 1-428.

Faber, P. & Riding, R. 1979. *Uraloporella* (microproblematicum) from the Middle Devonian of Eifel (West Germany). *Neues. Jb. Geol. Paläont. Mh., Stuttgart*, 1979, 139-146.

Faulkner, T.J. 1988. The Shipway Limestone of Gower: Sedimentation on a storm-dominated early Carboniferous ramp. *Geological Journal*, 23, 85-100.

Faulkner, T.J. 1989. The early Carboniferous (Courceyan) Middle Hope volcancis of Weston-super-Mare (near Bristol): Development and demise of an offshore volcanic high. *Proceedings of Geologists' Association*, 100, 93-106.

Floyd, P.A. 1982. Chemical variation in Hercynian basalts relative to plate tectonics. *Journal of Geological Society, London*, 139, 505-520.

Folk, R.L. & Assereto, R.A.M. 1976. Comparative fabrics of length-slow and length-fast calcite and calcitised aragonite in a Holocene speleothem, Carlsbad Caver, New Mexico. *Journal of Sedimentary Petrology*, 46, 486-496.

Gagan, M.K., Johnson, D.P., & Carter, R.M. 1988. The cyclone Winnifred storm bed, Central Great Barrier Reef shelf, Australia. *Journal of Sedimentary Petrology*, 58, 845-856.

Garven, G. 1985. The role of regional fluid flow in the genesis of the Pine Point deposit, western Canada sedimentary basin. *Economic Geology*, 80, 307-324.

Garven, G. & Freeze, R.A. 1984. Theoretical analysis of the role of groundwater flow in the genesis of stratabound ore deposits. *American Journal of Science*, 284, 1085-1124.

Gawthorpe, R.L. 1986. Sedimentation during carbonate ramp-to-slope evolution in a tectonically active area: Bowland Basin (Dinantian), Derbyshire, England. *Sedimentology*, 33, 185-206.

Gawthorpe, R.L. 1987. Burial dolomitization and porosity development in a mixed carbonate-clastic sequence: an examples from the Bowland Basin, northern England. *Sedimentology*, 34, 533-558.

Gayer, R. 1988. Variscan deformation of the South Wales coalfield - a foreland basin model. *Upper Palaeozoic basin evolution in South Wales.* Meeting of the geological Society of London (abstract). University College Cardiff (University of Wales).

George, T.N. 1970. *British Regional Geology: South Wales.* 3rd ed. H.M.S.O. London.

George, T.N. 1972. The classification of Avonian limestones. *Quarterly Journal of the Geological Society of London*, 128, 221-256.

George, T.N. 1974. The Cenozoic evolution of Wales. In: *The Upper Palaeozoic and Post-Palaeozoic rocks of Wales* (Ed. T.R. Owen) 85–115. University of Wales Press, Cardiff.

George, T.N. 1978. Eustasy and tectonics: Sedimentary rhythms and stratigraphical units in British Dinantian correlation. *Proceedings of the Yorkshire Geological Society*, 42, 229–262.

George, T.N., Johnson, G.A.L., Mitchell, M., Prentice, J.E., Ramsbottom, W.H.C., Sevastopulo, G. & Wilson, R.B. 1976. *A correlation of the Dinantian rocks of the British Isles.* Geol. Soc. London Special Report No. 7.

Ginsburg, R.N. & James, N.P. 1974. Holocene carbonate sediments of continental shelves. In: *The Geology of Continental Margins* (Eds C.A. Bank and C.L. Drake), 137–155. Springer-Verlag (Berlin).

Goldring, R. 1962. The Bathyal Lull: Upper Devonian and Lower Carboniferous sedimentation in the Variscan geosyncline. In: *Some aspects of the Variscan Fold Belt* (Ed. K. Coe) Manchester University Press, 75- 92.

Goldring, R. & Bridges, P. 1973. Sublittoral sheet sandstones. *Journal of Sedimentary Petrology*, 43, 736–747.

Grayson, R.F. & Oldham, L. 1987. A new structural framework for the northern British Dinantian as a basis for oil, gas and mineral exploration. In: *European Dinantian Environments* (Eds J. Miller, A.E. Adams & V.P. Wright), 33–59. Geological Journal Special Issue No. 12. John-Wiley (Chichester).

Green, G.W. & Welch, F.B.A. 1965. Geology of the country around Wells and Cheddar. *Memoir of the Geological Survey of Great Britain*, Sheet 280.

Greenwood, B. & Sherman, D.J. 1986. Hummocky cross-stratification in the surf zone: flow parameters and bedding genesis. *Sedimentology*, 33, 33–45.

Gregg, J.M. & Sibley, D.F. 1984. Epigenetic dolomitization and the origin of xenotopic dolomite texture. *Journal of Sedimentary Petrology*, 54, 908–931.

Gross, M.G. 1964. Variations in the O^{18}/O^{16} and C^{13}/C^{12} ratios of diagenetically altered limestones in the Bermuda Island. *Journal of Geology*, 72, 170–194.

Gutteridge, P. 1987. Dinantian sedimentation and the basement structure of the Derbyshire Dome. *Geological Journal*, 22, 25–41.

Hamblin, A.P. & Walker, R.G. 1979. Storm-dominated shallow marine deposits: the Fernie-Kootenay (Jurassic) transition, southern Rocky Mountains. *Canadian Journal of Earth Sciences*, 16, 1673–1690.

Hancock, P.L., Dunne, W.M. & Tringham, M.E. 1981. Variscan structures in southwest Wales. *Geologie en Mijnbouw*, 60, 81–88.

Handford, C.J. 1986. Facies and bedding sequences in shelf-storm-deposited carbonates-Fayettevile Shale and Pitkin Limestone (Mississippian), Arkanas. *Journal of Sedimentary Petrology*, 56, 123-137.

Hardie, L.A. 1987. Dolomitization: a critical view of some current views. *Journal of Sedimentary Petrology*, 57, 166-183.

Harms, J.C., Southard, J.B., Spearing, D.R. & Walker, R.G. 1975. Depositional environments as interpreted from primary sedimentary structures and stratified sequences. *Society of Economic Palaeontologists and Mineralogists*, Short Course, 2, 161.

Heckel, P.A. 1983. Diagenetic model for carbonate rocks in midcontinent Pennsylvanian eustatic cyclothems. *Journal of Sedimentary Petrology*, 53, 733-759.

Higgs, R. 1986. The 'South British Fault': 200km of Stephanian-early Permian dextral wrenching on an E-W fault through the Bristol Channel. Conference Abstract: *Controls of Upper Carboniferous Sedimentation, North-West Europe.* University of Keele.

Hird, K. 1986. *Petrography and geochemistry of some Carboniferous and Precambrian dolomites.* Unpublished Ph.D. thesis, University of Durham.

Hird, K. & Tucker, M.E. 1988. Contrasting diagenesis of two Carboniferous oolites from South Wales; a tale of climatic influence. *Sedimentology*, 35, 587-602.

Hird, K., Tucker, M.E. & Waters, R.A. 1987. Petrography, geochemistry and origin of Dinantian dolomites from South-east Wales. In: *European Dinantian Environments* (Eds J. Miller, A.E. Adams & V.P. Wright), 359-377. Geological Journal Special Issue No. 12. John-Wiley (Chichester).

Holder, M.T. & Leveridge, B.E. 1986. Correlation of the Rhenohercynian Variscides. *Journal of the Geological Society of London*, 143, 141-147.

Holder, M.T. & Leveridge, B.E. 1987. Discussion on the correlation of Rhenohercynian Variscides: reply. *Journal of the Geological Society of London*, 144, 353-354.

Hudson, J.D. 1982. Pyrite in ammonite-bearing shales from the Jurassic of England and Germany. *Sedimentology*, 29, 639-667.

Hunter, R.E. & Clifton, H.E. 1982. Cyclic deposits and hummocky cross-stratification of probable storm origin in Upper Cretaceous area, southwestern Oregon. *Journal of Sedimentary Petrology*, 52, 127-146.

Jacobs, L., Swennen, R., Van Orsmael, J., Notebaert, L., & Viaene, W. 1982. Occurences of pseudomorphs after evaporitic minerals in the Dinantian carbonate rocks of the eastern part of Belgium. *Bulletin de la Societé belge de Geologie*, 2, 105-123.

James, N.P. 1983. Reefs. In: *Carbonate Depositional Environments* (Eds P.A. Scholle, D.G. Bebout & C.H. Moore), 345-462. America Association of Petroleum Geologists, Memoir, 33.

Jeffreys, D.H. 1979. *Sedimentology of the Dinantian volcaniclastic and carbonate rocks of Middle Hope and Spring Cove, Weston-super-Mare.* Unpublished MSc. thesis, University of Reading.

Jeffreys, D.H. & Aigner, T. 1982. Storm sedimentation in the Carboniferous Limestones near Weston-super-Mare (Dinantian, SW-England). In: *Cyclic & Event Stratification* (Ed. A. Seilacher) 240-247. Springer-Verlag (Berlin).

Jodry, R.L. 1969. Growth and dolomitization of Silurian Reefs. St. Clair County, Michigan. *Bulletin of the American Association of Petroleum Geologists*, 53, 957-981.

Johnson, G.A.L. 1967. Basement control of Carboniferous sedimentation in northern England. *Proceedings of the Yorkshire geological Society*, 36, 175-194.

Johnson, G.A.L. 1982. Geographical changes in Britain during the Carboniferous period. *Proceedings of the Yorkshire Geological Society*, 44, 181-212.

Johnson, G.A.L. 1984. Precision in Dinantian geography. *European Dinantian Environments, First Meeting 1984, Abstracts*, 64-65. Department of Earth Sciences, Open University, Milton Keynes, U.K.

Jones, D.G. 1974. The Namurian Series in South Wales. In: *The Upper Palaeozic Rocks of Wales*, (Ed. T.R. Owen), 117-132. University of Wales Press, Cardiff.

Jones, G.L., Somerville, I.D. & Strogen, P. 1988. The Lower Carboniferous (Dinantian) of the Swords area: Sedimentation and tectonics in the Dublin Basin, Ireland. *Geological Journal*, 23, 221-248.

Junghanss, T., Goldring, R. & Simpson, J. 1984. The Dinantian between Rhosilli and Port Eynon (Gower, South Wales). In: *European Dinantian Environments, First Meeting*, 1984, *Abstracts*, 61-63. Department of Earth Sciences, Open University, U.K.

Kasig, W. 1980. Dinantian carbonates in the Aachen region. *F.R.G. Med. Rijka Geol. Dienst.*, 32-6, 44-52.

Kazmierczak, J. & Goldring, R. 1978. Subtidal flat-pebble conglomerate from the Upper Devonian of Poland: a multiprovenant high energy product. *Geological Magazine*, 115, 359-366.

Kelling, G. 1988. Silesian sedimentation and tectonics in the South Wales Basin: a brief review. In: *Sedimentation in a Synorogenic Basin Complex: the Upper Carboniferous of Northwest Europe* (Eds B.M. Besly and G. Kelling), 38-42. Blackie, Glasgow and London.

Kelling, G. & Williams, B.P.J. 1966. Deformation structures of sedimentary origin in the Lower Limestone Shales (basal Carboniferous) of South Pembrokeshire, Wales. *Journal of Sedimentary Petrology*, 36, 927-939.

Kendall, A.C. 1985. Radiaxial fibrous calcites: a reappraisal. In: *Carbonate cements* (Eds. N. Schneidermann and P.M. Harris). *Special publication of Society of Economic Paleontologists and Mineralogists*, 36, 59-77.

Kendall, A.C. & Broughton, P.L. 1978. Origin of fabrics in speleothems composed of columnar calcite crystals. *Journal of Sedimentary Petrology*, 48, 519-538.

Kendall, C.G. & Schlager W. 1981. Carbonates and relative changes in sea level. *Marine Geology*, 44, 181-212.

Kent, P.E. 1975. Review of North Sea Basin development. *Journal of the Geological Society of London*, 131, 435-468.

Klein, G.DEV. & Marsaglia, K.M. 1987. Hummocky cross-stratification, tropical hurricanes, and intense winter storms: discussion. *Sedimentology*, 34, 333-359.

Kobluk K.R. & Risk, M.L. 1977. Micritization and carbonate-grain binding by endolithic algae. *Bulletin American Association Petroleum Geologists*, 61, 1069-1081.

Kohout, F.A., Henry, H.R. & Banks, J.E. 1977. Hydrogeology related to geothermal conditions of the Floridan Plateau. In: *Geothermal Nature of the Floridan Plateau* (Eds K.L. Smith & G.M. Griffin), 1-34. Fla. Dept. Resour. Bur. Geol. Spec. Publ.

Komar, P.D., Nuedeck, R.H. & Kulm, L.D. 1972. Observations and significance of deep water oscillatory ripple marks on the Oregon continental shelf. In: *Shelf Sediment Transport, Process and Pattern*, 601-620. (Eds D.J.P. Swift, B.B. Duane & O.H. Pilkey) Dowden, Hutchinson and Ross, Pennsylvania.

Land, S.L. 1980. The isotopes and trace element geochemistry of dolomite: the state of the art. In: *Concepts and Models of Dolomitization* (Eds. D.H. Zenger, J.B. Dunham, & R.L. Ethington). *SEPM Special Publication* No. 28, Tulsa, Oklahoma, USA, 87-110.

Leckie, D.A. 1988. Wave-formed, coarse-grained ripples and their relationship to hummocky cross-stratification. *Journal of Sedimentary Petrology*, 58, 607-622.

Leckie, D.A. & Walker, R.G. 1982. Storm- and tide-dominated shorelines in Cretaceous Moosebar -lower Gates interval- outcrop equivalents of Deep Basin gas trap in western Canada. *American Association of Petroleum Geologists, Bulletin*, 66, 138-157.

Leeder, M.R. 1974. Sedimentary facies and the origins of basin subsidence along the northern margin of the supposed Hercynian ocean. *Tectonophysics*, 36, 167-179.

Leeder, M.R. 1976. Sedimentary facies and origins of basin subsidence along the northern margin of the supposed Hercynian ocean. *Tectonophysics*, 36, 167-179.

Leeder, M.R. 1982. Upper Palaeozoic basins of the British Isles-Caledonide inheritance versus Hercynian plate margin processes. *Journal of Geological Society, London*, 139, 479-491.

Leeder, M.R. 1987. Tectonic and palaeogeographic models for Lower Carbonifeous Europe. In: *European Dinantian Environments* (Eds J. Miller, A.E. Adams & V.P. Wright), 1-20. Geological Journal Special Issue No. 12. John-Wiley (Chichester).

Lees, A. 1964. The structure and origin of the Waulsortian (Lower Carboniferous) 'reefs' of west-central Eire. *Philosphical Transactions of the Royal Society of London*, B247, 483-531.

Lees, A. 1982. The paleoenvironmental setting and distribution of the Waulsortian facies of Belgium and southern Britain. In: *Symposium on the Environmental Setting and Distribution of the Waulsortian Facies*, 1-16 (Eds K. Bolton, H.R. Lane and D.V. LeMone), *El Paso Geological Society and University of Texas at El Paso*.

Lees, A., Hallet, V. & Hibo, D. 1985. Facies variation in Waulsortian buildups I. A model from Belgium. *Geological Journal*, 20, 133-158.

Lees, A. & Hennebert, M. 1982. Carbonate rocks of the Knap Farm Borehole at Cannington Park, Somerset. *Report of the Institute of Geological Sciences*, 85/5, 18-36.

Lees, A. & Miller, J. 1985. Facies variation in Waulsortian buildups II. Mid-Dinantian buildups from Europe and North America. *Geological Journal*, 20, 159-180.

Lees, A., Noel, B. & Bouw, P. 1977. The Waulsortian 'reefs' of Belgium: a progress report. *Memoir of the Institute of Geology Universite Louvain*, 29, 289-315.

Lippmann, F. 1973. Sedimentary Carbonate Minerals. New York, Springer-Verlag, 219.

Lovering, T.S. 1969. The origin and hydrothermal and low temperature dolomite. *Economic Geology*, 64, 743-754.

MacCarthy, I.A.J. 1987. Transgressive facies in the South Munster Basin, Ireland. *Sedimentology*, 34, 389-422.

MacCarthy, I.A.J. & Gardiner, P.R.R. 1987. Dinantian cyclicity: a case history from the Munster Basin of southern Ireland. In: *European Dinantian Environments* (eds J. Miller, A.E. Adams and V.P. Wright), 199-237. Geological Journal Special Issue no. 12. John Wiley (Chichester).

Macdonald, R., Gass, K.N., Thorpe, R.S. & Gass, I.G. 1984. Geochemistry and petrogenesis of the Derbyshire Carboniferous basalts. *Journal of Geological Society, London*, 141, 147-159.

Mac-Hargue, T.R. & Price, R.C. 1982. Dolomite from clay in argillaceous marine associated carbonates. *Journal of Sedimentary Petrology*, 52, 873-886.

Machel, H.G. 1984. Facies and dolomitization of the Upper Devonian Nisku formation in the Brazeau, Pembina, and Bigoray areas, Alberta, Canada. In: *Carbonates in Subsurface and Outcrop.* Canadian Society Petroleum Geologists Core Conference, 1984, 191-224.

Machel, H.G. & Mountjoy, E.W. 1986. Chemistry and environments of dolomitization- a reappraisal. *Earth-Science Reviews*, 23, 175-222.

Markello, J.R. & Read, J.F. 1981. Carbonate ramp-to-deeper shale shelf transitions of an Upper Cambrian intrashelf basin, Nolichucky Formation, Southwest Virginia Appalachians. *Sedimentology*, 28, 573-597.

Mattes, B.W. & Mountjoy, F.W. 1980. Burial dolomitization of the Upper Devonian Miette buildup, Jasper National Park, Alberta. In: *Concepts and Models of Dolomitization* (Eds. D.H. Zenger, J.B. Dunham, & R.L. Ethington), 259-297. Society of Economic Paleontologists and Mineralogists, Special Publication 28, Tulsa, Oklahoma, USA.

McRea, J.M. 1950. On the isotopic chemistry of carbonates and a palaeotemperature scale. *Journal of Chemistry & Physics*, 18, 849-857.

Milekovsky, S.A. 1971. Types of larval development in marine bottom invertebrates, their distribution and ecological significance: a re-evaluation. *Marine Biology*, 10, 193-213.

Miller, J. 1986. Facies relationships and diagenesis in Waulsortian mudmounds from the Lower Carboniferous of Ireland and N. England. In: *Reef Diagenesis* (Eds J.H. Schroeder & B.H. Purser) 311-335. Springer-Verlag (Berlin)

Miller, J. & Grayson, R.F. 1972. Origin and structure of the Lower Viséan 'reef' limestones near Clitheroe, Lancashire. *Proceedings of the Yorkshire Geological Society*, 38, 607-638.

Miller, J. & Grayson, R.F. 1982. The regional context of Waulsortian facies in Northern England. In: *Symposium of the palaeoenvironmental setting and distribution of the Waulsortian facies* (Eds K. Bolton, H.R. Lane & D.V. LeMone) 17-33. El Paso Geological Society and University of Texas, El Paso.

Mitchell, M. 1971. Annual report of Institute of Geological Sciences for 1970. 97-98.

Mitchell, M. 1972. The base of the Viséan in south-west and north-west England. *Proceedings Yorkshire Geological Society*, 39, 151-160.

Mitchell, M. 1980. The distribution of Tournaisian and early Viséan (Carboniferous) coral faunas from the Bristol and South Wales areas of Britain. *Acta Palaeontologica Polonica*, 25, 577-585.

Mitchell, M. & Green, G.W. 1965. Appendix I. The faunal succession in the Carboniferous Limestone of Burrington Combe. In: *Geology of the the country around Wells and Cheddar.* (Eds G.W. Green & F.B.A. Welch). Memoir of Geological Survey, Great Britain.

Mitchell, M., Reynolds, M.J., Laloux, M. & Owens, B. 1982. Biostratigraphy of the Knap Farm Borehole at Cannington Park, Somerset. *Report for the Institute of Geological Sciences*, 82/5, 8-17.

Mitchell, M., Strank, A.R.E., Thornbury, B.M. & Sevastopulo. 1986. The distribution of platform conodonts, corals and foraminifera from the Black Rock Limestone (late Tournaisian and early Viséan) of Tears Point, Gower, South Wales. *Proceedings of the Yorkshire Geological Society*, 46, 11-14.

Morgan, C.L. & Reynolds, S.H. 1904. The igneous rocks associated with the Carboniferous Limestone of the Bristol district. *Quarterly Journal Geological Society of London*, 69, 137-157.

Morton, R.A. 1981. Formation of storm deposits by wind-forced currents in the Gulf of Mexico and the North Sea. In: *Holocene Marine Sedimentation in the North Sea Basin* (Eds S.D. Nio, R.T.E. Shuttenhelm & Tj.C.E. Van Weering). *International Association of Sedimentologists Special Publication*, 5, 385-396.

Murphy, F.X. 1988. Facies variations within the Waulsortian Limestone Formation of the Dungarvan Syncline, southern Ireland. *Proceedings of the Geologists' Association*, 99, 205-219.

Murray, J.W. & Wright, C.A. 1971. The Carboniferous Limestone of Chipping Sodbury and Wick, Gloucestershire. *Geological Journal*, 7, 255-270.

Nelson, C.H. 1982. Modern shallow water graded sand layers from storm surges, Bering Shelf: a mimic of Bouma sequences and turbidite systems. *Journal of Sedimentary Petrology*, 52, 537-545.

Nolan, S.C. 1987. *The Carboniferous geology of the Dublin area.* Unpublished Ph.D. Thesis, University of Dublin.

Nottvedt, A. & Kreisa, R.D. 1987. Model for the combined-flow origin of hummocky cross-stratification. *Geology*, 15, 357-361.

Paine, R.T. 1970. The sediment occupied by Recent lingulid brachiopods and some palaeoecological implications. *Palaeogeography, Palaeoclimatology, Palaeoecology*, 7, 21-31.

Pearce, J.A. 1983. Role of the sub-continental lithosphere in magma genesis at active continental margins. In: *Continental basalts and mantle xenoliths* (Eds C.J. Hawkesworth & M.J. Norry), 230-249. Shiva Publishing, Nantwich.

Pearce, J., Alabaster, T., Shelton, A.W. & Searle, M.P. 1981. The Oman ophiolite as a Cretaceous arc-basin complex: evidence and implications. *Philosophical Transactions of the Royal Society London*, A300, 299-317.

Pearce, J.A. & Cann, J.R. 1973. Tectonic setting of basic volcanic rocks determined using trace element analyses. *Earth & Planetary Science Letters*, 19, 290-300.

Philcox, M.E. 1971. A Waulsortian bryozoan reef ('cumulative biostrome') and its off-reef equivalents, Ballybeg, Ireland. Compt. Rend. 6e Congr. Int. Strat. Geol. Carbonif. Sheffield 1967 4, 1359-1372.

Potts, P.J. 1987. *A handbook of silicate rock analysis.* Blackie (London & Glasgow).

Pratt, B.R. 1982. Stromatolitic framework of carbonate mud-mounds. *Journal of Sedimentary Petrology*, 52, 1203-1227.

de Raaf, J.F.M., Boersma, J.R. & van Gelder, A. 1977. Wave-generated structures from a shallow marine succession, Lower Carboniferous County Cork, Ireland. *Sedimentology*, 24, 451-483.

Radke, B.M. & Mathis, R.L. 1980. On the formation and occurrence of saddle dolomite. *Journal of Sedimentary Petrology*, 50, 1149-1168.

Ramsay, A.T. 1987. Depositional environments of Dinantian limestones in Gower, South Wales. In: *European Dinantian Environments* (Eds J. Miller, A.E. Adams & V.P. Wright) 265-308. Special Issue of the Geological Society No. 12. Wiley.

Ramsbottom, W.H.C. 1973. Transgressions and regressions in the Dinantian: a new synthesis of British Dinantian stratigraphy. *Proceedings of the Yorkshire Geological Society*, 39, 567-607.

Ramsbottom, W.H.C. 1977. Major cycles (Mesothems) in the Namurian. *Proceedings of Yorkshire Geological Society*, 41, 261-291

Ramsbottom, W.H.C. 1978. Carboniferous. In: *The Ecology of Fossils* (Ed W.S. McKerrow), 146-183. Duckworth.

Ramsbottom, W.H.C. 1979. Rates of transgression and regression in the Carboniferous of NW Europe. *Journal of the Geological Society of London*, 136, 147-153.

Ramsbottom, W.H.C. 1984. Developments from faunal studies in the Carboniferous of Wales. *Proceedings of the Geologists' Association*, 95, 365-371.

Ramsbottom, W.H.C. & Mitchell, M. 1980. The recognition and division of the Tournaisian Series in Britain. *Journal of the geological Society of London*, 137, 61-63.

Rankin, A.H. & Criddle A.J. 1984. Mineralizing fluids and metastable low-temperature inclusion brines at Llanharry iron deposit, South Wales. *Transactions of Institution Mining and Metallurgy* (Sect. B: Appl. earth sciences), 94, B126-B132.

Raven, M.R. 1983. *The diagenesis of the Oolite Group between Blaen Onnen and Pwll Du, Lower Carboniferous*, South Wales. Unpublished Ph.D. thesis, University of Nottingham, Great Britain.

Raymond, A., Parker, W.C. & Parrish, J.T. 1985. Phytogeography and paleoclimate of the Early Carboniferous. In: *Geological Factors and the Evolution of Plants* (Ed. B.H. Tiffney), 169-222. Yale University Press New Haven and London.

Read, J.F. 1982. Carbonate platforms of passive (extensional) continental margins: types, characteristics, and evolution. *Tectonophysics*, 81, 195-212.

Read, J.F. 1985. Carbonate platform facies models. *American Association of Petroleum Geologists, Bulletin*, 69, 1-21.

Reading, H.G. 1973. The tectonic environment of Southwest England. *Proceeding Geologist's Association* 84, 239-242.

Reineck, H. -E. & Singh, I.B. 1972. Genesis of laminated sand and graded rhythmites in storm-sand layers of shelf mud. *Sedimentology*, 18, 123-128.

Reynolds, R.C. 1984. Interstratified clay minerals. In: *Crystal structures of clay minerals and their X-ray identification*, 249-304 (Eds G.W. Brindley and G. Brown). Mineralogical Society of London.

Rhoads, D.C. 1967. Biogenic reworking of intertidal and subtidal sediments in Barnstable Harbor and Buzzards Bay, Massachusetts. *Journal of Geology*, 75, 461-476.

Rhoads, D.C. & Stanley, D.J. 1965. Biogenic graded bedding. *Journal of Sedimentary Petrology*, 35, 956-963.

Rhodes, F.H.T., Austin, R.L. & Druce, E.C. 1969. British Avonian (Carboniferous) conodont faunas, and their value in local and intercontinental correlation. *Bulletin of the Bristish Museum (Natural History) Geology*, Supplement 5.

Riding, R. & Jansa, L.F. 1974. *Uraloporella* Korde in the Devonian of Alberta. *Canadian Journal of Earch Sciences*, 11, 1414-1426.

Riding, R. & Jansa, L.F. 1976. Devonian occurrence of *Uraloporella* (?foraminifer) in the Canning Basin, Western Australia. *Journal of Paleontology*, 50, 805-807.

Riding, R. & Wright, V.P. 1981. Palaeosols and tidal-flat/ lagoon sequences on a Carboniferous carbonate shelf: sedimentary associations of triple disconformities. *Journal of Sedimentary Petrology*, 51, 1323-1339.

Robinson, D. & Wright, V.P. 1987. Ordered illite-smectite and kaolinite-smectite: pedogenic minerals in a Lower Carboniferous paleosol sequence, South Wales. *Clay minerals*, 22, 109-118.

Ross, C.A. & Ross, J.P. 1985. Late Paleozoic depositional sequences are synchronous and worldwide. *Geology*, 13, 194-197.

Ross, C.A. & Ross, J.P. 1987. Late Paleozoic sea levels and depositional sequences. *Cushman Foundation for Foraminiferal Research, Special Publication*, 24, 137-149.

Rowley, D.B., Raymond, A., Parish, J.T., Lottes, A.L., Scotese, C.R. & Ziegler, A.M. 1985. Carboniferous palaeogeographic, and paleoclimatic reconstructions. *International Journal of Coal Geology*, 5, 7-42.

Schofield, K. & Adams, A.E. 1985. Stratigraphy and depositional environments of the Woo Dale Limestones Formation (Dinantian), Derbyshire. *Proceedings of the Yorkshire Geological Society*, 45, 225-233.

Schofield, K. & Adams, A.E. 1985. Stratigraphy and depositional environments of the Woo Dale Limestones Formation (Dinantian), Derbyshire. *Proceedings of the Yorkshire Geological Society*, 45, 225-233.

Scotesce, C.R., Bambach, R.K., Banton, C., Van Der Voo, R. & Ziegler, A.M. 1979. Palaeozoic base maps. *Journal of Geology*, 87, 217-277.

Searl, A. 1988. Pedogenic dolomites from the Oolite Group (Lower Carboniferous) South Wales. *Geological Journal*, 23, 157-169.

Searl, A. 1989. Pedogenic columnar calcites from the Oolite Group (Lower Carboniferous), South Wales. *Sedimentary Geology*, 62, 47-58.

Selwood, E.B. & Thomas, J.M. 1987. Dinantian sedimentation in Southwest England. In: *European Dinantian Environments* (Eds J. Miller, A.E. Adams and V.P. Wright), 189-198. Geological Journal Special Issue No. 12. John Wiley (Chichester).

Sevastopulo, G.D. 1982. The age and depositional setting of the Waulsortian limestones in Ireland. In: *Symposium on the Paleoenvironmental Setting and Distribution of the Waulsortian Facies* (Eds K.R. Bolton, R.H. Lane, & D.V. LeMone) 65-79. El Paso Geological Society and University of Texas at El Paso.

Sevastopulo, G.D. & Nudds, J.R. 1987. Courceyan (Early Dinantian) biostratigraphy of Britain and Ireland: coral and conodont zones compared. *Cour. Forsch. -Inst. Senckenberg*, 98, 39-46.

Shinn, E.A., Lloyd, R.M. and Ginsburg, R.M. 1969. Anatomy of a modern carbonate tidal flat, Andros Island, Bahamas. *Journal of Sedimentary Petrology*, 39, 1202-1228.

Sibley, D.F. & Gregg, J.M. 1987. Classification of dolomite rock textures. *Journal of Sedimentary Petrology*, 57, 967-975.

Sibly, T.F. 1905. The Carboniferous Limestone of the Weston-super-Mare district (Somerset). *Quarterly Journal of Geological Society of London*, 69, 548-563.

Simms, M. 1984. Dolomitization by groundwater-flow systems in carbonate platforms. *Transactions of Gulf Coast Association Geological Society*, 34, 411-420.

Simpson, J. 1985. Stylolite-controlled layering in an homogeneous limestone pseudo-bedding produced by burial diagenesis. *Sedimentology*, 32, 495-505.

Simpson, J. 1987. Mud-dominated storm deposits from a Lower Carboniferous ramp. *Geological Journal*, 22, 191-206.

Smith, A.G. 1981. Phanerozoic Equal Area Maps. *Geol. Rundsch.*, 70, 91-127.

Smith, A.G., Briden, J.C. & Drewry, G.E. 1973. Phanerozoic World Maps. In: *Organsims and Continents through Time* 1.42 (Ed. N.F. Hughes). Palaeontological Assocation, London.

Soegaard, K. & Eriksson, K. 1985. Evidence of tide, storm, and wave interaction on a Precambrian siliciclastic shelf: the 1,700 m.y. Ortega Group, New Mexico. *Journal of Sedimentary Petrology*, 55, 672-684.

Somerville, I.D. 1979. Minor cyclicity in late Asbian limestones in the Llangollen district of North Wales. *Proceedings of the Yorkshire Geological Society*, 42, 317-341.

Somerville, I.D. & Jones, G.L. 1985. The Courceyan stratigraphy of the Pallaskenry borehole, County Limerick, Ireland. *Geological Journal*, 20, 377-400.

Somerville, I.D., Strank, A.R.E. & Welsh, A. 1989. Chadian faunas and flora from Dyserth: Depositional environments and palaeogeographic setting of Viséan strata in Northeast Wales. *Geological Journal*, 24, 49-66.

Speedyman, D.L. 1977. Volcanic rocks of the Bristol region. In: *Geological excursions in the Bristol district* (Ed. R.J.G. Savage), 47-54. University of Bristol press.

Starkey, H.C., Blackmon, P.D. & Hauff, P.L. 1984. The routine mineralogical analysis of clay-bearing samples. *Bulletin of the US Geological Survey.*

Strogen, P. 1988. The Carboniferous lithostratigraphy of southeast County Limerick, Ireland and, the origin of the Shannon Trough. *Geological Journal*, 23, 121-137.

Sullivan, R. 1960. *The Mid-Dinantian stratigraphy of a portion of central Pembrokeshire.* Unpublished Ph.D. thesis University of Glasgow, Great Britain.

Sullivan, R. 1965. The Mid-Dinantian stratigraphy of a portion of central Pembrokeshire. *Proceedings of the Geologists' Association London*, 76, 283-299.

Swennen, R., Boonen, P. & Viaene, W. 1982. Stratigraphy and lithogeochemistry of the Walhorn section (lower Viséan; Vesder Basin, E.-Belgium) and its implications. *Bulletin de la Societé belge de Geologie*, 4, 239-258.

Swennen, R., Viaene, W., Jacobs, L. & Van Orsmael, J. 1981. Occurrence of calcite pseudomorphs after gypsum in the Lower Carboniferous of the Vesder region (Belgium). *Bulletin de la Societé belge de Geologie*, 3, 231-247.

Swift, D.J.P., Figueiredo, A.G. (Jr), Freeland, G.L. & Oertel, G.F. 1983. Hummocky cross-stratification and megaripples a geological double standard. *Journal of Sedimentary Petrology*, 53, 1295-1317.

Swift, D.J.P., Hudelson, P.M., Brenner, R.L. & Thompson, P. 1987. Shelf construction in a foreland basin: storm beds, sandbodies, and shelf-slope depositional sequences in the Upper Cretaceous Mesarerde Group, Brook Cliffs, Utah. *Sedimentology*, 34, 423-457.

Swift, D.J.P. & Nummedal, D. 1987. Hummocky cross-stratification, tropical hurricanes, and intense winter storms: discussion. *Sedimentology*, 34, 338-344.

Tertian, R. & Claisse, F. 1982. *Principles of quantitative X-ray fluorescence analysis*. Haydon (London).

Thomas, L.P. 1974. The Westphalian (coal measures) in South Wales. In: *The Upper Palaeozoic and Post-Palaeozoic Rocks of Wales*, (Ed. T.R. Owen), 133-160. University of Wales Press, Cardiff.

Tucker, M.E. 1985. Shallow marine carbonate facies and facies models. In *Sedimentology: Recent Developments and Applied Aspects* (ed. P.J. Brenchley & B.P.J. Williams) 147-169. Geological Society of London, Special Publication no. 18.

Tudhope, A.W. & Scoffin, T.P. 1984. The effects of *Callianassa* bioturbation on the preservation of carbonate grains in Davies Reef Lagoon, Great Barrier Reef, Australia. *Journal Sedimentary Petrology*, 54, 1091-1096.

Turner, P. & Tarling, D.H. 1975. Implications of new palaeomagnetic results from the Carbonifeus System of Britain. *Journal of Geological Society of London*, 131, 469-488.

Upton B.G.J. 1982. Carboniferous to Permian volcanism in the stable foreland. In: *Igneous rocks of the British Isles* (Ed. D.S. Sutherland). Wiley.

Usdowski, H.E. 1968. The formation of dolomite in sediments. In: *Recent Developments in Carbonate Sedimentology in Central Europe* (Ed. G. Miller & G.M. Friedman) 21-32. Springer-Verlag, Berlin.

Vai, G.B. & Ricci-Lucchi, F. 1977. Algal crusts autochonous and clastic gypsum in a cannibalistic evaporite basin: a case history from the Messinian of the Northern Apennines. *Sedimentology*, 24, 211-244.

Van Der Zwan, C.J., Bouleter, M.C. & Hubbard, R.N.L.B. 1985. Climatic change during the Lower Carboniferous in Euramerica, based on multivariate statistical analysis of palynological data. *Palaeogeography, Palaeoclimatology, Palaeoecology*, 52, 1-20.

Varker, W.L. & Sevastopulo, G.D. 1985. The Carboniferous System: Part 1 - Conodonts of the Dinantian subsystem from great Britain and Ireland. In: *The stratigraphical index of conodonts* (Eds A.C. Higgins and R.L. Austin) 167-209. Cardiff: Ellis Horwood Ltd.

Vaughan, A. 1903. Notes on the corals and brachiopods obtained from the Avon section and preserved in the Stoddart Collection. *Proceedings of the Bristol Naturalists' Society.* (New Series), 10, 90-134.

Vaughan, A. 1905. Palaeontological sequence in the Carboniferous Limestone of the Bristol area. *Quarterly Journal of the Geological Society of London*, 61, 181-307.

Walkden, G.M. 1974. Paleokarstic surfaces in the Upper Viséan (Carboniferous) limestones of the Derbyshire Block, England. *Journal of Sedimentary Petrology*, 44, 1232-1247.

Walkden, G.M. 1987. Sedimentary and diagenetic styles in late Dinantian carbonates of Britain. In: *European Dinantian Environments* (eds J. Miller, A.E. Adams and V.P. Wright), 131-155. Geological Journal Special Issue no. 12. John Wiley (Chichester).

Walker, R.G., Duke, W.L. & Leckie, D.A. 1983. Hummocky stratification significance of its bedding sequence: discussion and reply. *Bulletin of the Geological Society of America*, 94, 1245-1251.

Wanless, H.R. 1979. Limestone response to stress: pressure-solution and dolomitization. *Journal of Sedimentary Petrology*, 49, 437-462.

Wanless, H.R., Lenore, P.T, & Tyrrell, K.M. 1988. Production of subtidal tubular and surficial tempestites by hurricane Kate, Caicos Platform, British West Indies. *Journal of Sedimentary Petrology*, 58, 739-750.

Waters, R.A. 1984. Some aspects of the Black Rock Limestone and Gully Oolite in the Eastern Vale of Glamorgan. *Proceedings of the Geologist's Association*, 95, 391-392.

Waters, R.A. & Lawrence, D.J.D. 1987. Geology of the South Wales Coalfield, Part III, the country around Cardiff. 3rd edition. *Memoir Bristish Geological Survey*, Sheet 263 (England and Wales).

Weedon, M.J. 1988. *The analysis of a peritidal lithosome: the Lower Carboniferous Clifton Down Mudstone and correlative Chadian/Arundian units.* Unpublished MSc thesis University of Bristol, UK.

Weimer, R.J., Howard, J.D. & Lindsay, D.R. 1982. Tidal flats. In: Sandstone Depositional Evironments (Eds by P.A. Scholle & D. Spearing). *Memoir of the American Association of Petroleum Geologists*, 31, 191-245.

Whittaker, A. & Green, G.W. 1983. Geology of the country around Weston-super-Mare. *Memoir of the Geological Survey of Great Britain*, Sheet 279 with parts of 263 and 295.

Whittaker, A. & Scrivener, R.C. 1982. The Knap Farm Borehole at Cannington Park, Somerset. *Report of Institute of Geological Sciences*, No. 82/5. 1-7.

Williams, G.D. & Chapman, T.J. 1986. The Bristol-Mendip foreland thrust belt. *Journal of the Geological Society of London*, 143, 63-73.

Wilson, D., Davies, J.R., Smith, M. & Waters, R.A. 1988. Structural controls on Upper Palaeozoic sedimentation in south-east Wales. *Journal of the Geological Society, London*, 145, 901-914.

Wilson, J.L. 1975. *Carbonate Facies in Geologic History.* Springer (New York).

Wilson, J.L. & Jordan, C. 1983. Middle shelf environment. In: *Carbonate depositional environments* (Eds P.A. Scholle, D.G. Bebout & C.H. Moore), 298-343. American Association of Petroleum Geologists, Memoir 33.

Woodhead, J.D. 1987. *Geochemistry of Mariana Island lavas.* Unpublished D. Phil. thesis University of Oxford.

Wright, V.P. 1982a. *Uraloporella* Korde from the Lower Carboniferous of South Wales. *Bulletin British Natural History Museum (Geology)*, 36, 151-155.

Wright, V.P. 1982b. Calcrete palaeosols from the Lower Carboniferous of South Wales. *Sedimentary Geology*, 52, 1-33.

Wright, V.P. 1982c. Omission surfaces the Lower Carboniferous of South Wales. *Neues fur Geol. und Palaeont., Monatshefte* 1982, 619-628.

Wright, V.P. 1984a. Facies patterns in the early Carboniferous of South West Britain. *European Dinantian Environments, First Meeting* 1984, *Abstracts*, 88-91. Department of Earth Sciences, Open University, Milton Keynes, U.K.

Wright, V.P. 1984b. Peritidal carbonate facies models: A review. *Geological Journal*, 19, 309-325.

Wright, V.P. 1986. Facies sequences on a carbonate ramp: the Carboniferous Limestone of South Wales. *Sedimentology* 33, 221-241.

Wright, V.P. 1987. The evolution of the Early Carboniferous Limestone Province in Southwest Britain. *Geological Magazine*, 124, 477-480.

Wright, V.P. 1989. Reefs. In: *Carbonate Sedimentology* (Eds M.E. Tucker, V.P. Wright & T.Dickson). *in press.*. Blackwell Scientific (Oxford).

Wright, V.P. & Peeters, C. *submitted.* The origins of crystalline calcrete mosaics revealed by cathodoluminescence. *Sedimentary Geology.*

Wright, V.P. & Robinson, D. 1988. Early Carboniferous floodplain deposits from South Wales: a case study fo the controls on palaeosol development. *Journal of the Geological Society, London*, 145, 847-857.

Wu, Xian-Tao. 1982. Storm-generated depositional types and associated trace fossils in Lower Carboniferous shallow-marine carbonates of Three Cliffs Bay and Ogmore-by-sea, South Wales. *Palaeogeography, Palaeoclimatology, Palaeoecology*, 39, 187-202.

Zenger, D.H. 1983. Burial dolomitization in the Lost Burro Formation (Devonian) eastcentral California and the significance of late diagenetic dolomitization. *Geology*, 11, 519-522.

Appendices A-R: Locality maps and sedimentary logs (KEY)

South Wales

Dyfed

A) Angle West
B) Castlemartin
C) Stackpole Quay
D) Caldey Island

Gower

E) Rhossili
F) Three Cliffs Bay

Glamorgan

G) Penhow
H) Barry Island

SW England

Forest of Dean

I) Drybrook Quarry

Bristol

J) Tytherington Quarry
K) Cromhall Quarry
L) Chipping Sodbury Quarry
M) Avon Gorge
N) Black Rock Quarry
O) Middle Hope

Mendip Hills

P) Burrington Combe
Q) Halecombe Quarry
R) Whatley Quarry

Appendices S-V: laboratory techniques

S) X-ray fluorescence
T) Atomic absorption spectrophotometer (AAS)
U) Determination of $\delta^{18}O$ and $\delta^{13}C$
V) X-ray diffraction (XRD)

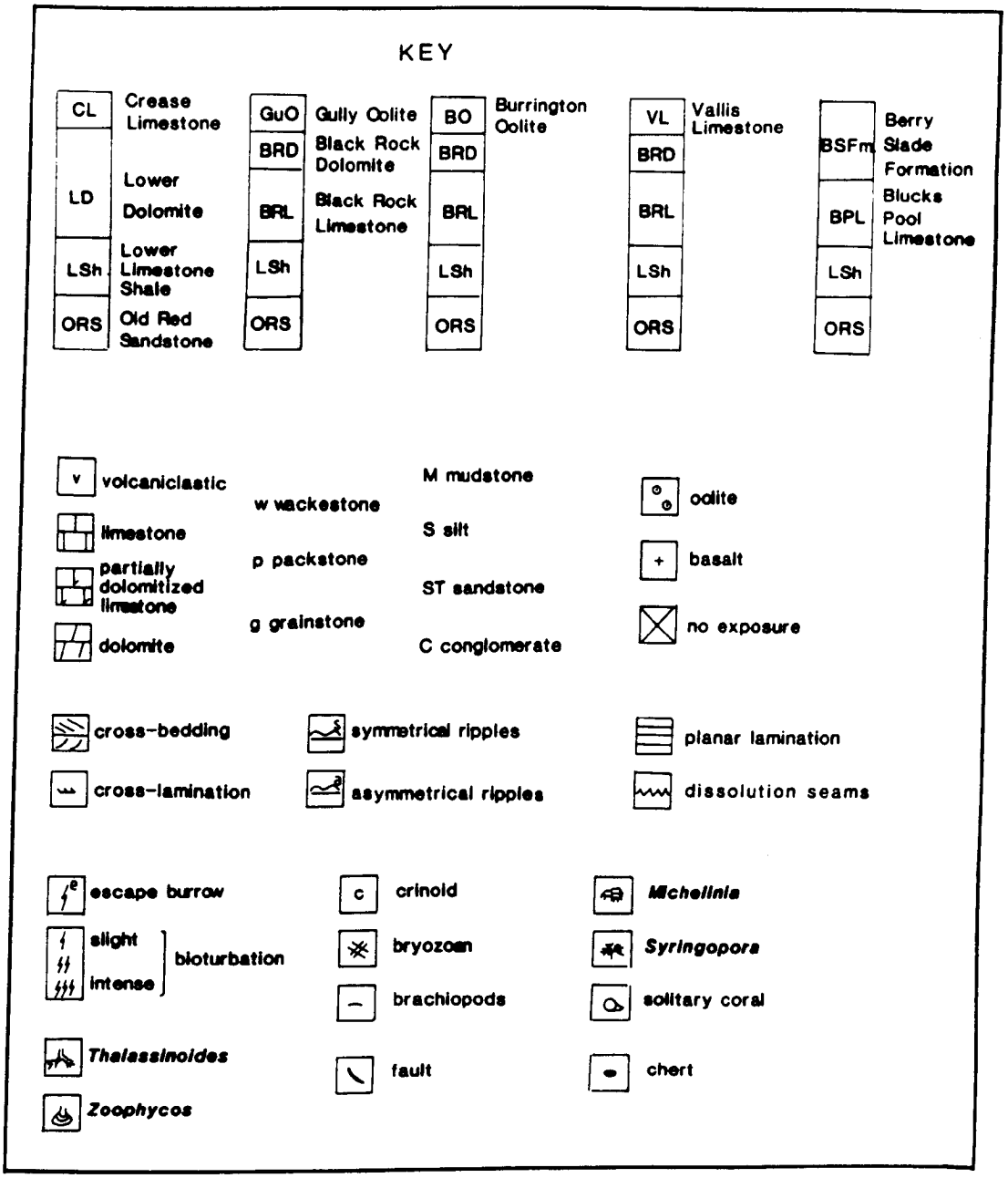
KEY
CL
Crease Limestone
LD
Lower Dolomite
LSh
Lower Limestone Shale
ORS
Old Red Sandstone
GuO
Gully Oolite
BRD
Black Rock Dolomite
BRL
Black Rock Limestone
LSh
ORS
BO
Burrington Oolite
BRD
BRL
LSh
ORS
VL
Vallis Limestone
BRD
BRL
LSh
ORS
BSFm
Berry Slade Formation
BPL
Blucks Pool Limestone
LSh
ORS
v volcaniclastic
limestone
partially dolomitized limestone
dolomite
w wackestone
p packstone
g grainstone
M mudstone
S silt
ST sandstone
C conglomerate
oolite
basalt
no exposure
cross-bedding
cross-lamination
symmetrical ripples
asymmetrical ripples
planar lamination
dissolution seams
escape burrow
slight
intense
bioturbation
Thalassinoides
Zoophycos
c crinoid
bryozoan
brachiopods
fault
Michelinia
Syringopora
solitary coral
chert

Appendix A

West Angle Bay

Grid ref. SM 850034

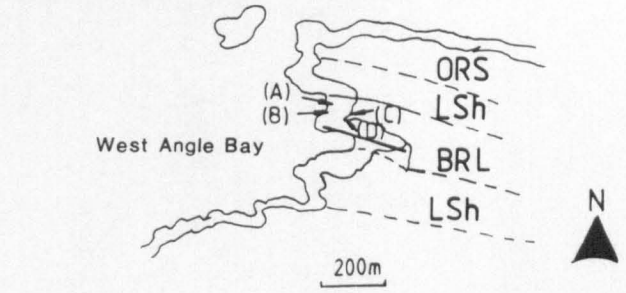

(D)
10
(C)
0
w p g
Fault
(B)
20
(A)
0
w p g

Appendix B

Castlemartin

Grid ref. SR 890975-882960

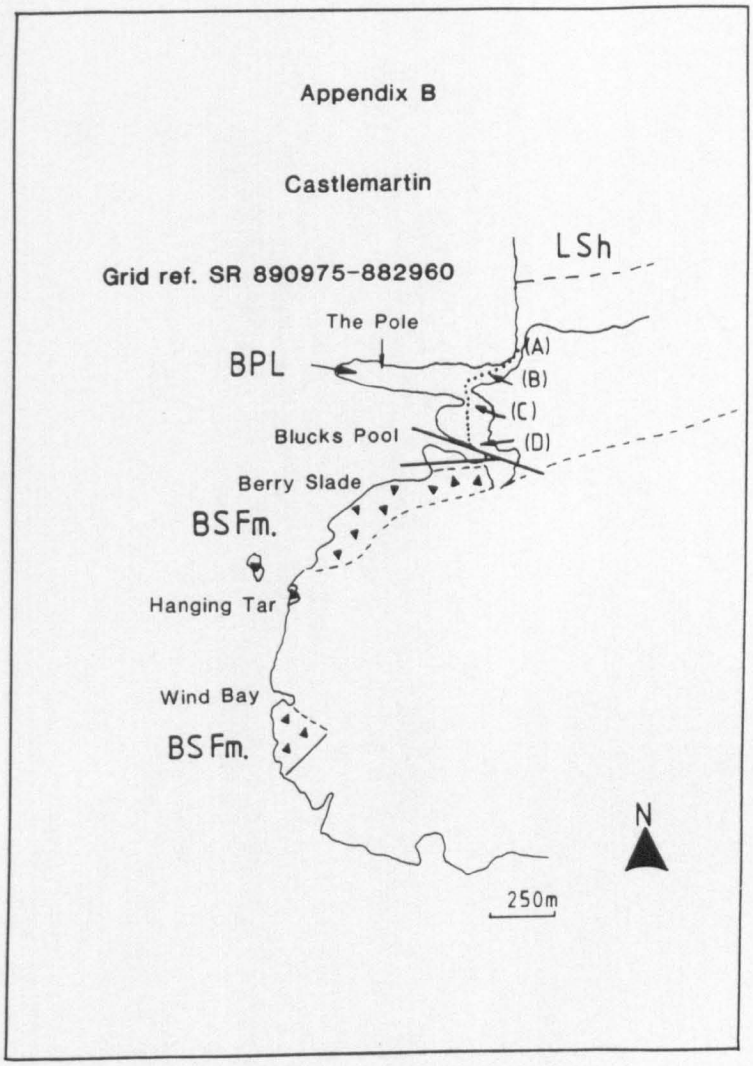

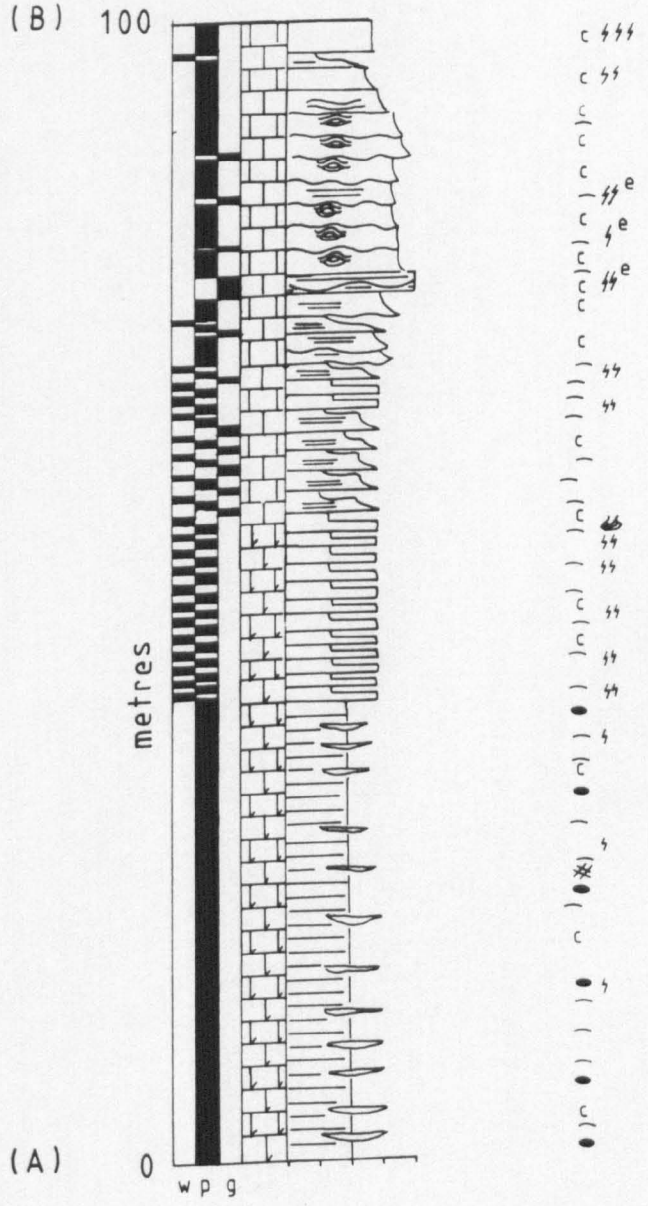
(B)
100
metres
0
(A)
w p g
e
e
e

(C) 200
(B) 100
w p g

300
200
w p g

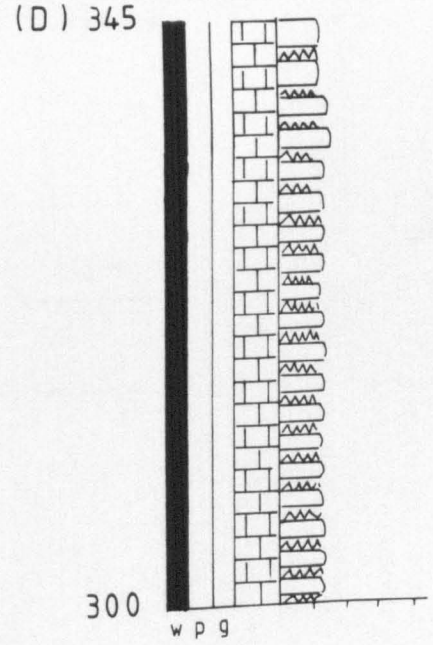
(D) 345
300
w p g

Appendix C

Stackpole Quay

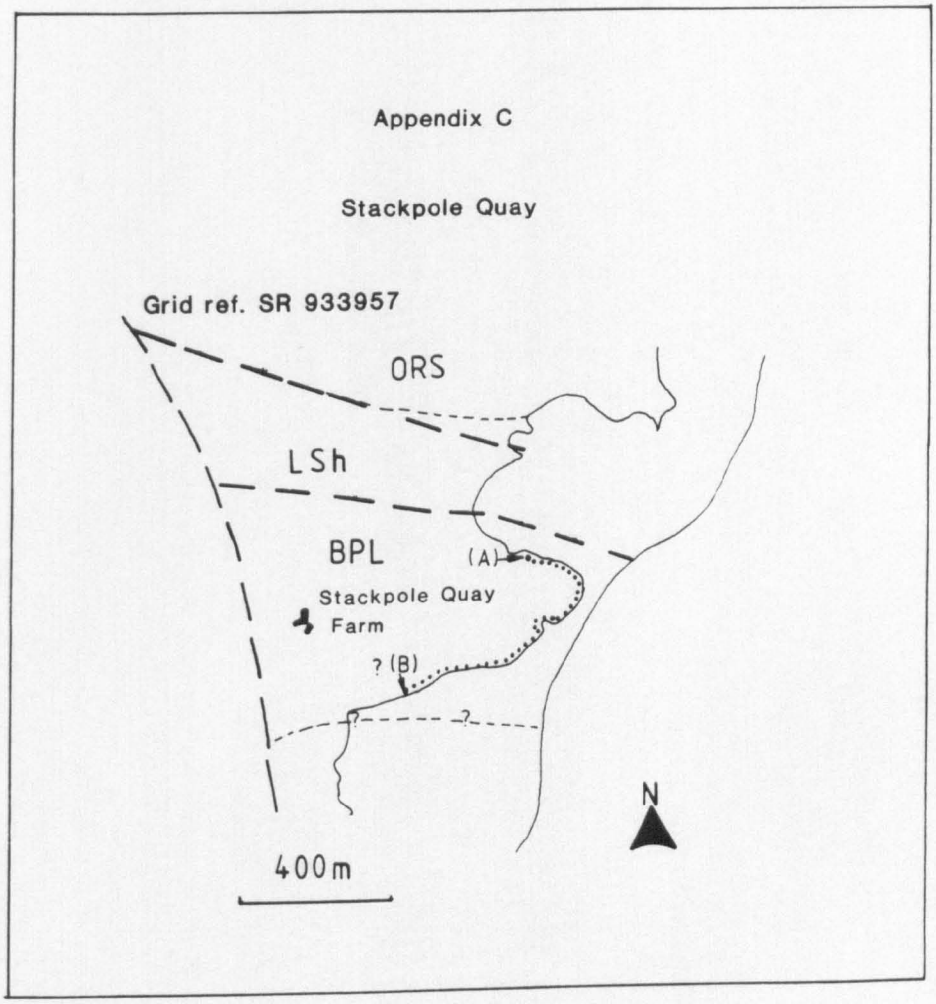

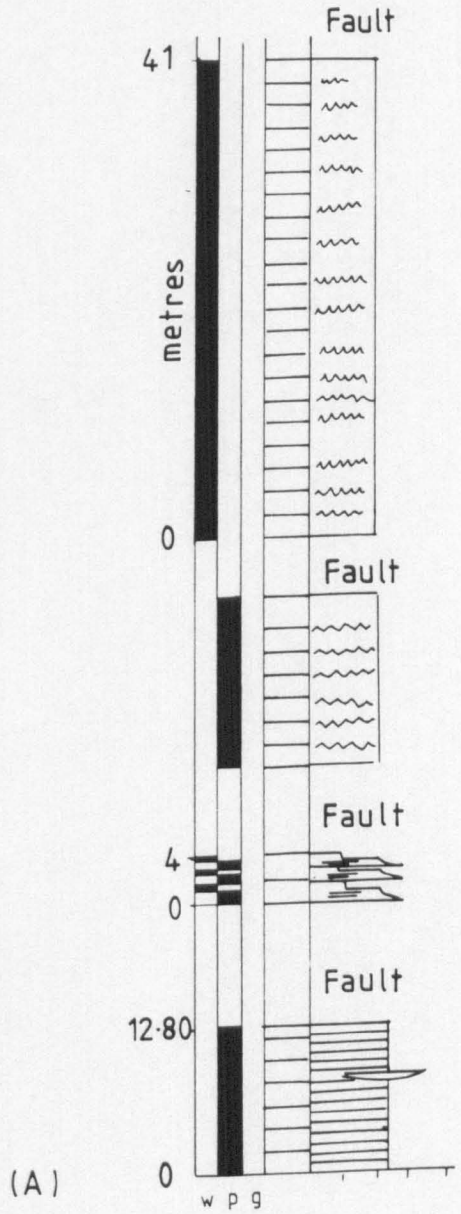
Fault
41
metres
0
Fault
Fault
4
0
Fault
12·80
0
(A)
w p g

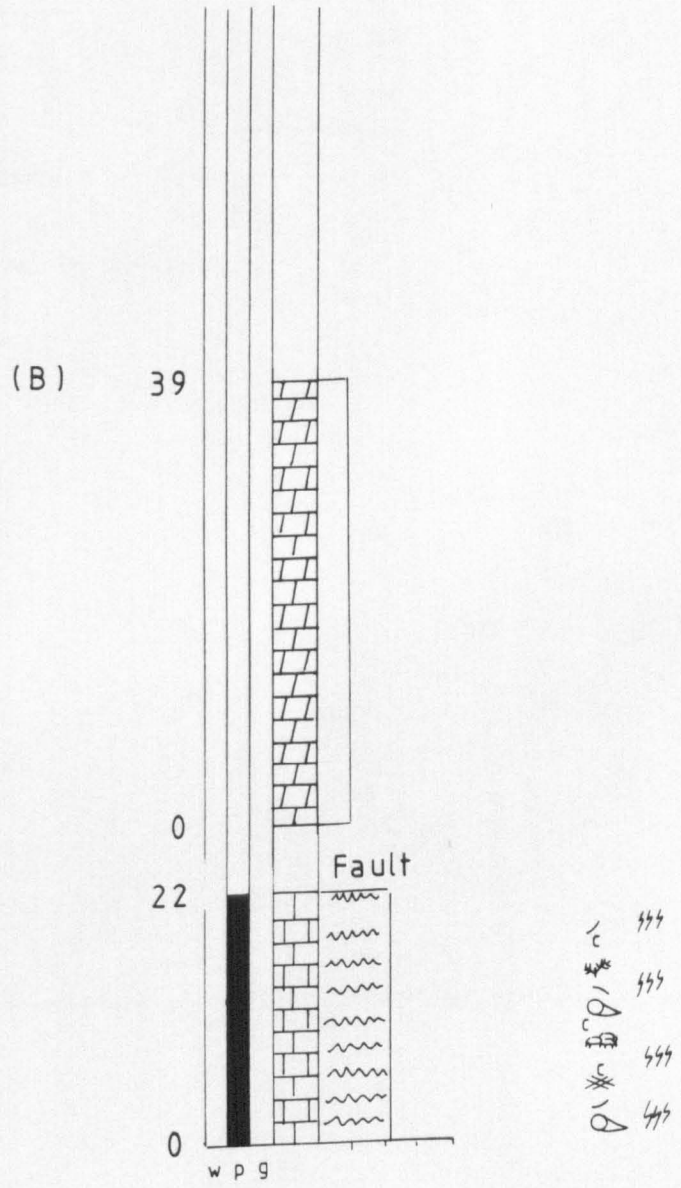
(B)
39
0
22
0
Fault
w p g

Appendix D

Caldey Island

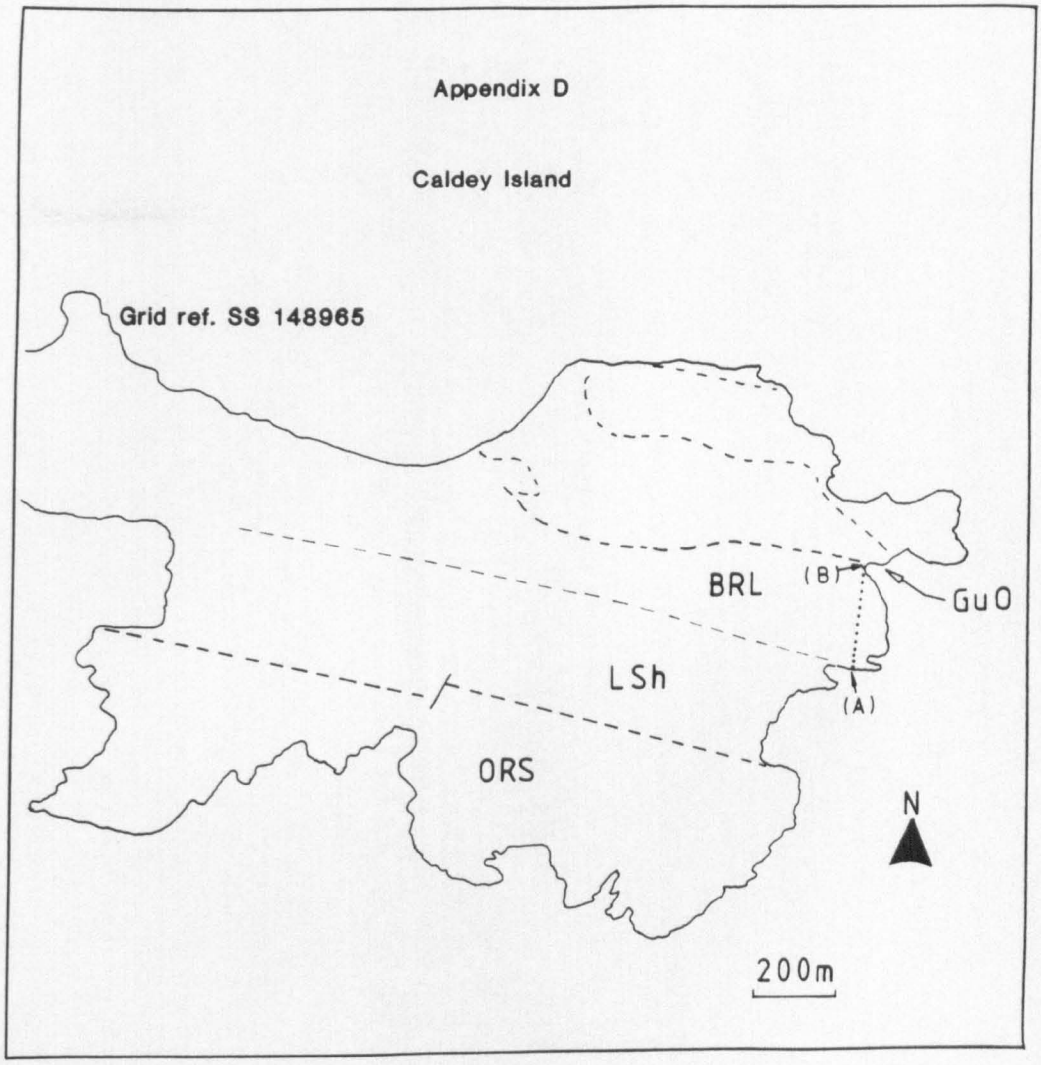

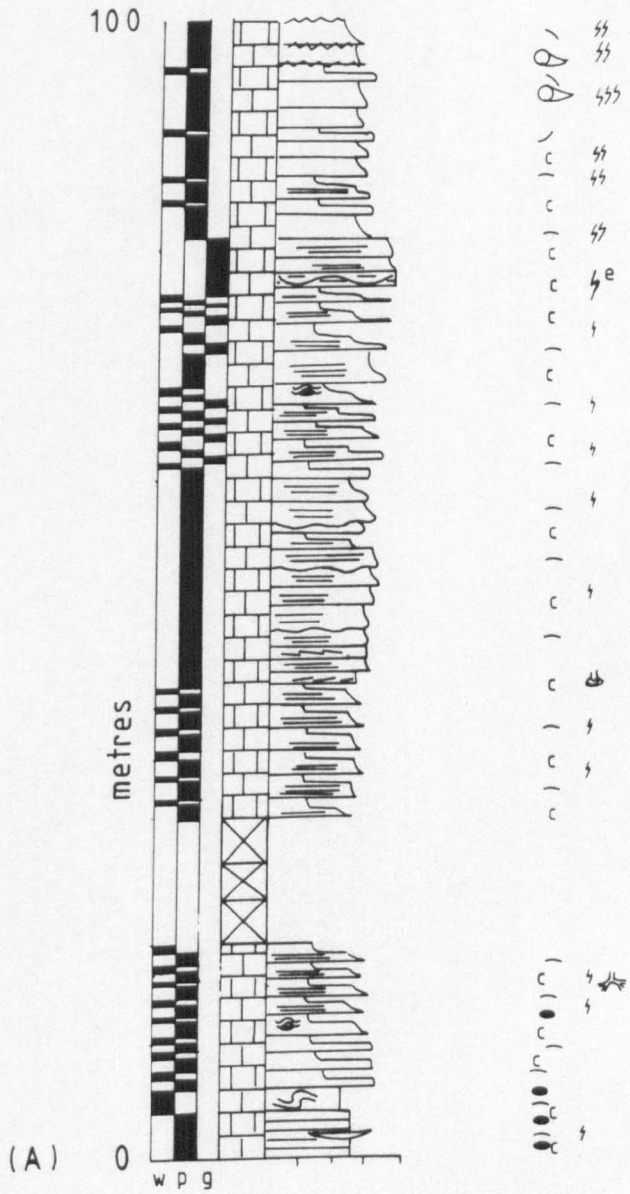
100
metres
0
(A)
w p g

(B) 183

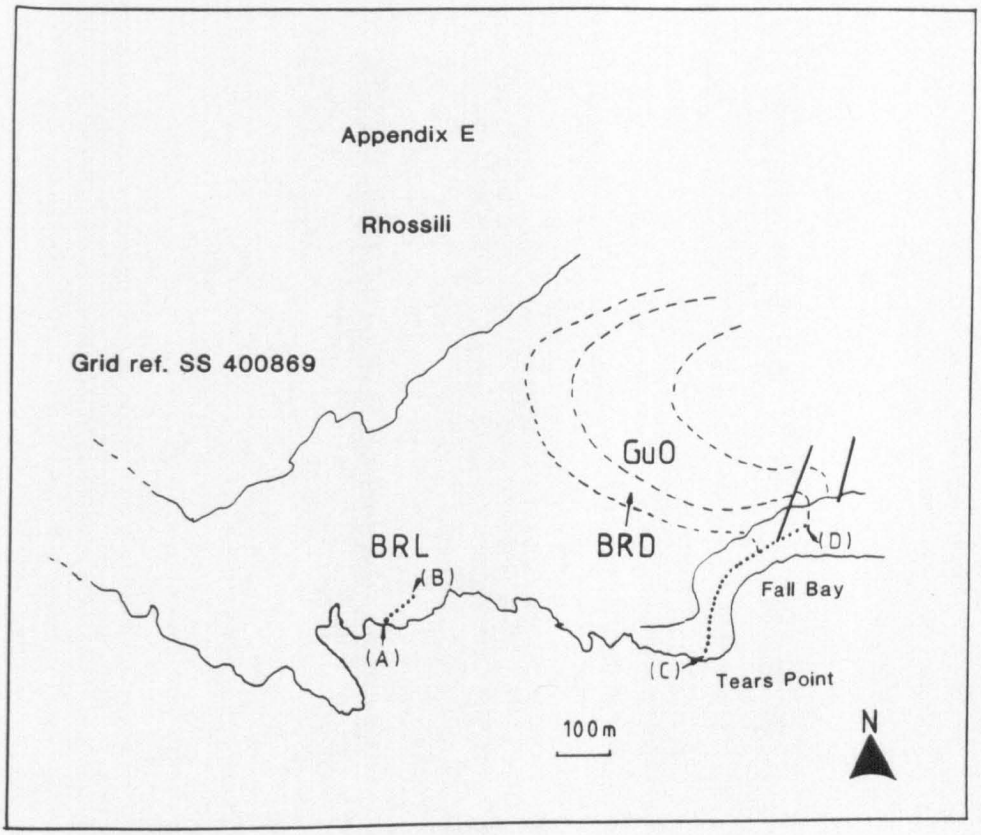
Appendix E
Rhossili
Grid ref. SS 400869
GuO
BRL
BRD
(B)
(A)
(C)
(D)
Fall Bay
Tears Point
100m
N

60
metres
0
33
metres
0
(C)
(B)
(A)
w p g

(D) 122
metres
60
w p g

Appendix F

Three Cliffs Bay

Grid ref. SS 535880

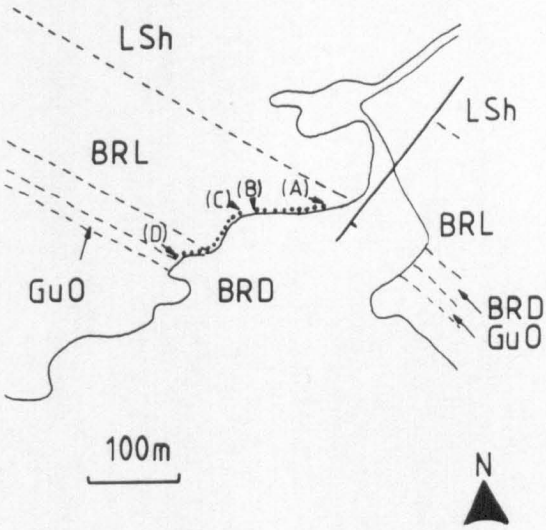

100
metres
0
(A)
(B)
(C)
w p g

(D)

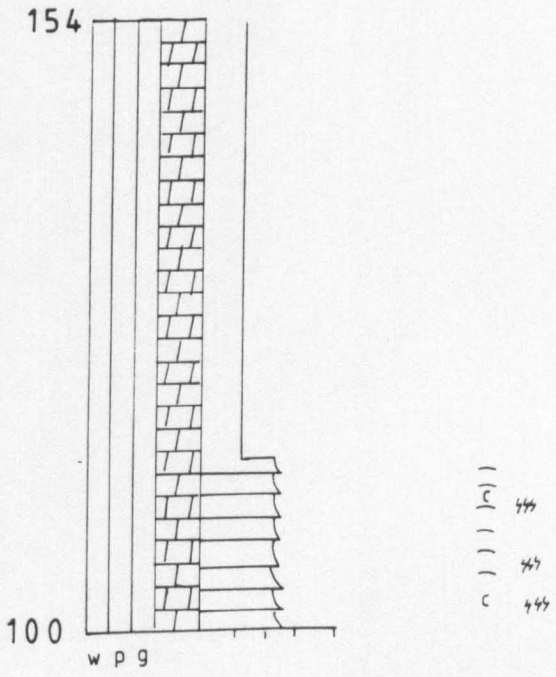

Appendix G

Penhow (ARC)

Grid ref. ST 425912

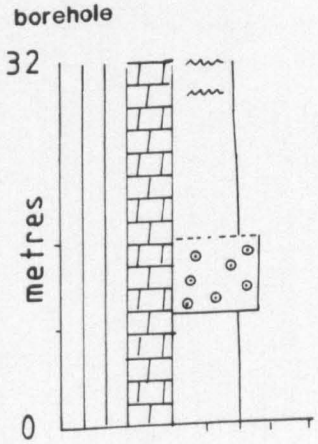

Appendix H

Barry Island

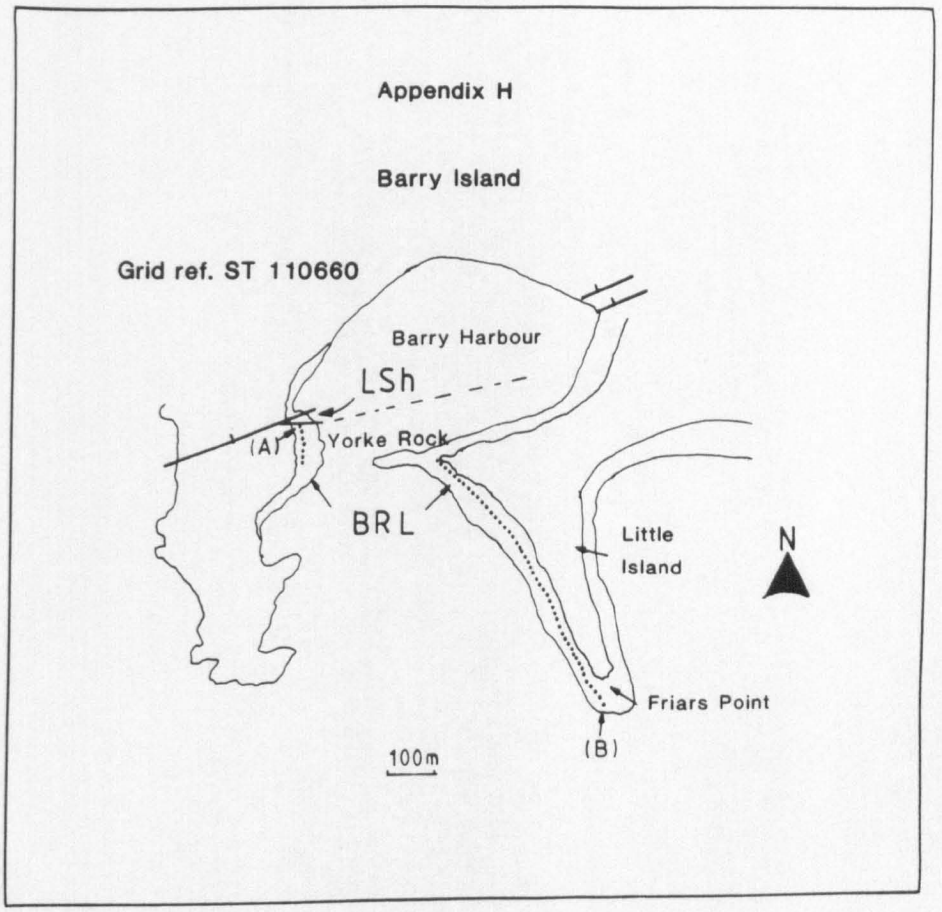

100
metres
0
(A)
w p g

200
metres
100
w p g

300
200
w p g

(B)
392
300
w p g

Appendix I

Drybrook Quarry (ARC)

Grid ref. SO 640180

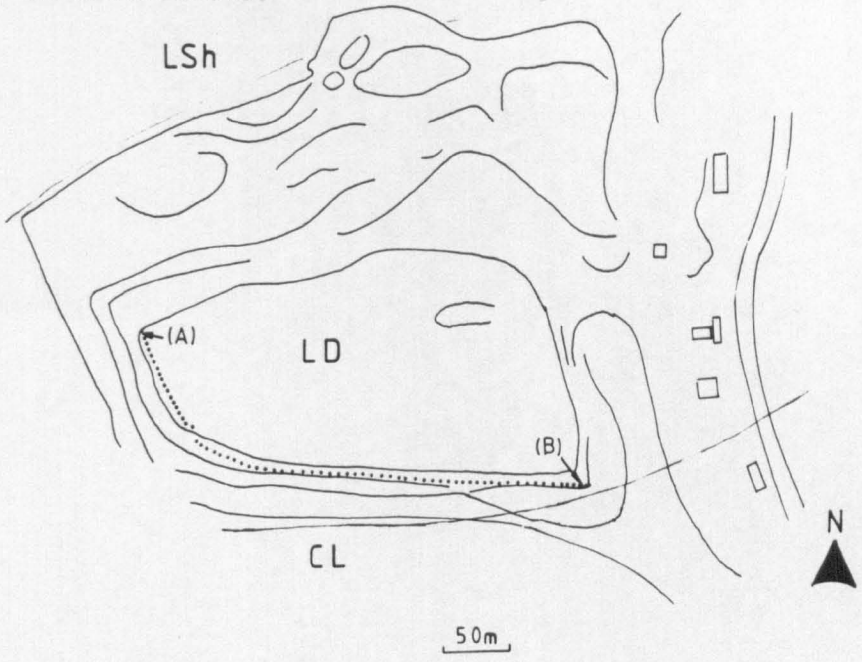

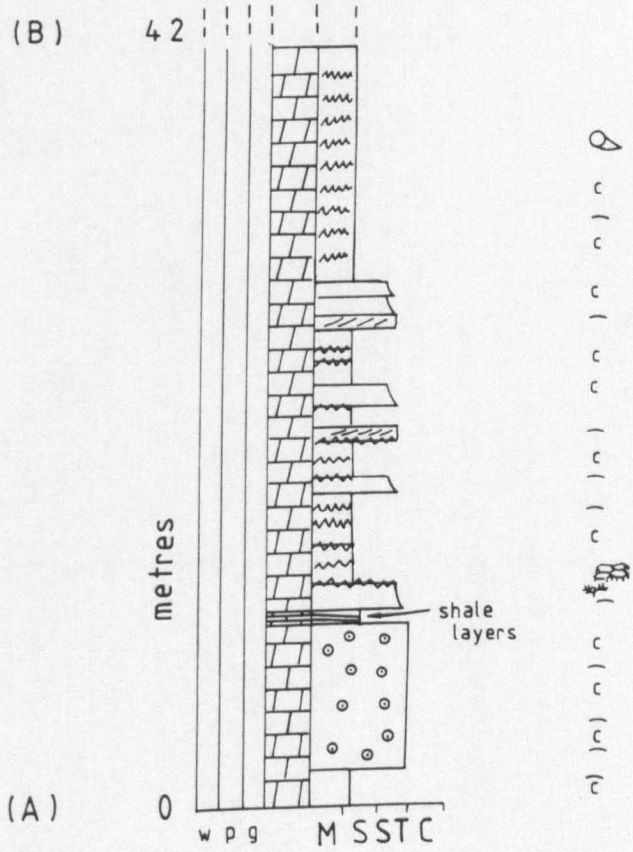
(B)
42
metres
shale
layers
(A)
0
w p g
M S S T C

Appendix J

Tytherington Quarry (ARC)

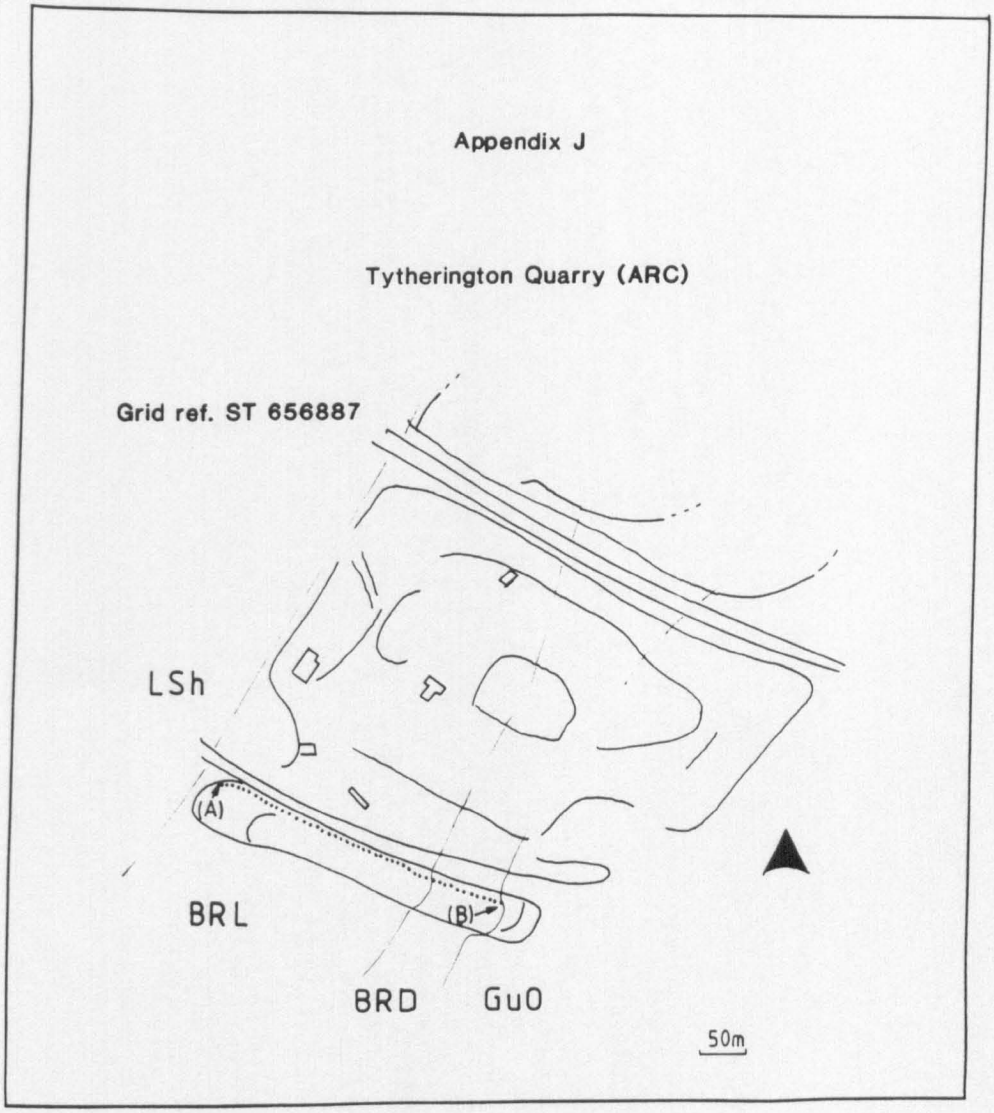

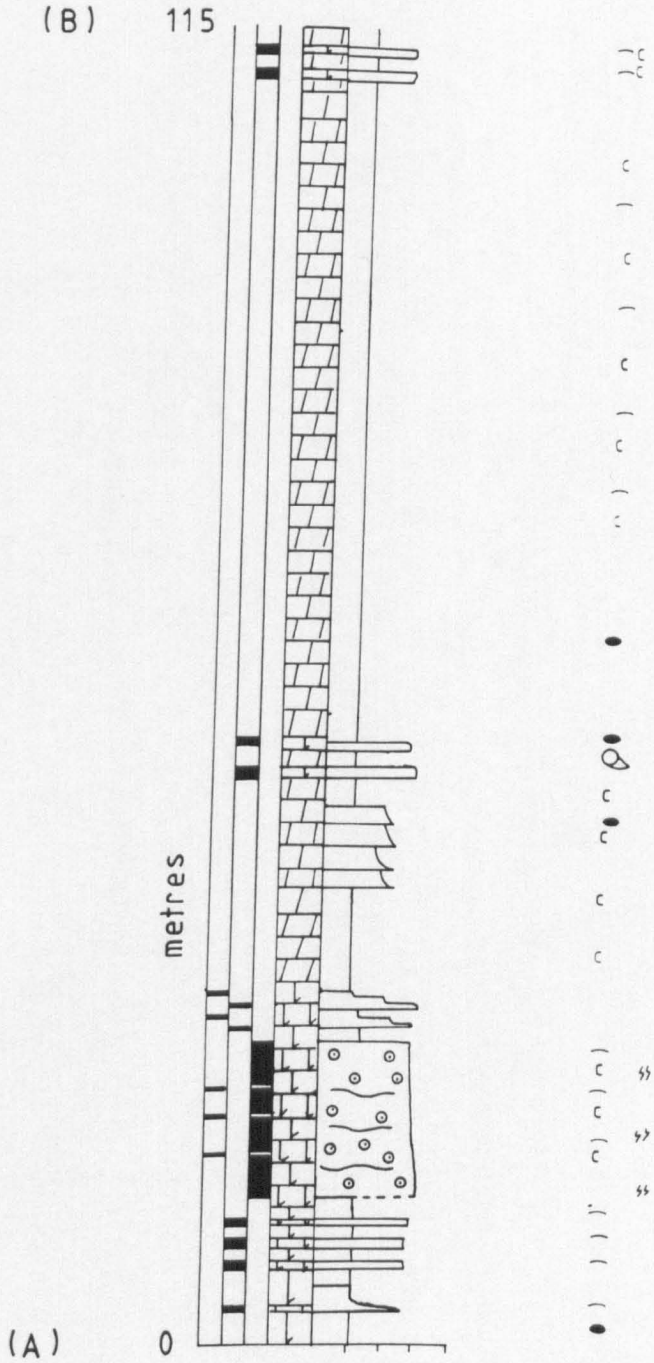
(B)
115
metres
(A)
0

Appendix K

Cromhall Quarry (ARC)

Grid ref. ST 706 916

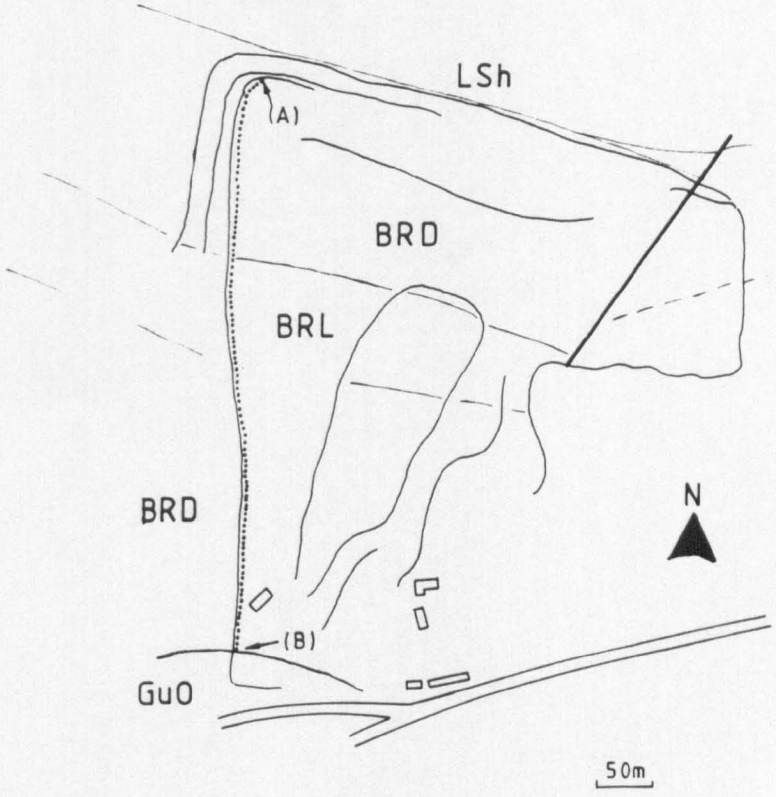

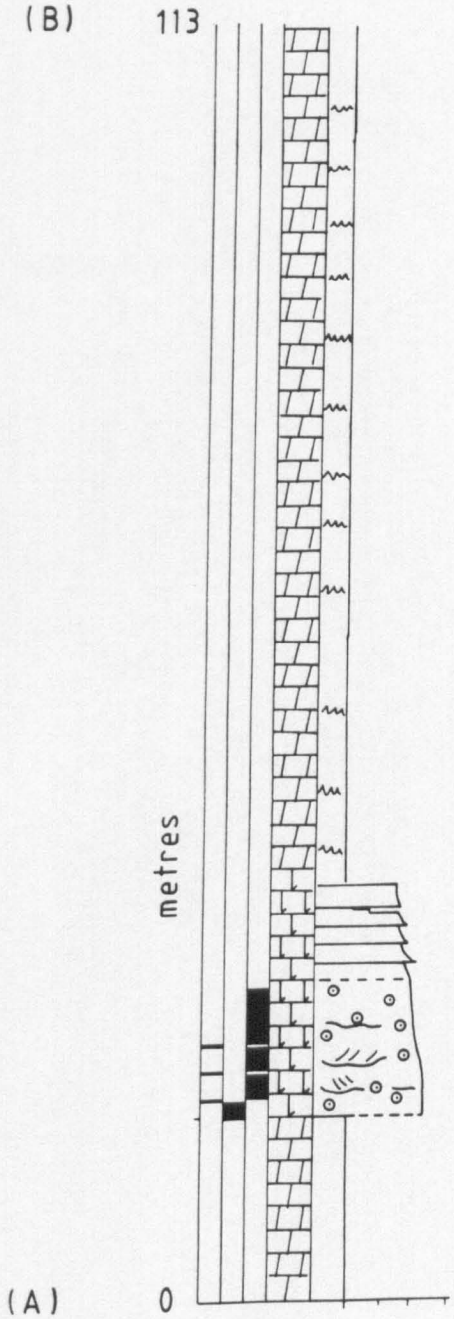
(B)
113
metres
(A)
0

Appendix L

Chipping Sodbury (ARC)

(Hampstead Farm)

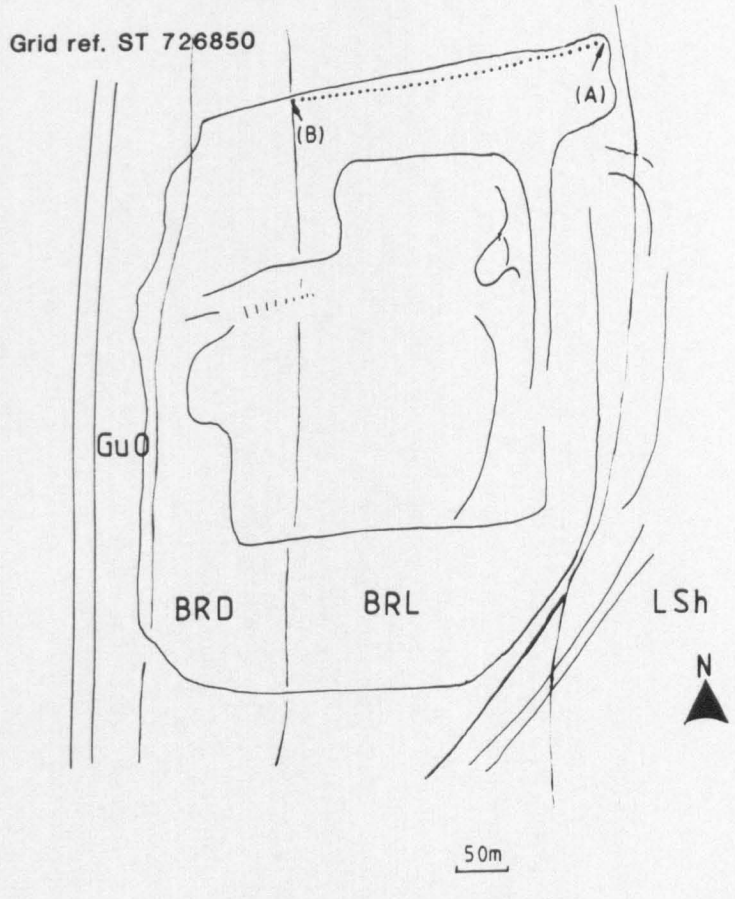

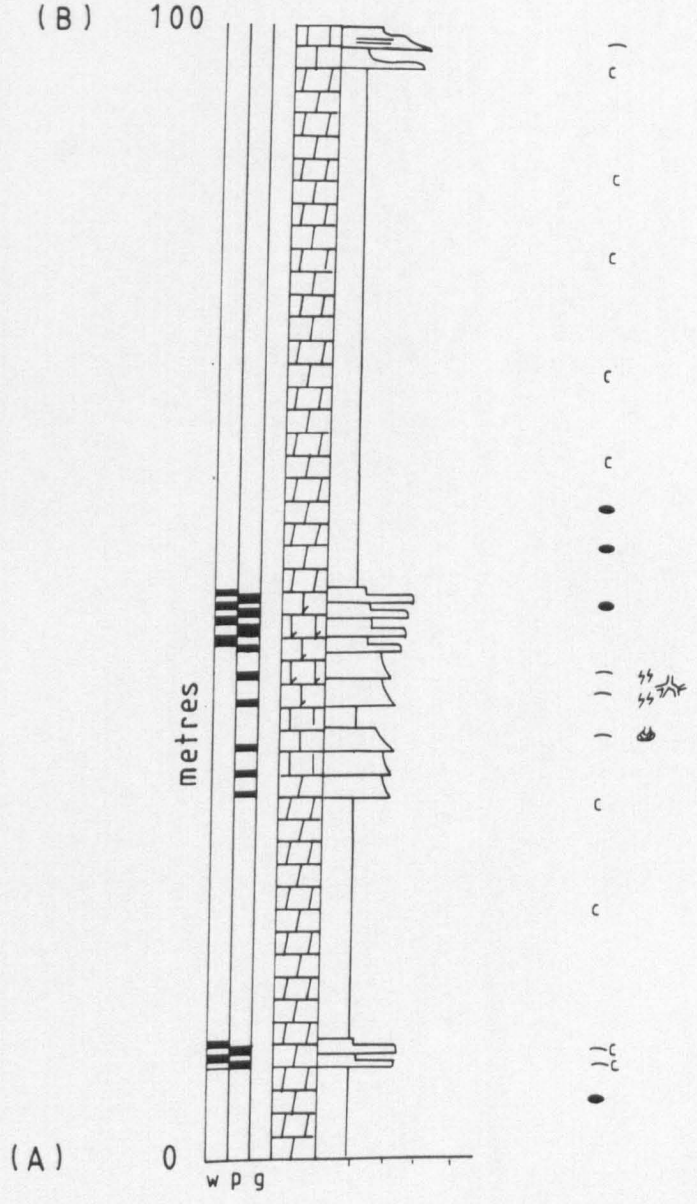
(B) 100
metres
(A) 0
w p g

Appendix M

Avon Gorge

Grid ref. ST 560745

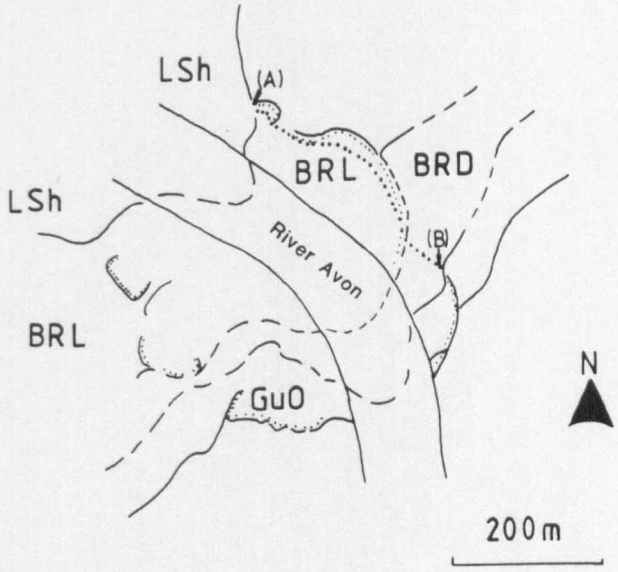

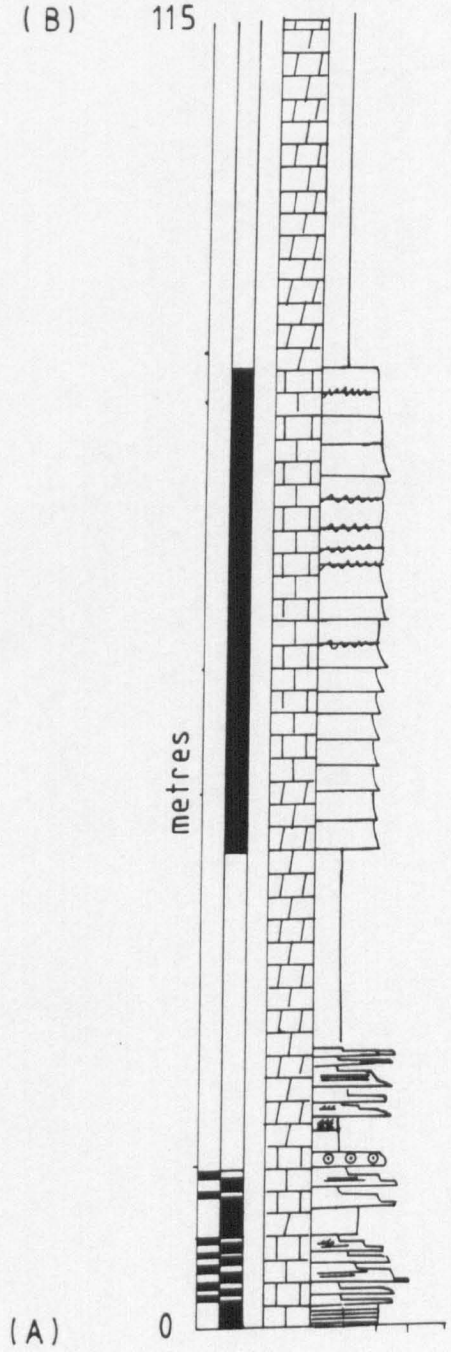
(B)
115
metres
0
(A)

Appendix N

Black Rock Quarry (ARC)

Grid ref. ST 452 747

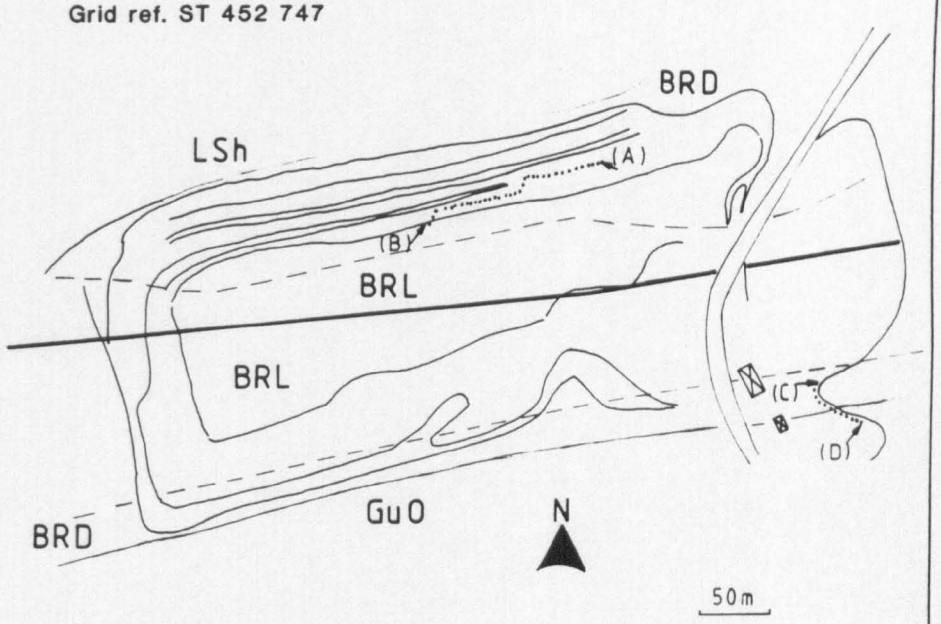

(B)
4
metres
(A)
0
w p g

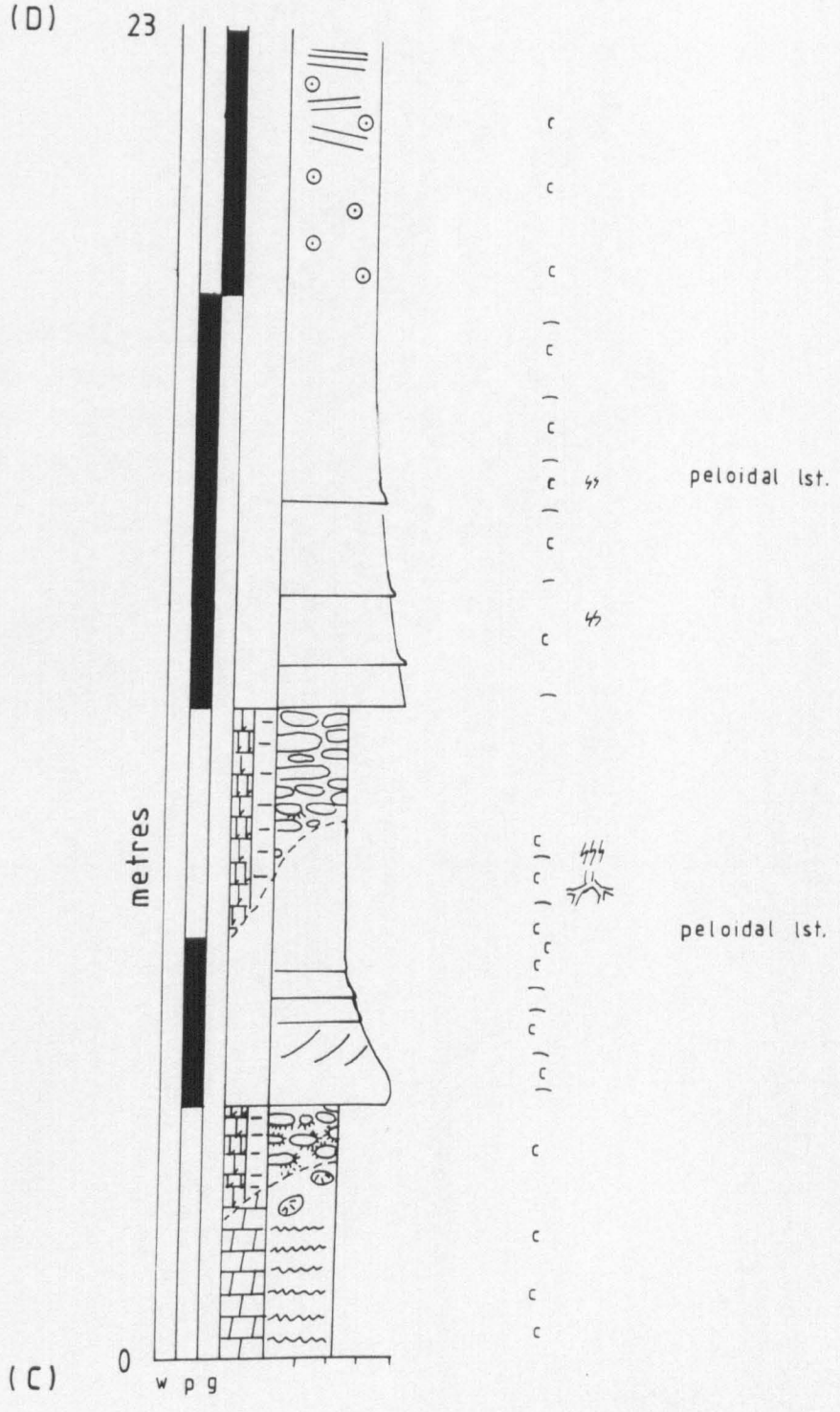
(D)
23
metres
0
(C)
w p g
peloidal lst.
peloidal lst.

Appendix O

Middle Hope

Grid ref. 1) ST 322661
2) 337664
3) 338666
4) 348669

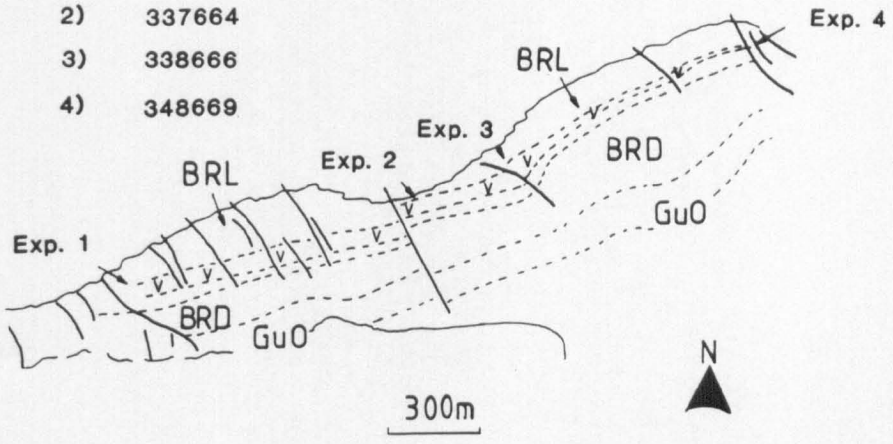

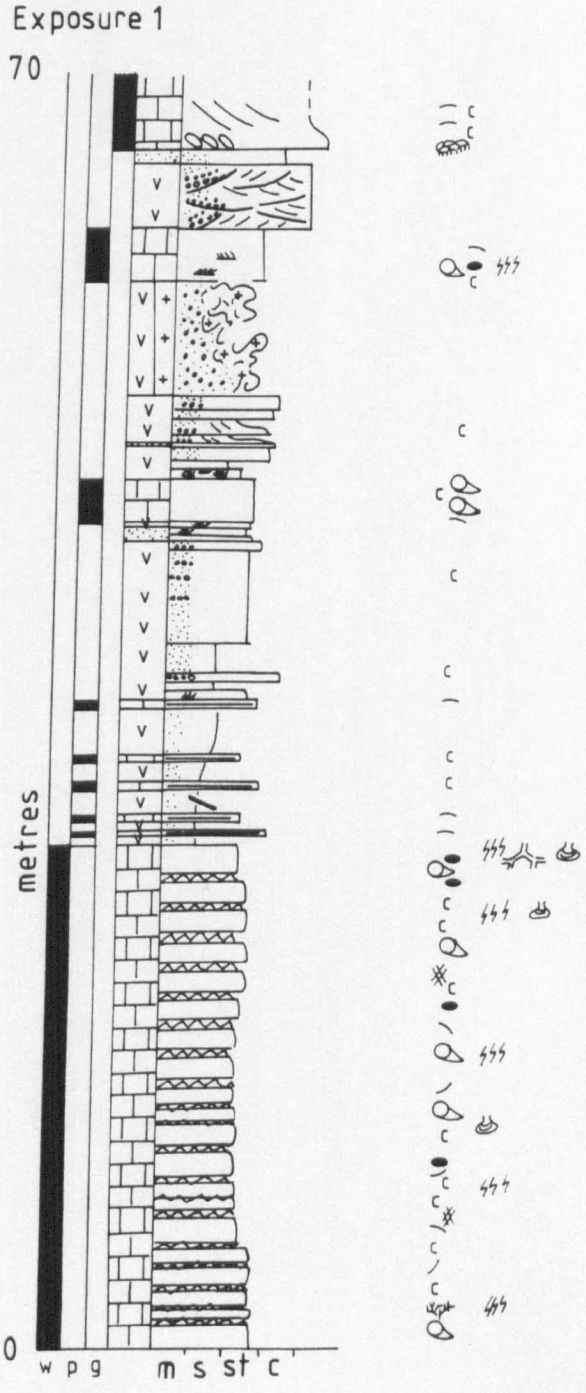
Exposure 1
70
0
metres
w p g
m s st c

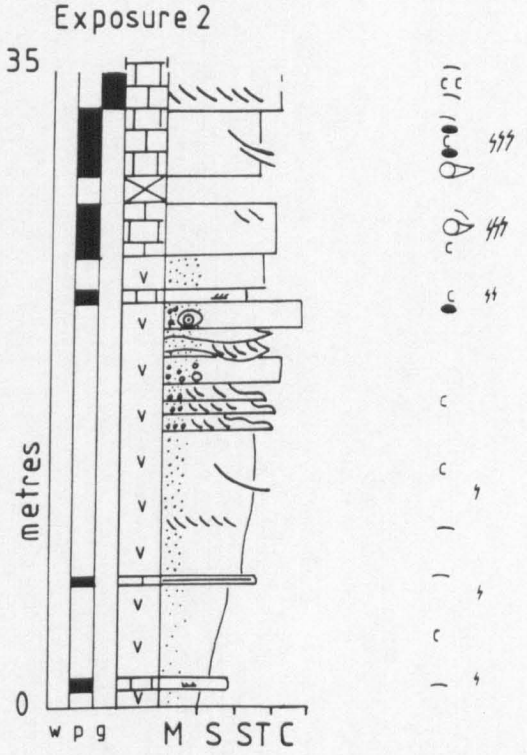
Exposure 2
35
metres
0
w p g
M S ST C

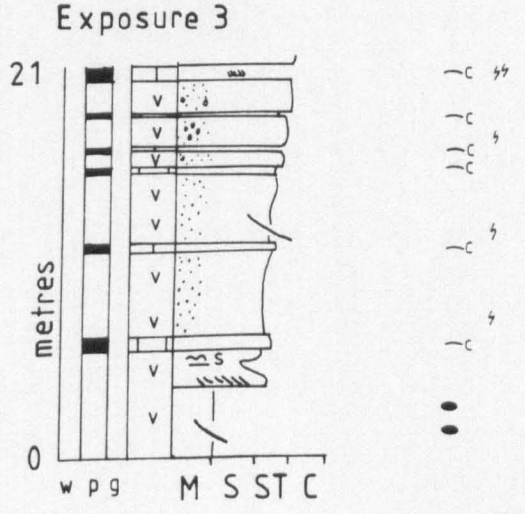
Exposure 3
21
metres
0
w p g
M S ST C

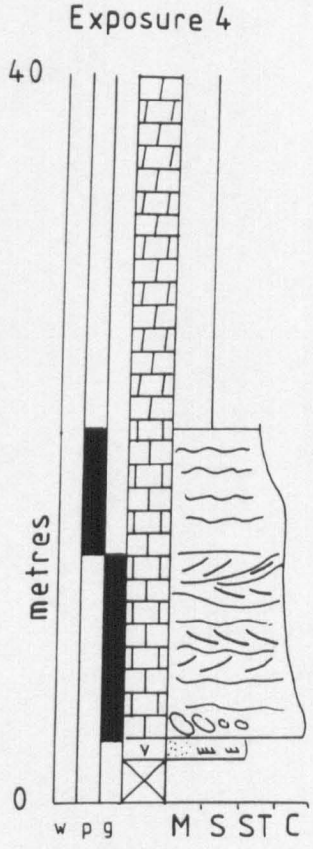
Exposure 4
40
metres
0
w p g
M S ST C

Appendix P

Burrington Combe

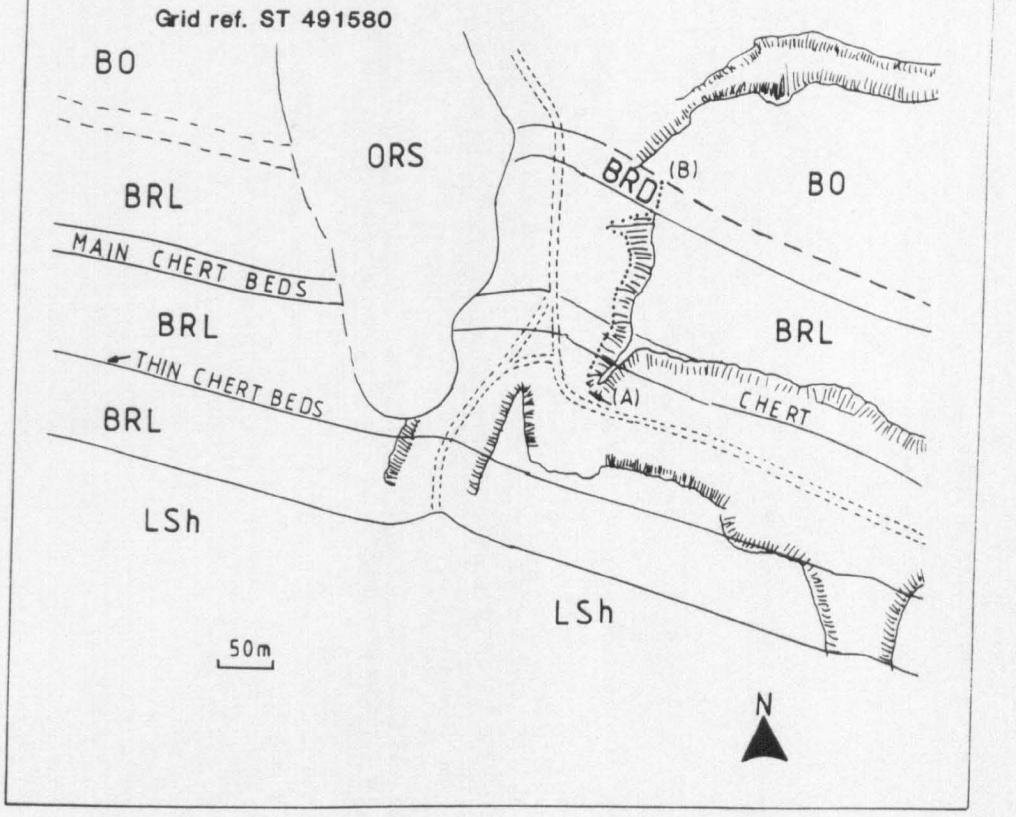

100
metres
0
(A)
w pg
M SST C

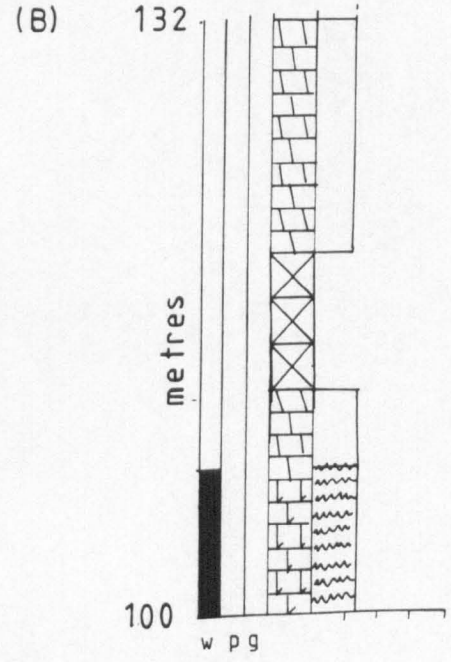
(B)
132
metres
100
w p g

Appendix Q

Halecombe Quarry

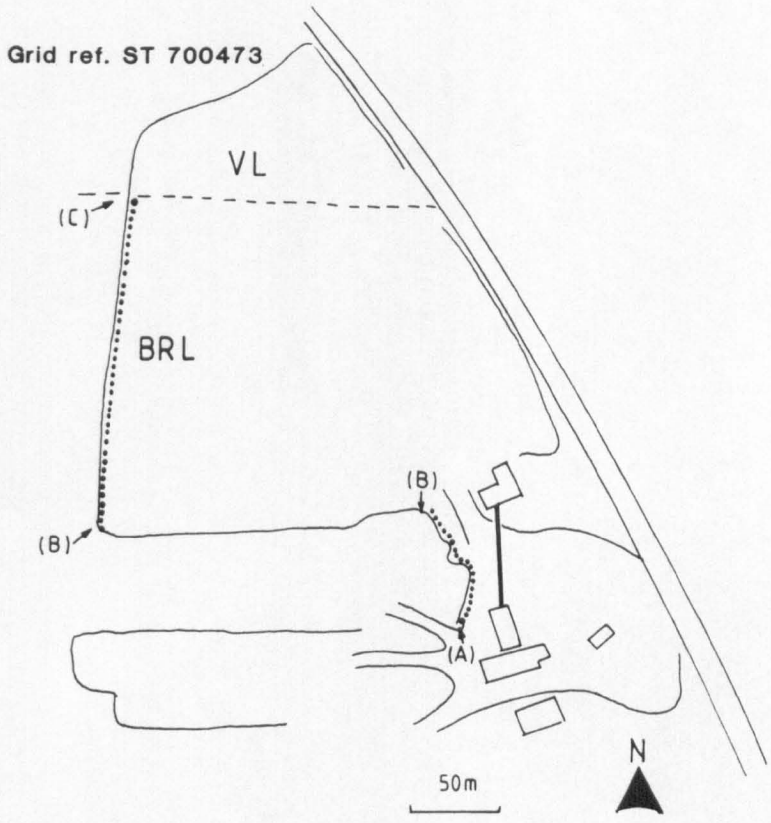

100
(B)
metres
(A)
0
w p g

200
metres
100
w p g

(C)

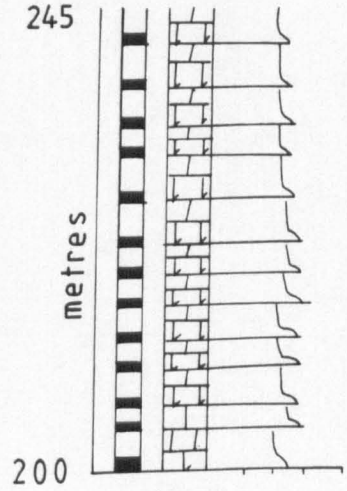

Appendix R

Whatley Quarry (ARC)

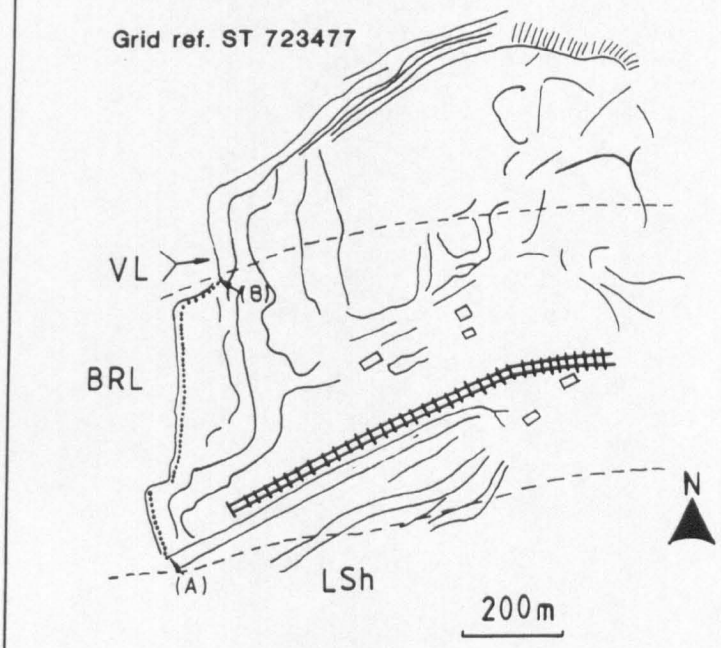

100
metres
0
w p g
(A)

200
100
metres
w p g

300
metres
200

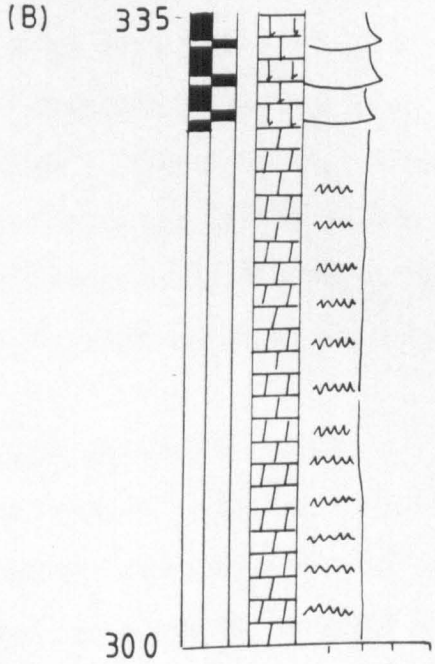
(B)
335
300

Appendix S: X-ray fluorescence

(Work undertaken by M. Widdowson, Oxford University)

S.1 Major elements

Major element analyses were carried out on a Philips PW1400 spectrometer with data processing using the X14 package on a PDP11 minicomputer. The analyses were performed on fused glass beads, made of 5.0000g of spectroflux 100 (lithium tetraborate containing no heavy absorber, dried at 600° for 6 hours) and 1.0000g of rock powder (pre-ignited at 1000° for at least 2 hours). The flux and rock powder were thoroughly mixed and fused in a zirconia grained 5% Au/Pt crucible at 1225° for about 15 minutes. The sample was swirled every 3 minutes to ensure homogeneity. The melt was then poured into a Pt/Au casting mould, and quenched over a compressed air jet. The crucible was cleaned between samples in boiling 50%HCl for 5 minutes.

As no heavy absorber (e.g. LaO) is present in Spectroflux 100, the X14 package provides on-line correction of the raw intensity data for the effects of mass absorption. This is achieved by the use of absorbance factors, or "alphas" (using the De Jongh formula), and an algorithm similar to the ZAP correction used for electron microprobe data. Major element calibration using up to 25 USGS standards, chosen to encompass the likely compositional range of the sample unknowns, was carried out before each run.

As the analyses were performed on pre-ignited materials, they should give major element oxide totals very close to 100% (less than 0.2 wt% of each specimen being composed of trace elements). Totals can therefore be used as a way of assessing of the quality of the analyses, and those between 99-101% are considered acceptable. Devey (1986) and Woodhead (1987) discuss the problems of machine drift and volatile loss,

and demonstrate that these introduce relatively little error. The major analytical errors seem to be in machine calibration and initial weighing.

S.2. Trace elements

The concentration of 13 trace elements were determined by the XRF technique. The elements concerned are Rb, Sr, Y, Zr, Nb, Pb, Zn, Cu, Ni, Co, Cr, V, and Ba. Analyses were determined on 10g pressed powder pellets, using 1.0ml of "Moviol" as a binding agent, and carried out on a Philips PW1400 spectrometer, with data processing on the PDP11 minicomputer.

Details of counting times and operating conditions for each element are given in Table S.1. A Rh anode tube was used in all cases and mass absorption corrections were made using the Rh Compton scatter peak, plus corrections for the Fe, Mn and Ti absorption edges, and line overlaps as necessary.

The precision of XRF data is usually extremely high, and readily verified from replicate analysis data (Potts 1987), as outlined below. The accuracy of the technique is however much more difficult to assess, and in practice this is done by calibrating the instrument against as many rock reference materials as possible. In the present study, calibration lines were constructed from analyses of up to 25 USGS recommened standards.

Data from replicate analyses (Widdowson pers. comm.) have also been used to calculate the "limit of determination", which is defined as the "the smallest signal that can be quantitatively measured" (Potts 1987). This is calculated at the 12-sigma level using the following equation:

	Element	Collimater	Detector	Crystal	kV	mA	Peak time	Bkg time
1	Rb	Ka	Scint	LiF220	95	25	100	80
2	Sr	Ka	Scint	LiF220	95	25	100	80
3	Y	Ka	Scint	LiF220	95	25	100	80
4	Zr	Ka	Scint	LiF220	95	25	100	80
5	Nb	Ka	Scint	LiF220	95	25	100	80
6	Zn	Ka	Flow/Scint	LiF220	60	40	100	80
7	Cu	Ka	Flow/Scint	LiF220	60	40	100	80
8	Ni	Ka	Flow/Scint	LiF220	60	40	100	80
9	V	Ka	Flow	LiF220	60	40	100	100
10	Cr	Ka	Flow	LiF220	60	40	100	80
11	Co	Ka	Flow	LiF220	60	40	100	80
12	Ba	La	Flow	LiF200	60	40	100	100

Table S.1 Operating conditions and count times. In all cases a Rh anode tube is used.

		Bkgrnd T:sec	Gross pk T:sec	Sample S15	Rate Bkgrnd (R_B)	Rate Peak (R_G)	Net Peak ($R_G - R_B$)	M Cnt:sec	LoD
1	SiO2	20	200	48.4	147	19346	19199	396.67	0.082
2	TiO2	10	100	2.78	44	4652	4608	1657.55	0.015
3	Al2O3	10	100	13.52	37	4618	4581	338.83	0.068
4	Cr2O3	80	200	0.02	36.5	75	38.5	1925.00	0.004
5	Fe2O3T	16	16	15.42	293	130452	130159	8440.92	0.006
6	MnO	16	40	0.23	293	1808	1515	6586.96	0.008
7	MgO	40	100	6.13	24.5	444	419.5	68.43	0.137
8	CaO	2	20	11	198	64608	64410	5855.45	0.020
9	Na2O	40	100	2.46	53.5	243	189.5	77.03	0.180
10	K2O	20	100	0.24	221	1114	893	3720.83	0.011
11	P2O5	40	100	0.27	18	157	139	524.81	0.016
12	Zn ppm	80	100	108.5	306.5	854	547.5	5.05	4.65
13	Cu ppm	80	100	207.8	250	1214	964	4.64	4.57
14	Ni ppm	80	100	83.6	205.5	496	290.5	3.47	5.53
15	Co ppm	80	100	54.4	187	239	52	0.96	19.19
16	Cr ppm	80	100	89.8	36	104	68	0.76	10.63
17	V ppm	100	100	364.2	32	283	251	0.69	9.85
18	Ba ppm	100	100	85.8	32	90	58	0.68	10.04
19	Ga ppm	100	100	•	•	•	•	•	[illegible]
20	Rb ppm	80	100	11.5	231.5	336	104.5	9.09	2.25
21	Sr ppm	80	100	247.2	292	1826	1534	6.21	3.69
22	Y ppm	80	100	34.7	384	590	206	5.94	4.43
23	Zr ppm	80	100	163.7	364	1852	1488	9.12	2.81
24	Nb ppm	80	100	12.8	541	628	87	6.80	4.59
25	Pb ppm	80	100	4.2	202	209	7	1.63	11.71
26	Th ppm	80	100	•	•	•	•	•	•
27	U ppm	80	100	•	•	•	•	•	•

Table S.2 Limit of determination.

Bkgrnd = Background, T = time, sec = seconds, Cnt = count, & LoD = limit of determination.

(Tertian & Claisse 1982)

$$LoD = 3x \frac{4C}{R_G - R_B} \times \frac{\sqrt{R_B T_B}}{T_B(R_G - T_B)}$$

where LoD is the limit of determination, R_B the background count rate, T_B the count rate for which the signal was accumulated, R_G the gross peak count rate, T_P the count rate for which that signal was accumulated, and C the concentration of the element (Table S.2). Given this, the limit of detection will vary from sample to sample, but, for example, in basaltic compositions, the variation within the range of compositions is minimal. Thus the limits of determination for the 13 trace elements used in the present study are given in Table S.1.

Appendix T: Atomic absorption spectrophotometer (AAS)

Approximately 0.2g of sample was added to 50ml of 0.5M acetic acid and boiled on a hot plate for half an hour, filtered and then made up to 100ml. The carbonate fraction was calculated by subtracting the weight of the residue collected during filtration from the original starting weight (0.2g). The choice of standard for a given sample analysis depended upon the approximate element concentration in that sample, thus ensuring the most accurate calibration. Operation of the AAS was undertaken by A. Kemp (Bristol University). The precision of the instrument in the air/acetylene flame is between 0.3% to 1.0%.

Appendix U: Determination of $\delta^{18}O$ and $\delta^{13}C$

(Work undertaken by M.T. Burchell at BP Sunbury on Thames)

Measurement was made by mass spectometry on carbon-dioxide gas prepared from de-organified samples. The raw data produced by the spectrometers was corrected for various analytical effects and adjusted to produce final results relative to an international calibration scale. The corrections to be made were a) instrumental effects arising from deficiencies in the measuring process; b) mass overlap due to coinciding CO_2 mass combinations; c) isotopic fractionation (separation) during sample preparation from the original phase to the measurement standard; and d) calibration against a laboratory standard and adjustment to an international reference scale - in this instance the PDB belemnite standard (see below0. In the system used at BP, these corrections are performed automatically by a computerised data handling package. The first two are programmed from the work of Craig (1957) and Deines (1970), whilst the third adjustment is made using a "sigma" (o) correction factor defined as:

$$\sigma_{(A-B)}=R_{(A)}/R_{(B)}$$

where $R_{(X)}$ is the isotopic ratio ($^{13}C/^{12}C$, $^{18}O/^{16}O$) of the sample and A & B are respectively, reactant and product of the fractionating reaction.

Methodology

After removal of organic-matter by plasma oxidation (2 hours), extraction of CO_2 from the carbonate followed the procedure of McRea (1950). Outgassed phosphoric acid was reacted for 15 hours with the dolomite sample after equilibration at 60.0°C. The liberated gas was passed

through an acetone cold-trap (-90°C to remove water and phosphoric acid) into a liquid nitrogen cold-trap (-196°C). Keeping the nitrogen trap filled, gas-collection vessels were evacuated to remove nitrogen gas, leaving evolved carbon-dioxide frozen down in the trap. Laboratory standards (SSB) calcibrated to PDB were prepared in a similar way and included in each batch of samples so that analytical precision could be monitored.

The isotopic character of the sample and standard CO_2 volumes was measured using a VG Isotopes SIRA 12 triple collector mass spectrometer. Solid-gas phase oxygen fractionation was corrected using a sigma coefficient for dolomite at 60°C was calculated using:

$$\sigma_{(T)}=mT + C$$

where m= -3.91429×10^5 and C=1.012069. Hence for the reaction at T=60°C, $\sigma_{(60)}=1.00972$.

All figures in the text and tables are expressed in the "del" notation as permil (‰) deviation from the PDB belemnite standard such that:

$\delta^{13}C$ = [(Rc sample/Rc PDB)-1]x1000‰, where $Rc=^{13}C/^{12}C$

and

$o^{18}O$=[(Ro sample/Ro PDB)-1]x1000‰, where $Ro=^{18}O/^{16}O$

Accuracy considerations

Precision of the various isotopic measurements was determined by observing the variability of results in 25 SSB laboratory standard analyses. Overall standard error margins were found to be 0.005‰ for carbon and 0.10‰ for oxygen. The errors in instrumental measurement (quoted for manufacturer) of 0.02‰ should be added to the above to give total standard error ranges of 0.07‰ for $\delta^{13}C$ and 0.12‰ for $\delta^{18}O$.

Although repeat analyses were not generally conducted for actual unknown samples, the few that were re-analysed showed reproducability well within these tolerance levels. In such cases the figures quoted as means.

Appendix V: X-ray diffraction (XRD)

(Work undertaken by L. Garvie, University of Bristol)

Two samples from each of the Portishead Paleosol Bed were collected and analysed. All samples were disaggregated in an ultrasonic tank and the <2um (e.s.d.) fraction separated using centrifuge and subsequent filtration techniques. The collected filtrate was smeared onto a glass slide to obtain an orientated sample and each mount was irradiated after the following pre-treatments: 1) air-dried, 2) solvation with ethylene glycol and heated at 300° for 30 minutes, 3) heating at 500° for 30 minutes. Analysis was undertaken using a Philips 2 kW diffractometer using Ni-filtered Cu-K_{alpha} radation at a setting of 40 kV and 40 mA. An automatic divergence silt and graphite monochromator were used and calibration of the instrument checked by using tetradecanol.

The tables of Brindley and Brown (1980) and Starkey *et al.* (1984) were used as a guide in determining the mineralogy of the samples from the XRD traces (pers. comm. L. Garvie).